The following notice applies to any unclassified (including originally classified and now declassified) technical reports released to "qualified U.S. contractors" under the provisions of DoD Directive 5230.25, Withholding of Unclassified Technical Data From Public Disclosure.

NOTICE TO ACCOMPANY THE DISSEMINATION OF EXPORT-CONTROLLED TECHNICAL DATA

1. Export of information contained herein, which includes, in some circumstances, release to foreign nationals within the United States, without first obtaining approval or license from the Department of State for items controlled by the International Traffic in Arms Regulations (ITAR), or the Department of Commerce for items controlled by the Export Administration Regulations (EAR), may constitute a violation of law.

2. Under 22 U.S.C. 2778 the penalty for unlawful export of items or information controlled under the ITAR is up to ten years imprisonment, or a fine of $1,000,000, or both. Under 50 U.S.C., Appendix 2410, the penalty for unlawful export of items or information controlled under the EAR is a fine of up to $1,000,000, or five times the value of the exports, whichever is greater; or for an individual, imprisonment of up to 10 years, or a fine of up to $250,000, or both.

3. In accordance with your certification that establishes you as a "qualified U.S. Contractor", unauthorized dissemination of this information is prohibited and may result in disqualification as a qualified U.S. contractor, and may be considered in determining your eligibility for future contracts with the Department of Defense.

4. The U.S. Government assumes no liability for direct patent infringement, or contributory patent infringement or misuse of technical data.

5. The U.S. Government does not warrant the adequacy, accuracy, currency, or completeness of the technical data.

6. The U.S. Government assumes no liability for loss, damage, or injury resulting from manufacture or use for any purpose of any product, article, system, or material involving reliance upon any or all technical data furnished in response to the request for technical data.

7. If the technical data furnished by the Government will be used for commercial manufacturing or other profit potential, a license for such use may be necessary. Any payments made in support of the request for data do not include or involve any license rights.

8. A copy of this notice shall be provided with any partial or complete reproduction of these data that are provided to qualified U.S. contractors.

DESTRUCTION NOTICE

For classified documents, follow the procedure in DoD 5220.22-M, National Industrial Security Program, Operating Manual, Chapter 5, Section 7, or DoD 5200.1-R, Information Security Program Regulation, Chapter 6, Section 7. For unclassified, limited documents, destroy by any method that will prevent disclosure of contents or reconstruction of the document.

AD NUMBER

AD864281

LIMITATION CHANGES

TO:

Approved for public release; distribution is unlimited.

FROM:

Distribution authorized to U.S. Gov't. agencies and their contractors; Critical Technology; DEC 1969. Other requests shall be referred to Army Aviation Materiel Laboratories, Fort Eustis, VA. This document contains export-controlled technical data.

AUTHORITY

USAAMRDL ltr, 23 Jun 1971

AD

USAAVLABS TECHNICAL REPORT 69-10A

ADVANCEMENT OF SMALL GAS TURBINE COMPONENT TECHNOLOGY, ADVANCED SMALL AXIAL COMPRESSOR

VOLUME I

ANALYSIS AND DESIGN

By

James V. Davis

December 1969

U. S. ARMY AVIATION MATERIEL LABORATORIES
FORT EUSTIS, VIRGINIA

CONTRACT DA 44-177-AMC-296(T)

CONTINENTAL AVIATION AND ENGINEERING CORPORATION

DETROIT, MICHIGAN

176

DISCLAIMER NOTICE

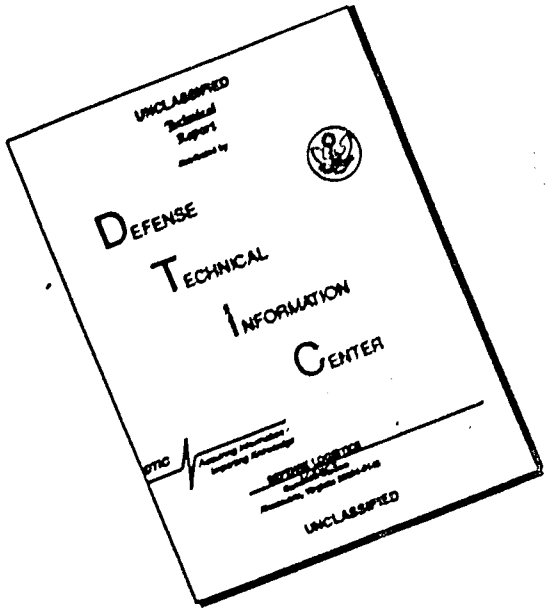

THIS DOCUMENT IS BEST QUALITY AVAILABLE. THE COPY FURNISHED TO DTIC CONTAINED A SIGNIFICANT NUMBER OF PAGES WHICH DO NOT REPRODUCE LEGIBLY.

BLANK PAGES
IN THIS
DOCUMENT
WERE NOT
FILMED

DISCLAIMERS

The findings in this report are not to be construed as an official Department of the Army position unless so designated by other authorized documents.

When Government drawings, specifications, or other data are used for any purpose other than in connection with a definitely related Government procurement operation, the United States Government thereby incurs no responsibility nor any obligation whatsoever; and the fact that the Government may have formulated, furnished, or in any way supplied the said drawings, specifications, or other data is not to be regarded by implication or otherwise as in any manner licensing the holder or any other person or corporation, or conveying any rights or permission, to manufacture, use, or sell any patented invention that may in any way be related thereto.

DISPOSITION INSTRUCTIONS

Destroy this report when no longer needed. Do not return it to the originator.

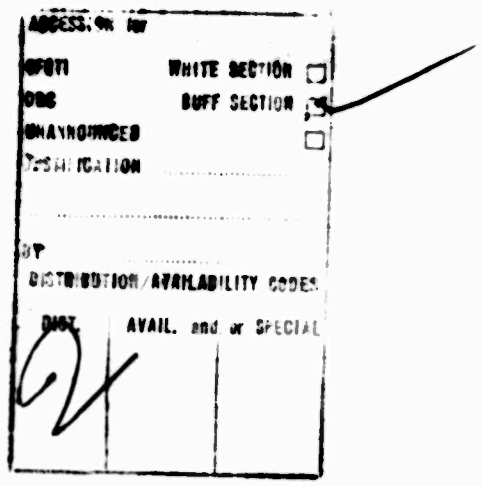

DEPARTMENT OF THE ARMY
U.S. ARMY AVIATION MATERIEL LABORATORIES
FORT EUSTIS, VIRGINIA 23604

The research described herein, which was conducted by Continental Aviation and Engineering Corporation, was performed under U.S. Army Contract DA 44-177-AMC-296(T). The work was performed under the technical management of Mr. David B. Cale, Propulsion Division, U.S. Army Aviation Materiel Laboratories.

Appropriate technical personnel of this Command have reviewed this report and concur with the conclusions contained herein.

The findings and recommendations outlined herein were considered in planning the subsequent phases of the program.

The aerodynamic design portion of this report is published as a classified addendum under separate cover.

Task 1G162203D14413
Contract DA 44-177-AMC-296(T)
USAAVLABS Technical Report 69-10A
December 1969

ADVANCEMENT OF SMALL GAS TURBINE COMPONENT TECHNOLOGY, ADVANCED SMALL AXIAL COMPRESSOR

VOLUME I
ANALYSIS AND DESIGN

Continental Report No. 1033

By

James V. Davis

Prepared By

Continental Aviation and Engineering Corporation
Detroit, Michigan

for

U. S. ARMY AVIATION MATERIEL LABORATORIES
FORT EUSTIS, VIRGINIA

SUMMARY

This report deals with the preliminary design and analysis of an advanced axial-centrifugal compressor for small gas turbines, and with the detail design of the axial stages.

The purposes are to advance and demonstrate efficient high pressure ratio axial compressor technology to the level where, when matched analytically with both the advanced centrifugal compressor technology supplied by U. S. Army Aviation Materiel Laboratories (USAAVLABS) and the conventional engine component characteristics, a potential for a 0.460-pound-per-horsepower-hour specific fuel consumption (SFC) turboshaft engine at 2500°F turbine inlet gas temperature shall be provided.

A cursory design study of the gas generator involving the preliminary design and analysis of a family of axial compressors was conducted. Each axial compressor was designed to be capable of match with the USAAVLABS advanced centrifugal technology. The minimum overall axial-centrifugal design pressure ratio for each compressor configuration was 16:1. The engine performance using the characteristics of the compressor designs was evaluated and an optimum gas generator configuration was selected.

The axial compressor for the optimum gas generator configuration was detail designed for test rig evaluation. This axial compressor has two stages and a 3.0:1 design pressure ratio. The design flow rate is 5.0 pound-per-second and the inlet tip radius is 2.72 inches.

FOREWORD

This report, prepared by Continental Aviation and Engineering Corporation, presents Phase I of a three-phase small axial compressor program for the advancement of small gas turbine component technology.

The program was sponsored by the United States Army Aviation Materiel Laboratories under Contract DA 44-177-AMC-296(T), Task 1G162203 D14413.

Phase I presents a study of a family of advanced axial compressors. It is reported as Volume I with an addendum under a separate cover. The addendum is the analysis and design.

Phases II and III are presented in Volume II. Phase II presents the axial compressor fabrication and test. Phase III presents the axial compressor redesign, fabrication, and test.

TABLE OF CONTENTS

LIST OF ILLUSTRATIONS

LIST OF ILLUSTRATIONS (CONTINUED)

LIST OF ILLUSTRATIONS (CONTINUED)

LIST OF ILLUSTRATIONS (CONTINUED)

LIST OF ILLUSTRATIONS (CONTINUED)

LIST OF TABLES

LIST OF TABLES (CONTINUED)

INTRODUCTION

This report presents the work accomplished in Phase I of Contract DA 44-177-AMC-296(T) for the United States Army Aviation Materiel Laboratories, Fort Eustis, Virginia.

The project objectives are to advance and demonstrate efficient high pressure ratio axial compressor technology to the level where, when matched analytically with the advanced centrifugal compressor technology supplied by USAAVLABS and the conventional engine component characteristics, a potential for a 0.460-pound-per-horsepower-hour SFC turboshaft engine at 2500°F turbine inlet gas temperature shall be provided.

The Phase I objectives are to select and design the optimum advanced axial compressor for a 0.460-pound-per-horsepower-hour SFC turboshaft engine at 2500°F turbine inlet gas temperature. The advanced axial compressor performance objectives are:

1. At least 16:1 overall design pressure ratio in analytical combination with the advanced centrifugal technology.

2. Axial compressor pressure ratio not less than 2.5:1.

3. Capability of operation at all required engine speeds, permitting engine acceleration in a reasonable time interval.

4. Five-pound-per-second airflow.

5. Not more than two stages.

The work included a cursory design of a gas generator and an aerodynamic and mechanical design of an advanced two-stage axial compressor.

The cusory design of the gas generator involved the preliminary design and analysis of a family of advanced axial compressors capable of being matched with the USAAVLABS advanced centrifugal technology. Eight cursory compressor designs were completed, flow paths were constructed, and overall engine performance was estimated. For each compressor design, engine flow path drawings were constructed.

From the analysis, the four candidate engines embodying the best engine performance were selected. Each of the four candidate engines was further assessed for configuration compactness and complexity, part-power fuel consumption and flow range, and the need for variable componentry. The optimum engine and compressor configuration was then determined from the four candidates.

A complete aerodynamic and mechanical design was prepared for the optimum axial compressor. The optimum axial compressor consists of two transonic stages and has a 0.494 inlet hub/tip ratio. The design aerodynamic performance is 3.0:1 pressure ratio and 82.3 percent efficiency at 1415-foot-per-second tip speed.

CURSORY DESIGN OF GAS GENERATOR

PRELIMINARY AERODYNAMIC DESIGN OF COMPRESSOR CONFIGURATIONS

Axial Pressure Range

Since the axial compressor configurations are required to match with the USAAVLABS centrifugal compressor technology, a preparatory study was conducted to determine the range of axial pressure ratio that would both match the centrifugal technology and obtain the required overall engine performance.

Both two-stage and single-stage axial compressors with pressure ratios less than 2.8:1 were eliminated from the cursory design study as follows:

1. The single-stage compressors with pressure ratios below 2.8:1 were eliminated because the relative low efficiencies predicted for this type of compressor in this pressure ratio level prevent the axial centrifugal compressor combination from obtaining the target overall 16:1 pressure ratio. Figure 1 shows this effect. The predicted axial efficiency for a 2.8:1 pressure ratio single-stage axial compressor is 78 percent. Note in Figure 1 that the combined axial-centrifugal compressor pressure ratio for this 2.8:1 pressure ratio axial compressor is barely 16:1, and that lower single-stage axial pressure ratios would result in combined axial-centrifugal pressure ratios lower than 16:1.

2. The two-stage transonic compressors with pressure ratios lower than 2.8:1 were eliminated because the lower pressure ratio compressors do not represent a significant advance in two-stage axial compressor technology. Continental's family of two-stage compressors includes two transonic axial compressors in the 2.5:1 pressure ratio range.

An upper limit of 3.1:1 axial pressure ratio was used for the cursory design study and is described as follows:

1. Above this pressure ratio level, the supersonic compressors exhibit low predicted efficiencies, so that the target brake specific fuel consumption (BSFC) is not obtained when the

axial-centrifugal compressor performance is integrated into an engine performance analysis. The predicted efficiency for a 3.1:1 single-stage axial compressor is 76.5 percent. Note in Figure 1 that the BSFC for this axial-centrifugal-engine combination is close to 0.47. Above 3.1:1 axial pressure ratio, the rotor and stator shock losses increase rapidly and decrease the axial compressor efficiency so that the BSFC for the axial-centrifugal-engine combination is higher than the target value of 0.47.

2. The 3.1:1 axial pressure ratio limit was also applied to the transonic axial compressors for the cursory design study. As shown in Figure 1, the predicted efficiency for the 3.1:1 pressure ratio transonic compressor (82.5 percent) is high enough so that the axial-centrifugal pressure ratio is nearly 17.3:1 and the engine BSFC is close to 0.45. Both of these values are high enough to exceed the targets for 16:1 axial-centrifugal pressure ratio and the 0.47 BSFC.

Axial Compressor Design Method

Eight axial flow compressors were designed to the extent of generating velocity triangles within the pressure ratio range determined. The predicted aerodynamic design points of these compressors are shown in Table I.

TABLE I
AXIAL COMPRESSOR DESIGN POINT TABLE

Spool	Axial Stage	Axial Pressure Ratio	Axial Efficiency	Axial Tip Speed, Feet per Second
1	1	2.8	0.780	1500
1	1	3.1	0.765	1560
1	2	2.8	0.840	1350
1	2	3.1	0.825	1420
2	1	2.8	0.780	1500
2	1	3.1	0.765	1560
2	2	2.8	0.840	1350
2	2	3.1	0.825	1420

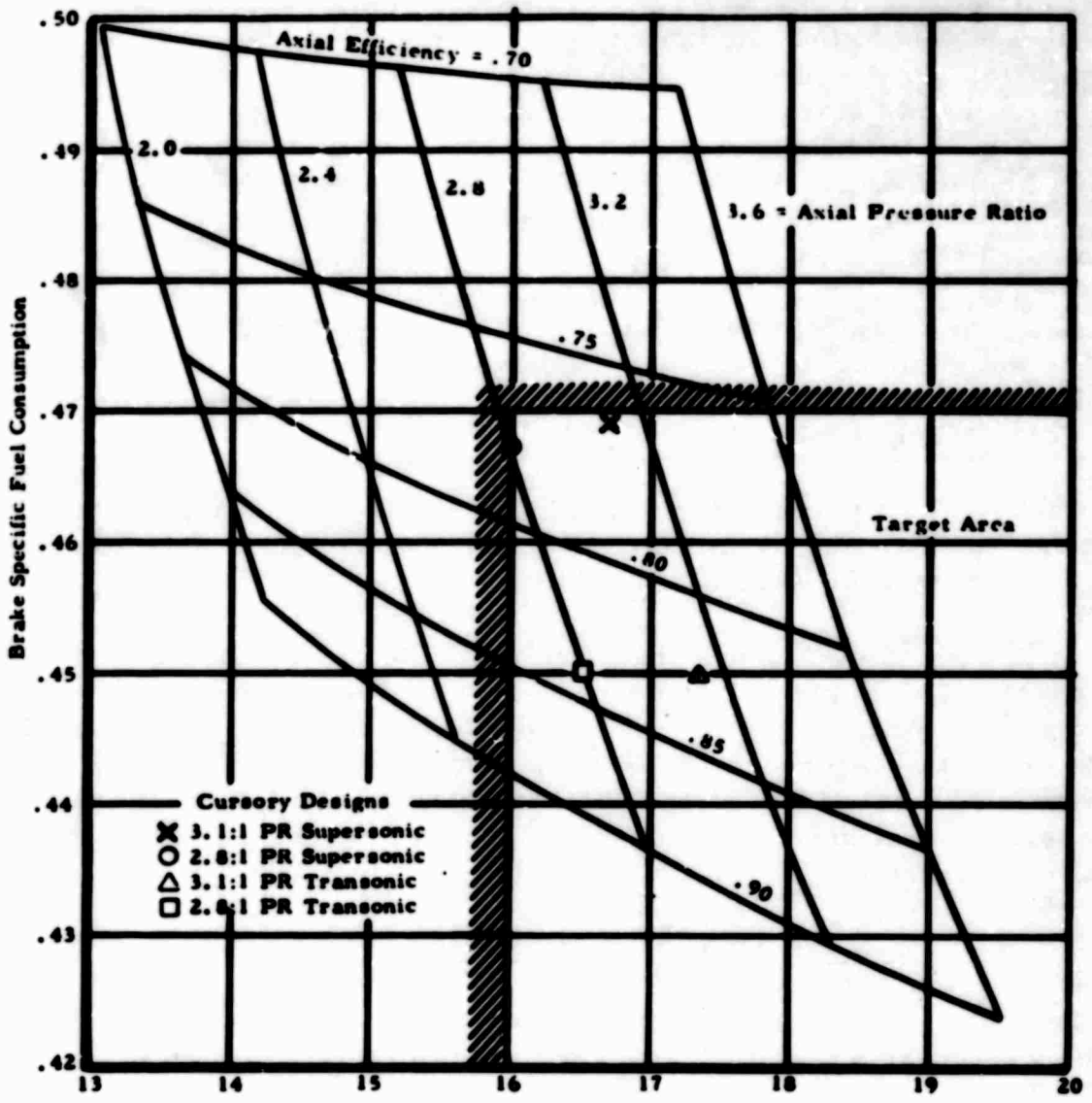

Figure 1. The Effect of Overall Axial-Centrifugal Compressor Pressure Ratio and Axial Compressor Performance on Brake Specific Fuel Consumption.

Single-Stage Supersonic Axial Compressors. The performance of the single-stage axial compressors was predicted by a detailed study involving rotor and stator Mach number levels and tip speed. A similar preliminary study was performed during the proposal stage of this contract. For the 2.8:1 pressure ratio single-stage axial compressor, the detailed study indicated nearly a constant single-stage axial efficiency for tip speeds from 1400 to 1500 feet per second. Below 1400 feet per second, stator shock losses become excessive and decrease stage efficiency. Conversely, above 1500 feet per second, rotor shock losses become excessive and decrease stage efficiency. Between 1400 and 1500 feet per second, the stator and rotor shock losses vary in such a manner as to maintain nearly constant stage efficiency.

The relatively high value of tip speed (1500 feet per second) was selected because it offered the lowest rotor diffusion, lowest rotor turning, and lowest stator Mach numbers all with a reasonable inlet relative rotor Mach number.

The tip speed for the 3.1:1 pressure ratio single-stage compressor was calculated similarly to tip speed for the 2.8:1 pressure ratio single-stage compressor.

Predicted 2.8:1 pressure ratio supersonic axial performance is presented in Figure 2. This compressor map is also used as a basis for the 3.1:1 pressure ratio supersonic axial compressor. Since the pressure ratio difference between the two designs is relatively small, conventional scale factors are used to obtain the 3.1:1 pressure ratio supersonic axial performance from the 2.8:1 pressure ratio supersonic axial performance.

Two-Stage Transonic Axial Compressors. The performance of the transonic compressors was calculated by utilizing proven Continental transonic axial compressor design techniques. Rotor tip speed was selected to limit rotor diffusion to acceptable values.

Predicted transonic axial compressor performance for the 2.8:1 pressure ratio design is presented in Figure 3. This compressor map is also used as a basis for the 3.1:1 pressure ratio transonic axial compressor, similar to the two different pressure ratio level supersonic compressor maps.

Single- and Twin-Spool Compressors. As noted in Table I, the axial compressor efficiency for similar pressure ratio levels and stages is the same for both twin- and single-spool configurations. Actually, the single-spool axial efficiency should be somewhat lower than the twin-

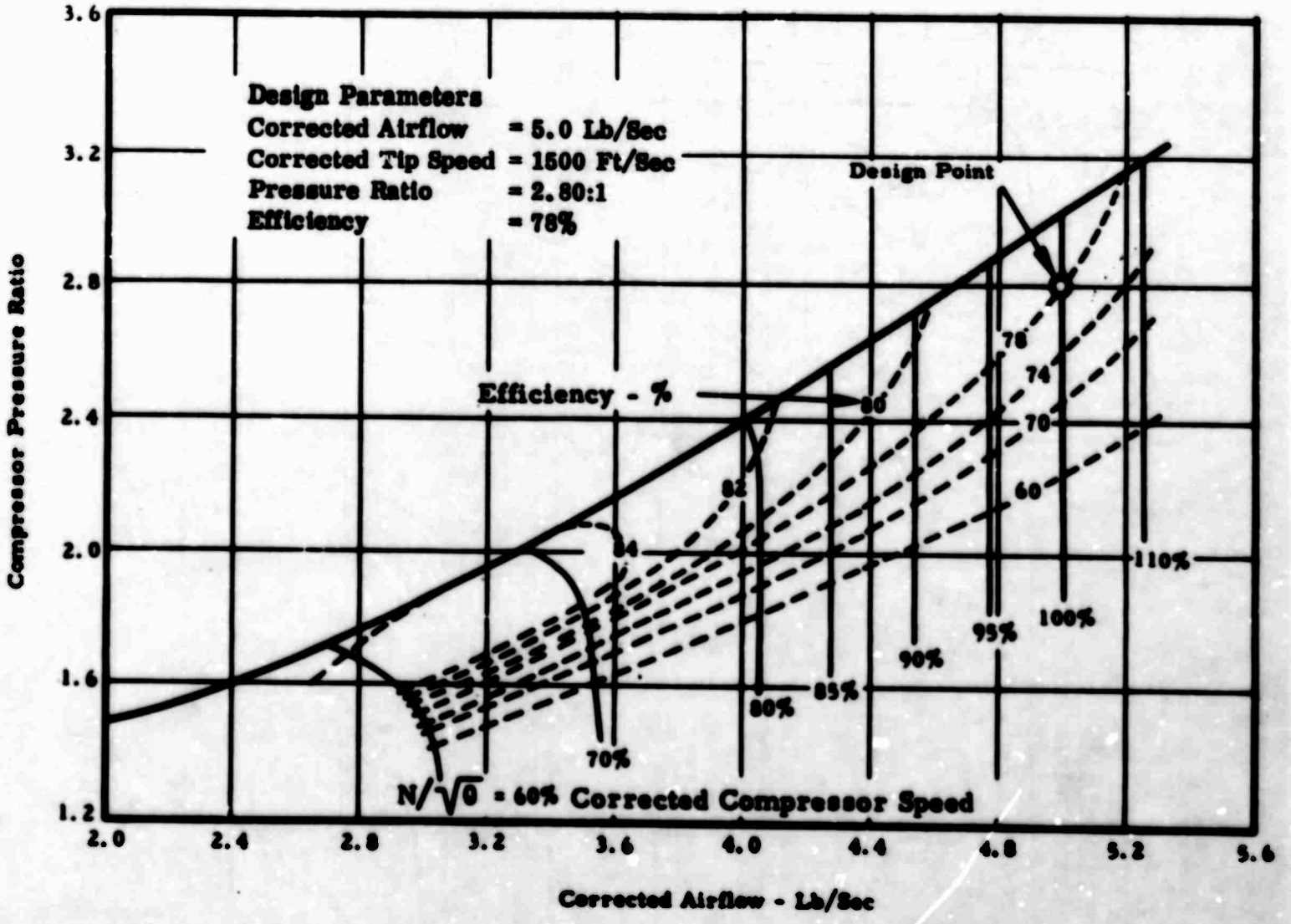

Figure 2. Estimated Performance Map for Single-Stage Supersonic Compressor.

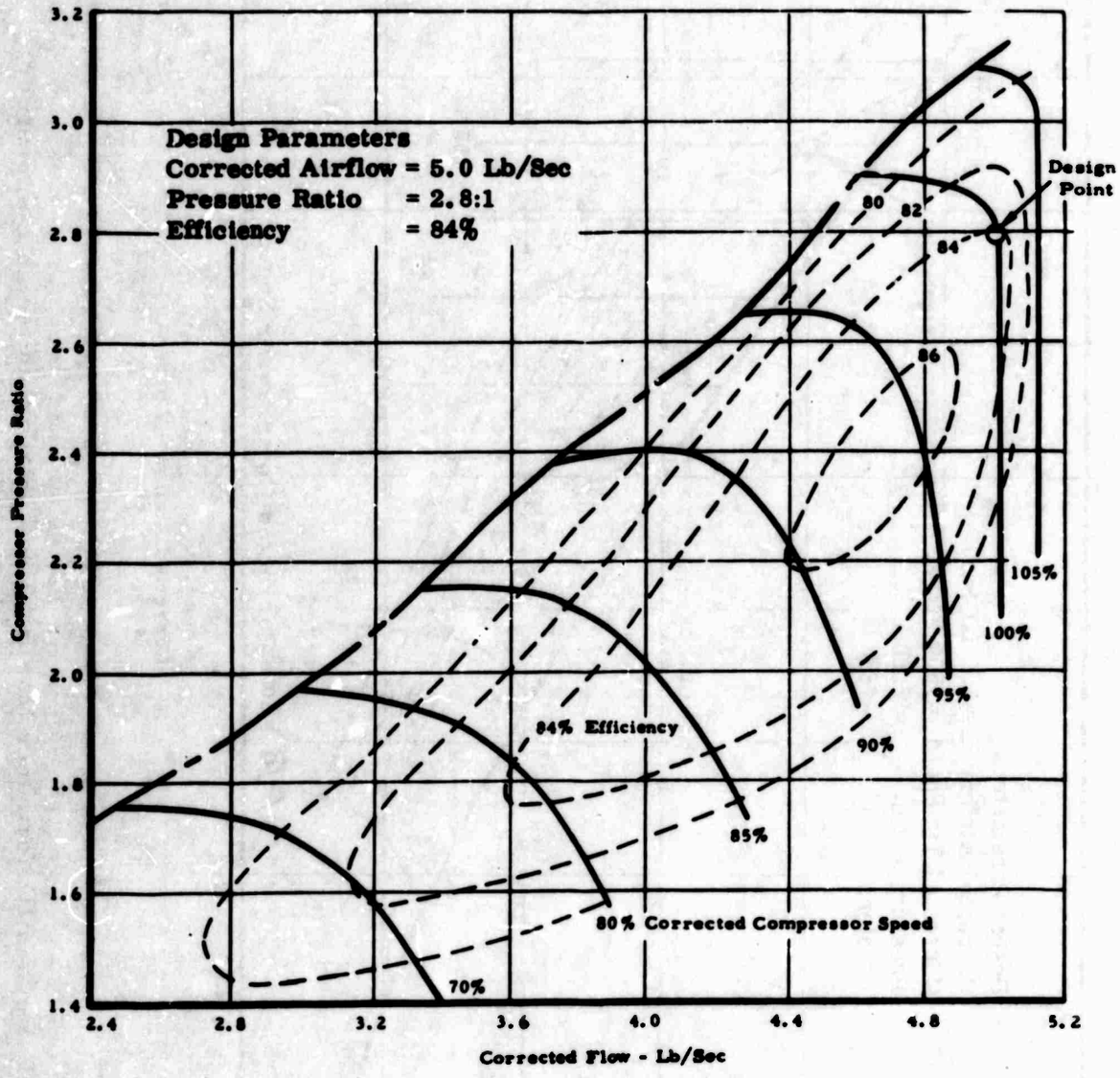

Figure 3. Estimated Performance Map for Two-Stage Transonic Compressor.

spool efficiency, if the differences in transition duct losses are taken into account and are included in the efficiency calculations. However, the efficiency differences are small enough to be neglected in the cursory gas generator design study.

Transition Duct Design. A method was devised to provide a consistent transition duct length comparison between the eight axial centrifugal compressor configurations. A radius of curvature for the hub of all 16 transition ducts was selected from previous test data and experience. This value of radius of curvature was held constant for all configurations.

Thus, for large hub radii differences between the axial exit and the centrifugal inlet, relatively long transition duct lengths were calculated, and vice versa. The transition duct shrouds were designed to provide a constant area passage between the axial exit and the centrifugal inlet.

Analysis of Compressor Designs

Aerodynamic Parameters. Table II summarizes each of the eight designs, and Figures 4 through 11 present each axial compressor flow path with two transition ducts. The shorter transition duct matches into the USAAVLABS radial flow centrifugal impeller (RFI) and the longer transition duct matches into the mixed flow impeller (MFI). A difference in transition duct length is necessary to accommodate the difference in inlet hub-tip ratio between the two centrifugal compressors. Notice that for a given axial-transition duct configuration, the RFI centrifugal compressor presents a more compact geometric form.

The axial rotor tip relative Mach number and air turning angles are listed in the aerodynamic section of Table II along with the axial compressor aerodynamic performance confidence level. The confidence level of the transonic axial compressors is rated as good, and the level of the supersonic axial compressors is rated as fair. This rating is based on the relationship between the tip Mach number and the tip air turning. The transonic axial compressors have relatively low to medium tip Mach numbers and low values of tip air turning, while the supersonic axial compressors exhibit high tip Mach numbers and high values of tip air turning.

It is the combination of high tip Mach number with high air turning that necessitates the rating of fair for the aerodynamic performance confidence level of the supersonic axial compressors. It must be emphasized, however, that even though the transonic compressors are

TABLE II
AXIAL CENTRIFUGAL COMPRESSOR DESIGN COMPARISON

DEFINITION			PERFORMANCE			GEOMETRY			AERODYNAMICS		
Flow-Path Fig. No.	Spool	No. of Axial Stages	Axial Pressure Ratio	Axial Efficiency	Overall Axial Cent. Pressure Ratio	Engine BSFC	Axial Tip Radius (Inches)	Axial Inlet Hub-Tip Radius Ratio	Axial Comp. Length *(Inches)	Axial Comp. Aerodynamic Perf. Confidence Level	Axial Rotor Tip Relative Mach Number	Axial Rotor Tip Air Turning Angle
3a	1	1	2.8	0.780	16.0	0.466	3.762	0.776	6.97	Fair	1.503	35.9°
3b	1	1	3.1	0.765	16.7	0.467	3.828	0.797	6.77	Fair	1.582	37.4°
3c	1	2	2.8	0.840	16.5	0.449	3.345	0.712	5.87	Good	1.386	5.0°
3d	1	2	3.1	0.825	17.3	0.449	3.427	0.731	5.88	Good	1.450	5.1°
3e	2	1	2.8	0.780	16.0	0.466	3.170	0.666	6.58	Fair	1.506	35.2°
3f	2	1	3.1	0.765	16.7	0.467	2.91	0.605	6.18	Fair	1.580	38.2°
3g	2	2	2.8	0.840	16.5	0.449	2.720	0.500	5.71	Good	1.383	5.9°
3h	2	2	3.1	0.825	17.3	0.449	2.720	0.500	5.89	Good	1.442	5.7°

*Includes transition duct length for axial compressors matched with Boeing centrifugal RFI.

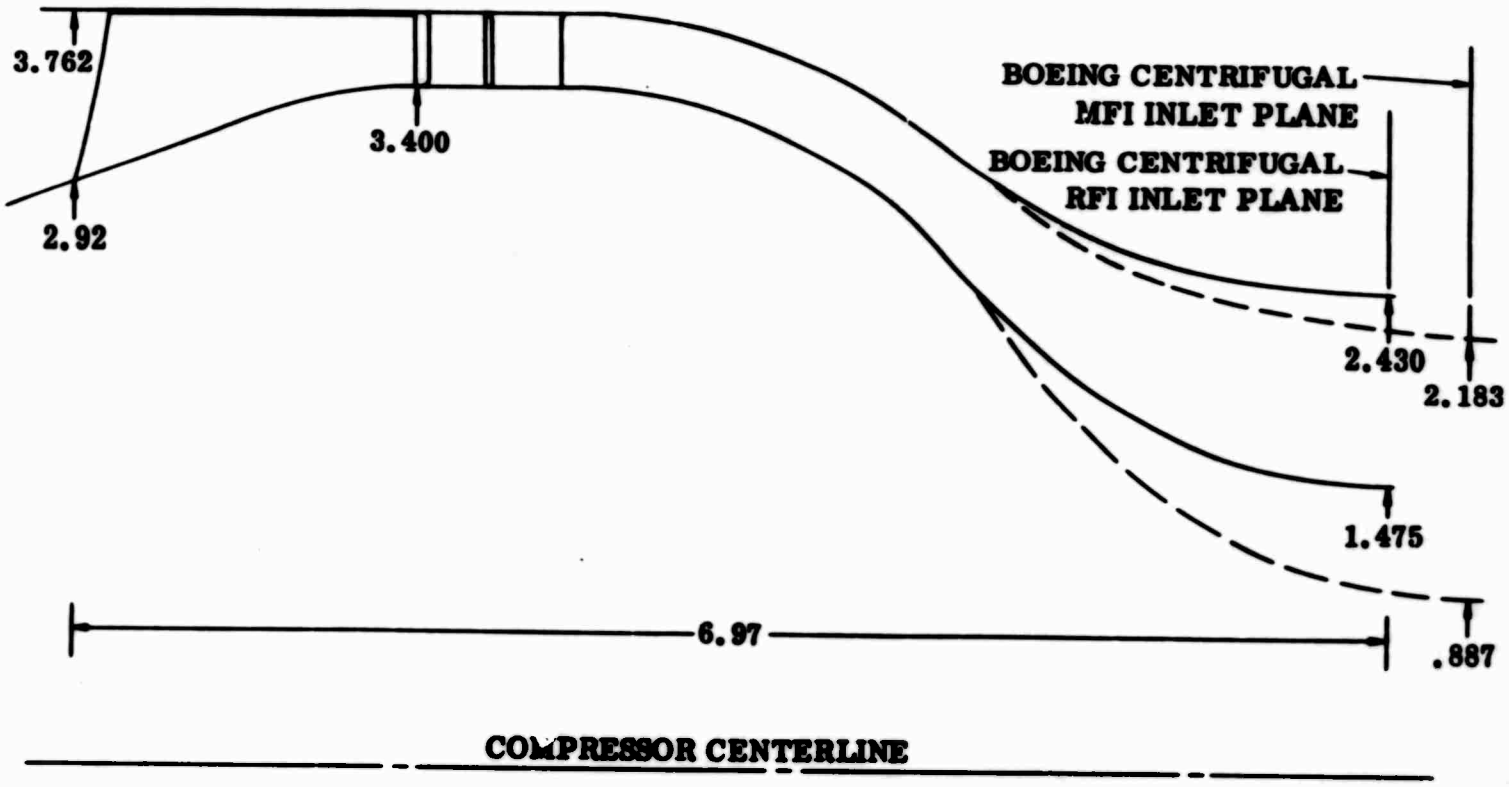

Figure 4. Preliminary Flow Path for Single-Spool Single-Stage Supersonic Compressor, Pressure Ratio = 2.8:1.

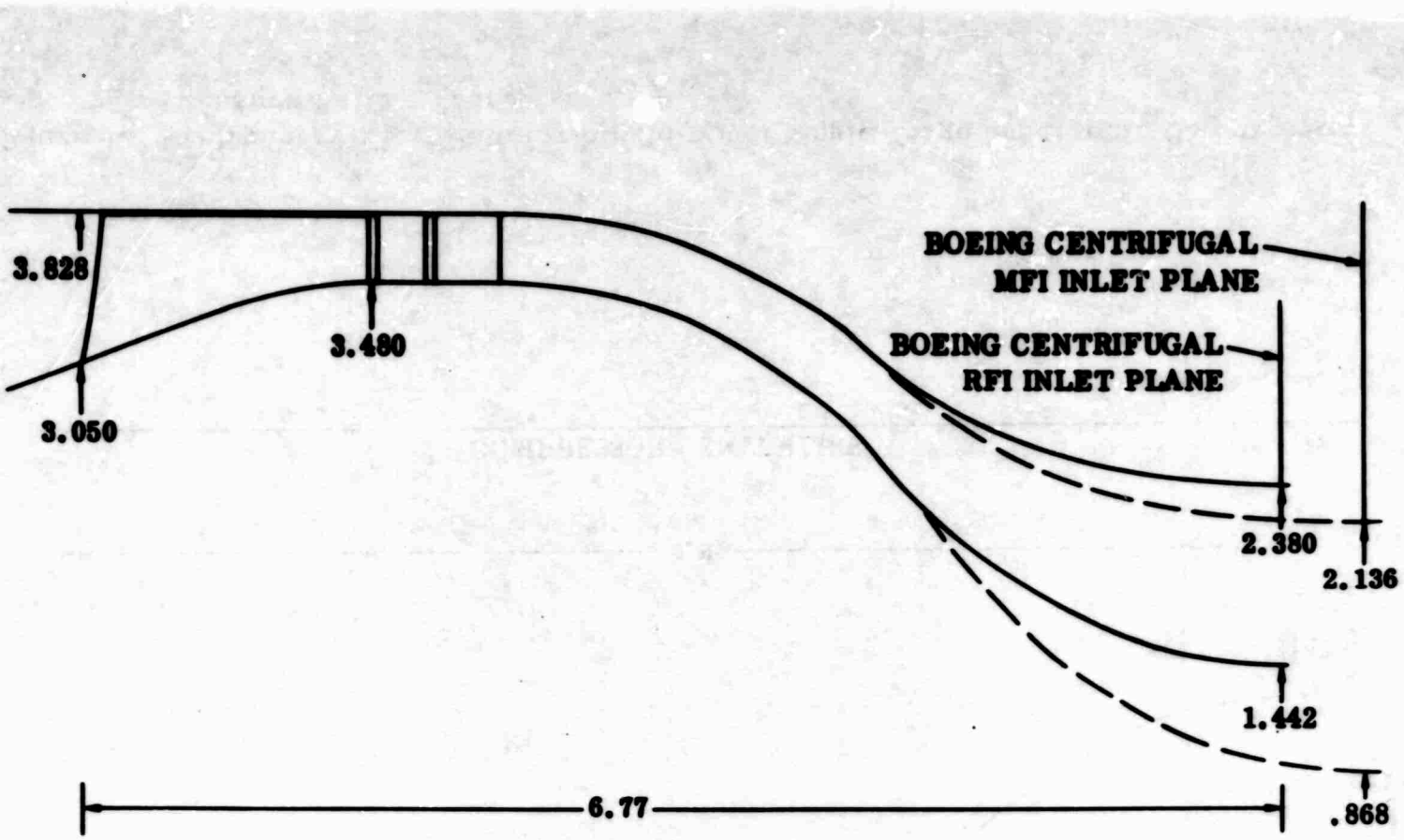

Figure 5. Preliminary Flow Path for Single-Spool Single-Stage Supersonic Compressor, Pressure Ratio = 3.1:1.

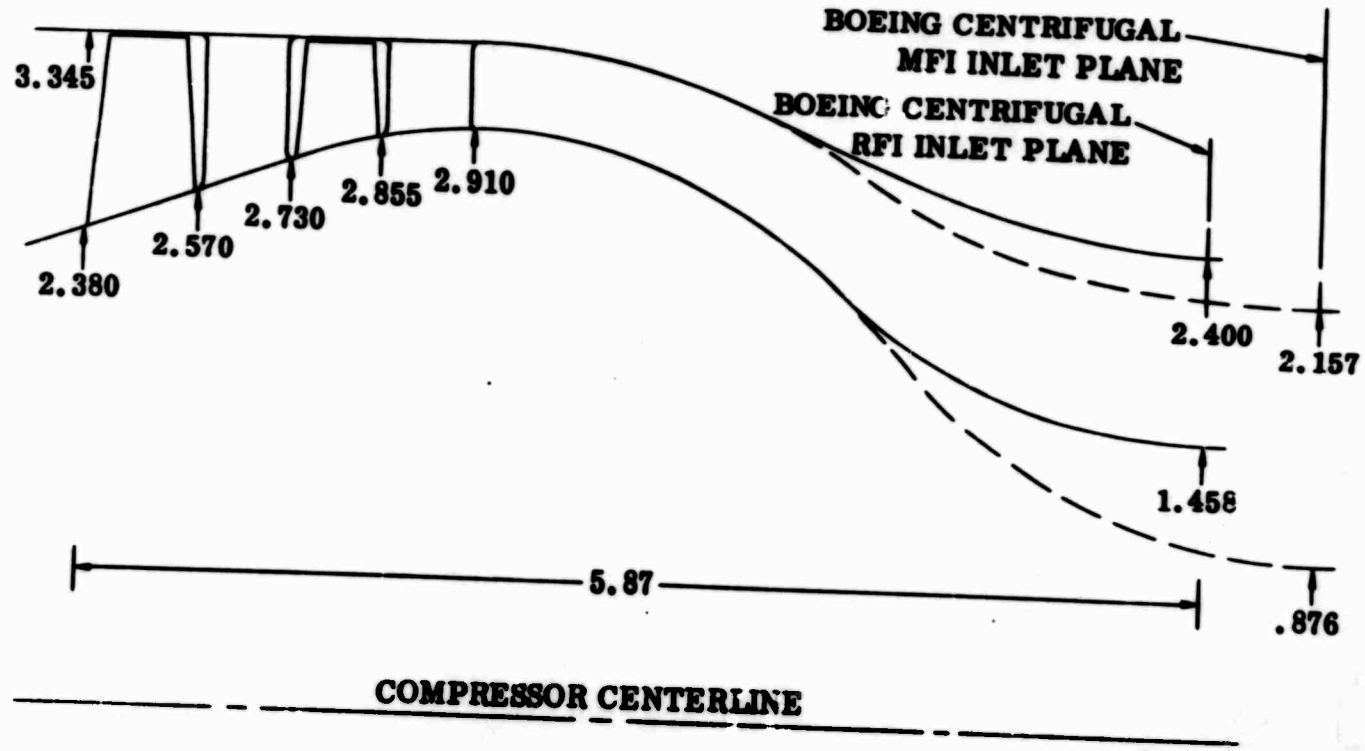

Figure 6. Preliminary Flow Path for Single-Spool Two-Stage Transonic Compressor, Pressure Ratio = 2.8:1.

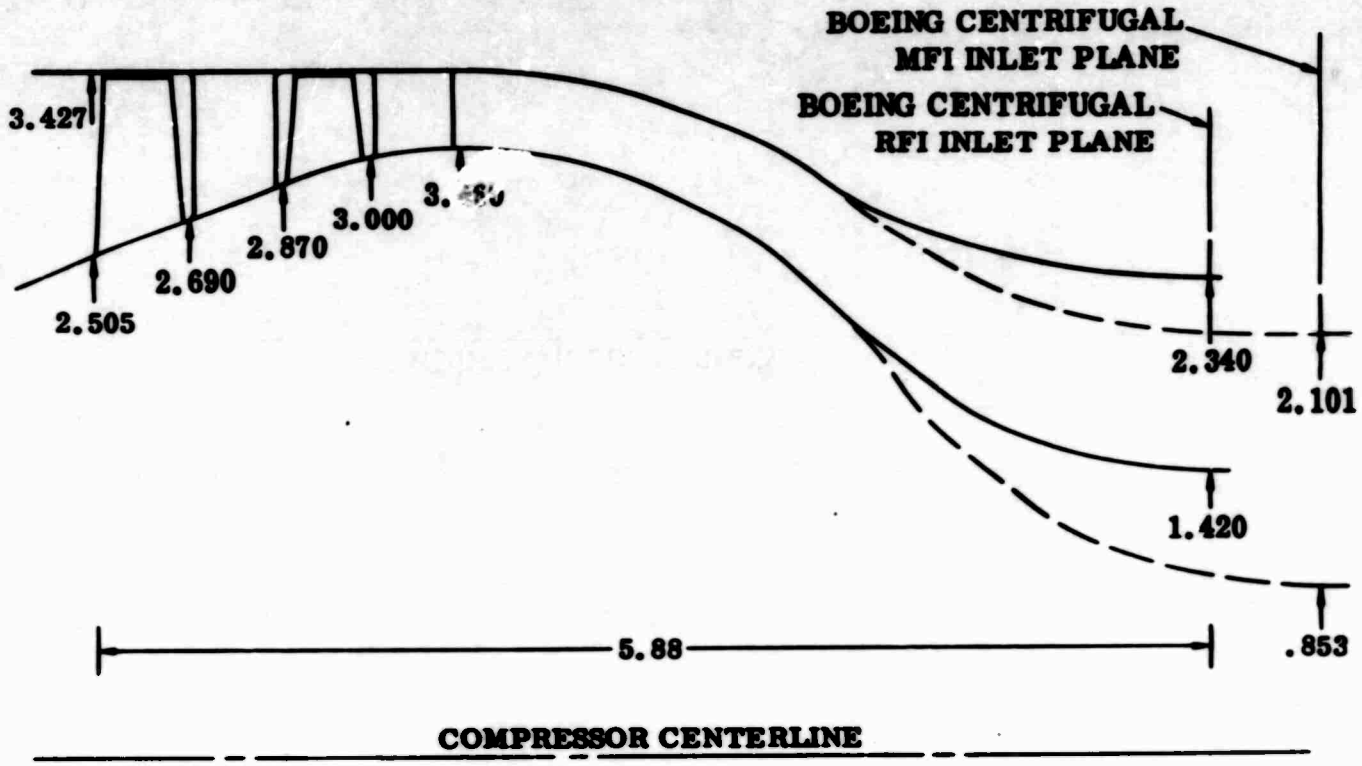

Figure 7. Preliminary Flow Path for Single-Spool Two-Stage Transonic Compressor, Pressure Ratio = 3.1:1.

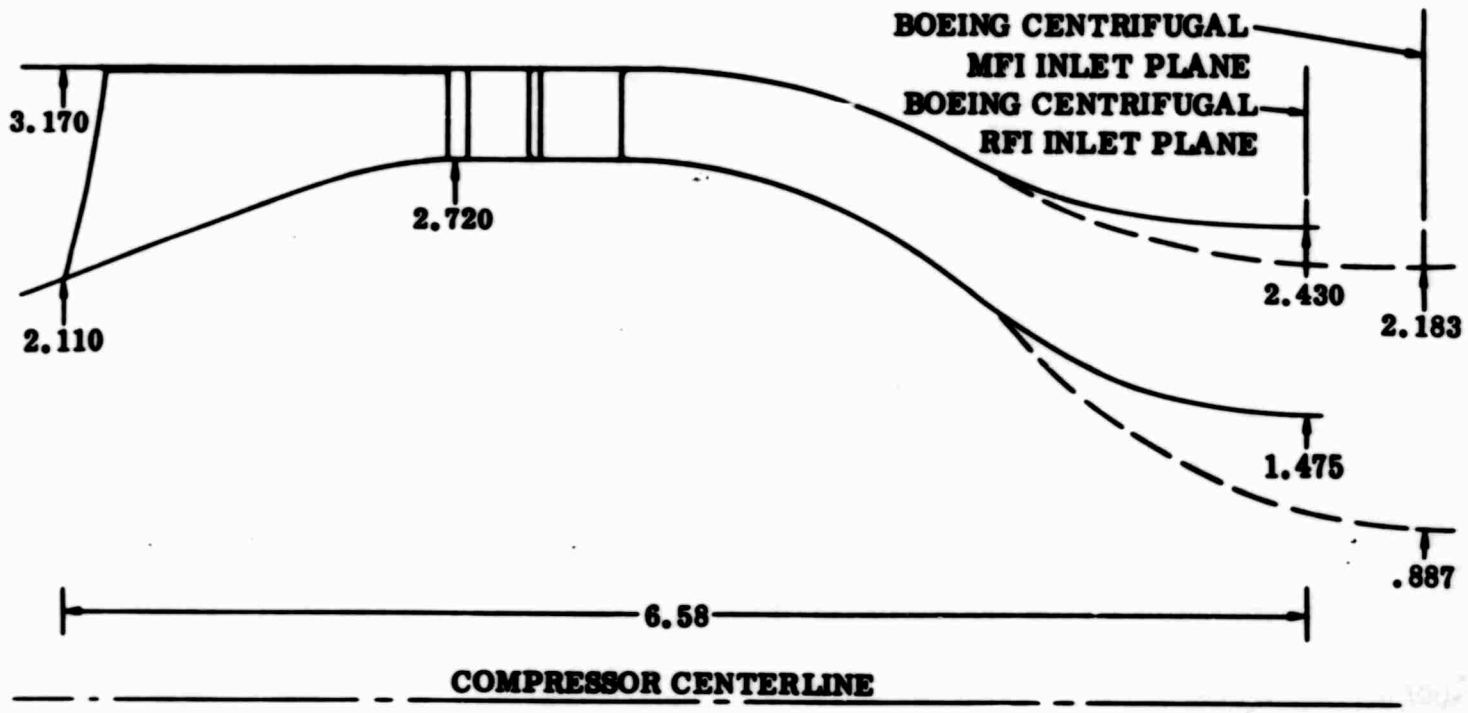

Figure 8. Preliminary Flow Path for Twin-Spool Two-Stage Supersonic Compressor, Pressure Ratio = 2.8:1.

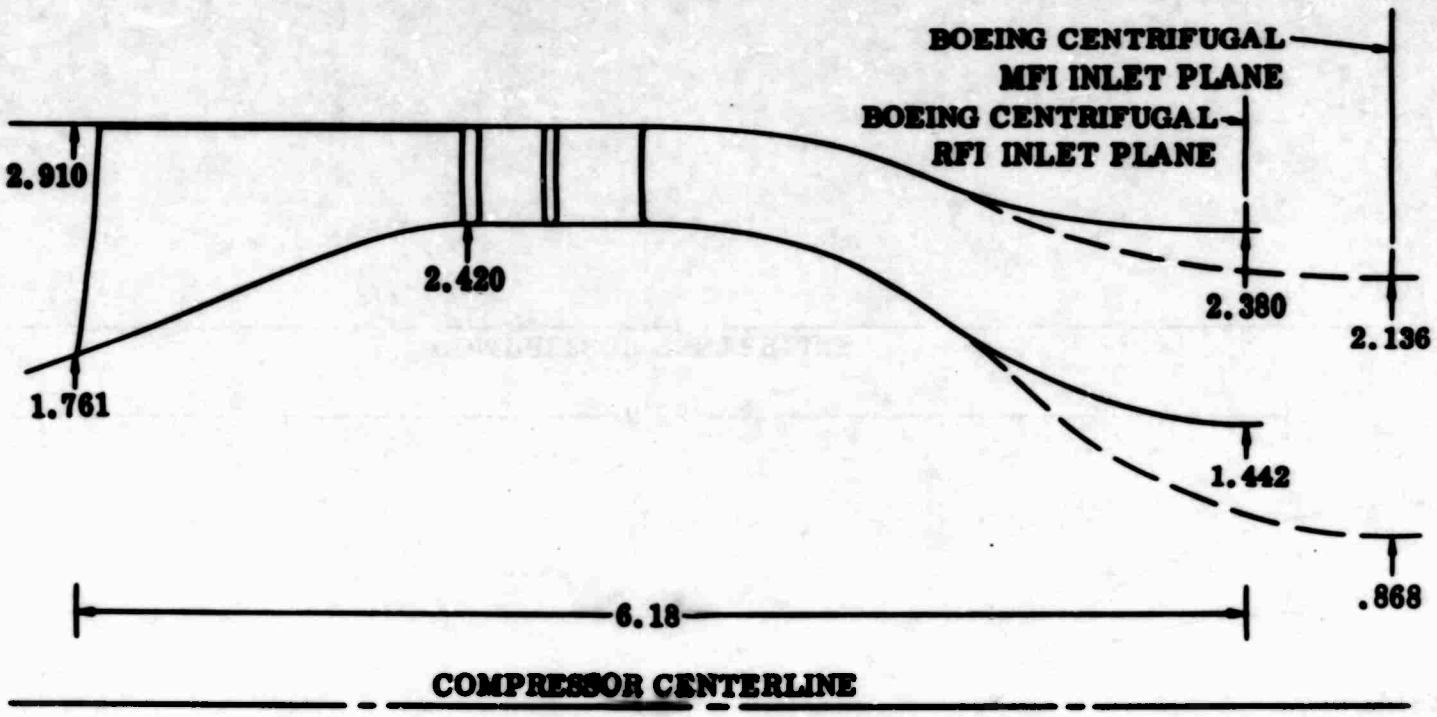

Figure 9. Preliminary Flow Path for Twin-Spool Single-Stage Supersonic Compressor, Pressure Ratio = 3.1:1.

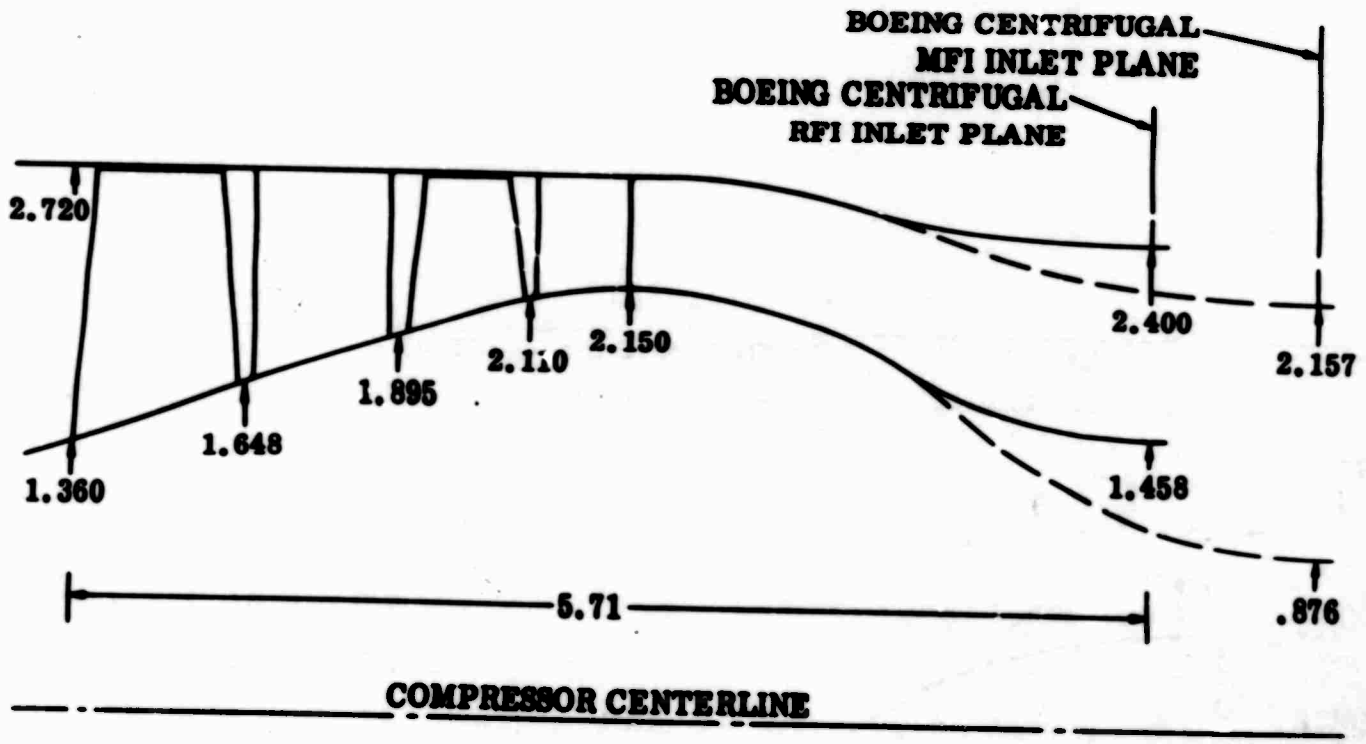

Figure 10. Preliminary Flow Path for Twin-Spool Two-Stage Transonic Compressor, Pressure Ratio = 2.8:1.

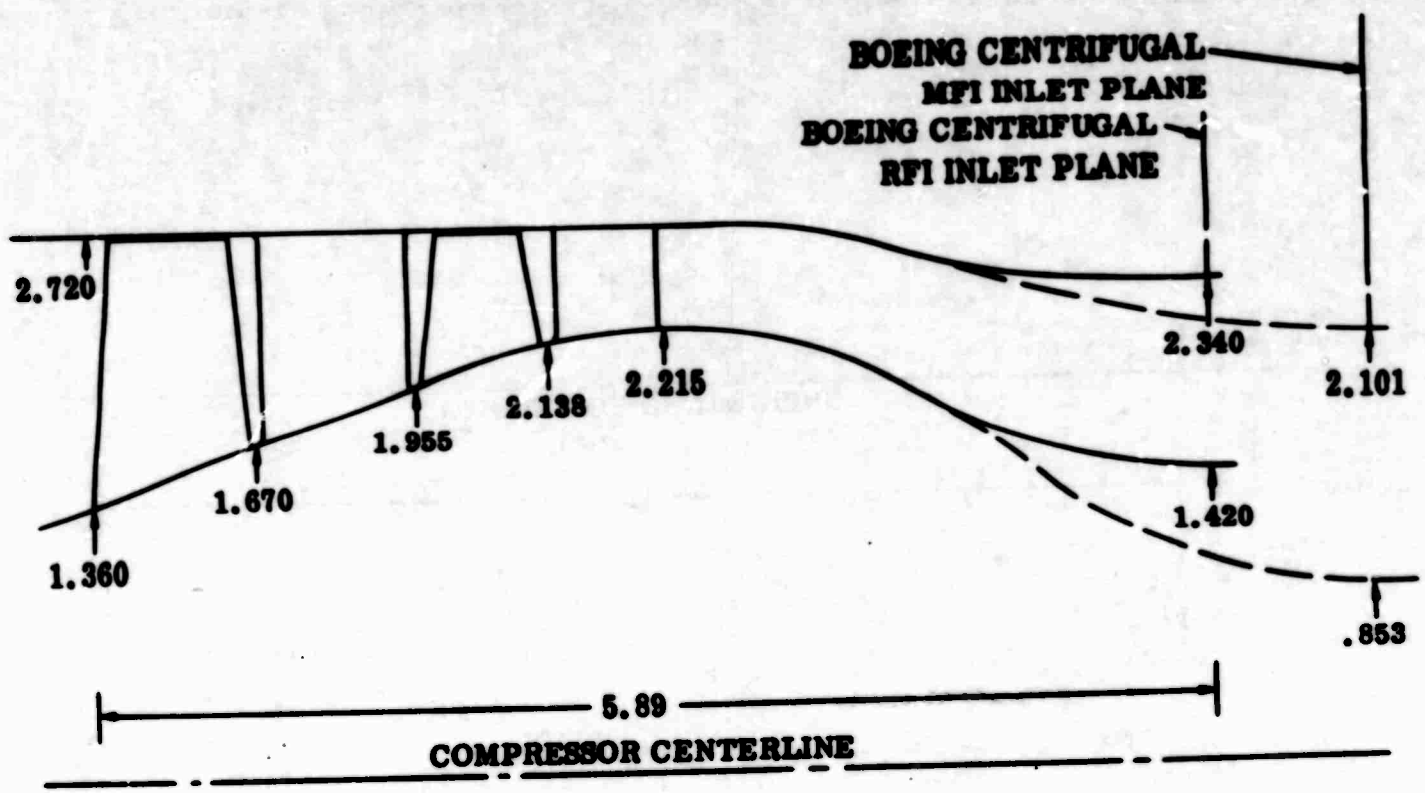

Figure 11. Preliminary Flow Path for Twin-Spool Two-Stage Transonic Compressor, Pressure Ratio = 3.1:1.

rated as good in aerodynamic performance confidence level, they do represent an equivalent advance in axial compressor technology, since the predicted performance is well above the actual test performance of any known existing two-stage axial compressor.

Geometric Configuration. A comparison of the axial compressor geometry and corresponding transition duct geometry is shown in Figures 4 through 11. It can be seen that the transonic axial compressors present a smaller geometric envelope for a given spool configuration than the supersonic axial compressors. For example, the single-spool, 2.8:1 pressure ratio transonic axial compressor (Figure 6) is 0.834 inch smaller in diameter and 1.10 inch shorter in length than the single-spool, 2.8:1 pressure ratio supersonic axial compressor (Figure 4).

The above length values include the RFI transition duct lengths. Based on outside-dimension volume, the volume of the transonic compressor is two-thirds the volume of the supersonic axial compressor. Thus, even though the supersonic axial compressor has one less stage than the transonic axial compressor, the supersonic compressor has a larger physical envelope than the transonic compressor. Actually, so far as blade row reduction is concerned, the transonic axial compressors have possibly only one more blade row than the supersonic axial compressors since the latter requires two stator rows (one to reduce the stator Mach numbers to a subsonic value and the other to turn the flow to the axial direction). The same type of comparison may be made with the compressors which produce a pressure ratio of 3.1:1.

The supersonic axial compressors require a larger envelope than the transonic axial compressors because of two factors. First, both single- and two-spool supersonic compressors require a high tip speed in order to achieve the desired pressure ratio in only one stage. For single-spool operation, the high tip speed necessitates a relatively high tip radius since the rotational speed is fixed by the centrifugal compressor. The high tip radius in turn requires a long transition duct configuration to match the inlet of the centrifugal compressor. For twin-spool operation, the high tip speed and the requirement of supersonic relative Mach numbers over the entire span of the inlet to the rotor necessitates a tip radius which is higher than that of a corresponding transonic axial compressor. Secondly, the high pressure ratio also requires a low rotor aspect ratio and therefore, a relatively long chord, as can be seen on the flow path drawings (Figures 4, 5, 8, and 9). This is confirmed by Continental's experience on the effect of aspect ratio on the flow range, pressure ratio level, and efficiency of axial compressors.

Engine Design Point Performance. As can be seen on Table II, the transonic axial-centrifugal configurations show nearly a 0.017 reduction in design point BSFC engine performance and a comparable higher overall axial-centrifugal pressure ratio. This performance difference is due to the relatively higher transonic compressor efficiencies.

PRELIMINARY FLOW PATH LAYOUTS OF GAS GENERATOR CONFIGURATIONS

The gas generator flow path layouts of the four candidate compressor configurations are presented on Figures 12 and 13.

The gas generator flow paths for the 2.8:1 and the 3.1:1 pressure ratio single-spool transonic axial compressors are presented on Figure 12, and those of the 2.8:1 and 3.1:1 pressure ratio twin-spool compressors are presented on Figure 13. As shown on the compressor flow paths in Figures 4 through 11, a very small geometric difference between transonic axial compressors is noticed for the two levels of design axial pressure ratio. For example, the difference in tip radius between the two single-spool transonic axial compressors is less than 0.1 inch. Thus, this difference is not noticed on the reduced flow path drawings.

It must be emphasized that even though discs, shafts, bearings, and combustors are shown, these items are included only to define possible problem areas associated with small high performance gas generators and to supplement the flow path drawings. Moreover, the design concepts shown for these items are cursory in nature.

The following accessories were not shown, as they were considered beyond the scope of the contractual requirements for the preliminary gas generator flow paths:

1. Oil pump
2. Fuel pump
3. Fuel control
4. Starting system
5. Power takeoff

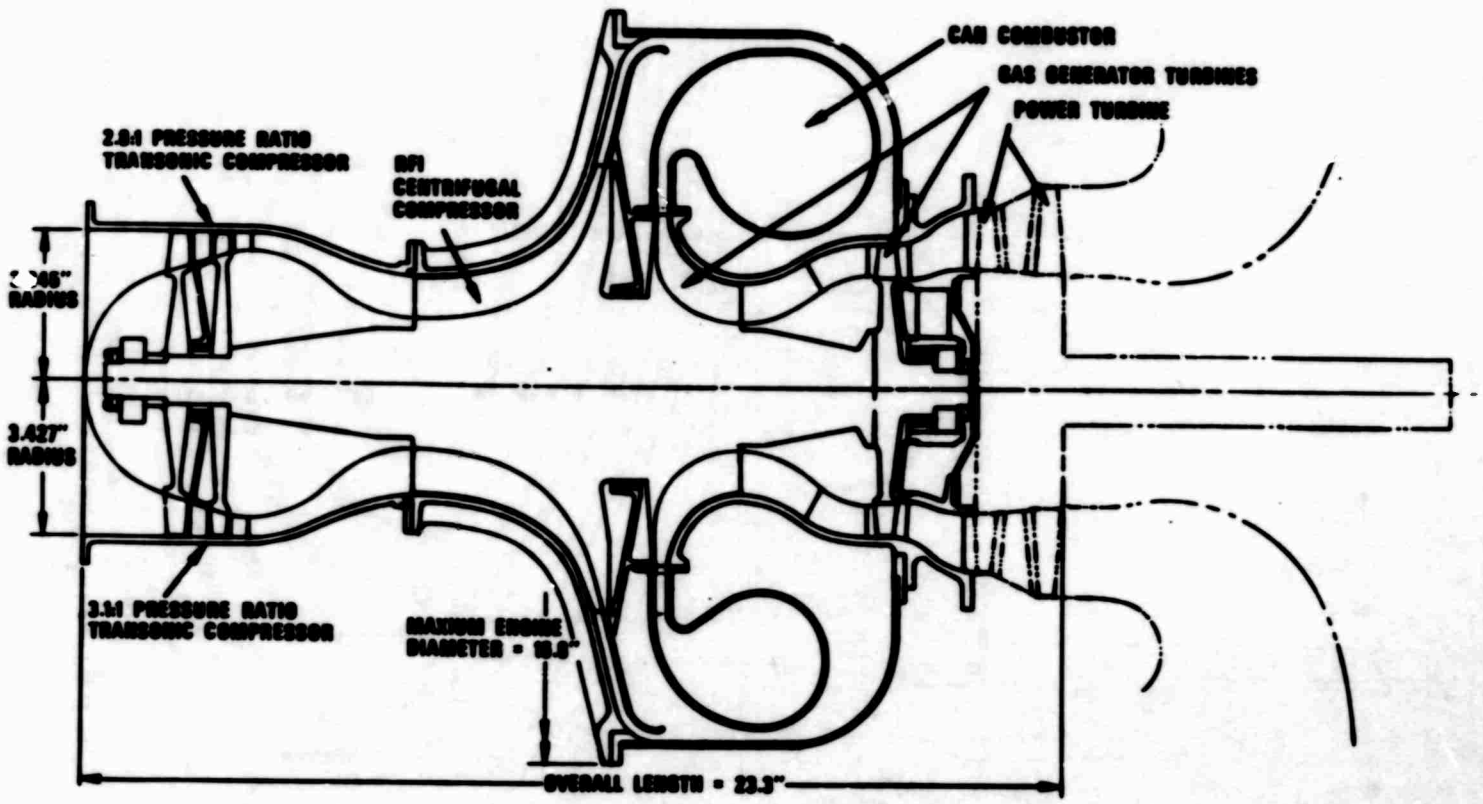

Figure 12. Single-Spool Free Shaft Power Turbine Gas Generator Flow Path - Two-Stage Transonic Axial Compressor.

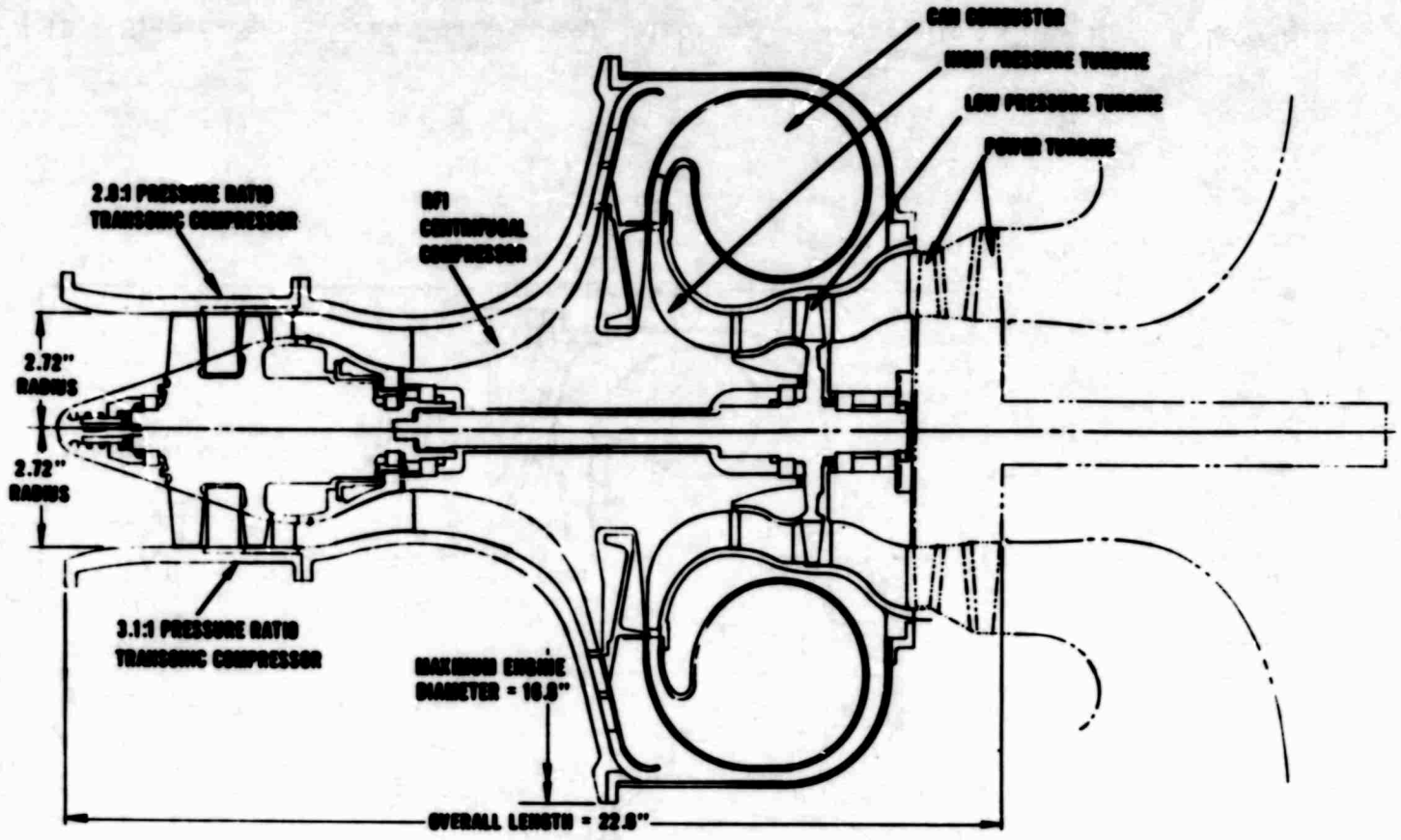

Figure 13. Twin-Spool Free Shaft Power Turbine Gas Generator Flow Path - Two-Stage Transonic Axial Compressor.

In addition, it is noted that some problem areas do exist (such as radial turbine cooling and engine thrust balancing of turbines and compressors) and that these areas were also considered beyond the scope of the contractual requirements.

The above accessories and problem areas may require modifications to the flow path when these items are considered for the gas generator. However, these modifications will be minor and will not affect the flow paths to a degree which will prevent the advanced compressor technology from being used.

The following discussion briefly summarizes the configurations, compactness, and complexity of the four candidate gas generator flow paths.

Compressors

A comparison between the single-spool transonic axial compressor configuration (Figure 12) and that of the twin spool (Figure 13) shows that the twin-spool axial compressors appear to be more rugged and compact. This is because the twin-spool version is free to operate at near optimum rpm for maximum weight flow per unit frontal area (W/A_f) and thus has larger blade heights and chords. The single-spool axials are literally tied to the specified centrifugal rpm and are thus required to operate at lower than optimum rpm for maximum W/A_f. Since the airflow is invariant, larger tip radii and therefore smaller blade heights result for the single-spool axials.

Because the twin-spool transonic axial compressors do appear more advanced (higher W/A_f) and rugged, a study was initiated to use the USAAVLABS centrifugal compressor technology to design a centrifugal compressor that would be adaptable to the twin-spool axial compressors in a single-spool mode of operation. This would allow an axial compressor designer to be free to select the most advanced axial compressor regardless of single-spool or twin spool variations. The study indicated that if the specific speed of either the USAAVLABS centrifugal compressor or the USAAVLABS radial outflow compressor were increased by about 25 percent, single-spool compatibility between the most advanced axial compressor and the above centrifugal compressor would result.

Figures 14 and 15 show the 2.8 pressure ratio single-stage supersonic compressors. These are shown for comparison purposes, as they have been eliminated because of inadequate performance. Notice that as far as geometric configuration is concerned, the twin-spool supersonic compressor (Figure 14) is much more compact than the single-spool

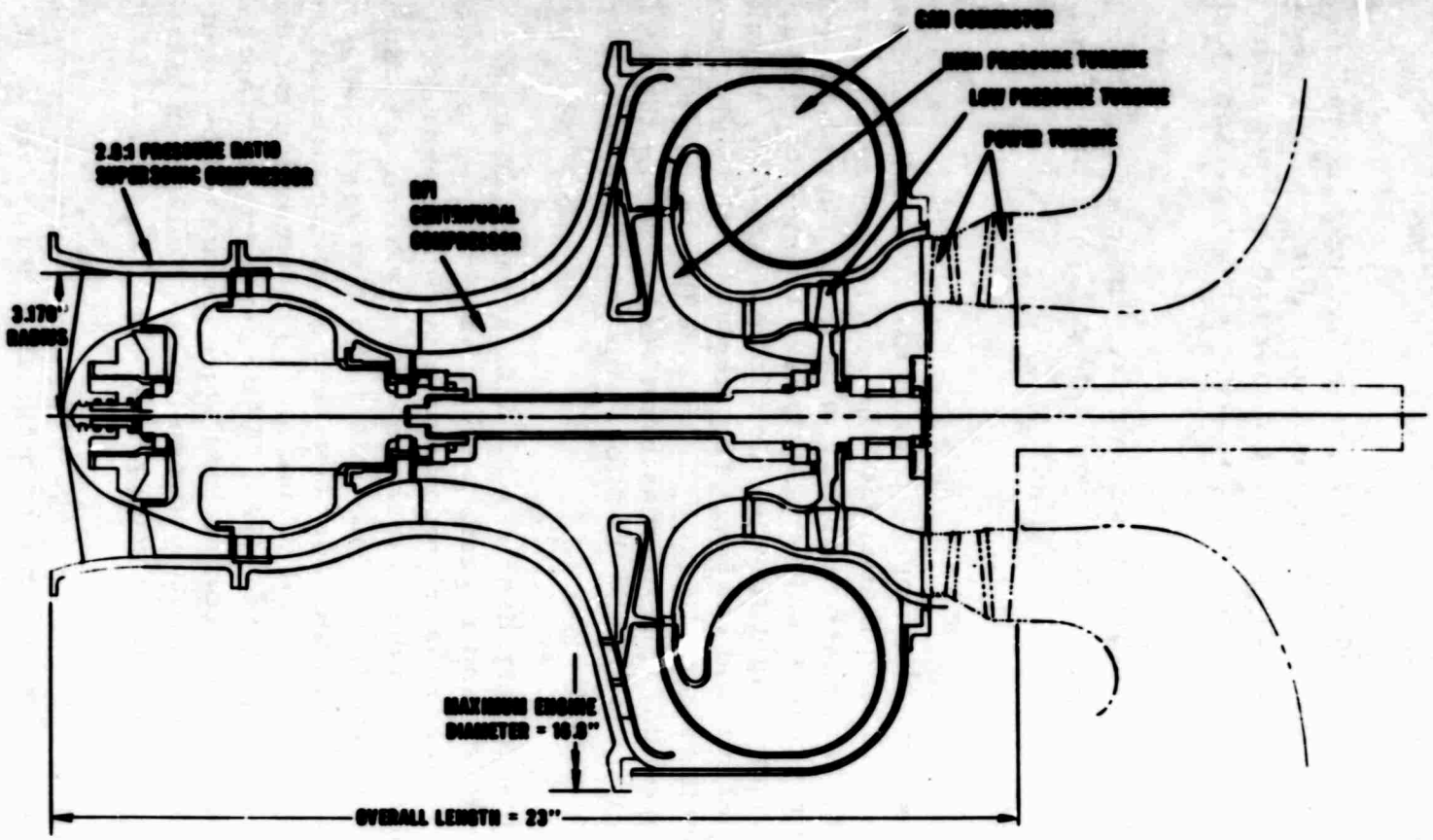

Figure 14. Twin-Spool Free Shaft Power Turbine Gas Generator Flow Path - Single-Stage Supersonic Axial Compressor.

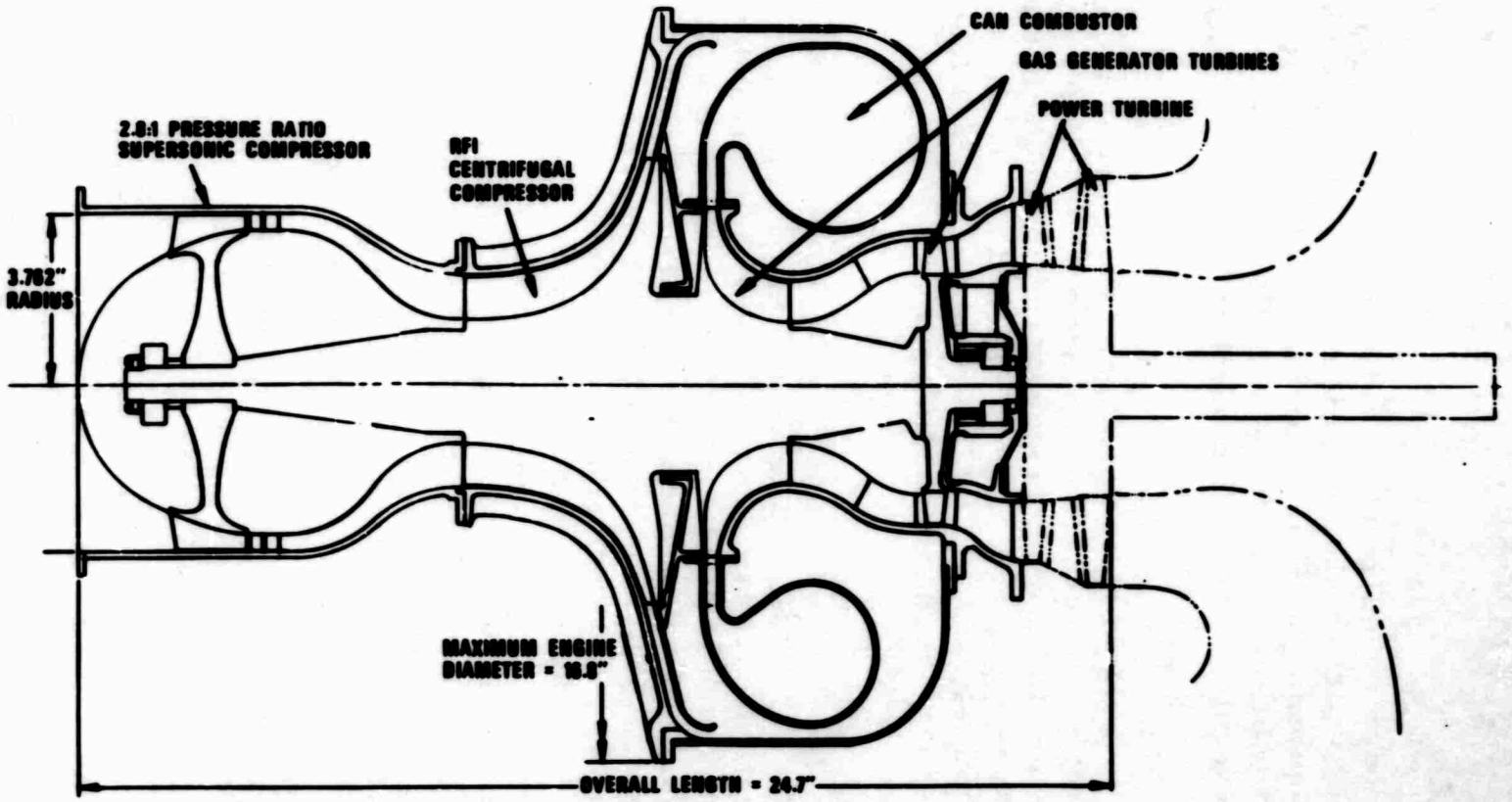

Figure 15. Single-Spool Free Shaft Power Turbine Gas Generator Flow Path - Single-Stage Supersonic Axial Compressor.

supersonic compressor (Figure 15). Again, this is because the single-spool supersonic axial rotor has to rotate at the same speed as the centrifugal rotor.

Combustor

A can combustor configuration was selected for the gas generators. This configuration, which is shown on Figures 12 and 13, is preliminary and has not been optimized. The combustor pressure drop from the centrifugal compressor diffuser exit to the radial turbine inlet nozzle is estimated at 4-1/2 percent. This value is identical to the cycle combustor pressure drop.

An annular combustor configuration, which would have a pressure drop of approximately 2 percent, was considered for this type of gas generator. However, the can combustor was preferred because it would have only one-fifth as much cooled metal exposed to the intense flame radiation (approximately 250,000 BTU per hour per square foot radiation heating) as the annular combustor configuration.

Turbines

As noticed on the flow path drawings, the high pressure turbine is of radial configuration. At an airflow of 5 pounds per second, 16:1 overall compressor pressure ratio levels, and at rotational speeds near 50,000 rpm, a radial inflow turbine is more suitable for the high pressure turbine than an axial. The combination of the three parameters prevents an efficient high-work axial turbine design because of small blade heights which in turn produce excessive end wall losses.

There are two methods of obtaining an efficient axial design: (1) reducing the wall boundary layer by such methods as suction or blowing; (2) increasing the blade height by designing the turbine at a lower radius. The latter method requires that additional turbine stages be added to maintain work/speed ratios consistent with high efficiency turbines.

An indication of the problem associated with maintaining turbine blade height is illustrated in Figure 16. Imposing a 0.7 inch minimum blade height shows that a 16:1 pressure ratio compressor requires eight axial turbine stages as contrasted to one turbine stage to drive a 9:1 pressure ratio compressor. This curve was generated for a minimum diameter turbine, positive reaction in all stages, constant hub diameter, axial discharge and equal work per stage. Relaxing some of these limitations allows a fewer number of stages to be used but the same efficiency level cannot be maintained. Achievement of 83 to 85 percent efficiency

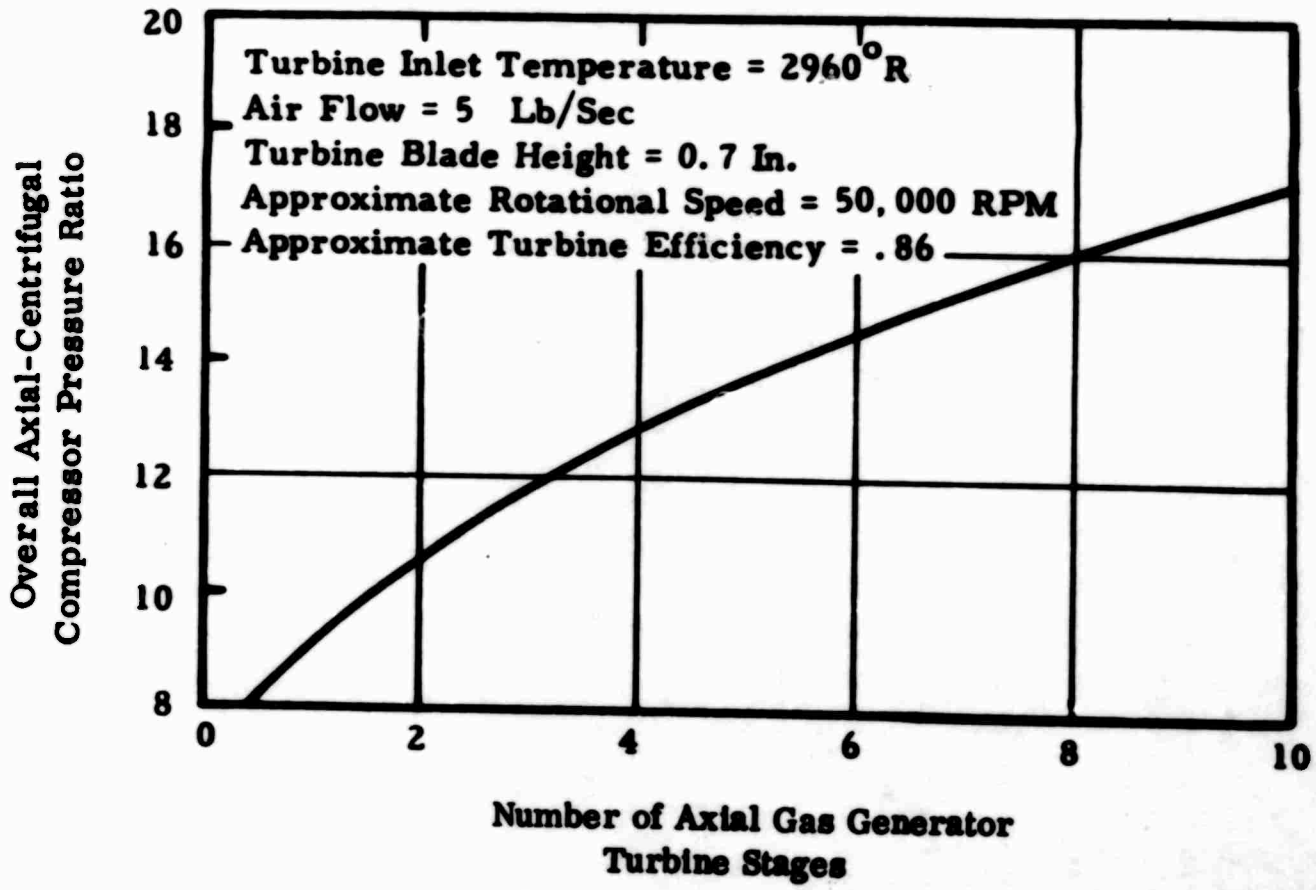

Figure 16. The Effect of Compressor Pressure Ratio on Number of Axial Gas Generator Turbine Stages.

in two stages for a 16:1 gas generator presents a formidable task in lieu of size and loading parameters.

The two methods for increasing the effectiveness of the high pressure axial turbine were discarded in favor of the radial high pressure turbine.

The turbines shown on the flow paths were designed for the following approximate efficiencies which are consistent with the turbine efficiencies mentioned in the contract.

High pressure turbine efficiency	83.9 percent
Low pressure turbine efficiency	86.0 percent
Power turbine efficiency	88.1 percent

These efficiencies are based on uncooled turbines constructed of advanced materials. If turbine cooling is considered, these efficiencies would probably be lower than as shown above.

The cursory turbine stress analysis was based on 100-hour-life advanced nickel-chrome base alloy goals. Maximum centrifugal turbine stresses are close to 55,000 psi.

Fixed shaft power turbines were not considered practical because the gas generator rotational speeds are too high for efficient, reasonably stressed turbines. In order to design a mechanically feasible fixed shaft power turbine, an efficiency penalty of greater than 3 percent would result.

PERFORMANCE EVALUATION OF CANDIDATE CONFIGURATIONS

PLAN OF ATTACK

The plan of attack in evaluating the candidate compressors in a complete engine is shown in Figure 17. Four basic engines in 32 different configurations were evaluated. These engines are shown schematically in Figure 18 and are defined below.

Single-Spool Connected Power Turbine

The gas generator compressor and turbine, and the power turbine are connected to a common shaft.

Two-Spool Connected Power Turbine

The gas generator compressor and turbine are split into a low pressure spool and a high pressure spool. The compressor and turbine of each spool are connected by separate concentric shafts. The power turbine is affixed directly to the low pressure spool shaft. Connected power turbine engines are also called fixed shaft engines in this report.

Single-Spool Free Power Turbine

The gas generator compressor and turbine are connected to a common shaft. The power turbine is on a separate shaft.

Two-Spool Free Power Turbine

This configuration has the same arrangement as the two-spool fixed shaft engine except the power turbine is on a separate shaft. Free power turbine engines are also called free shaft engines in this report.

The cursory analysis of the 32 engines included examining the compressor off-design operating line and the significant performance parameters along that line in order to determine:

Operational potential; i.e., examine turbine, variable nozzles, inlet guide vanes (IGV), and so forth.

The four candidate compressors for further detailed gas generator studies.

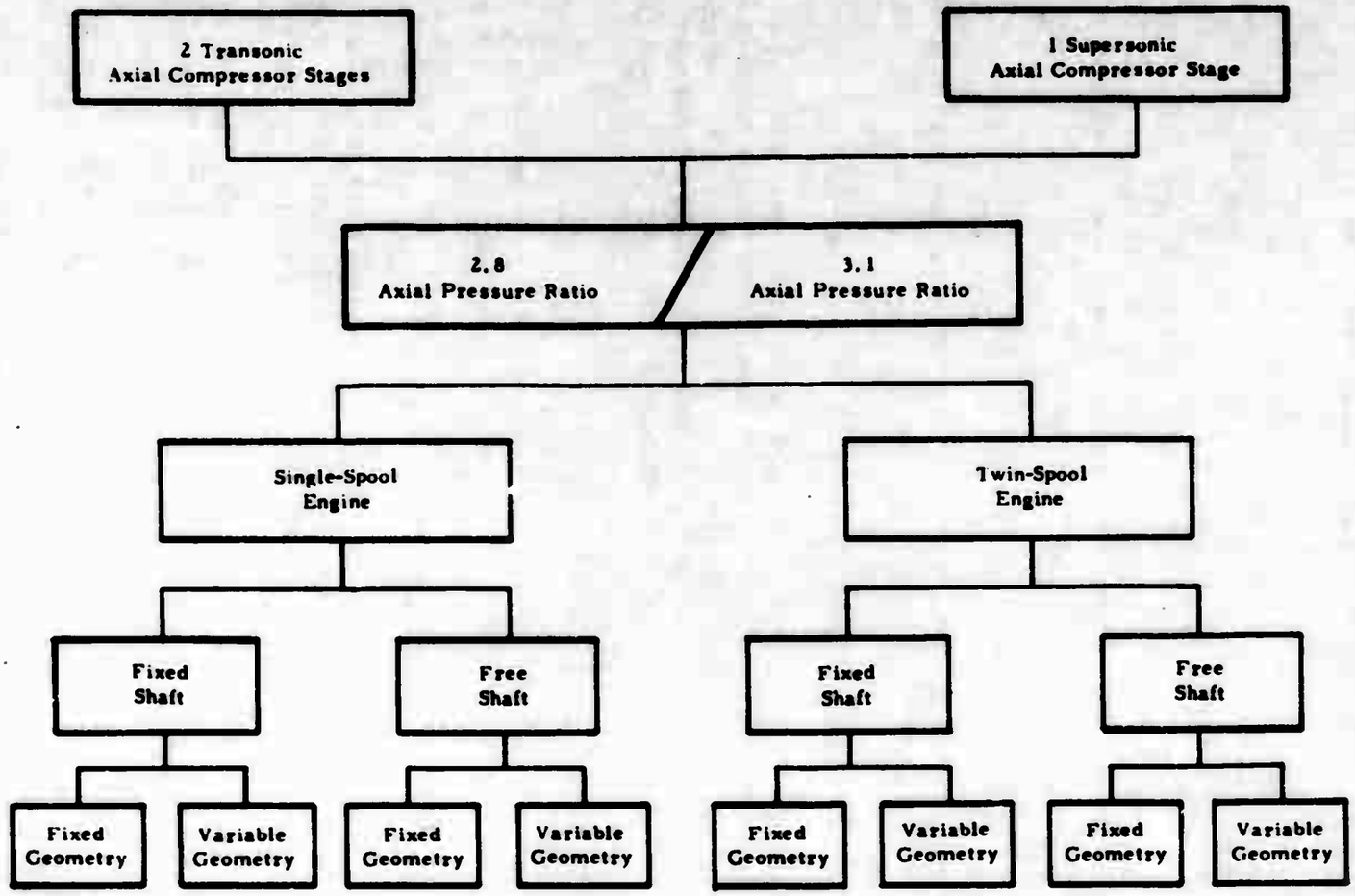

Figure 17. Engine Performance Evaluation of 2.8:1 Axial Pressure Ratio Candidate Compressors.

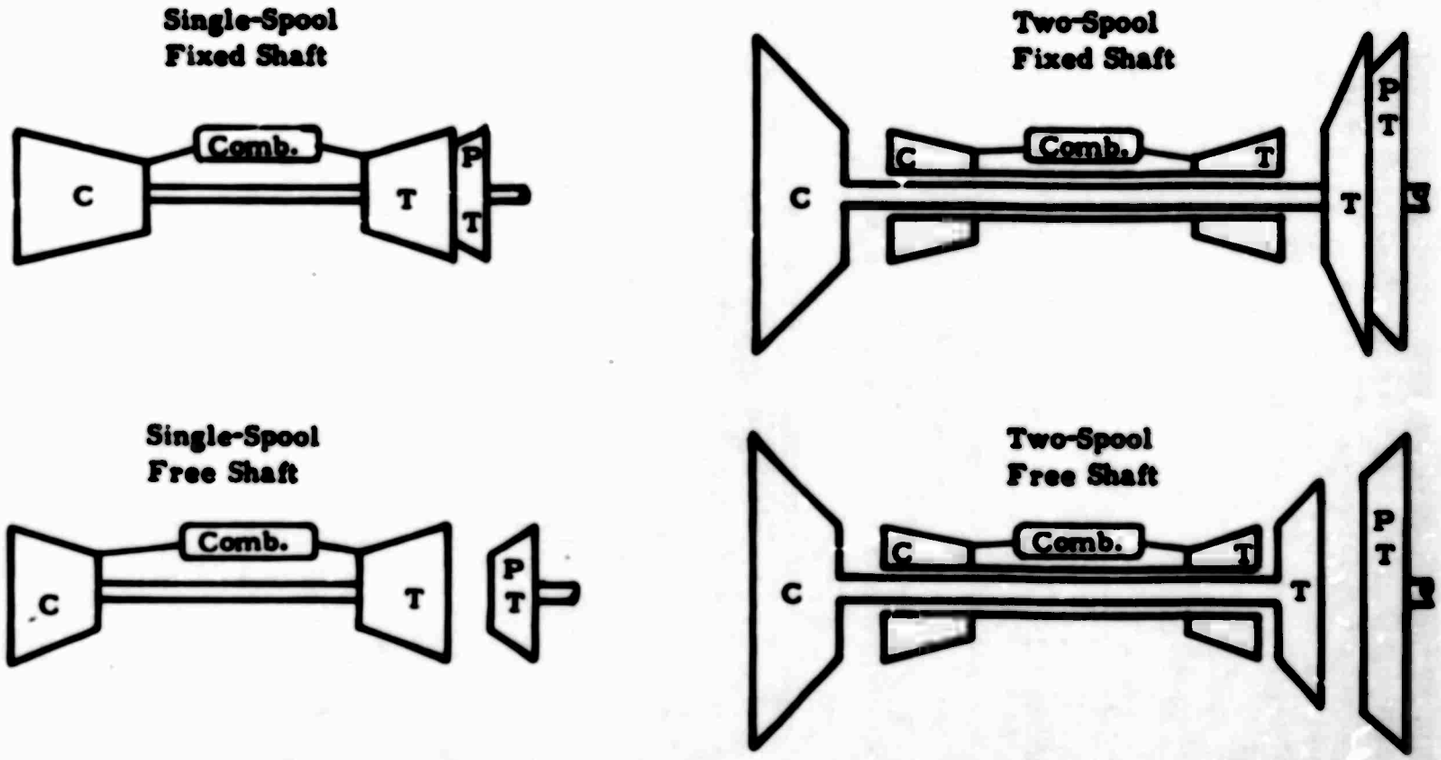

Note: Fixed Shaft = Fixed Power Turbine = Connected Power Turbine
C = Compressor
T = Gas Generator Turbine
P_T = Power Turbine

Figure 18. Engine Configuration Definition.

It should be noted that some of the 32 candidates can be clearly eliminated from detailed study without generating an operating line. For example, some single-spool engines may be eliminated by inspecting the compressor maps (i.e., large surge regions). The thermodynamic analysis carried out for two-spool engines in order to select the candidate axial compressor is discussed below.

TWO-SPOOL ENGINE CONFIGURATIONS

Two-Spool Engine - Free Power Turbine

Design Point Analysis. A summary of the design point data is given in Table III. A design point was established for each two-spool free turbine cycle. The complete output computation for these points is included in Tables IV through VII. A schematic diagram giving the engine station designation is presented on Figure 19. The symbolic definitions of the computer output format are given on page 38.

Low Spool - One Supersonic Stage - Axial Pressure Ratio = 2.8:1. Figure 20 shows the operating line on the low pressure spool for both fixed and variable turbine geometry configurations.

It is evident that:

Inadequate surge margin exists in the fixed geometry configuration.

Adequate surge margin exists with variable turbine geometry with part-power (BSFC) approximately 1.0 percent lower, as can be seen on Figures 20 and 21. In addition, the surge margin of the high pressure compressor is very narrow at part-power, with variable turbine nozzles, as shown in Figure 22. Included in Figures 21 and 22 for comparison are the 3.1 pressure ratio data.

It should be noted that all of the points shown in Table III represent comparable matches along the given centrifugal operating line. Because of its higher efficiency, the transonic compressor performance provides the highest shaft horsepower (SHP) and lowest BSFC.

TABLE III
DESIGN POINT DATA

	Supersonic Axial Stage		Transonic Axial Stages	
P_3/P_2	2.8:1	3.1:1	2.8:1	3.1:1
SHP	1058	1037	1107	1091
BSFC	0.466	0.467	0.449	0.449
TIT - °R	2960	2960	2960	2960
P_5/P_2	16.0:1	16.7:1	16.5:1	17.27:1
Eff LP Comp.	78.0	76.5	84.0	82.5
Eff HP Comp.	79.9	79.8	79.9	79.8
Eff LP Turbine	86.0	86.0	86.0	86.0
Eff HP Turbine	83.9	83.9	83.9	83.9
Eff Power Turbine	88.1	88.1	88.1	88.1

Axial Pressure Ratio = 3.1:1. Incated in Figure 23 is the low pressure spool operating line for both fixed and variable turbine geometry. The results here are almost identical to the 2.8 pressure ratio stage.

From the above, the following can be concluded concerning a two-spool free-shaft engine using a supersonic axial stage as the low-pressure spool at a pressure ratio of 2.8 or 3.1:1.

A fixed geometry engine is not feasible because of inadequate part-power surge margin.

Little improvement is obtained in part-power (BSFC) with incorporation of variable turbine nozzles, and high pressure spool part-power surge margin problems may be encountered.

An engine with only variable inlet axial compressor guide vanes or variable power turbine geometry may be feasible.

TABLE IV

PERFORMANCE DESIGN POINT, TWO-SPOOL FREE POWER TURBINE,
SUPERSONIC AXIAL, 2.8:1 PRESSURE RATIO

OUTPUT

M	0.0000E-99	ALT	0.0000E-99	V-KNOTS	0.0000E-99		
TA	5.1868E+02	PA	1.4695E+01	NL/ST2	1.0000E+02	NH/ST4	8.3438E+01
T2	5.1868E+02	P2	1.4622E+01	WST/D2	5.0251E+00	WST/D4	2.1509E+00
T3	7.4505E+02	P3	4.0942E+01	(WST/D)3	2.1509E+00	WST4/D5	3.7641E-01
T4	7.4505E+02	P4	4.0942E+01	P3/P2	2.8000E+00	P5/P4	5.7142E+00
T5	1.3166E+03	P5	2.3395E+02	ETACL	7.8000E-01	ETACH	7.9880E-01
T6	1.3166E+03	P6	2.3395E+02	NL/T9C	4.6473E+01	NH/T7C	4.2594E+01
T7-TIT	2.9600E+03	P7	2.2343E+02	WND609	1.4319E+00	WND607	5.5232E-01
T8	2.4806E+03	P8	8.6178E+01	DH/TC-TL	1.2023E+01	DH/TC-TH	2.6498E+01
T9	2.4806E+03	P9	8.6178E+01	P11/P12C	4.0633E+00	P7/P8C	2.7842E+00
T10	2.2945E+03	P10	5.7876E+01	ETATL	8.6000E-01	ETATH	8.3900E-01
T11	2.2945E+03	P11	5.7876E+01	WSTP2	7.7875E+00	NPT/T11C	4.8227E+01
T12	1.7586E+03	P12	1.5701E+01	WSTP3	3.3333E+00	WN/D6011	2.1322E+00
T14	1.7586E+03	P13	1.4916E+01	WSTP4	3.3333E+00	DH/TC-PT	3.6226E+01
T15	1.7244E+03	P14	1.4916E+01	WSTP5	7.5996E-01	P9/P10C	1.5172E+00
		P15	1.4916E+01	WSTP7	1.2265E+00	ETAPT	8.8100E-01
WA	5.0000E+00			WSTP8	2.9110E+00	DHCL	5.4554E+01
W4	5.0000E+00	DP/PN	0.0000E-99	WSTP9	2.9110E+00	DHCH	1.4313E+02
W5	4.9000E+00	F/A	2.7951E-02	WSTP10	4.1688E+00	DHTH	1.4605E+02
W7	5.0369E+00	WFPTRH	0.0000E-99	WSTP11	4.1688E+00	DHTL	5.5668E+01
W9	5.0369E+00	WFLPRH	0.0000E-99	WSTP12	1.3452E+01	DHPT	1.5575E+02
W11	5.0369E+00	WFP	4.9306E+02	WSTP15	1.4300E+01		
W15	5.1369E+00	WF	4.9306E+02	F/A9	2.7951E-02	P15/PA	1.0149E+00
				F/A11	2.7951E-02	FG	4.7365E+01
BSFC	4.6590E-01	EBSFC	4.5771E-01	AJ	1.0800E+02	FN	4.7365E+01
SHP	1.0583E+03	ESHP	1.0772E+03	TAU	5.5583E+04	P5/P2	1.5999E+01

TABLE V

PERFORMANCE DESIGN POINT, TWO-SPOOL FREE POWER TURBINE, SUPERSONIC AXIAL, 3.1:1 PRESSURE RATIO

OUTPUT							
M	0.0000E-99	ALT	0.0000E-99	V-KNOTS	0.0000E-99		
TA	5.1868E+02	PA	1.4695E+01	NL/ST2	1.0000E+02	NH/ST4	8.1765E+01
T2	5.1868E+02	P2	1.4622E+01	WST/D2	5.0251E+00	WST/D4	1.9924E+00
T3	7.7584E+02	P3	4.5329E+01	(WST/D)3	1.9825E+00	WST4/D5	3.6829E-01
T4	7.7584E+02	P4	4.5103E+01	P3/P2	3.1000E+00	P5/P4	5.4100E+00
T5	1.3463E+03	P5	2.4400E+02	ETACL	7.6500E-01	ETACH	7.9765E-01
T6	1.3463E+03	P6	2.440E+02	NL/T9C	4.6477E+01	NH/T7C	4.2592E+01
T7-TIT	2.9600E+03	P7	2.3424E+02	WND609	1.3671E+00	WND607	5.2657E-01
T8	2.4796E+03	P8	9.0222E+01	DH/TC-TL	1.3677E+01	DH/TC-TH	2.6528E+01
T9	2.4796E+03	P9	9.0222E+01	P11/P12C	4.0036E+00	P7/P8C	2.7879E+00
T10	2.2676E+03	P10	5.7184E+01	ETATL	8.6000E-01	ETATH	8.3900E-01
T11	2.2676E+03	P11	5.7184E+01	WSTP2	7.7875E+00	NPT/T11C	4.8504E+01
T12	1.7409E+03	P12	1.5701E+01	WSTP3	3.0723E+00	WN/D6011	2.1570E+00
T14	1.7409E+03	P13	1.4916E+01	WSTP4	3.0878E+00	DH/TC-PT	3.5914E+01
T15	1.7070E+03	P14	1.4916E+01	WSTP5	7.3684E-01	P9/P10C	1.6133E+00
		P15	1.4916E+01	WSTP7	1.1693E+00	ETAPT	8.8100E-01
WA	5.0000E+00			WSTP8	2.7787E+00	DHCL	6.2049E+01
W4	5.0000E+00	DP/PN	0.0000E-99	WSTP9	2.7787E+00	DHCH	1.4330E+02
W5	4.9000E+00	F/A	2.7483E-02	WSTP10	4.1925E+00	DHTH	1.4623E+02
W7	5.0346E+00	WFPTRH	0.0000E-99	WSTP11	4.1925E+00	DHTL	6.3315E+01
W9	5.0346E+00	WFLPPH	0.0000E-99	WSTP12	1.3379E+01	DHPT	1.5265E+02
W11	5.0346E+00	WFP	4.8480E+02	WSTP15	1.4222E+01		
W15	5.1346E+00	WF	4.8480E+02	F/A9	2.7483E-02	P15/PA	1.0149E+00
				F/A11	2.7483E-02	FG	4.7104E+01
BSFC	4.6740E-01	EBSFC	4.5906E-01	AJ	1.0741E+02	FN	4.7104E+01
SHP	1.0372E+03	ESHP	1.0560E+03	TAU	5.4477E+04	P5/P2	1.6687E+01

TABLE VI
PERFORMANCE DESIGN POINT, TWO-SPOOL FREE POWER TURBINE
TRANSONIC AXIAL, 2.8:1 PRESSURE RATIO

OUTPUT							
M	0.0000E-99	ALT	0.0000E-99	V-KNOTS	0.0000E-99		
TA	5.1868E+02	PA	1.4695E+01	NL/ST2	1.0000E+02	NH/ST4	8.4350E+01
T2	5.1868E+02	P2	1.4622E+01	WST/D2	5.0251E+00	WST/D4	2.1383E+00
T3	7.2901E+02	P3	4.0942E+01	(WST/D)3	2.1276E+00	WST4/D5	3.6182E-01
T4	7.2901E+02	P4	4.0738E+01	P3/P2	2.8000E+00	P5/P4	5.9100E+00
T5	1.3025E+03	P5	2.4076E+02	ETACL	8.4000E-01	ETACH	7.9950E-01
T6	1.3025E+03	P6	2.4076E+02	NL/T9C	4.6482E+01	NH/T7C	4.2595E+01
T7-TIT	2.9600E+03	P7	2.3113E+02	WND609	1.3871E+00	WND607	5.3403E-01
T8	2.4799E+03	P8	8.8983E+01	DH/TC-TL	1.1168E+01	DH/TC-TH	2.6547E+01
T9	2.4799E+03	P9	8.8983E+01	P11/P12C	4.3570E+00	P7/P8C	2.7903E+00
T10	2.3073E+03	P10	6.1552E+01	ETATL	8.6000E-01	ETATH	8.3900E-01
T11	2.3073E+03	P11	6.1552E+01	WSTP2	7.7875E+00	NPT/T11C	4.8094E+01
T12	1.7469E+03	P12	1.5701E+01	WSTP3	3.2973E+00	WN/D6011	2.0053E+00
T14	1.7469E+03	P13	1.4916E+01	WST/4	3.3138E+00	DH/TC-PT	3.7679E+01
T15	1.7129E+03	P14	1.4916E+01	WSTP5	7.3451E-01	P9/P10C	1.4704E+00
		P15	1.4916E+01	WSTP7	1.1859E+00	ETAPT	8.8100E-01
WA	5.0000E+00			WSTP8	2.8195E+00	DHCL	5.0659E+01
W4	5.0000E+00	DP/PN	0.0000E-99	WSTP9	2.8195E+00	DHCH	1.4338E+02
W5	4.9000E+00	F/A	2.8174E-02	WSTP10	3.9316E+00	DHTH	1.4631E+02
W7	5.0380E+00	WFPTRH	0.0000E-99	WSTP11	3.9316E+00	DHTL	5.1693E+01
W9	5.0380E+00	WFLPRH	0.0000E-99	WSTP12	1.3410E+01	DHPT	1.6289E+02
W11	5.0380E+00	WFP	4.9699E+02	WSTP15	1.4256E+01		
W15	5.1380E+00	WF	4.9699E+02	F/A9	2.8174E-02	P15/PA	1.0149E+00
				F/A11	2.8174E-02	FG	4.7217E+01
BSFC	4.4900E-01	EBSFC	4.4147E-01	AJ	1.0767E+02	FN	4.7217E+01
SHP	1.1068E+03	ESHP	1.1257E+03	TAU	5.8133E+04	P5/P2	1.6465E+01

TABLE VII

PERFORMANCE DESIGN POINT, TWO-SPOOL FREE POWER TURBINE, TRANSONIC AXIAL, 3.1:1 PRESSURE RATIO

OUTPUT							
M	0.0000E-99	ALT	0.0000E-99	V-KN	0.0000E-99		
TA	5.1868E+02	PA	1.4695E+01	NL/ST2	1.0000E+02	NH/ST4	8.2758E+01
T2	5.1868E+02	P2	1.4622E+01	WST/D2	5.0251E+00	WST/D4	1.9685E+00
T3	7.5734E+02	P3	4.5329E+01	(WST/D)3	1.9587E+00	WST4/D5	3.5153E-01
T4	7.5734E+02	P4	4.5103E+01	P3/P2	3.1000E+00	P5/P4	5.6000E+00
T5	1.3293E+03	P5	2.5257E+02	ETACL	8.2500E-01	ETACH	7.9840E-01
T6	1.3293E+03	P6	2.5257E+02	NL/T9C	4.6481E+01	NH/T7C	4.2593E+01
T7-TIT	2.9600E+03	P7	2.4247E+02	WND609	1.3220E+00	WND607	5.0884E-01
T8	2.4795E+03	P8	9.3329E+01	DH/TC-TL	1.2686E+01	DH/TC-TH	2.6547E+01
T9	2.4795E+03	P9	9.3329E+01	P11/P12C	4.3268E+00	P7/P8C	2.7904E+00
T10	2.2831E+03	P10	6.1246E+01	ETATL	8.6000E-01	ETATH	8.3900E-01
T11	2.2831E+03	P11	6.1246E+01	WSTP2	7.7875E+00	NPT/T11C	4.8340E+11
T12	1.7291E+03	P12	1.5701E+01	WSTP3	3.0355E+00	WN/D6011	2.0145E+00
T14	1.7291E+03	P13	1.4916E+01	WSTP4	3.0507E+00	DH/TC-PT	3.7537E+01
T15	1.6954E+03	P14	1.4916E+01	WSTP5	7.0731E-01	P9/P10C	1.5548E+00
		P15	1.4916E+01	WSTP7	1.1299E+00	ETAPT	8.8100E-01
WA	5.0000E+00			WSTP8	2.6869E+00	DHCL	5.7543E+01
W4	5.0000E+00	DP/PN	0.0000E-99	WSTP9	2.6869E+00	DHCH	1.4340E+02
W5	4.9000E+00	F/A	2.7752E-02	WSTP10	3.9288E+00	DHTH	1.4633E+02
W7	5.0359E+00	WFPTRH	0.0000E-99	WSTP11	3.9288E+00	DHTL	5.8717E+01
W9	5.0359E+00	WFLPRH	0.0000E-99	WSTP12	1.3337E+01	DHPT	1.6063E+02
W11	5.0359E+00	WFP	4.8955E+02	WSTP15	1.4177E+01		
W15	5.1359E+00	WF	4.8955E+02	F/A9	2.7752E-02	P15/PA	1.0149E+00
				F/A11	2.7752E-02	FG	4.6957E+01
BSFC	4.4852E-01	EBSFC	4.4094E-01	AJ	1.0707E+02	FN	4.6957E+01
SHP	1.0914E+03	ESHP	1.1102E+03	TAU	5.7325E+04	P5/P2	1.7273E+01

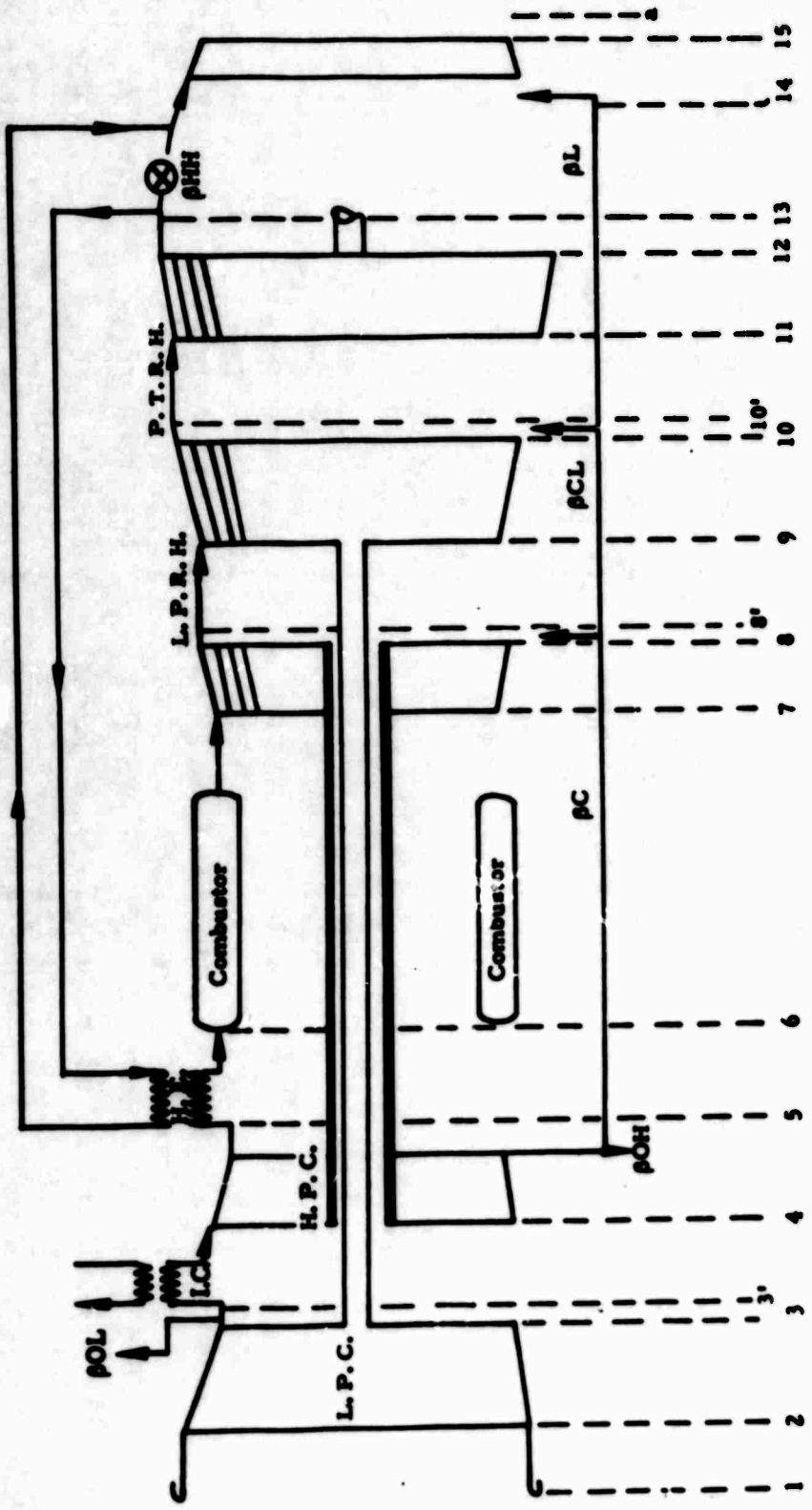

Figure 19. Gas Generator Station Designation.

SYMBOLS

M	-	Mach number (flight)
TA	-	Ambient temperature - ^{o}R
T	-	Temperature at appropriate station - ^{o}R
W	-	Airflow - lb/sec
BSFC	-	Brake specific fuel consumption - lb/SHP/hr
SHP	-	Shaft horsepower
ALT	-	Altitude - feet
PA	-	Ambient pressure - psia
P	-	Pressure at appropriate station - psia
DP/PN	-	Exhaust nozzle pressure loss
F/A	-	Fuel to air ratio
WF	-	Total fuel flow - lb/hr
EBSFC	-	Equivalent brake specific fuel consumption - lb/SHP/hr
ESHP	-	Equivalent shaft horsepower
V-KNOTS	-	True airspeed - knots
NL/ST2	-	Referred low pressure spool speed - $(N/\sqrt{\theta})_2$ - rpm
WST/D2	-	Referred airflow $(W\sqrt{\theta}/\delta)_2$ - lb/sec
(WST/D)3	-	Referred airflow $(W\sqrt{\theta}/\delta)_3$ - lb/sec
P3/P2	-	Low pressure spool compressor pressure ratio
ETACL	-	Low pressure spool compressor adiabatic efficiency
NL/T9C	-	Referred low pressure turbine speed - $(N_L/\sqrt{\theta_{cr}})_9$ - rpm
WN/D609	-	Low pressure turbine speed-flow parameter - $(WN/\delta 60)_9$ - lb-rev/sec^2
DH/TC-TL	-	Referred low pressure turbine work - $(\Delta h/\theta_{cr})_9$ - BTU/lb
P11/P12C	-	Corrected low pressure turbine pressure ratio
ETATL	-	Low pressure turbine adiabatic efficiency
WSTP	-	Flow parameter - $W\sqrt{T}/P$ at appropriate station
F/A9	-	Fuel to air ratio at station 9
F/A11	-	Fuel to air ratio at station 11
AJ	-	Exhaust nozzle area
TAU	-	Output shaft torque
NH/ST4	-	Referred high pressure compressor speed - $(N_H/\sqrt{\theta})_4$ - rpm
WST/D4	-	Flow parameter - $W\sqrt{\theta_4}/\delta_5$ - lb/sec
P5/P4	-	High pressure compressor pressure ratio
ETACH	-	High pressure compressor adiabatic efficiency
NH/T7C	-	Referred high pressure turbine speed $(N_H/\sqrt{\theta_c})_7$ - rpm
P15/PA	-	Exhaust nozzle total to static pressure ratio
FG	-	Gross thrust
FN	-	Net thrust
P5/P2	-	Overall cycle pressure ratio
T7-TIT-^{o}R	-	Turbine inlet temperature - ^{o}R

WND607	-	High pressure turbine speed-flow parameter $(WN/\delta 60)_7$ lb-rev/sec^2
DH/TC-TH	-	Referred high pressure turbine work - $(\Delta h/\theta_{cr})_7$ - Btu/lb
P7/P8C	-	Corrected high pressure turbine pressure ratio
ETATH	-	High pressure turbine adiabatic efficiency
NPT/T11C	-	Referred power turbine speed $(N_{PT}/\sqrt{\theta}_{cr})11$ - rpm
WN/D6011	-	Power turbine speed-flow parameter $(WN/\delta 60)11$ - lb-rev/sec^2
DH/TC-PT	-	Power turbine referred work $(\Delta h/\theta_{cr})_{11}$ - Btu/lb
P_9/P10C	-	Corrected power turbine pressure ratio
ETAPT	-	Power turbine adiabatic efficiency

Low Spool = Two Transonic Stages - Axial Pressure Ratio = 2.8:1. Figure 24 indicates the operating line on the low spool for both fixed and variable turbine geometry configurations. It can be seen that:

Adequate surge margin exists in the fixed geometry configuration.

Adequate surge margin exists with variable turbine nozzles, and part-power (BSFC) is reduced by approximately 1.9 percent (see Figure 25). Also, similar to the supersonic case, the surge margin of the high pressure spool is reduced considerably at part-power with variable turbine geometry (Figure 26). Shown in Figures 25 and 26 for comparison are the 3.1 pressure ratio data.

Axial Pressure Ratio = 3.1:1. Shown in Figure 27 is the low pressure spool operating line for both fixed and variable turbine geometry. The results are again very similar to the 2.8 pressure ratio stage.

From the above cursory analysis, the following can be concluded concerning a two-spool free shaft engine using two transonic axial stages as the low pressure spool at a pressure ratio of 2.8 or 3.1:1.

A fixed or variable geometry engine appears to be feasible.

An engine with only variable turbine nozzles may encounter possible high-spool part-power surge margin problems.

Variable inlet guide vanes on the low spool are not required.

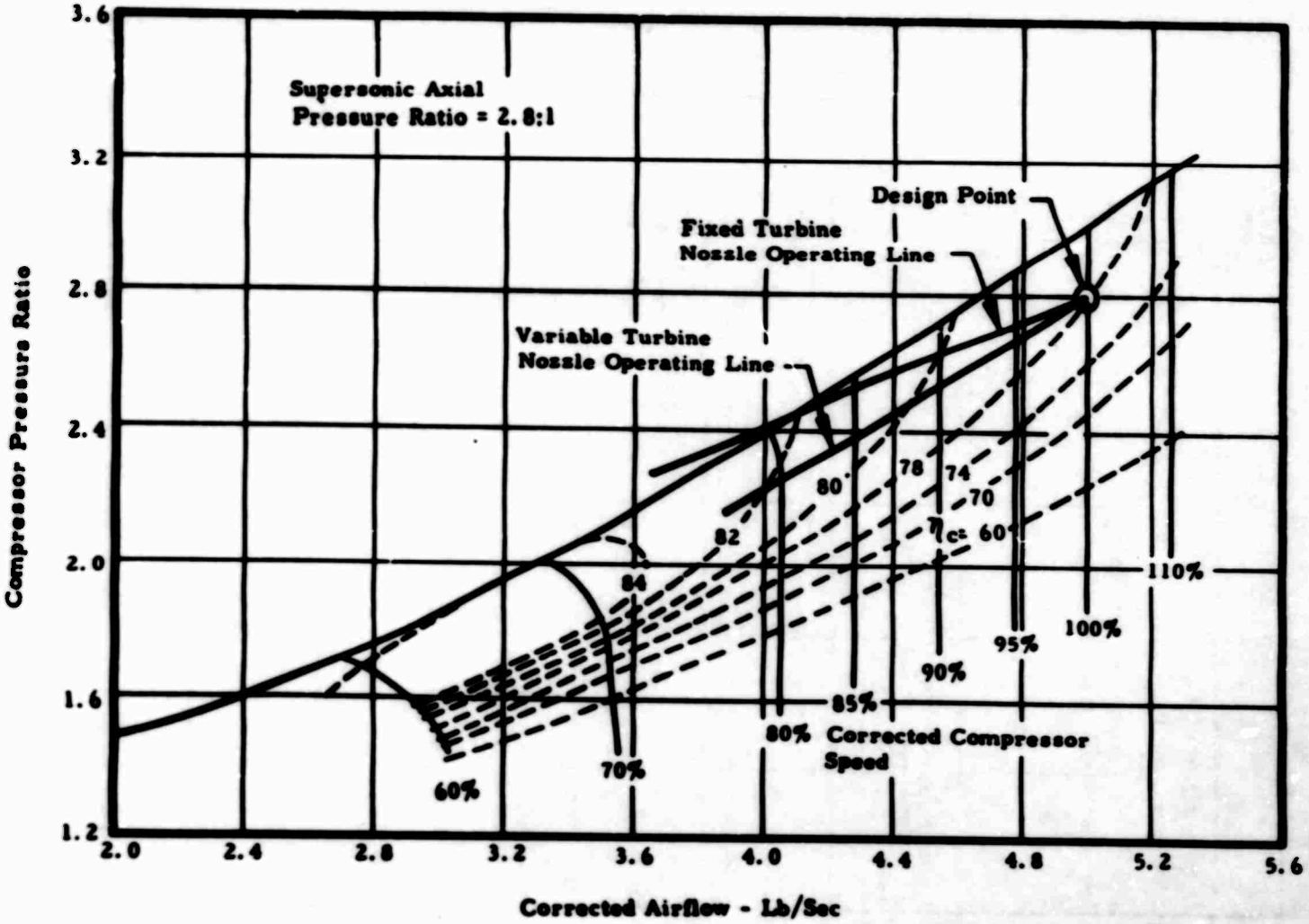

Figure 20. Estimated Performance Map for Single-Stage Supersonic Compressor With Two-Spool Free Shaft Engine Operating Lines.

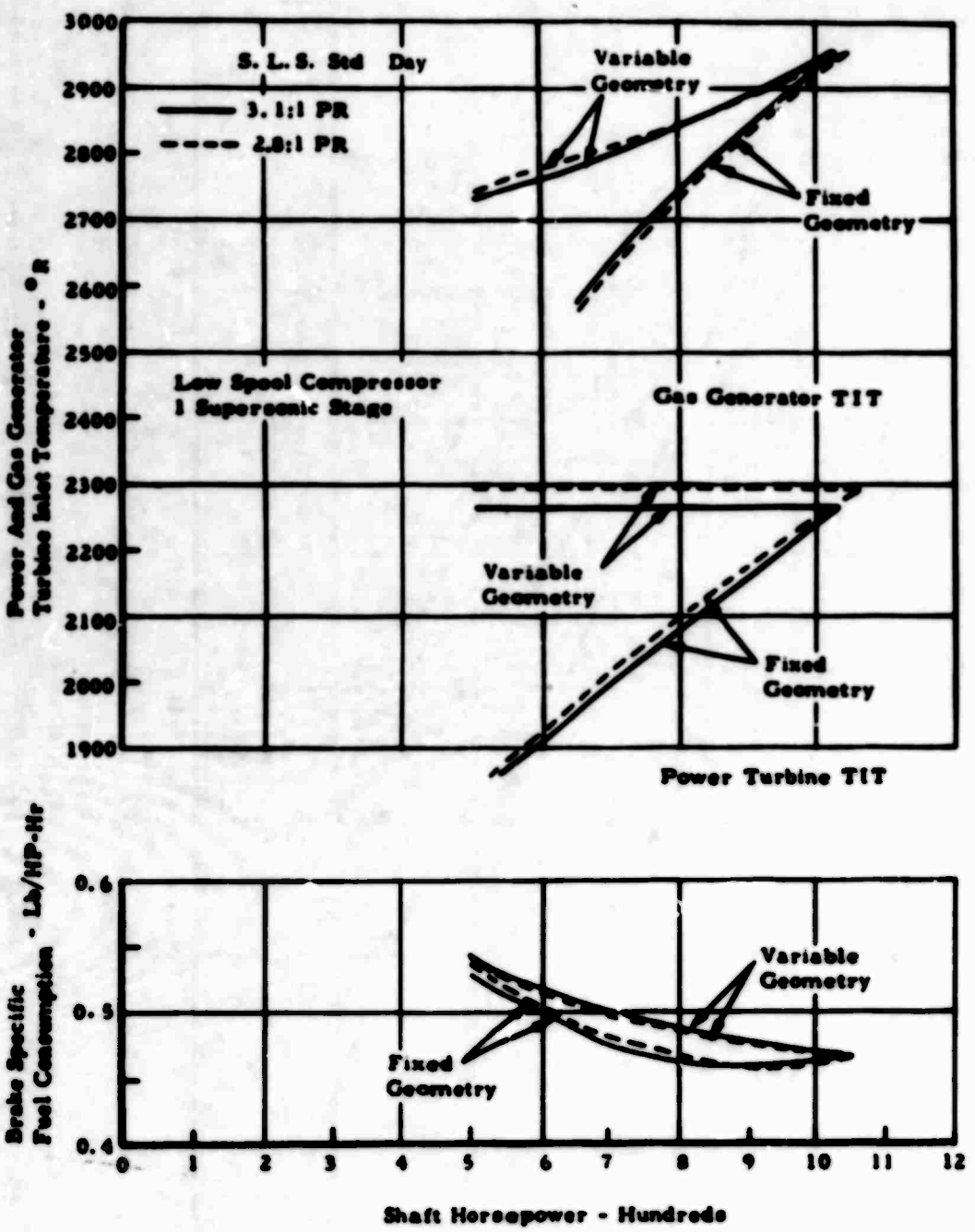

Figure 21. USAAVLABS Compressor Design - Supersonic Axial.

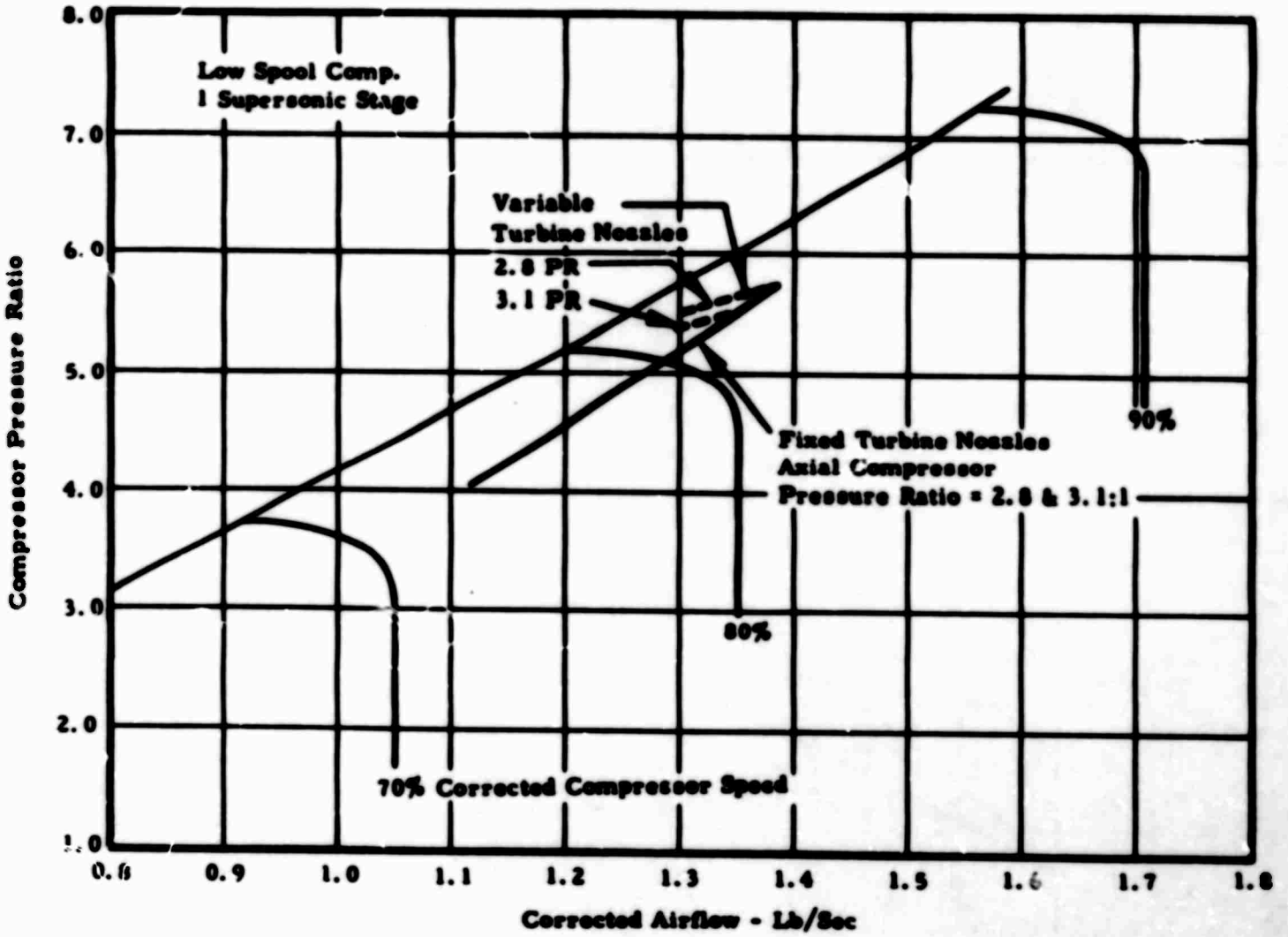

Figure 22. Estimated Performance Map for High Pressure Ratio Centrifugal Compressor With Two-Spool Free Shaft Engire Operating Lines.

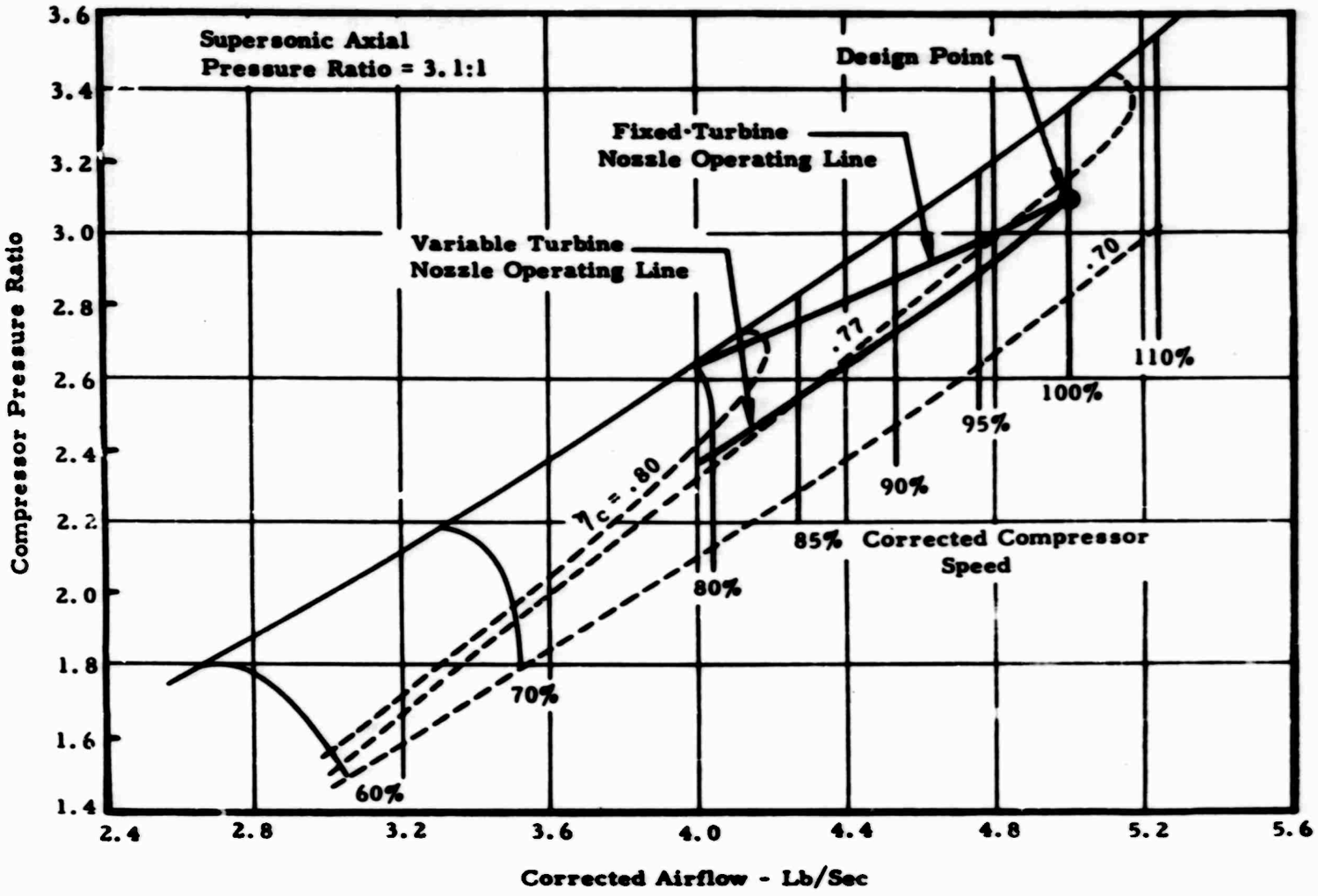

Figure 23. Estimated Performance Map for Single-Stage Supersonic Compressor With Two-Spool Free Shaft Engine Operating Lines.

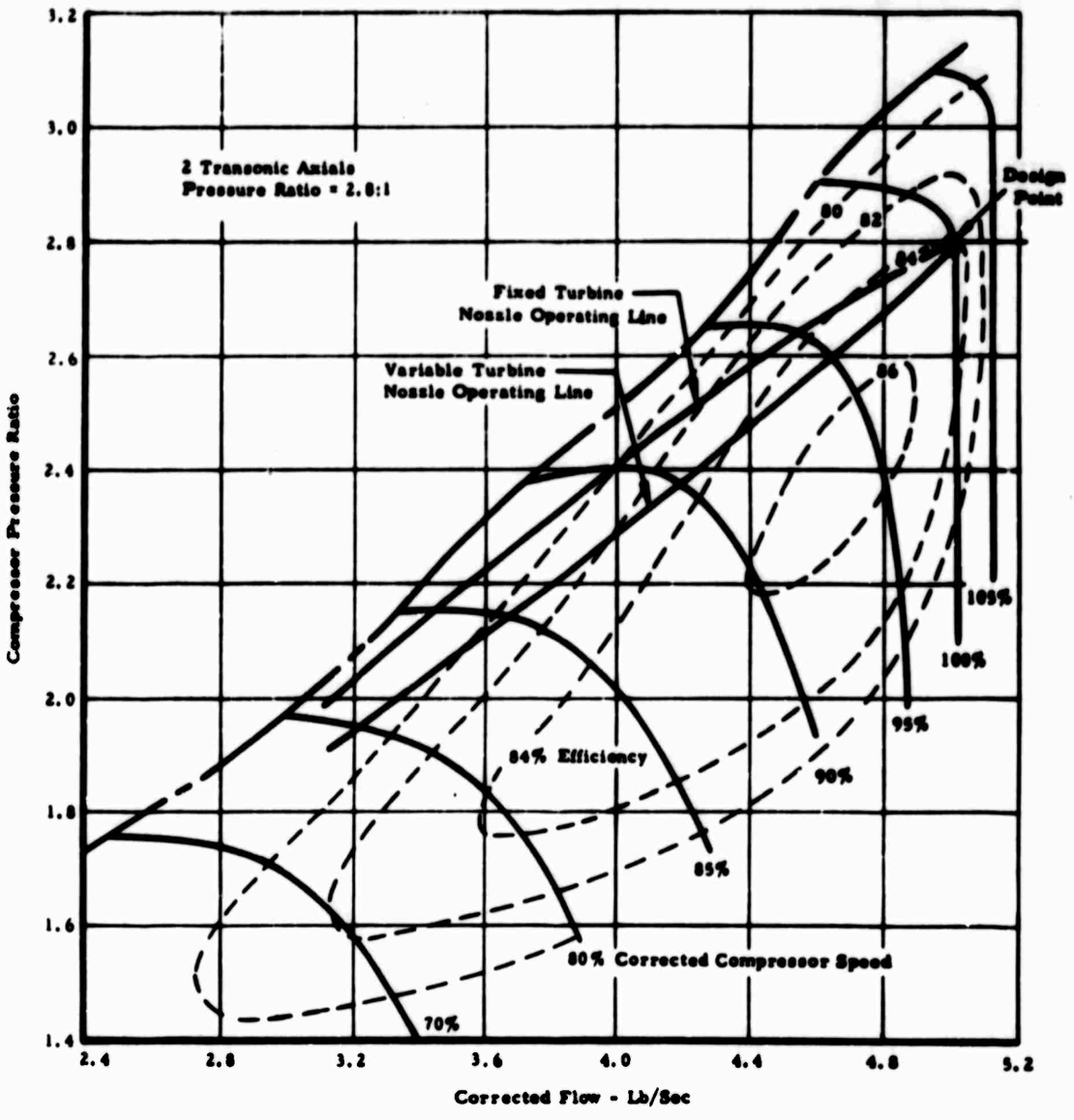

Figure 24. Estimated Performance Map for Two-Stage Transonic Compressor With Two-Spool Free Shaft Engine Operating Lines.

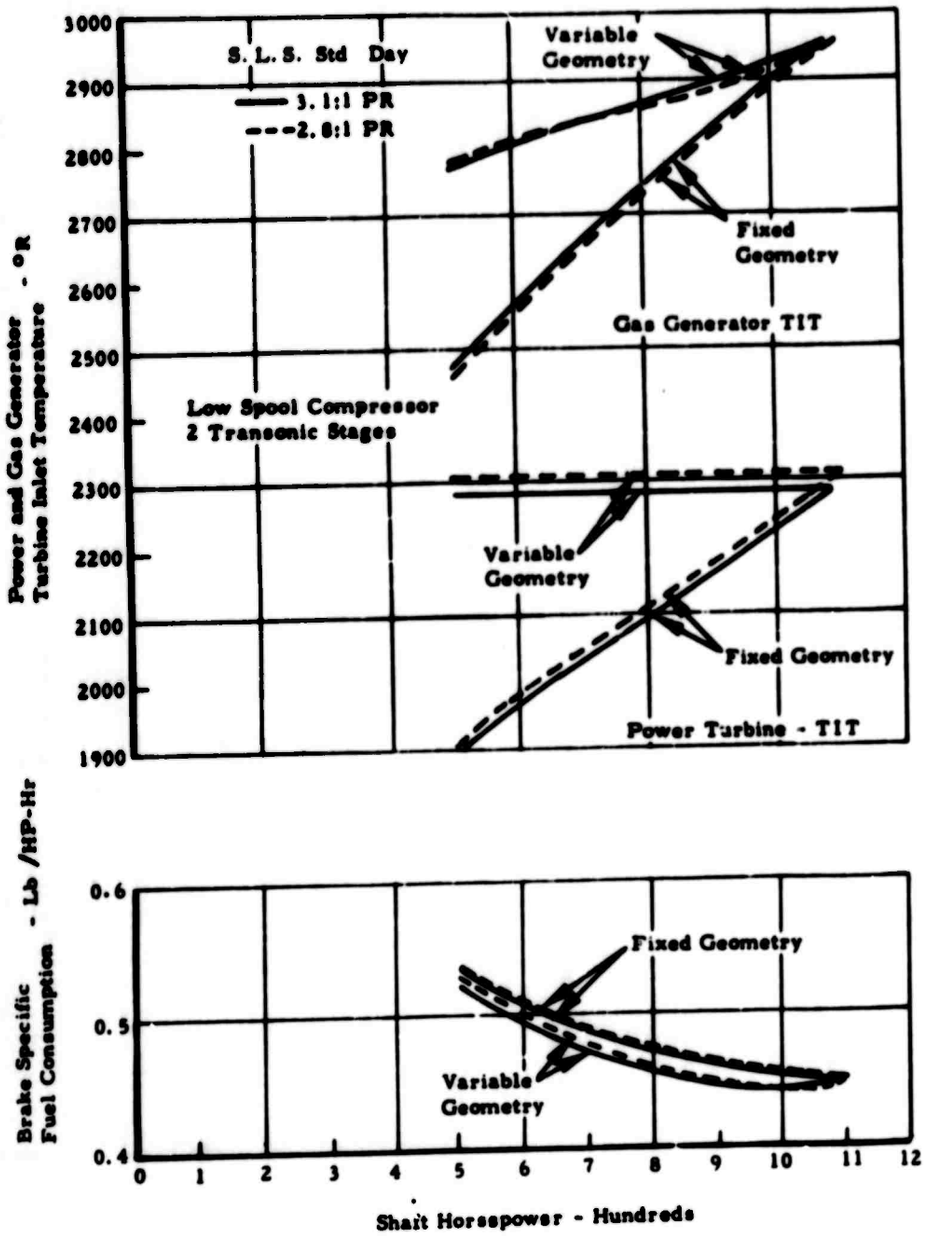

Figure 25. USAAVLABS Compressor Design - Transonic Axial.

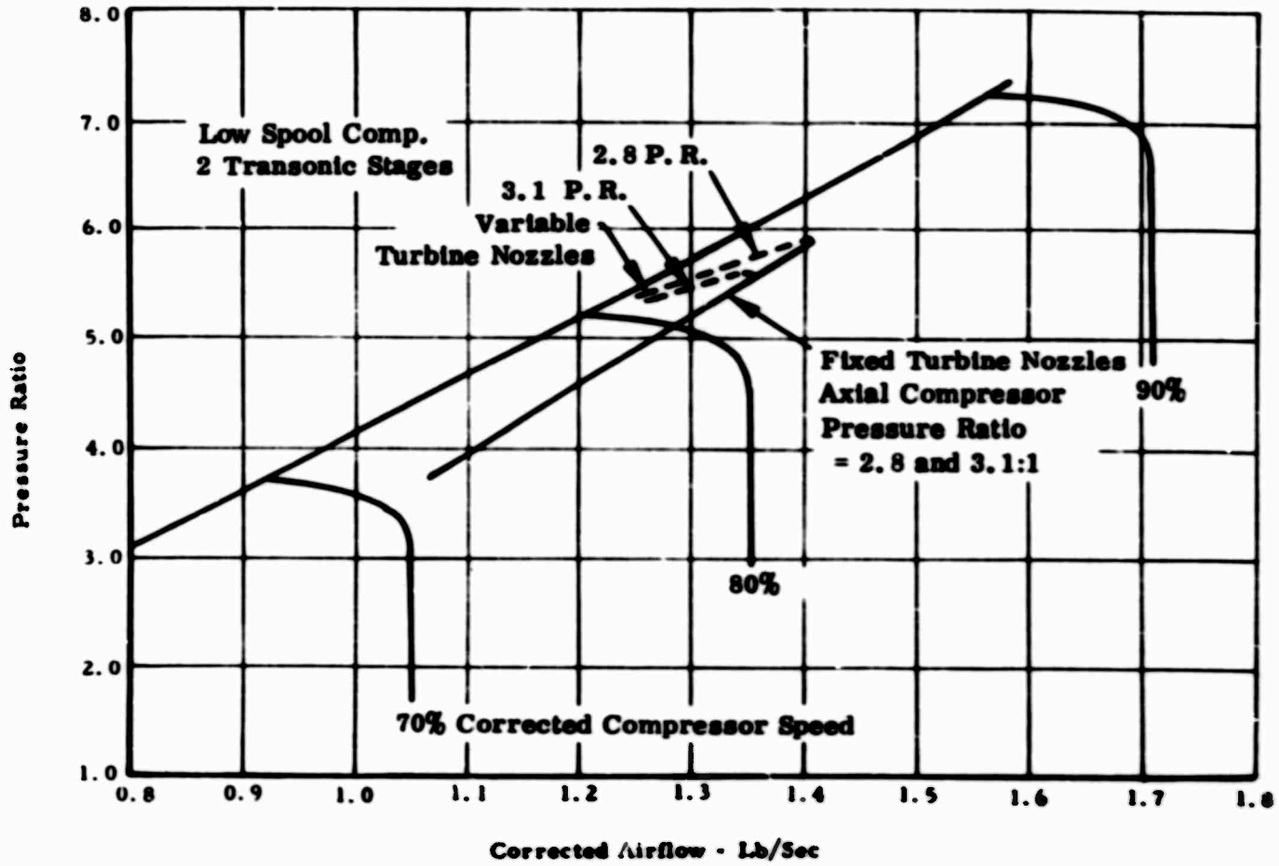

Figure 26. Estimated Performance Map for High Pressure Ratio Centrifugal Compressor With Two-Spool Free Shaft Engine Operating Lines.

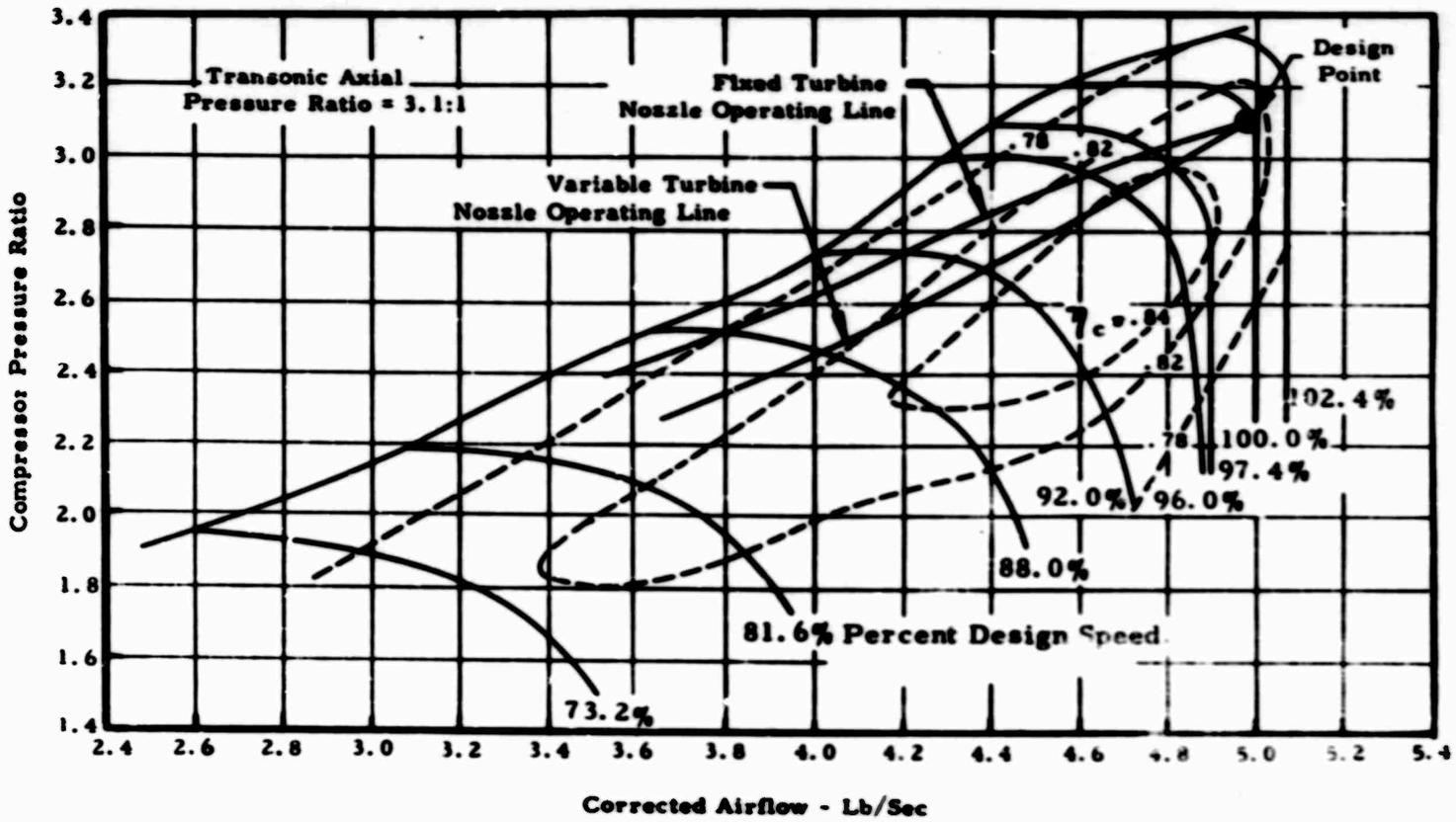

Figure 27. Estimated Performance Map for Two-Stage Transonic Compressor With Two-Spool Free Shaft Engine Operating Lines.

Variable Geometry Analysis - Two-Spool Free Shaft

The work in evaluating each compressor in two-spool engine configurations also included an examination of:

Variable inlet guide vanes on the low pressure compressor spool only.

Variable inlet guide vanes on the low pressure compressor spool with variable power turbine nozzles.

Variable inlet guide vanes on the high pressure compressor spool only.

Each item is discussed in detail below.

Variable Inlet Guide Vanes* on the Low Pressure Compressor Spool Only. In order to evaluate the effect of variable inlet guide vanes on a two-spool free shaft engine, an engine utilizing a single-stage 2.8:1 pressure ratio supersonic axial stage was used as the low pressure spool compressor.

The effect of variable inlet guide vanes (VIGV) can be clearly seen by examining what happens to a particular operating point on a given compressor speed line when the inlet guide vane position is changed. Figure 29 shows the migration of the given point to lower flows and pressures as the inlet guide vane is closed. It is significant that:

The 90 percent speed line migrates to lower flows and pressures as the inlet guide vane is closed, thus carrying the operating point to the reduced flow condition.

The surge line remains essentially unchanged with respect to flow and pressure ratio. Closing the guide vane eventually forces the low pressure operating point into the surge region (at about 13° of prewhirl).

This effect results from the fact that as the guide vane is closed, prewhirl is introduced which causes a loss in stage pressure ratio. For a single axial stage, the stage surge pressure ratio decreases

---

* For Continental terminology, a positive inlet guide vane setting angle is always in the direction of rotation and is associated with a reduction in flow. A negative inlet guide vane setting angle is against direction of rotation and is associated with an increase in flow. (See Figure 28.)

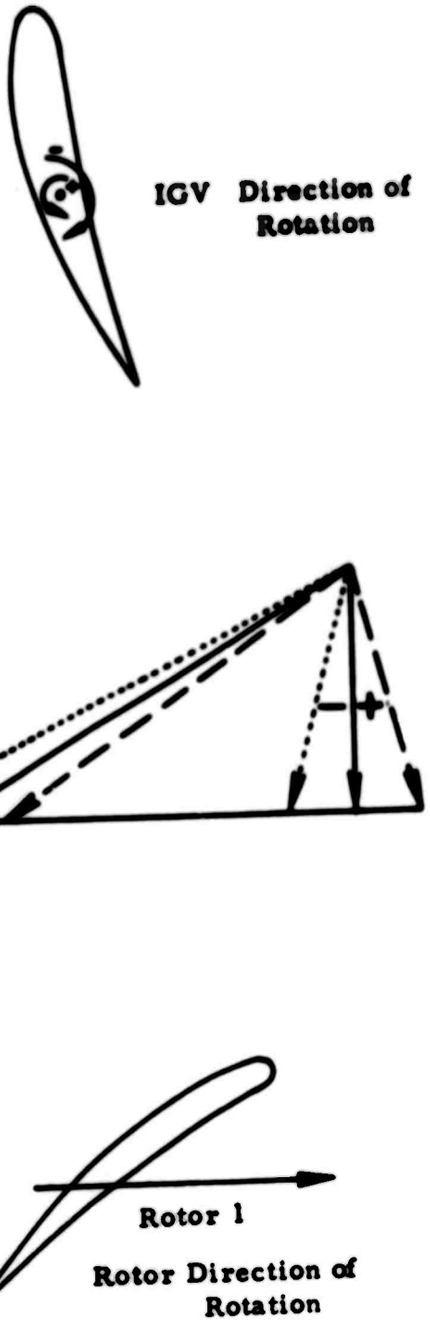

Figure 28. Continental Variable Inlet Guide Vane Nomenclature.

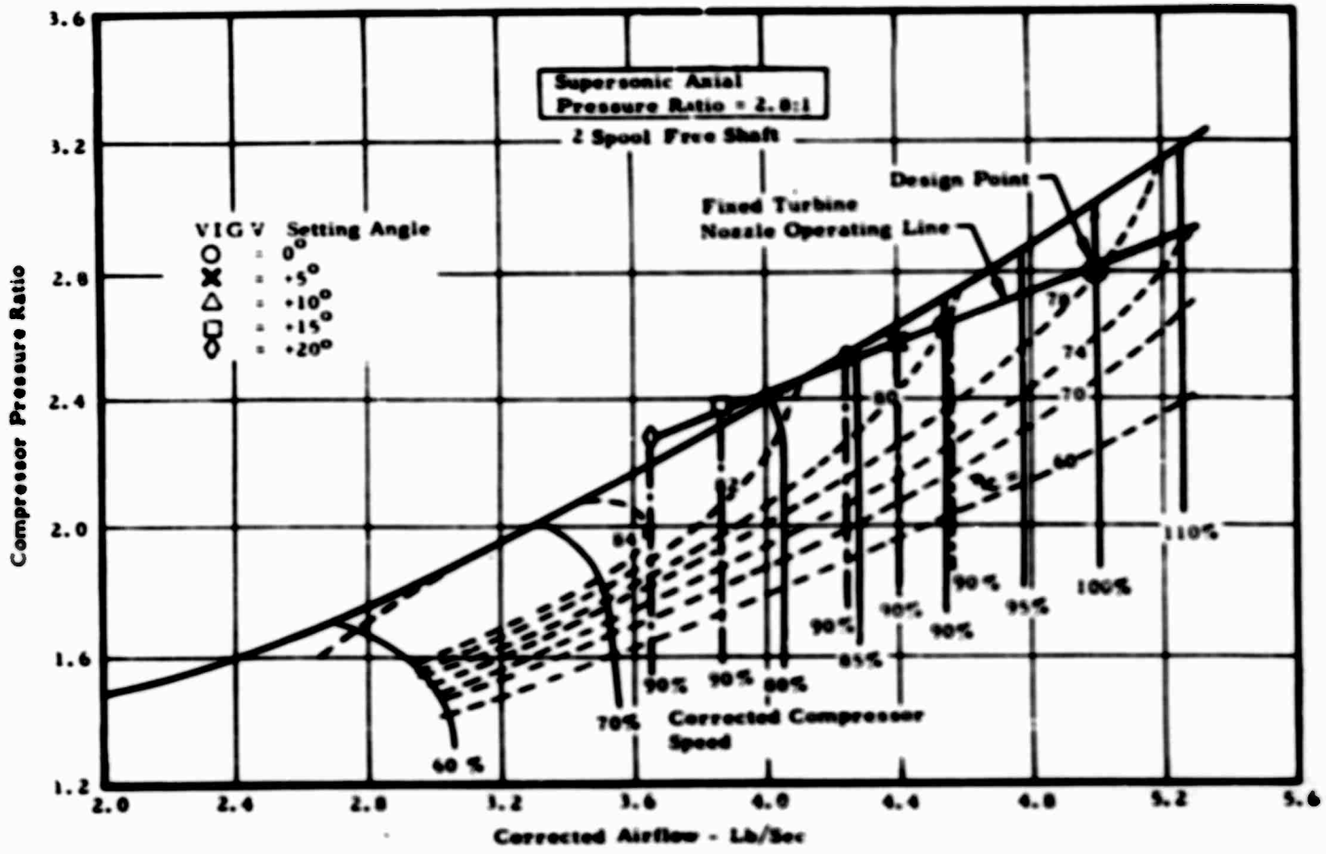

Figure 29. Estimated Performance Map for Single-Stage Supersonic Compressor With Low Spool (Variable Inlet Guide Vane) Operating Line.

at approximately the same rate as the flow; hence there is no surge line change. Figure 30 shows some Continental test results for a single-stage transonic axial rotor with various inlet guide vane setting angles which were used in this analysis.

Figure 31 shows the migration of an operating point on the high pressure compressor spool when closing down the inlet guide vanes on the low pressure spool and holding constant low pressure rotor speed. The point moves down the same operating line as a fixed geometry engine with a decreasing high pressure rotor speed.

Variable Inlet Guide Vanes on the Low-Pressure Compressor Spool With Variable Power Turbine Nozzles. This configuration was not investigated, since it was unnecessary. Figure 20 shows that with variable turbine nozzles only, the low-pressure spool surge margin is adequate.

Variable Inlet Guide Vanes on the High-Pressure Compressor Spool Only. In order to evaluate the effect of variable inlet guide vanes on the high spool of a two-spool free shaft engine, an engine utilizing a single-stage 2.8:1 pressure ratio supersonic axial stage was again used as the low pressure compressor in conjunction with USAAVLABS centrifugal as the high spool.

Figures 32 and 33 show the operating lines with the introduction of prewhirl on the high pressure compressor at -10° and $+40^{\circ}$, respectively. As can be seen by comparison of these two figures, the surge line is moved to lower flows, improving the high pressure surge margin.

Increasing the prewhirl causes a loss in pressure ratio which is similar to the axial compressor. However, in the case of the centrifugal compressor, because of the difference in inlet and exit tip speeds, the surge pressure ratio decreases at a slower rate than the flow; hence the surge margin improvement.

Figure 34 shows Continental test results for a single-stage centrifugal compressor for various inlet guide vane setting angles. The test results substantiate predictions that the surge margin improves with introduction of prewhirl.

However, the effect of variable inlet guide vanes on the high pressure compressor has a detrimental effect of the low pressure compressor operating line. Figure 35 shows the low pressure compressor operating line in surge with $+40^{\circ}$ of high pressure compressor prewhirl angle.

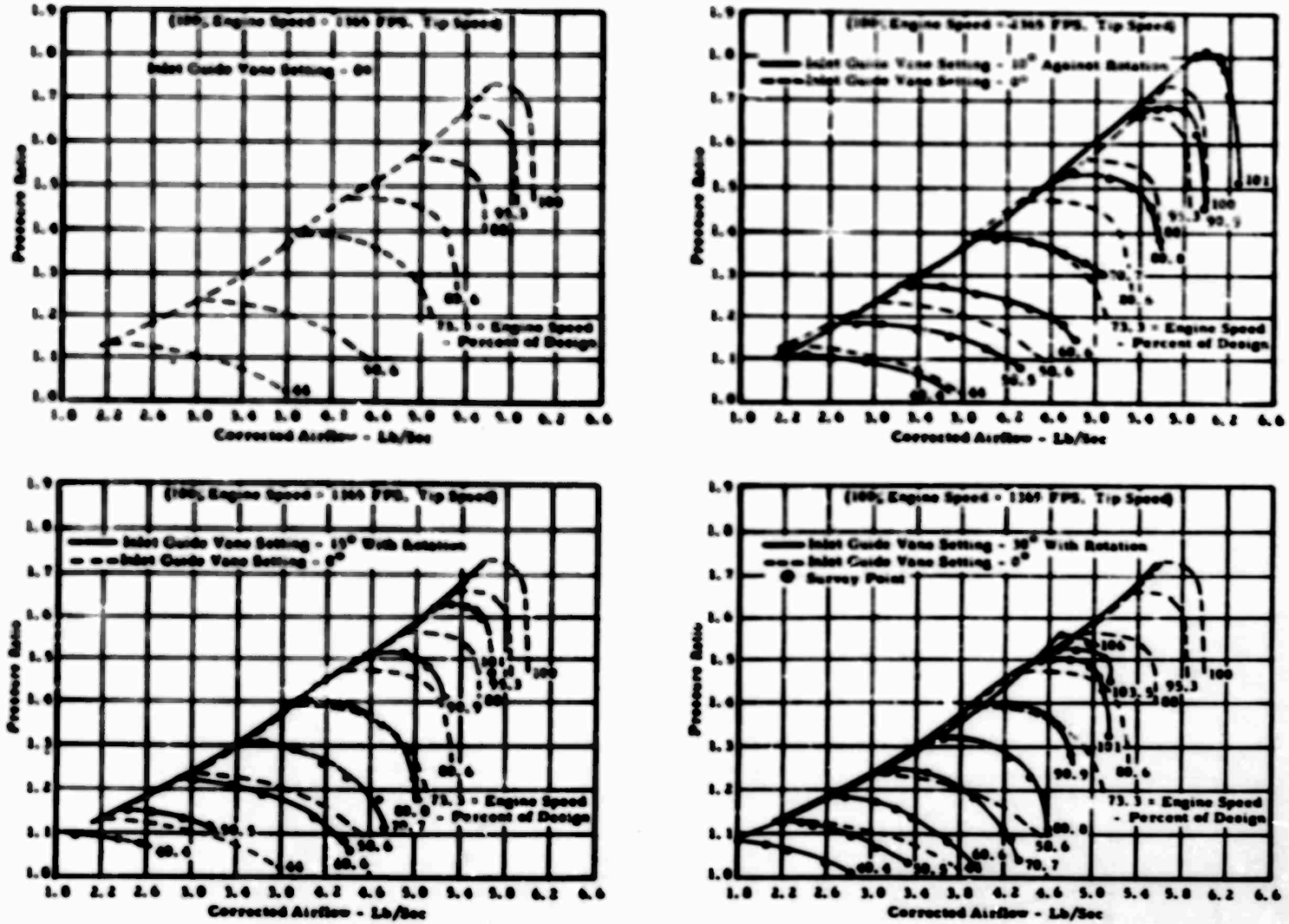

Figure 30. Test Results for Single-Stage Transonic Axial Rotor With Various Inlet Guide Vane Settings.

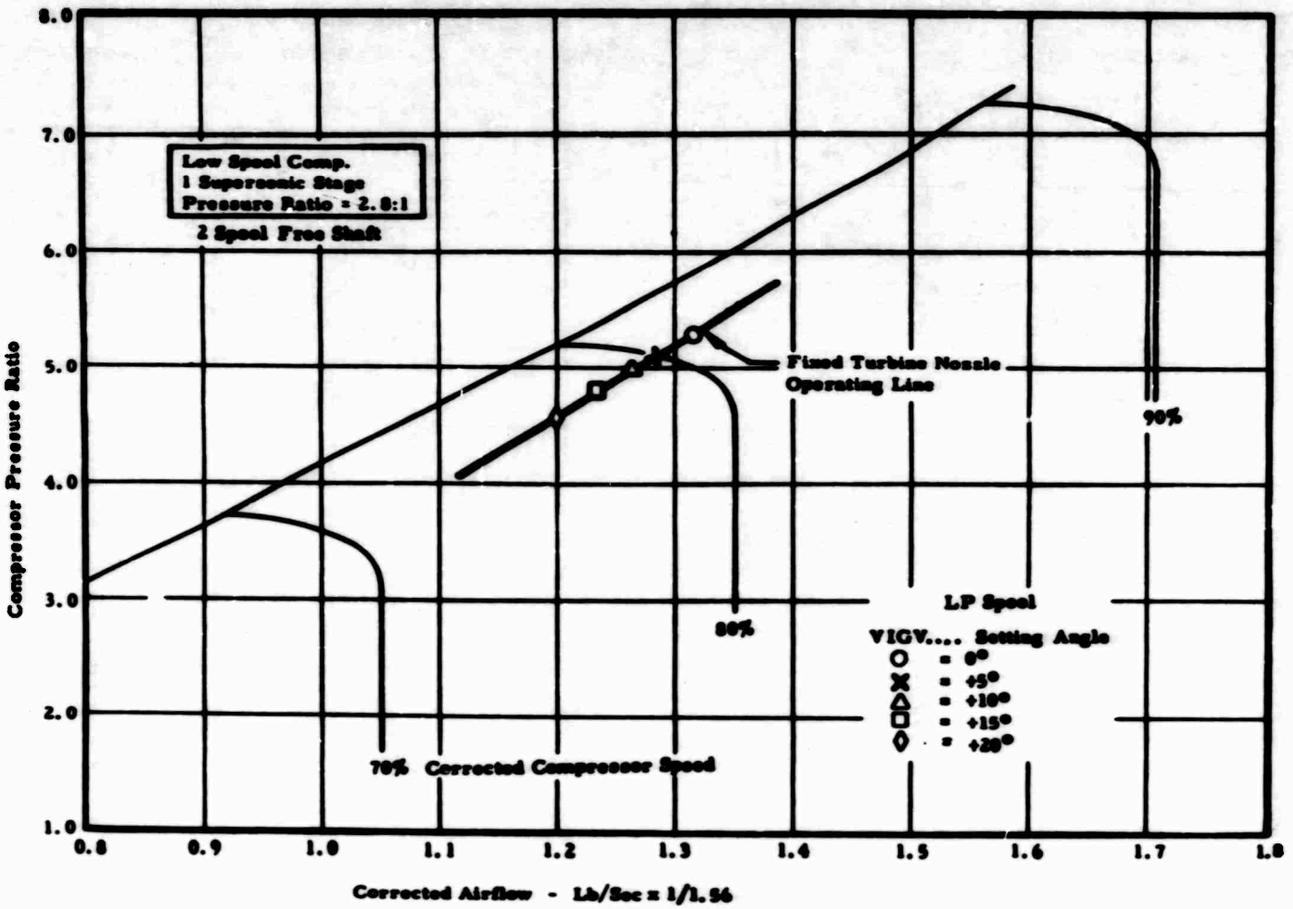

Figure 31. Estimated Performance Map for High Pressure Ratio Centrifugal Compressor With High Spool Operating Line.

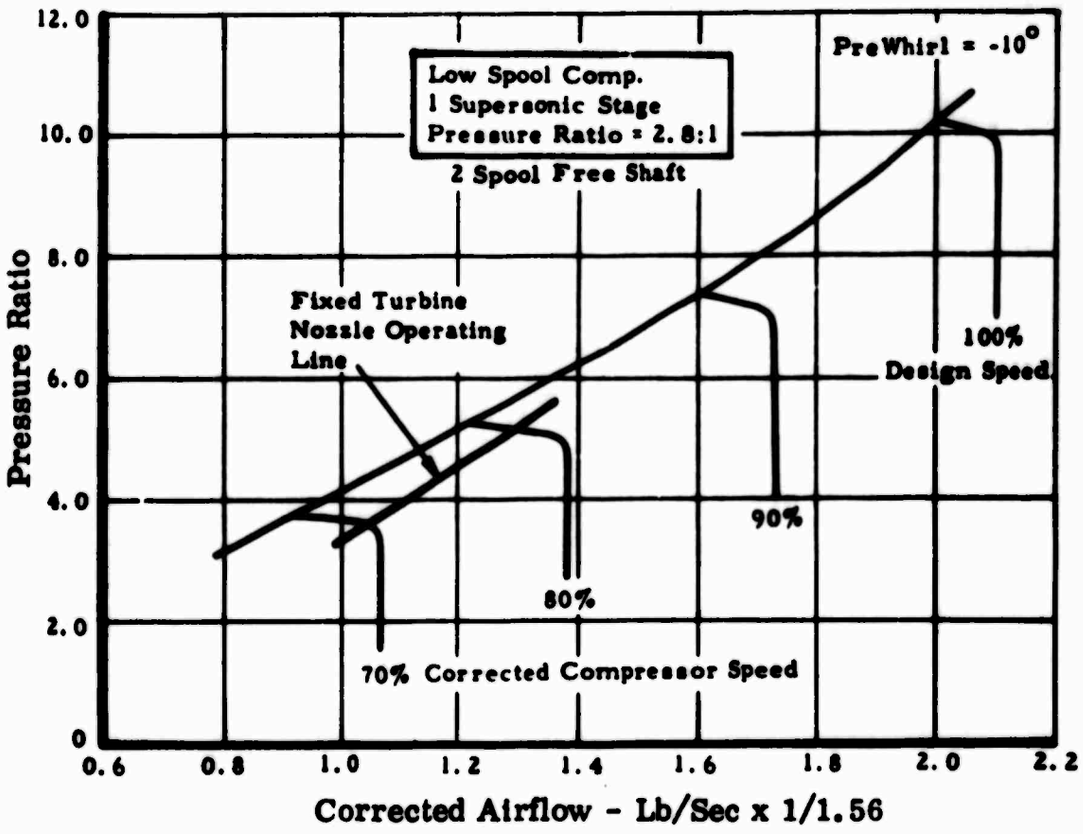

Figure 32. Estimated Performance Map for High Pressure Ratio Centrifugal Compressor With High Spool Operating Line.

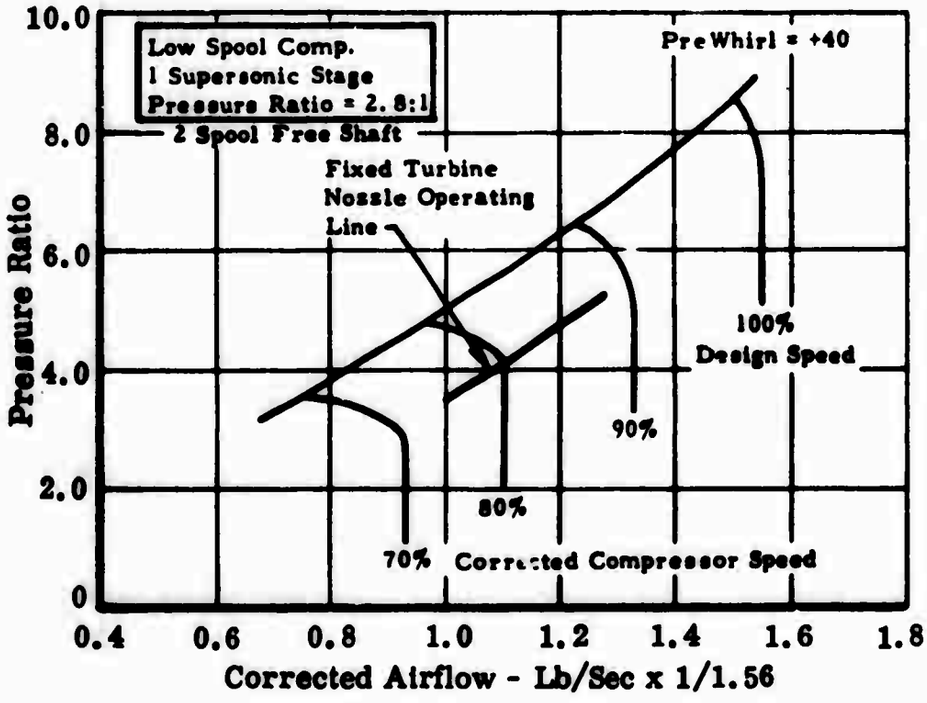

Figure 33. Estimated Performance Map for High Pressure Ratio Centrifugal Compressor With High Spool Operating Line.

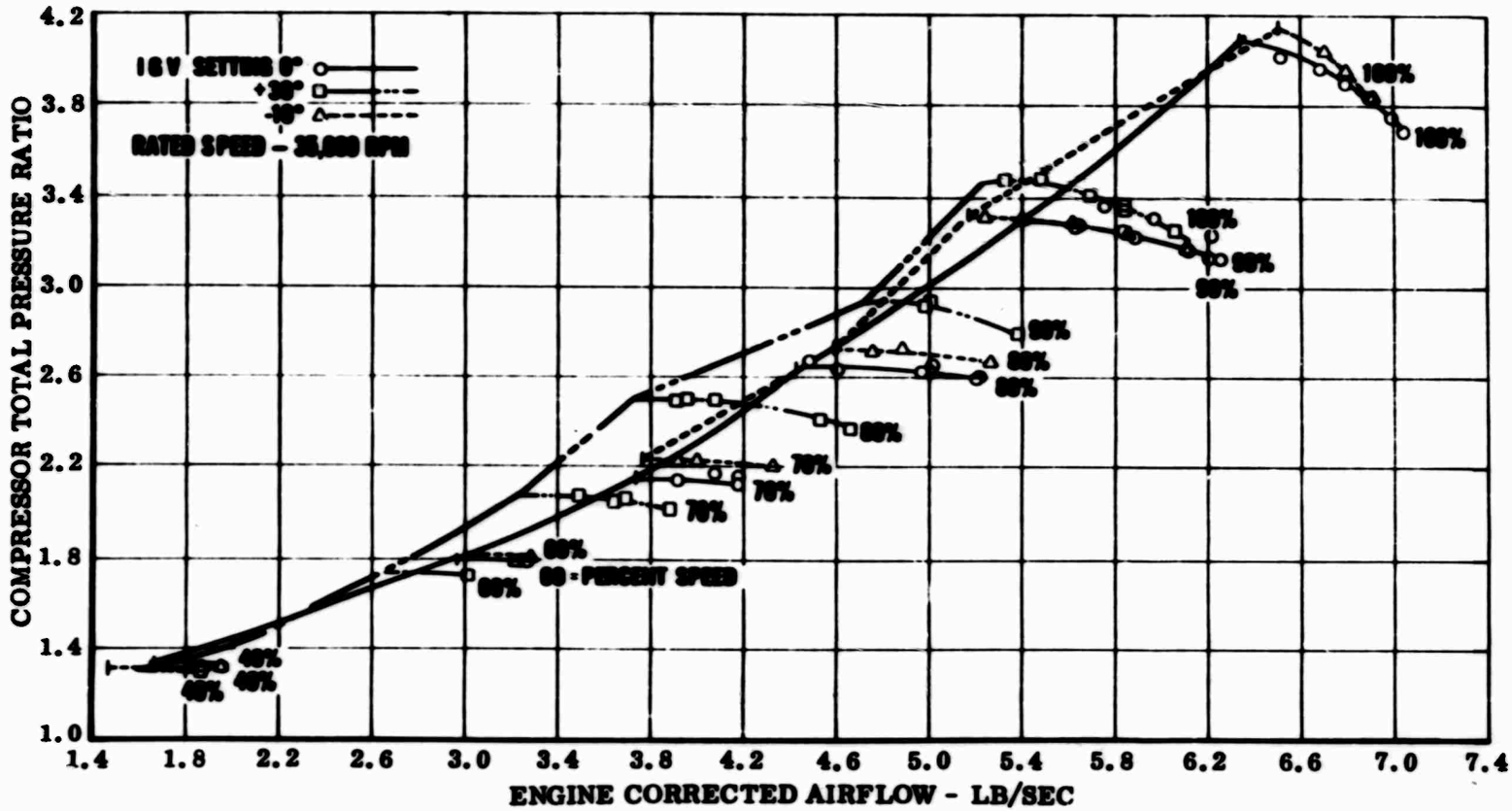

Figure 34. Continental Test Data for Single-Stage Centrifugal Compressor With Variable Inlet Guide Vanes.

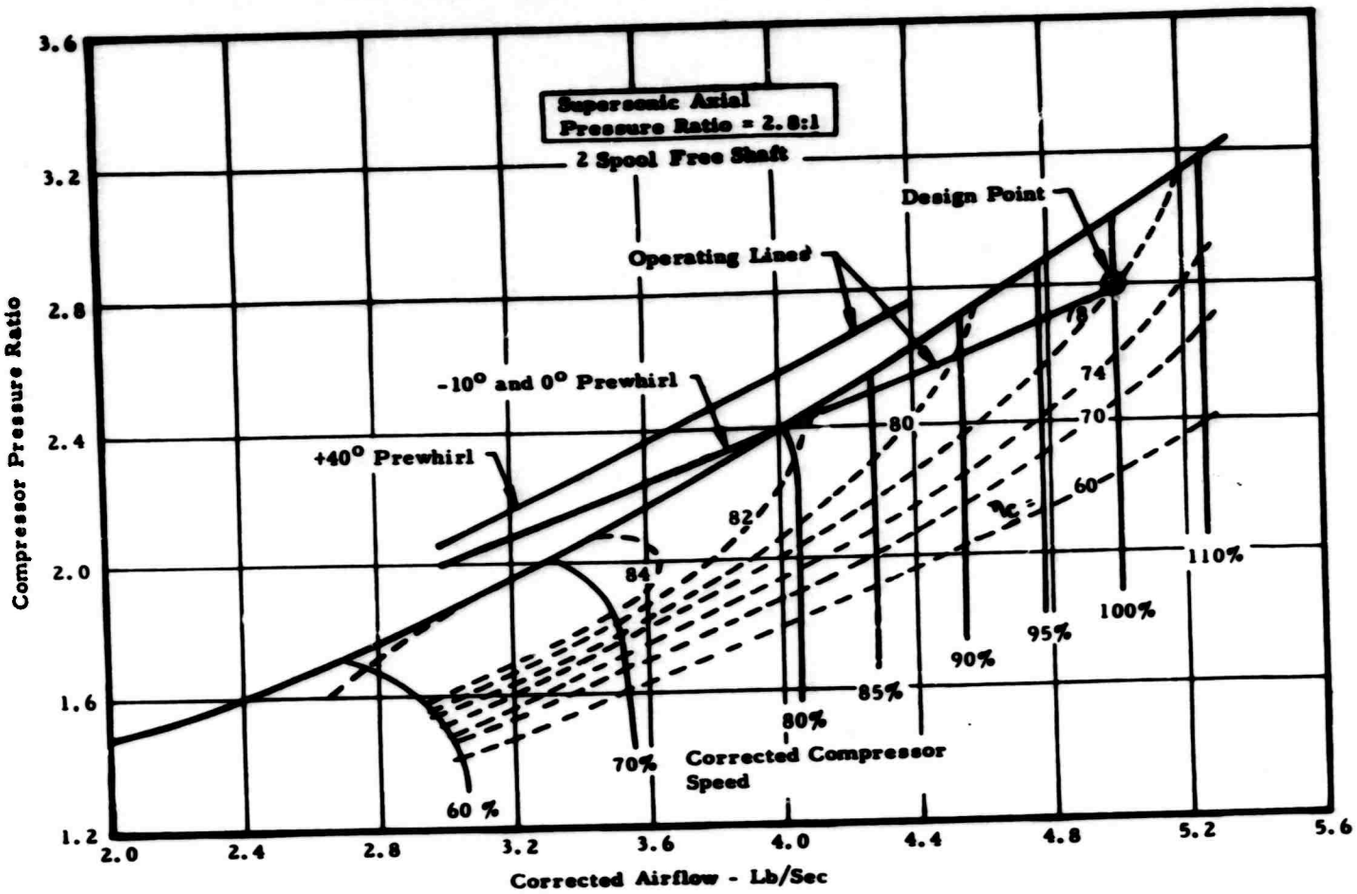

Figure 35. Estimated Performance Map for Single-Stage Supersonic Compressor With Low Spool Operating Lines.

Two-Spool Fixed (Connected) Power Turbine

Design Point Analysis. A summary of the design point data is shown in Table VIII. The design point was established for each of the two-spool fixed (connected) power turbine cycles. The complete output computation for these points is included in Tables IX through XII, respectively. The engine station designation is presented in Figure 36. The symbols used on the computer output are given below and on page 69.

TABLE VIII
DESIGN POINT DATA

	One Supersonic Stage		Two Transonic Stages	
Axial Pressure Ratio	2.8:1	3.1:1	2.8:1	3.1:1
SHP	1056	1033	1106	1088
BSFC Lb/HP-Hr	0.466	0.469	0.449	0.449
T7-TIT ^{o}R	2960	2960	2960	2960
P_5/P_2	16.0	16.77	16.55	17.36
Eff. LP Comp.- %	78	76.5	84	82.5
Eff. HP Comp.- %	79.9	79.8	79.9	79.8
Eff. LP Turb. - %	86.5	86.5	86.5	86.5
Eff. HP Turb. - %	83.9	83.9	83.9	83.9

All of the above points represent comparable matches along the given centrifugal operating line.

The off-design work carried on for two-spool fixed (connected) power turbine engines is discussed below.

Low Spool = One Supersonic Stage

Axial Pressure Ratio = 2.8:1. Figure 37 shows the operating lines, for selected high pressure spool mechanical speeds, on the low-pressure spool compressor map. Figures 38 through 40 present selected engine performance characteristics.

SYMBOLS

TA	-	Ambient temperature - ^{o}R
T	-	Temperature at appropriate station - ^{o}R
EFFECT	-	Heat exchanger effectiveness
DP/PHC	-	Heat exhcanger pressure loss - cold

TABLE IX

DESIGN POINT PERFORMANCE, TWO-SPOOL FIXED POWER TURBINE, SUPERSONIC AXIAL COMPRESSOR 2.8:1 PRESSURE RATIO

OUTPUT 30.040

TA	5.1868E+02	PA	1.4695E+01	NL/RTH2	1.0000E+02	NH/RTH4	8.3437E+01
T2	5.1868E+02	P2	1.4622E+01	WRTH/D2	5.0251E+00	WRTH/D4	2.1509E+00
T3	7.4505E+02	P3	4.0942E+01	P3/P2	2.8000E+00	P5/P4	5.7142E+00
T4	7.4505E+02	P4	4.0942E+01	EAT CL	7.8000E-01	ETA CH	7.9880E-01
T5	1.3166E+03	P5	2.3395E+02	ETAC AV	7.4674E-01	P5/P2	1.6000E+01
T6	1.3166E+03	P6	2.3395E+02	NL/RTH9	4.6603E+01	NH/RTH7	4.2594E+01
T7	2.9600E+03	P7	2.2343E+02	WN/D609	1.4319E+00	WN/D607	5.5232E-01
T8	2.4806E+03	P8	8.6178E+01	DHT/TH9	4.4574E+01	DHT/TH7	2.6498E+01
T9	2.4806E+03	P9	8.6178E+01	ETA TL	8.6600E-01	ETA TH	8.3900E-01
T10	1.7733E+03	P10	1.5701E+01	P9/P10	5.4885E+00	P7/P8	2.5926E+00
T11	1.7733E+03	P11	1.4916E+01	NTL	1.0000E+02	NTH	1.0000E+02
T12	1.7644E+03	P12	1.4916E+01	DHTL	2.0700E+02	DHTH	1.4605E+02
EFFECT	0.0000E-99	P13	1.4916E+01	DHTL/NL	2.0700E-02	DHTH/NH	1.4605E-02
DP/PHC	0.0000E-99	TAU H	0.0000E-99	P12/PA	1.0150E+00	ETAT AV	0.0000E-99
DP/PHH	0.0000E-99	TAU L	0.0000E-99	P13/PA	1.0149E+00	AJ	1.0925E+02
FN	4.7911E+01	FG	4.7911E+01	DP/PN	0.0000E-99	F/A	2.7951E-02
SHP	1.0566E+03	BSFC	4.6663E-01	ESHP	1.0758E+03	EBSFC	4.5831E-01

TABLE X

DESIGN POINT PERFORMANCE, TWO-SPOOL FIXED POWER TURBINE SUPERSONIC AXIAL COMPRESSOR, 3.1:1 PRESSURE RATIO

OUTPUT 30.040

TA	5.1868E+02	PA	1.4695E+01	NL/RTH2	1.0000E+02	NH/RTH4	8.1765E+01
T2	5.1868E+02	P2	1.4622E+01	WRTH/D2	5.0251E+00	WRTH/D4	1.9825E+00
T3	7.7584E+02	P3	4.5329E+01	P3/P2	3.1000E+00	P5/P4	5.4100E+00
T4	7.7584E+02	P4	4.5329E+01	EAT CL	7.6500E-01	ETA CH	7.9765E-01
T5	1.3463E+03	P5	2.4523E+02	ETAC AV	7.3565E-01	P5/P2	1.6771E+01
T6	1.3463E+03	P6	2.4523E+02	NL/RTH9	4.6407E+01	NH/RTH7	4.2592E+01
T7	2.9600E+03	P7	2.3419E+02	WN/D609	1.3674E+00	WN/D607	5.2668E-01
T8	2.4796E+03	P8	9.0203E+01	DHT/TH9	4.5518E+01	DHT/TH7	2.6528E+01
T9	2.4796E+03	P9	9.0203E+01	ETA TL	8.6600E-01	ETA TH	8.3900E-01
T10	1.7562E+03	P10	1.5701E+01	P9/P10	5.7449E+00	P7/P8	2.5963E+00
T11	1.7562E+03	P11	1.4916E+01	NTL	1.0000E+02	NTH	1.0000E+02
T12	1.7482E+03	P12	1.4916E+01	DHTL	2.1134E+02	DHTH	1.4623E+02
EFFECT	0.0000E-99	P13	1.4916E+01	DHTL/NL	2.1134E-02	DHTH/NH	1.4623E-02
DP/PHC	0.0000E-99	TAU H	0.0000E-99	P12/PA	1.0150E+00	ETAT AV	0.0000E-99
DP/PHH	0.0000E-99	TAU L	0.0000E-99	P13/PA	1.0149E+00	AJ	1.0870E+02
FN	4.7670E+01	FG	4.7670E+01	DP/PN	0.0000E-99	F/A	2.7483E-02
SHP	1.0331E+03	BSFC	4.6925E-01	ESHP	1.0522E+03	EBSFC	4.6075E-01

TABLE XI

DESIGN POINT PERFORMANCE, TWO-SPOOL FIXED POWER TURBINE, TWO-STAGE TRANSONIC AXIAL COMPRESSOR, 2.8:1 PRESSURE RATIO

OUTPUT 30.040

TA	5.1868E+02	PA	1.4695E+01	NL/RTH2	1.0000E+02	NH/RTH4	8.4350E+01
T2	5.1868E+02	P2	1.4622E+01	WRTH/D2	5.0251E+00	WRTH/D4	2.1276E+00
T3	7.2901E+02	P3	4.0942E+01	P3/P2	2.8000E+00	P5/P4	5.9100E+00
T4	7.2901E+02	P4	4.0942E+01	EAT CL	8.4000E-01	ETA CH	7.9950E-01
T5	1.3025E+03	P5	2.4197E+02	ETAC AV	7.7445E-01	P5/P2	1.6548E+01
T6	1.3025E+03	P6	2.4197E+02	NL/RTH9	4.6409E+01	NH/RTH7	4.2595E+01
T7	2.9600E+03	P7	2.3108E+02	WN/D609	1.3874E+00	WN/D607	5.3414E-01
T8	2.4799E+03	P8	8.8964E+01	DHT/TH9	4.5247E+01	DHT/TH7	2.6547E+01
T9	2.4799E+03	P9	8.8964E+01	ETA TL	8.6600E-01	ETA TH	8.3900E-01
T10	1.7619E+03	P10	1.5701E+01	P9/P10	5.6660E+00	P7/P8	2.5974E+00
T11	1.7619E+03	P11	1.4916E+01	NTL	1.0000E+02	NTH	1.0000E+02
T12	1.7530E+03	P12	1.4916E+01	DHTL	2.1007E+02	DHTH	1.4631E+02
EFFECT	0.0000E-99	P13	1.4916E+01	DHTL/NL	2.1007E-02	DHTH/NH	1.4631E-02
DP/PHC	0.0000E-99	TAU H	0.0000E-99	P12/PA	1.0150E+00	ETAT AV	0.0000E-99
DP/PHH	0.0000E-99	TAU L	0.0000E-99	P13/PA	1.0149E+00	AJ	1.0892E+02
FN	4.7766E+01	FG	4.7766E+01	DP/PN	0.0000E-99	F/A	2.8174E-02
SHP	1.1061E+03	BSFC	4.4930E-01	ESHP	1.1252E+03	EBSFC	4.4168E-01

TABLE XII
DESIGN POINT PERFORMANCE, TWO-SPOOL FIXED POWER TURBINE,
TWO-STAGE TRANSONIC AXIAL COMPRESSOR, 3.1:1 PRESSURE RATIO

OUTPUT 30.040

TA	5.1868E+02	PA	1.4695E+01	NL/RTH2	1.0000E+02	NH/RTH4	8.2757E+01
T2	5.1868E+02	P2	1.4622E+01	WRTH/D2	5.0251E+00	WRTH/D4	1.9587E+00
T3	7.5734E+02	P3	4.5329E+01	P3/P2	3.1000E+00	P5/P4	5.6000E+00
T4	7.5734E+02	P4	4.5329E+01	EAT CL	8.2500E-01	ETA CH	7.9840E-01
T5	1.3293E+03	P5	2.5384E+02	ETAC AV	7.6555E-01	P5/P2	1.7360E+01
T6	1.3293E+03	P6	2.5384E+02	NL/RTH9	4.6408E+01	NH/RTH7	4.2593E+01
T7	2.9600E+03	P7	2.4242E+02	WN/D609	1.3222E+00	WN/D607	5.0895E-01
T8	2.4795E+03	P8	9.3309E+01	DHT/TH9	4.6227E+01	DHT/TH7	2.6547E+01
T9	2.4795E+03	P9	9.3309E+01	ETA TL	8.6600E-01	ETA TH	8.3900E-01
T10	1.7447E+03	P10	1.5701E+01	P9/P10	5.9427E+00	P7/P8	2.5980E+00
T11	1.7447E+03	P11	1.4916E+01	NTL	1.0000E+02	NTH	1.0000E+02
T12	1.7366E+03	P12	1.4916E+01	DHTL	2.1463E+02	DHTH	1.4633E+02
EFFECT	0.0000E-99	P13	1.4916E+01	DHTL/NL	2.1463E-02	DHTH/NH	1.4633E-02
DP/PHC	0.0000E-99	TAU H	0.0000E-99	P12/PA	1.0150E+00	ETAT AV	0.0000E-99
DP/PHH	0.0000E-99	TAU L	0.0000E-99	P13/PA	1.0149E+00	AJ	1.0837E+02
FN	4.7524E+01	FG	4.7524E+01	DP/PN	0.0000E-99	F/A	2.7752E-02
SHP	1.0884E+03	BSFC	4.4976E-01	ESHP	1.1074E+03	EBSFC	4.4204E-01

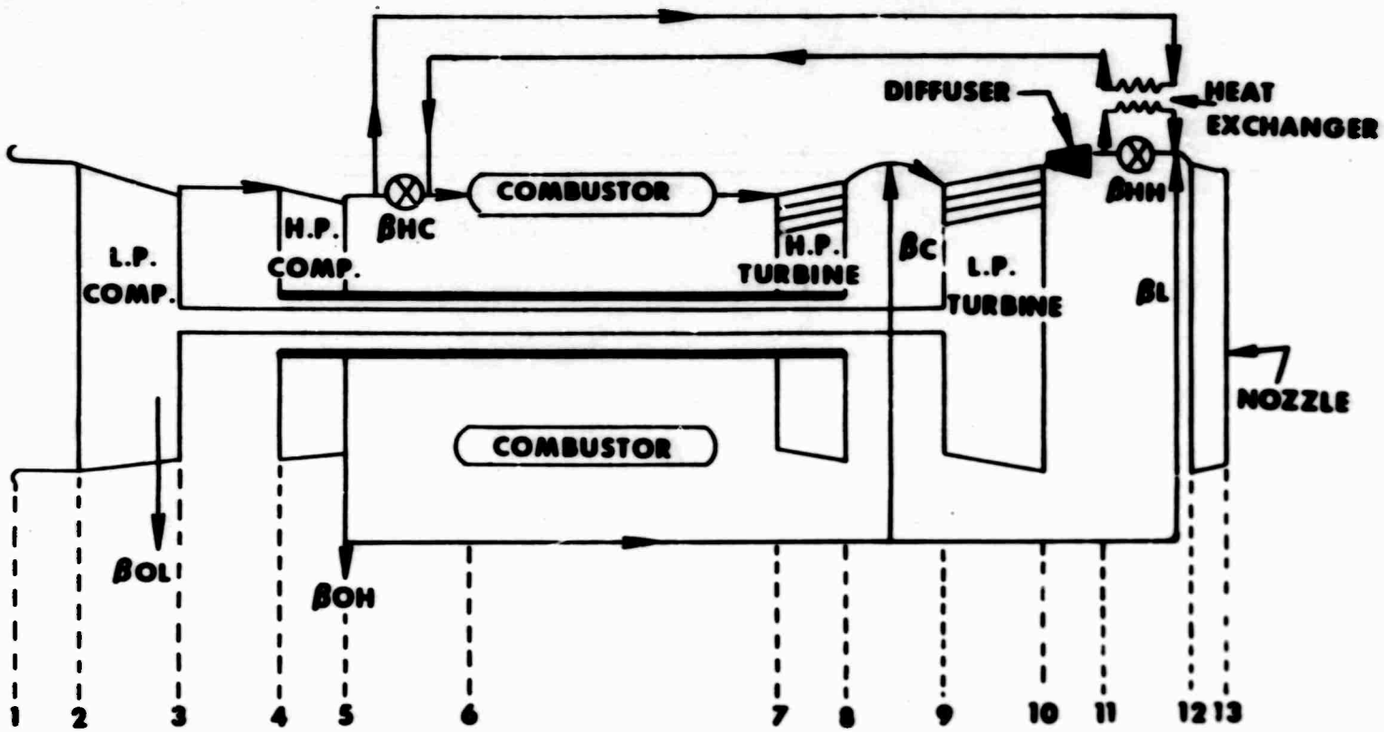

Figure 36. Schematic Drawing and Station Designation, Two-Spool Fixed Power Turbine, Turboshaft Engine.

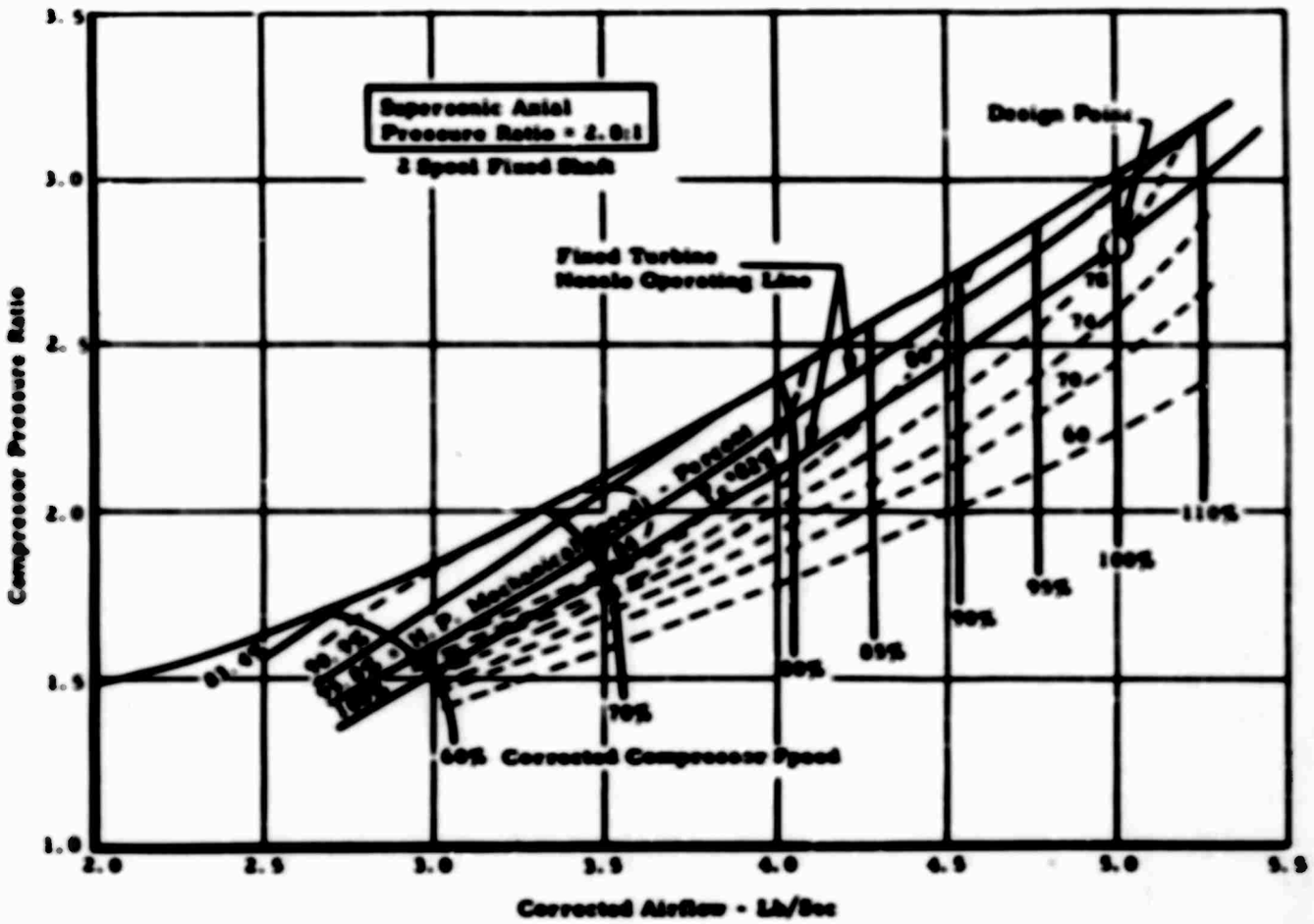

Figure 37. Estimated Performance Map for a Single-Stage Supersonic Compressor With Selected Low Spool Operating Lines.

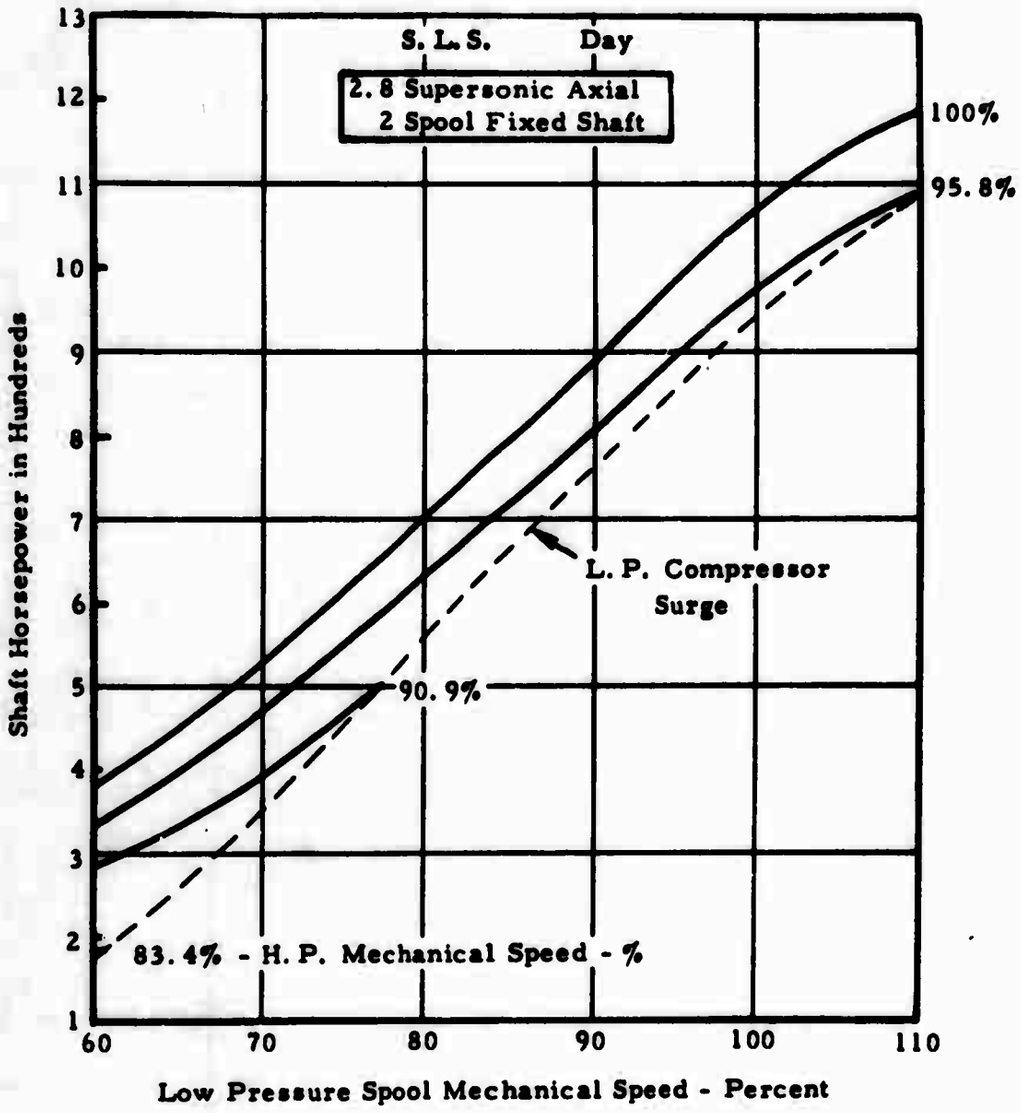

Figure 38. Estimated Horsepower Characteristics.

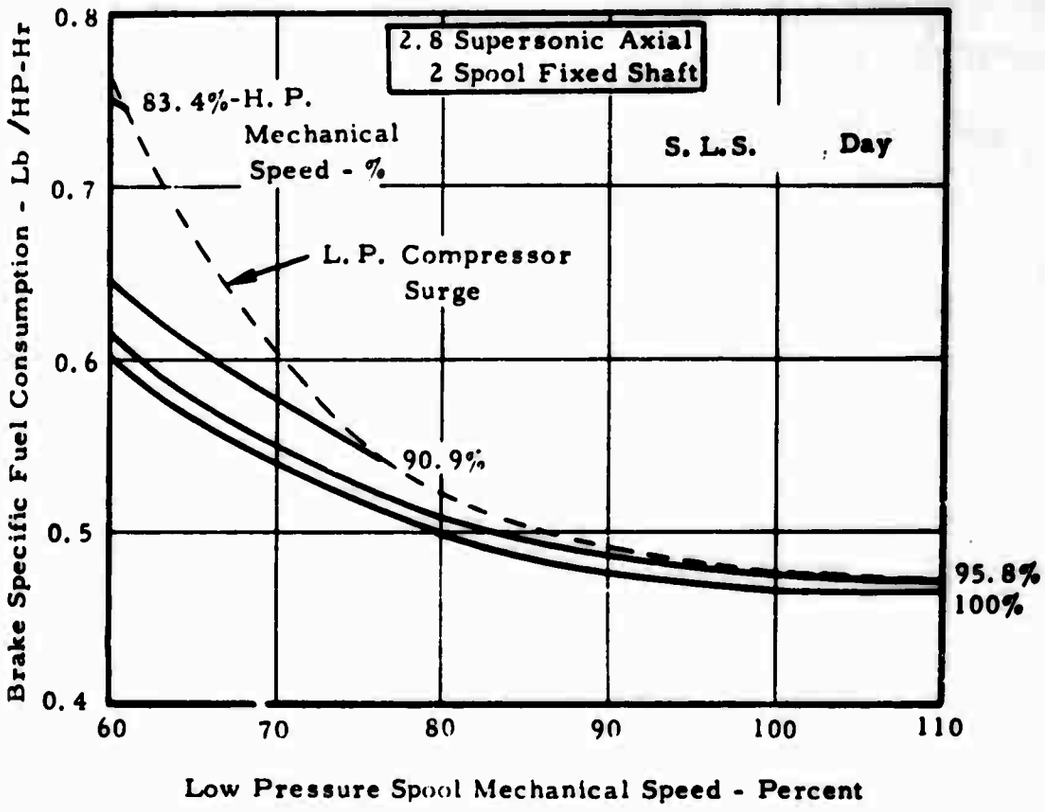

Figure 39. Estimated BSFC Characteristics.

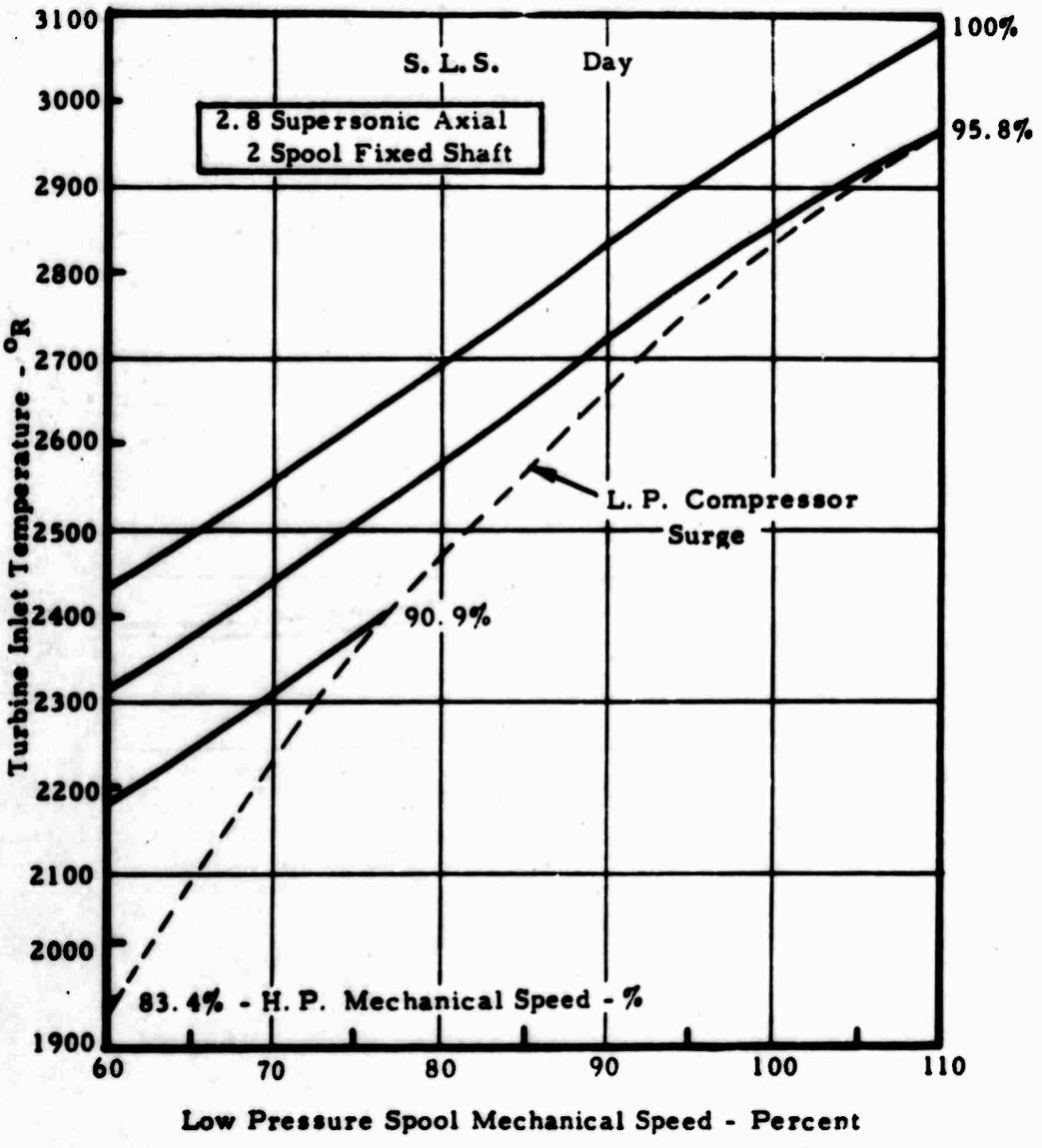

Figure 40. Estimated Gas Generator Turbine Inlet Temperature Characteristics.

DP/PHH	-	Heat exchanger pressure loss - hot
FN	-	Net thrust
SHP	-	Shaft horsepower
PA	-	Ambient pressure - PSIA
P	-	Pressure at appropriate station - PSIA
TAU H	-	Torque - HP compressor
TAU L	-	Torque - LP compressor
FG	-	Gross thrust
BSFC	-	Brake specific fuel consumption - Lb/SHP/Hr
NL/RTH2	-	Referred low pressure spool speed - $NL/\sqrt{\theta_2}$ - rpm
WRTH/D2	-	Referred airflow - $(W\sqrt{\theta}/\delta)_2$ - lb/sec
P_3/P_2	-	Low pressure spool compressor pressure ratio
ETA CL	-	Low pressure spool compressor adiabatic efficiency
ETAC AV	-	Overall compressor efficiency
NL/RTH 9	-	Referred low pressure turbine speed - $NL/\sqrt{\theta_{cr}})_9$ - rpm
WN/D609	-	Low pressure turbine speed - flow parameter - $(WN/\delta 60)_9$ - (lb-rev/sec^2)
DHT/TH9	-	Referred low pressure turbine work - $(\Delta h/\theta_{cr})_9$ - Btu/lb
ETA TL	-	Low pressure turbine adiabatic efficiency
P_9/P_{10}	-	Low pressure turbine pressure ratio
NTL	-	Low pressure turbine speed - rpm
DHTL	-	Low pressure turbine work - Btu/lb
DHTL/NL	-	Low pressure turbine work - speed parameter - $\Delta h/NL^2$
P12/PA	-	Exhaust nozzle total to static pressure ratio
P13/PA	-	Exhaust nozzle total to static pressure ratio
DP/PN	-	Exhaust nozzle pressure loss
ESHP	-	Equivalent shaft horsepower
NH/RTH4	-	Referred high pressure compressor speed - $N_H/\sqrt{\theta_4}$ - rpm
WRTH/D4	-	Referred high pressure compressor flow - $(W\sqrt{\theta}/\delta)_4$ - lb/sec
P_5/P_4	-	High pressure compressor pressure ratio
ETA CH	-	High pressure compressor adiabatic efficiency
P_5/P_2	-	Overall cycle pressure ratio
NH/RTH7	-	Referred high pressure turbine speed $(N_H/\sqrt{\theta_c})_7$ - rpm
WN/D607	-	High pressure turbine speed flow parameter $(WN/\delta 60)_7$ - lb-rev/sec^2
DHT/TH7	-	Referred high pressure turbine work - $(\Delta h/\theta_c)_7$ - Btu/lb
ETA TH	-	High pressure turbine adiabatic efficiency
P_7/P_8	-	High pressure turbine pressure ratio
NTH	-	High pressure turbine speed - rpm

DHTH	-	High pressure turbine work - Btu/lb
DHTH/NH	-	High pressure turbine work - speed parameter - $\Delta h/N_H 2$
ETAT AV	-	Overall turbine efficiency
AJ	-	Exhaust nozzle area
F/A	-	Fuel to air ratio
EBSFC	-	Equivalent brake specific fuel consumption - lb/SHP/hr

Axial Pressure Ratio = 3.1:1. Data similar to the above are presented in Figures 41 through 44 for the 3.1:1 axial stage. Figure 45 shows good operating margin on the high pressure spool for both levels of low spool pressure ratio.

These engine configurations do not show any significant performance change between the 2.8 and 3.1:1 pressure ratio low spool supersonic axial stage compressors.

Low Spool = Two Transonic Stages

Axial Pressure Ratio = 2.8:1. Figure 46 shows the operating lines for several high pressure spool mechanical speeds, on the low pressure compressor map. Figures 47 through 49 present selected engine performance characteristics.

Axial Pressure Ratio = 3.1:1. Data similar to the above are presented in Figures 50 through 53 for the 3.1:1 axial stage.

Figure 54 shows good surge margin on the high pressure compressor for both levels of low spool pressure ratio. Again, these engine configurations do not show any significant performance change when using either 2.8 or 3.1:1 pressure ratio transonic axial, low spool compressors. However, the transonic low spool compressor engines consistently provide a larger operating range (compare horsepower curves, Figures 38 and 47, and better BSFC, Figure 55) than the supersonic low spool compressor engines. This is due to the higher transonic compressor efficiency.

Variable Geometry Analysis - Two-Spool Fixed Shaft

The effect of variable area turbine nozzles on the low pressure spool turbine engine performance was investigated. The purpose of using variable geometry is to increase part-power turbine inlet temperature, thus increasing the cycle efficiency. With the two-spool fixed-shaft engine, the temperature gains were off-set by lower pressure ratios and compressor efficiencies. A BSFC comparison is provided in Figure 56.

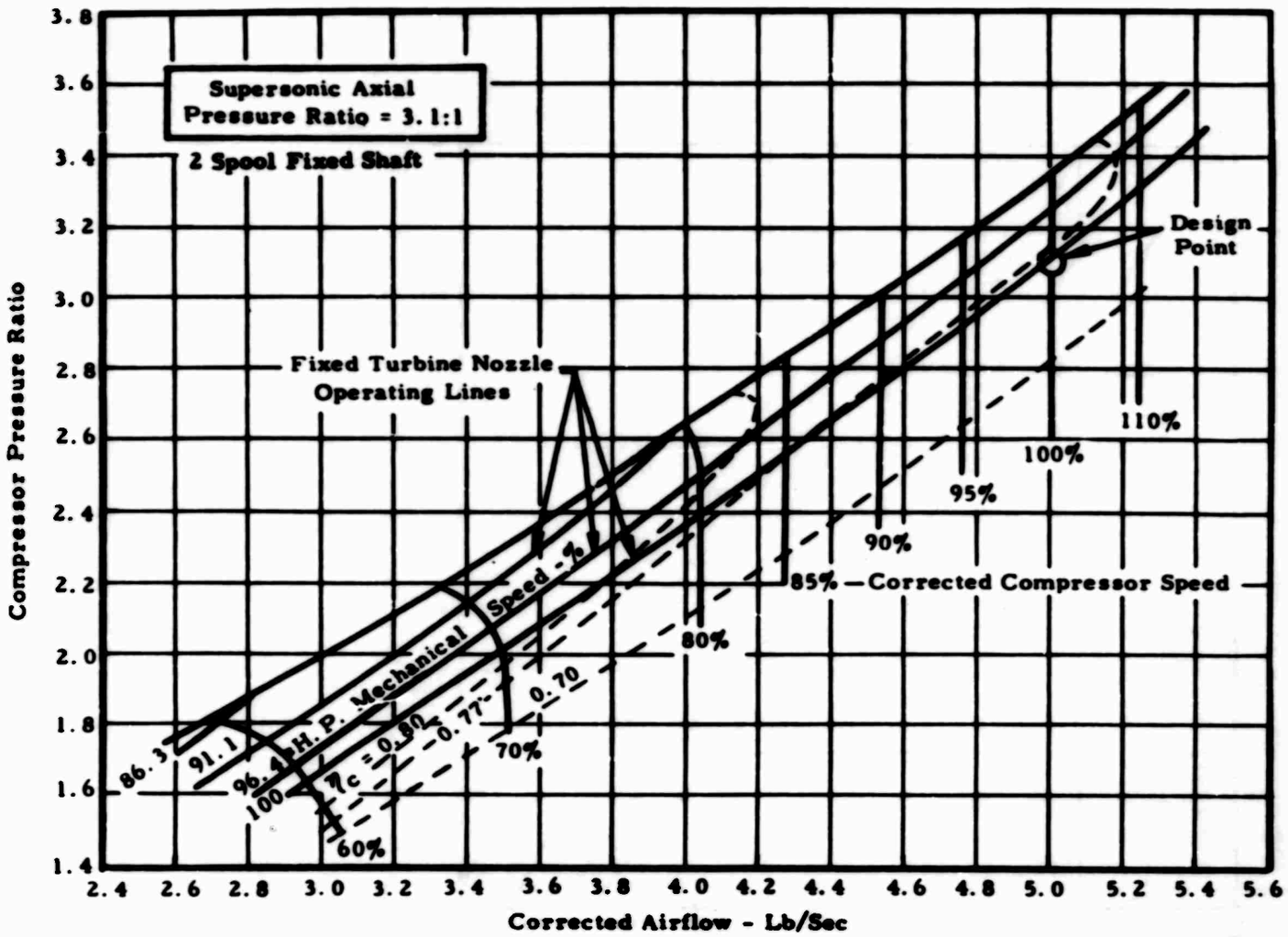

Figure 41. Estimated Performance Map for a Single-Stage Supersonic Compressor With Selected Low Spool Operating Lines.

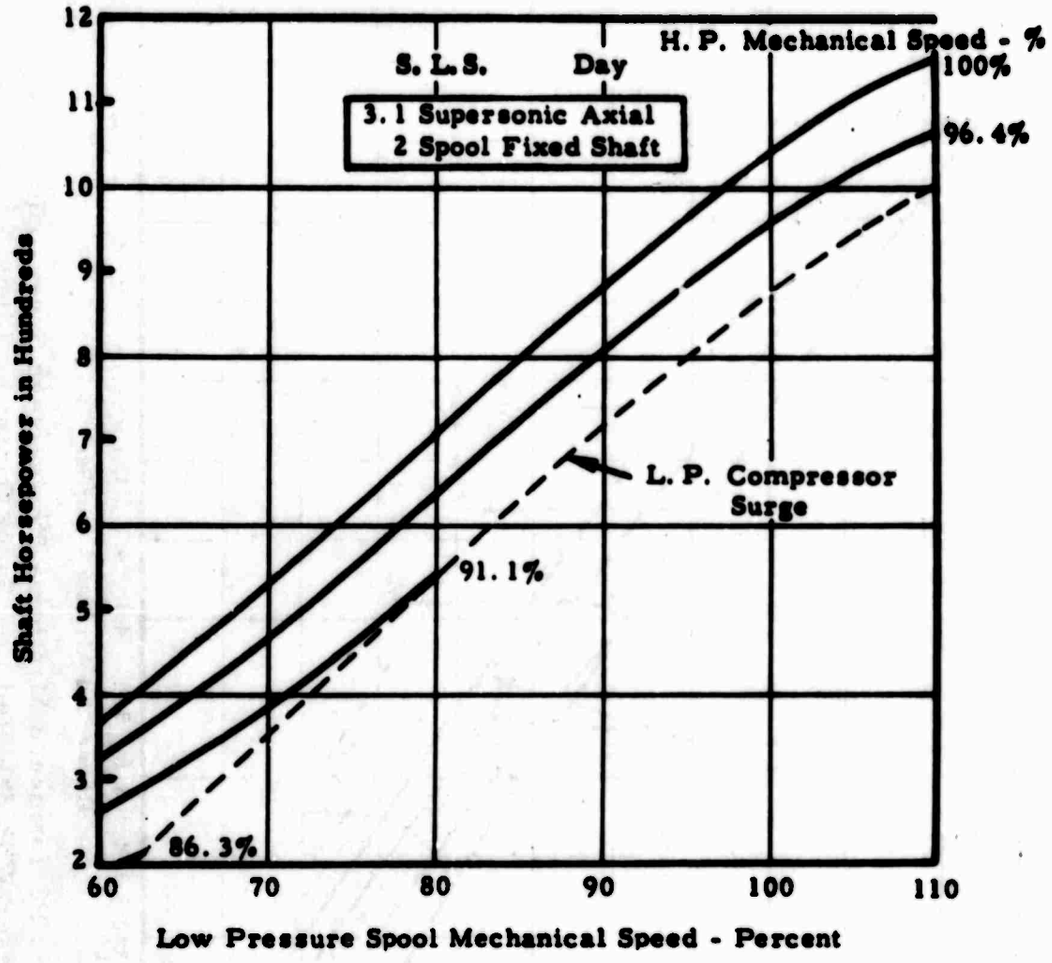

Figure 42. Estimated Horsepower Characteristics.

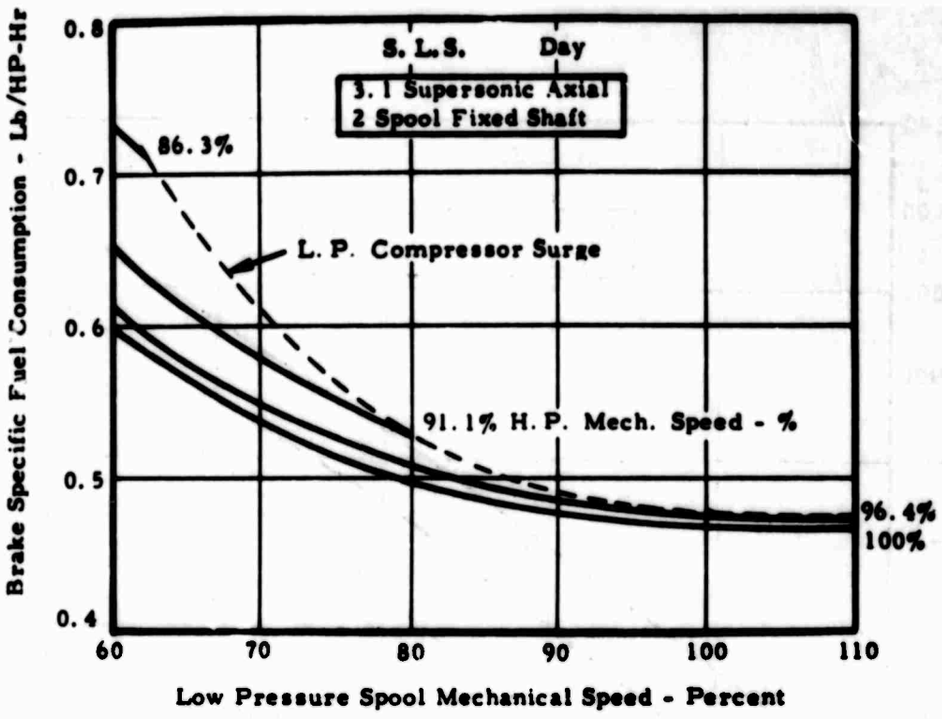

Figure 43. Estimated BSFC Characteristics.

Concurrent turbine structural and aerodynamic studies carried on with the thermodynamic studies also indicated that:

Combining the low pressure and power turbine to operate at the low pressure speed results in an overstressed design.

Reducing the stresses to acceptable level results in an undesirable aerodynamic low pressure spool turbine design.

Therefore, the fixed shaft configuration is less desirable than the free for both thermodynamic and structural reasons.

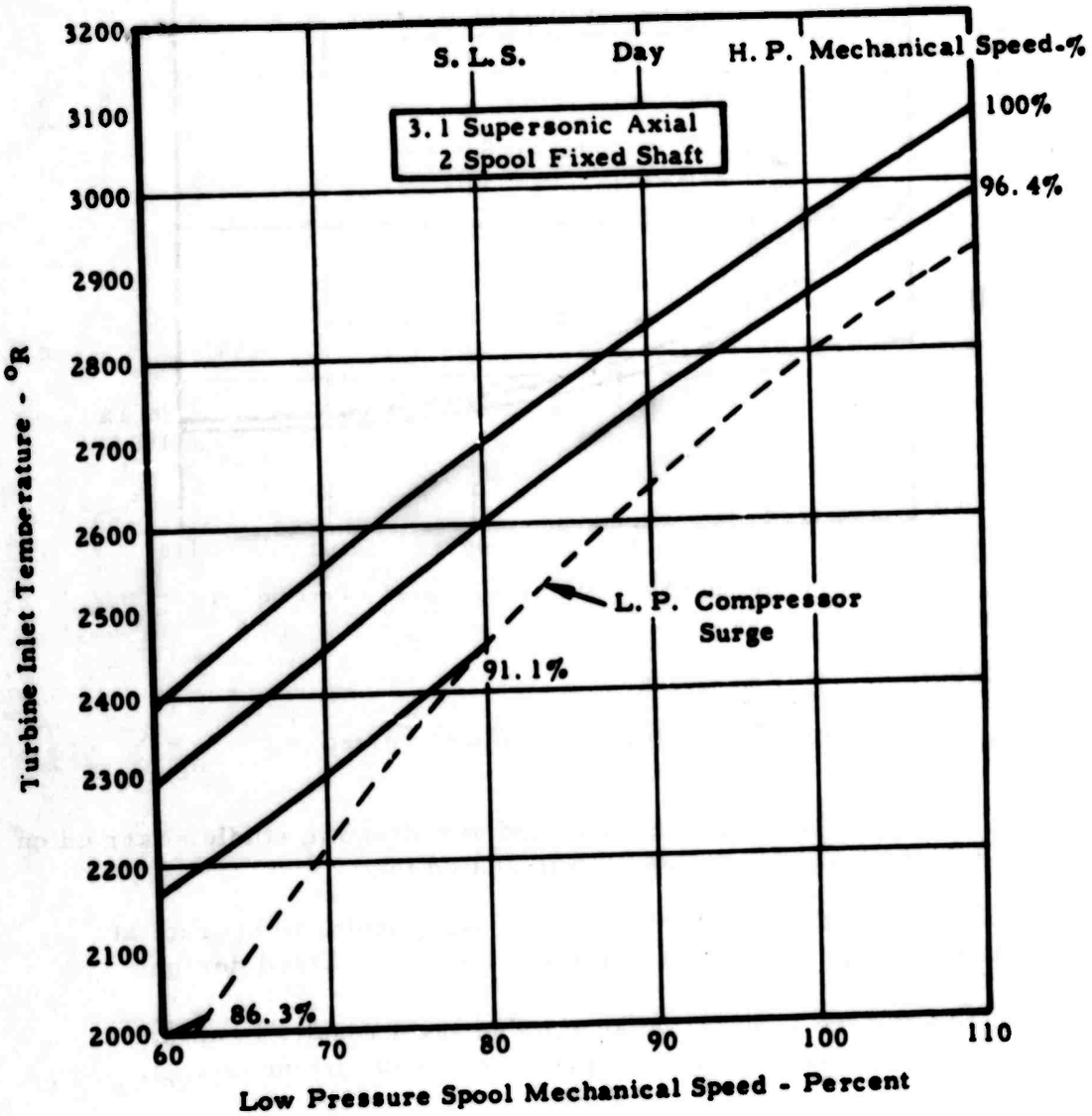

Figure 44. Estimated Gas Generator Turbine Inlet Temperature Characteristics.

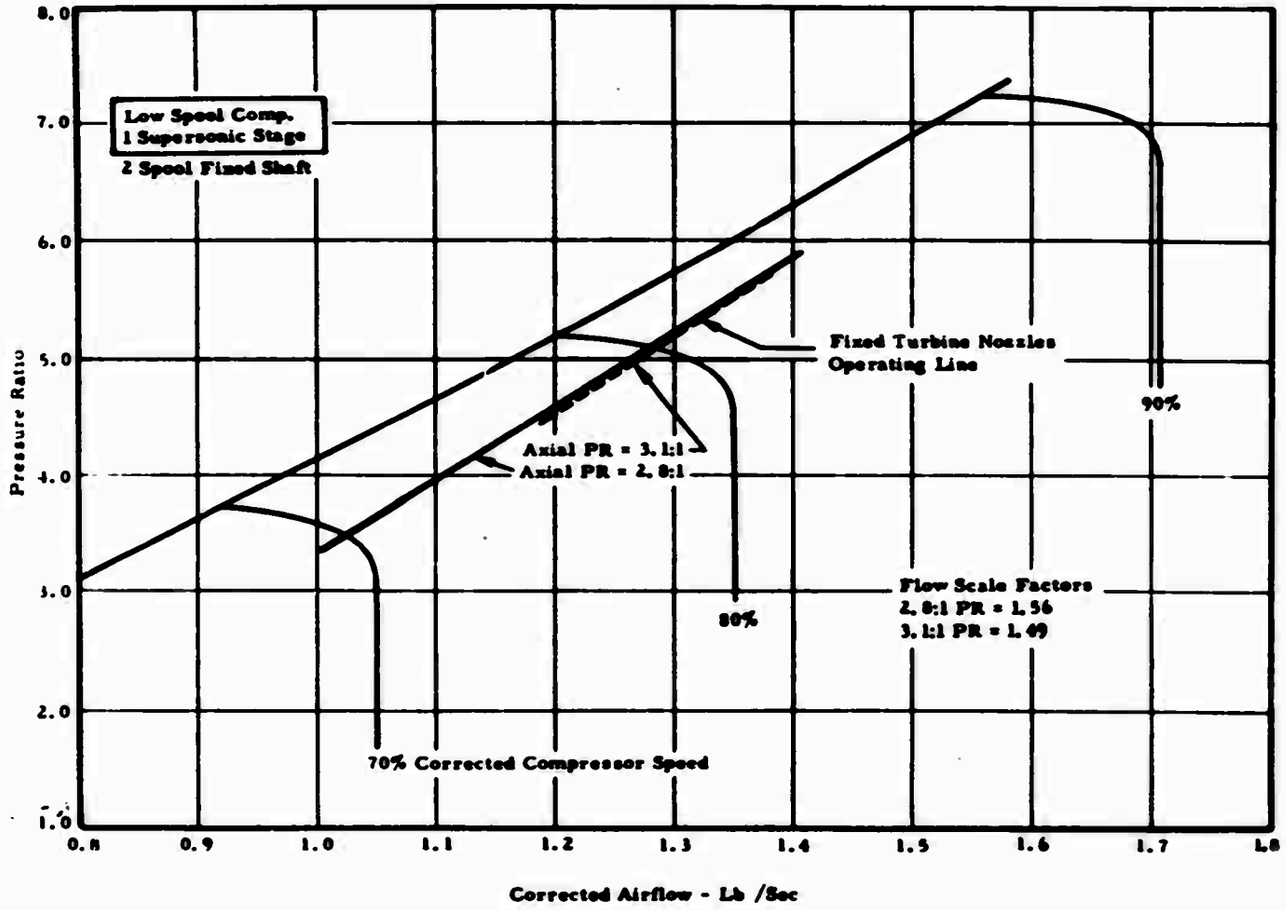

Figure 45. Estimated Performance Map for a High Pressure Ratio Centrifugal Compressor With High Spool Operating Lines.

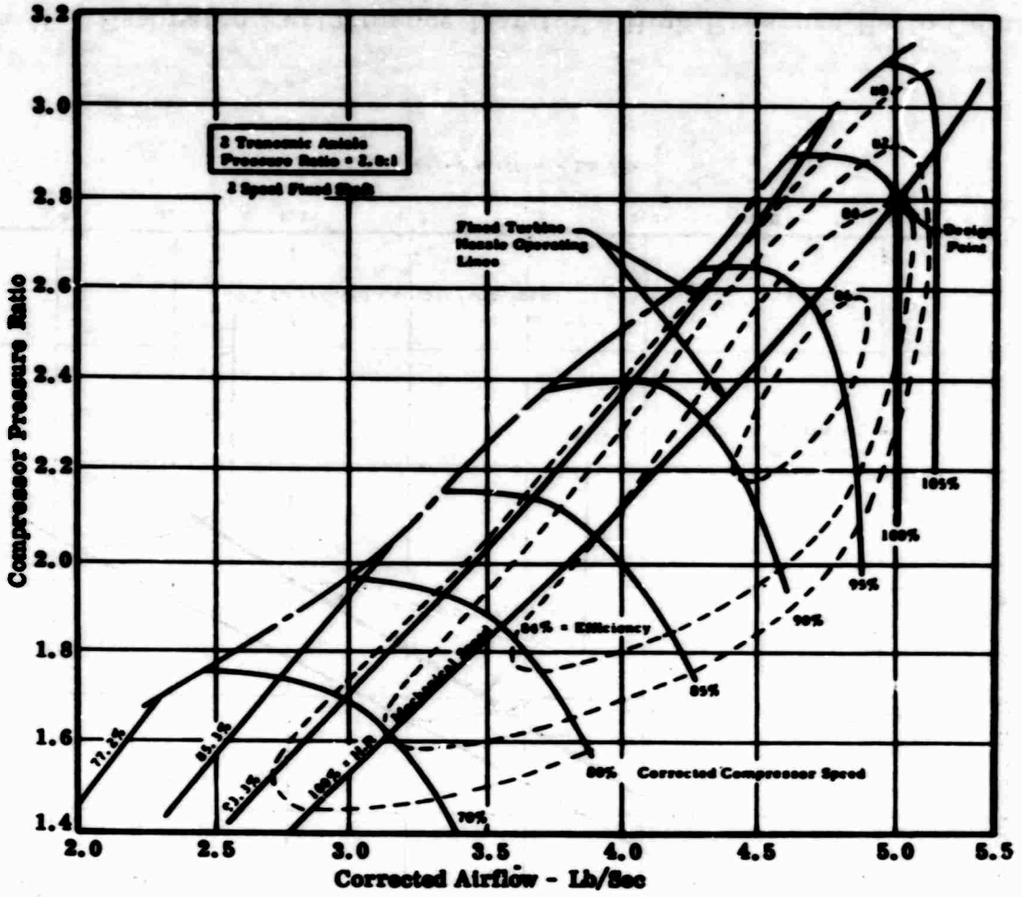

Figure 46. Estimated Performance Map for a Two-Stage Transonic Compressor With Selected Low Spool Operating Lines.

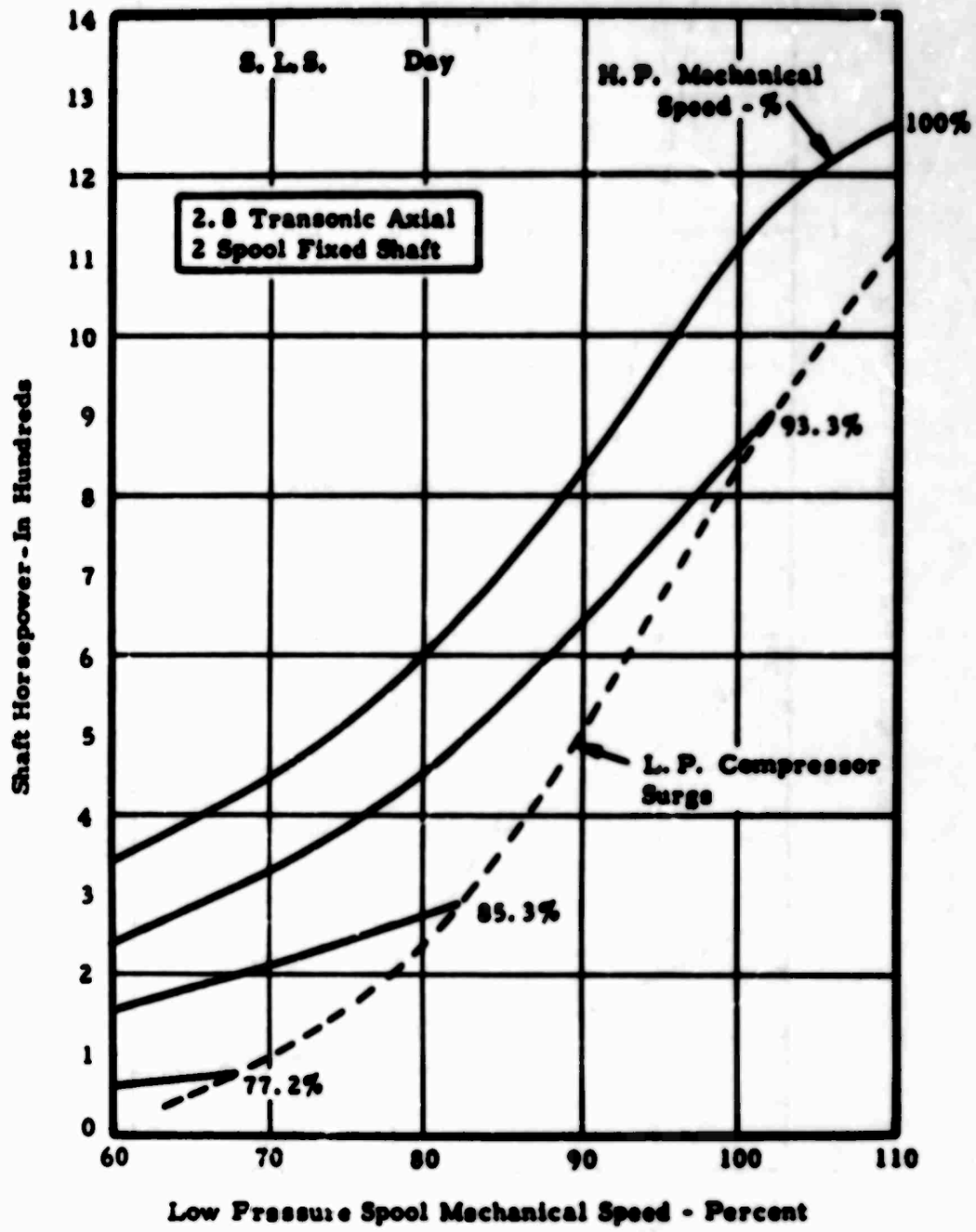

Figure 47. Estimated Horsepower Characteristics.

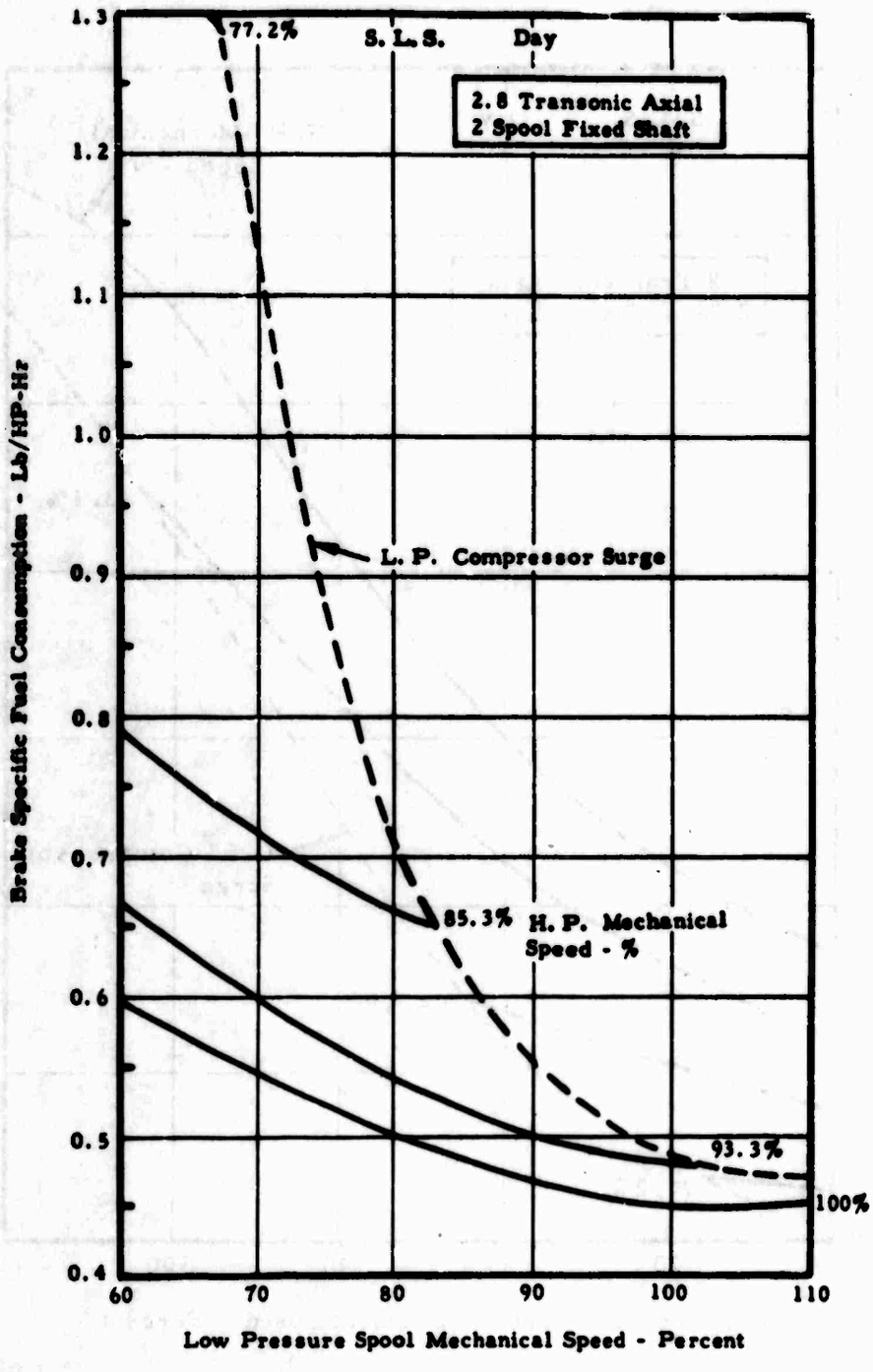

Figure 48. Estimated BSFC Characteristics.

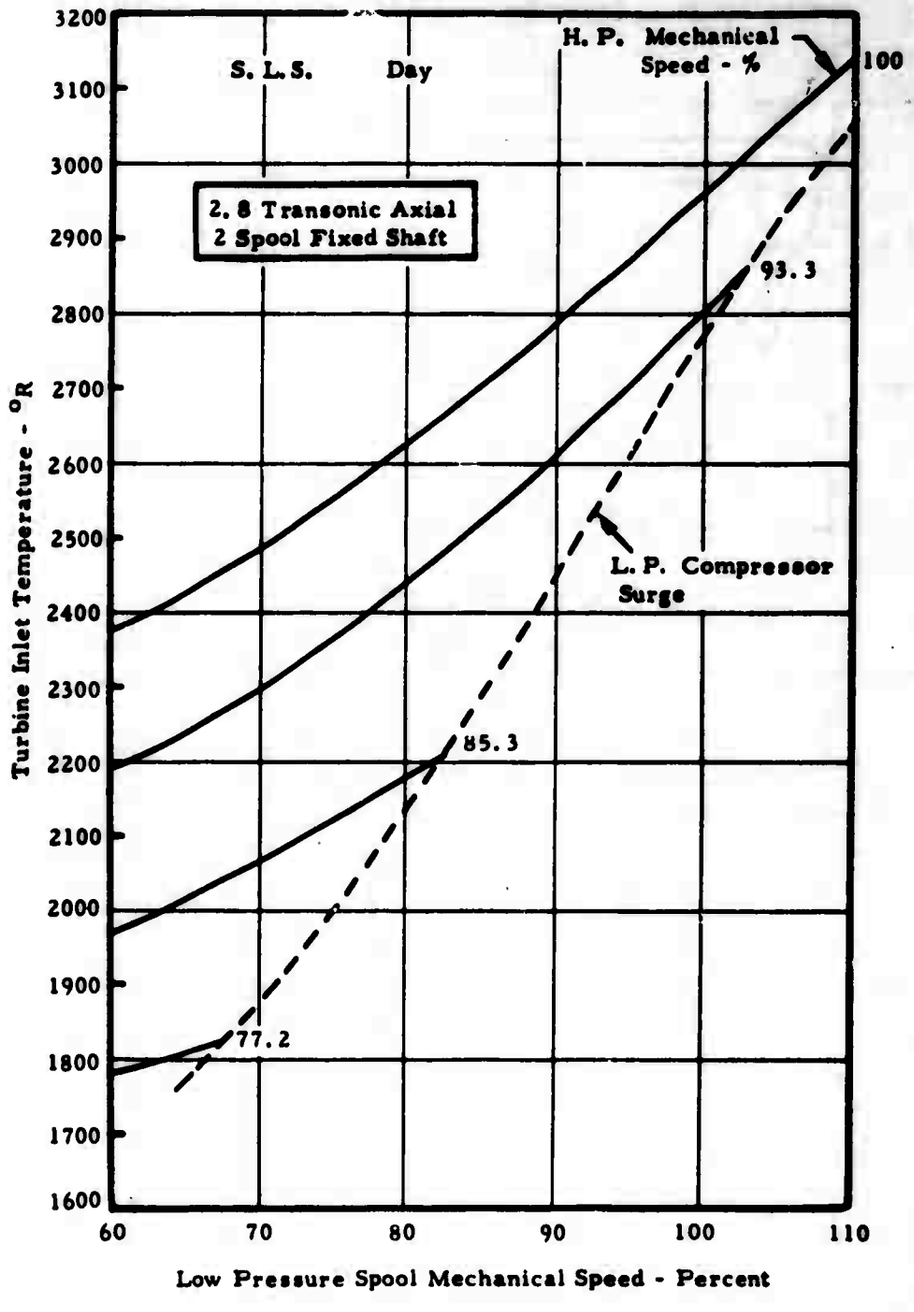

Figure 49. Estimated Gas Generator Turbine Inlet Temperature Characteristics.

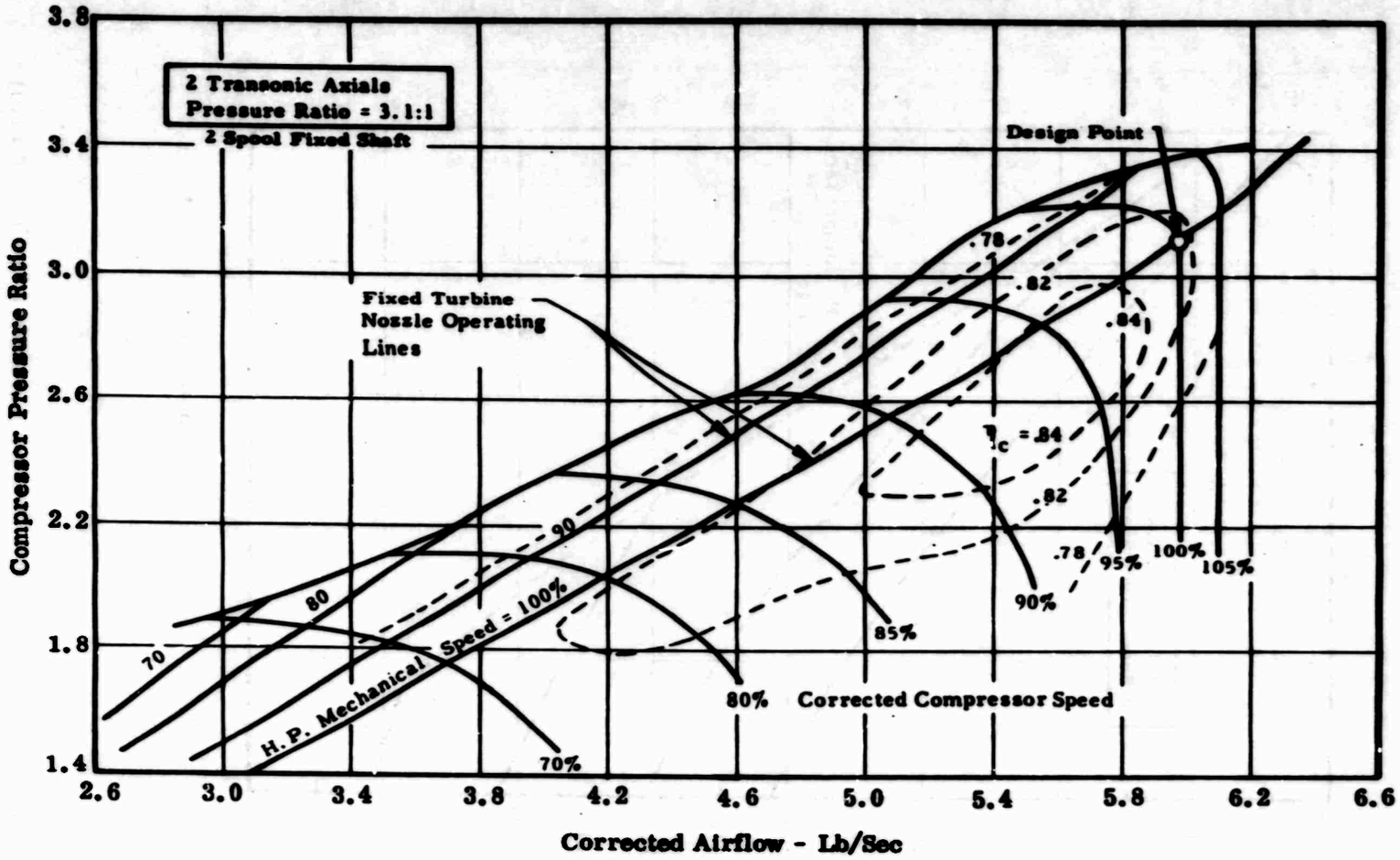

Figure 50. Estimated Performance Map for a Two-Stage Transonic Compressor With Selected Low Spool Operating Lines.

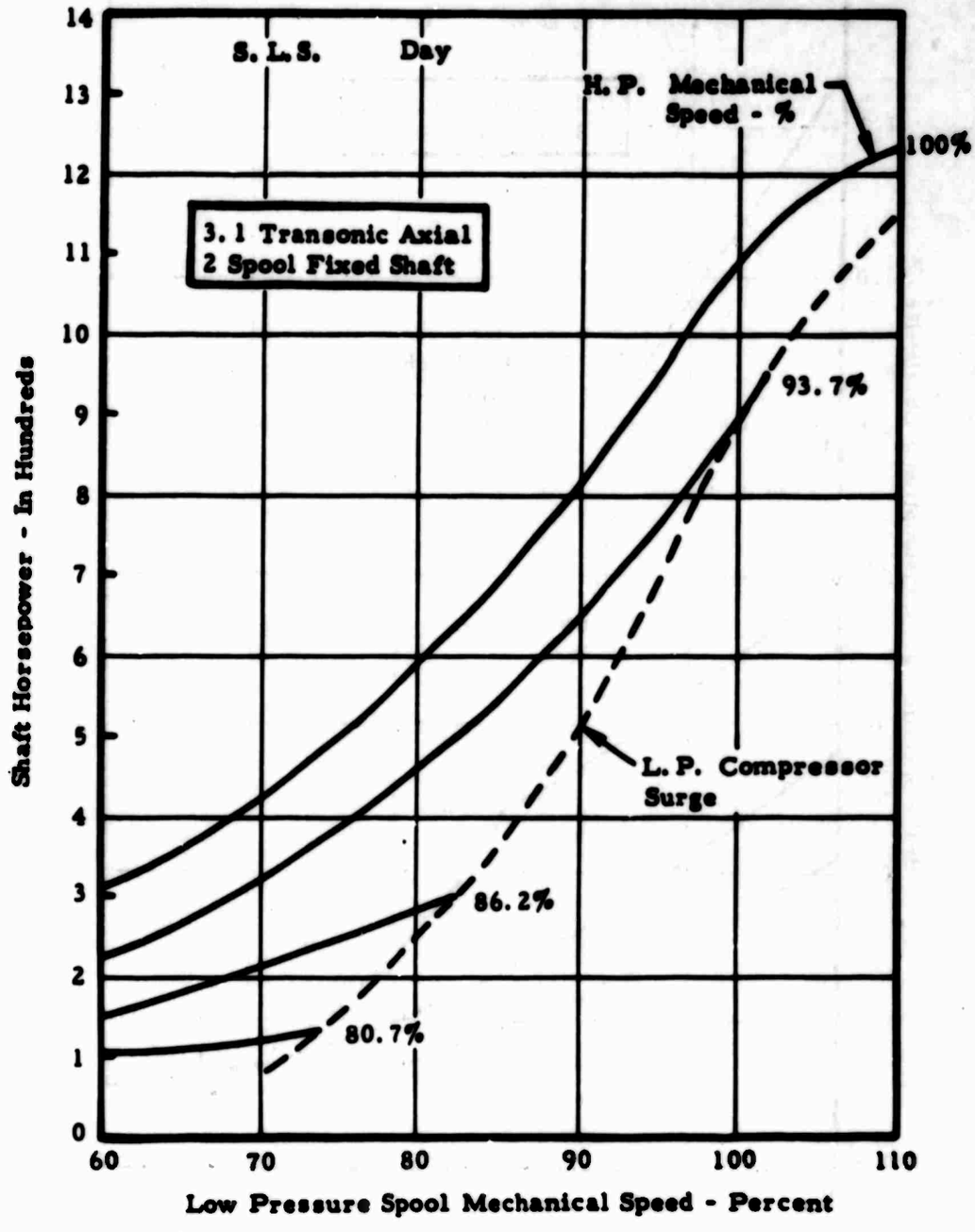

Figure 51. Estimated Horsepower Characteristics.

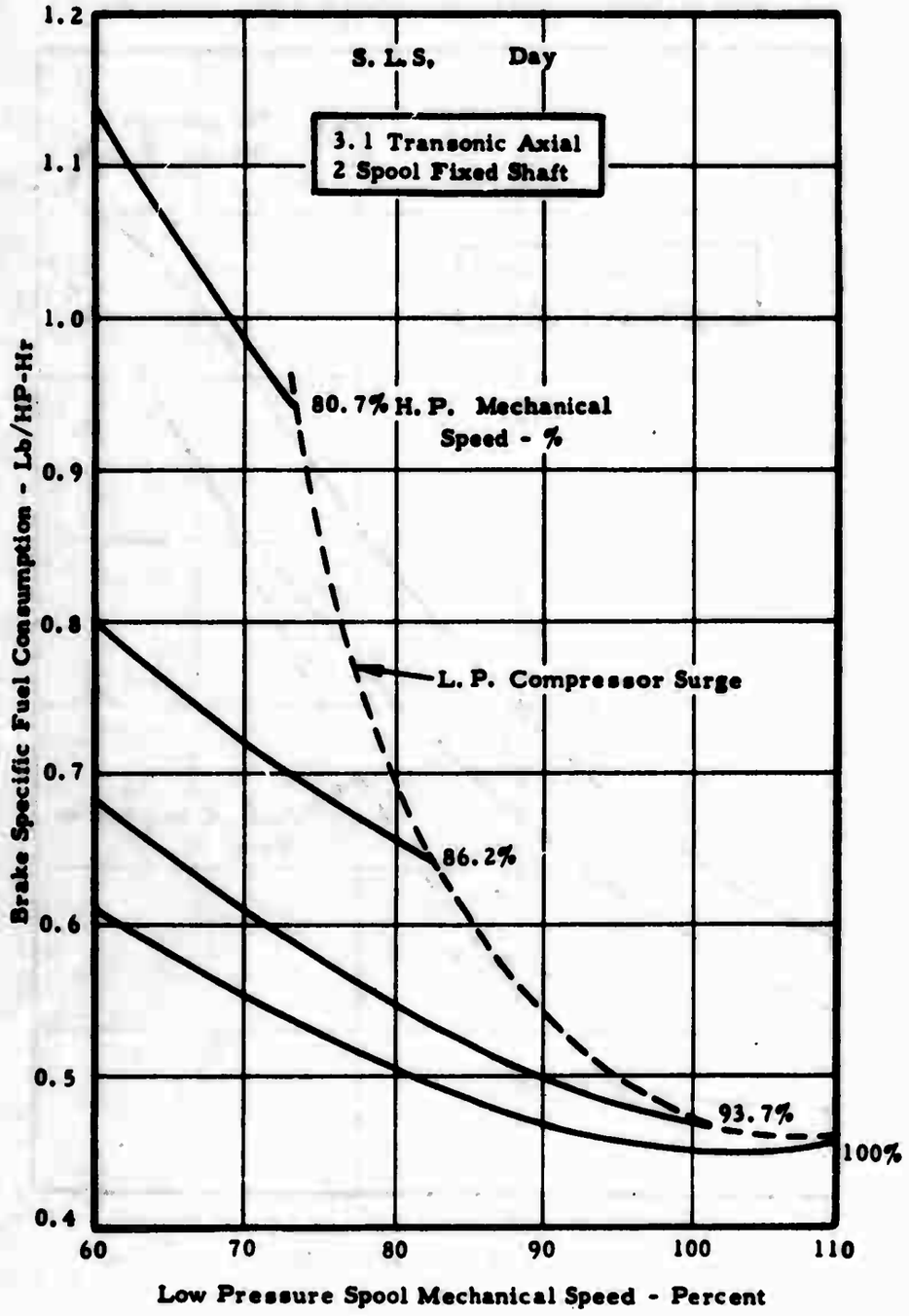

Figure 52. Estimated BSFC Characteristics.

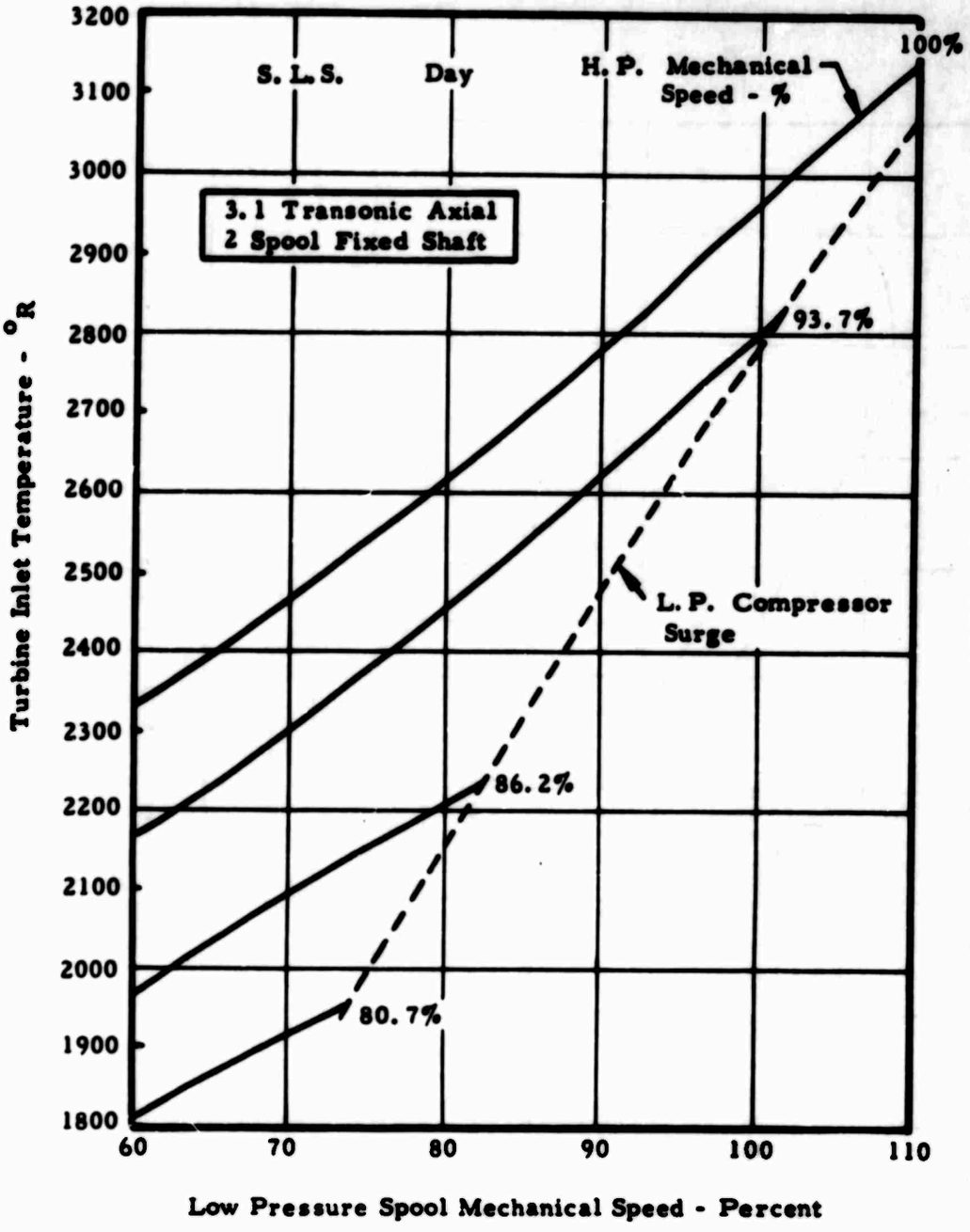

Figure 53. Estimated Gas Generator Turbine Inlet Temperature Characteristics.

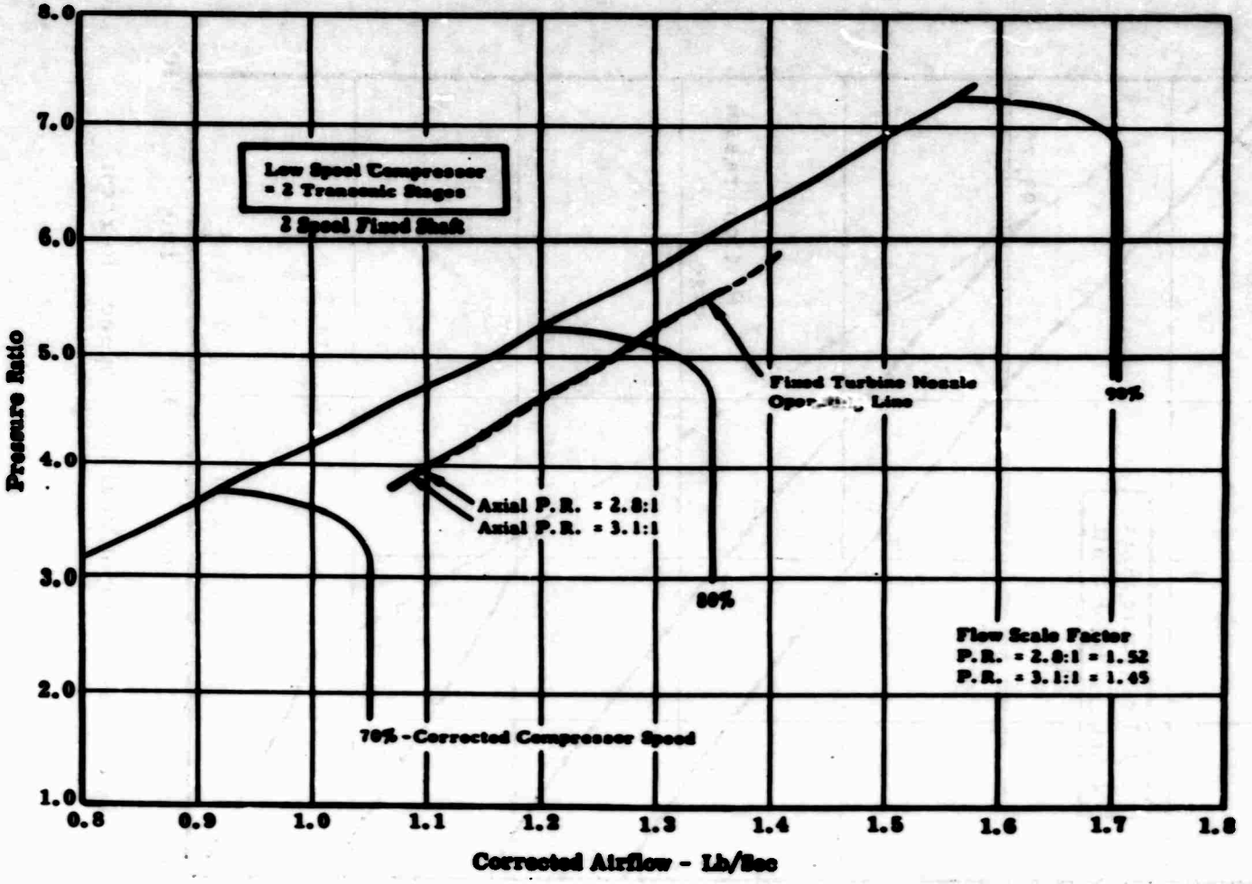

Figure 54. Estimated Performance Map for a High Pressure Ratio Centrifugal Compressor With High Spool Operating Lines.

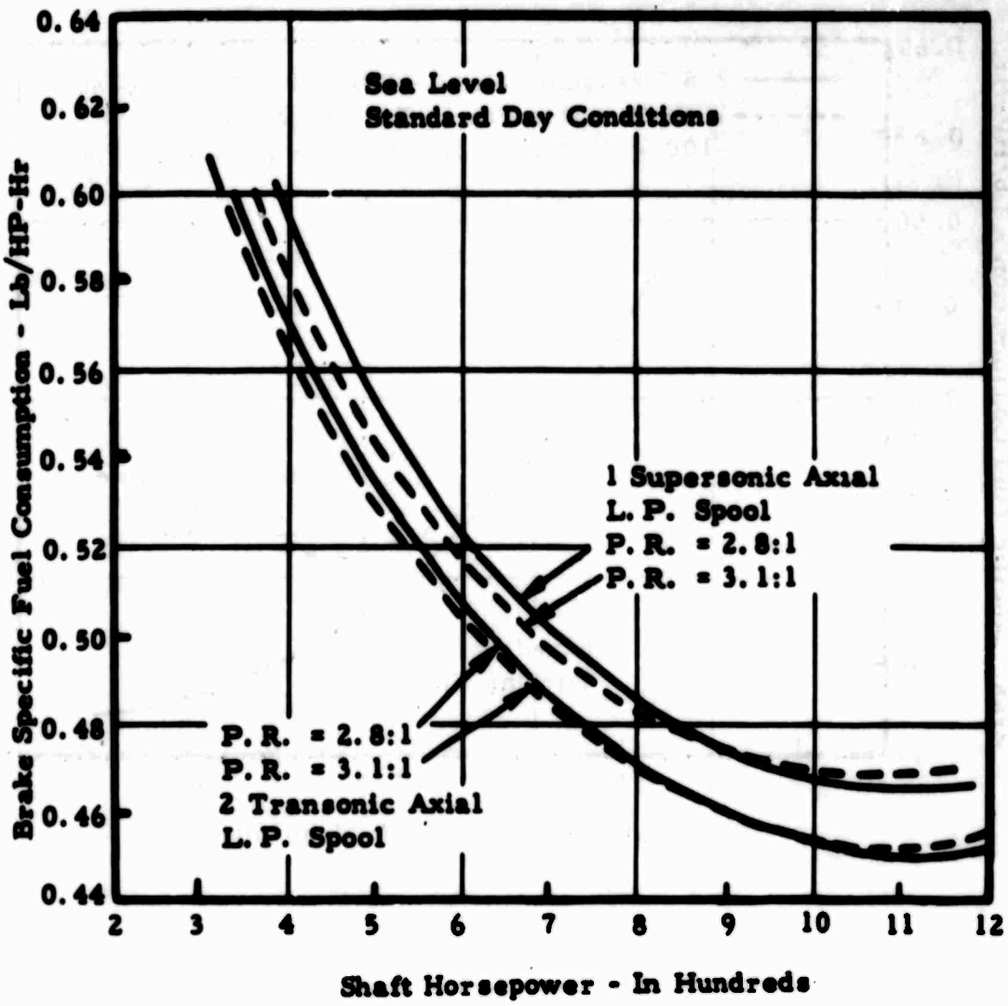

Figure 55. Comparison of BSFC - Horsepower Characteristics, Two-Spool Fixed Power Turbine.

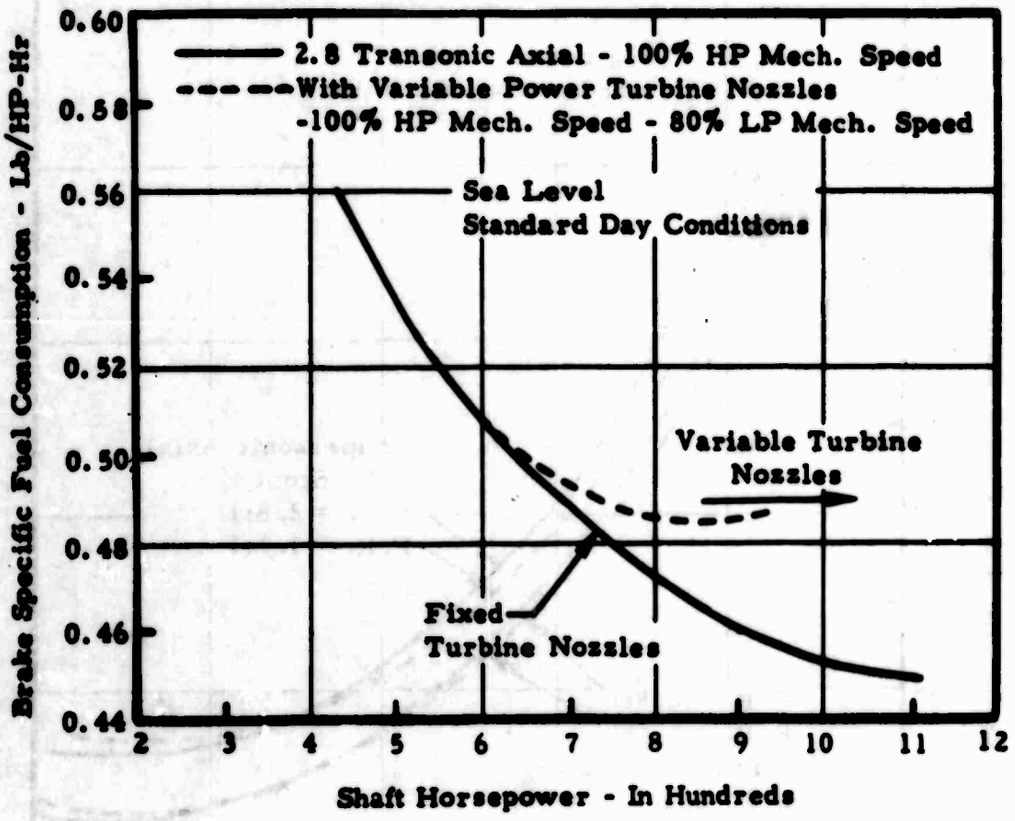

Figure 56. Effect of Variable Power Nozzles on Engine Performance, Two-Spool Fixed Power Turbine.

SINGLE-SPOOL ENGINE CONFIGURATIONS

Compressor Matching Studies

The thermodynamic analysis carried out for single-spool engines in order to select the candidate axial compressor is discussed in detail below.

The work on single-spool engines included matching the axial compressor to the centrifugal compressor to obtain a combined overall compressor map for each configuration.

These combined maps were required to generate single-spool off-design data. The matching was done using Continental Computer Program 30-090 "Compressor Stage Matching". In most cases several compressor matches were examined in order to obtain the optimum combined map. The matches completed include those listed below.

Supersonic Stage

2.8 pressure ratio - no inlet guide vanes and variable inlet guide vanes

3.1 pressure ratio - no inlet guide vanes

Transonic Stage

2.8 pressure ratio - no inlet guide vanes and variable inlet guide vanes

3.1 pressure ratio - no inlet guide vanes and variable inlet guide vanes

These single-spool maps are described in Figure 57.

The compressor map consists of a single-stage 2.8:1 pressure ratio supersonic axial compressor matched to the USAAVLABS high pressure ratio centrifugal compressor. No inlet guide vanes are used. Also shown are the axial and centrifugal compressor surge lines. It is evident that this combined compressor has a very narrow operating range because the axial surge line crosses over at a high speed and flow. An engine using this configuration was therefore discarded without further consideration.

Using the 3.1:1 pressure ratio supersonic axial, the combined overall map produced a narrower operating range than that of the 2.8:1. Therefore, since the 2.8:1, with variable inlet guide vanes, results in a marginal engine, the 3.1:1 supersonic axial in a single-spool configuration was not considered further.

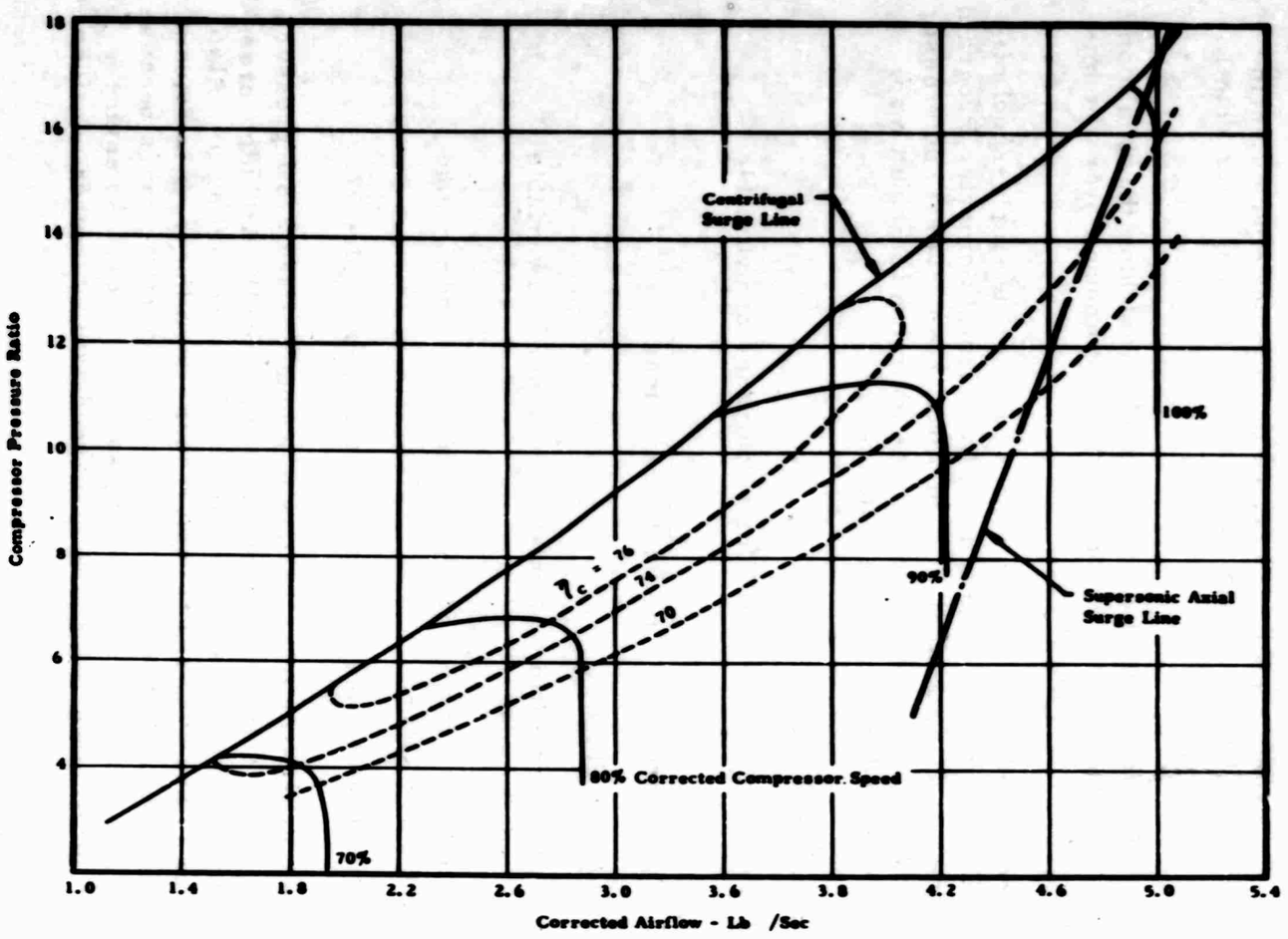

Figure 57. Estimated Performance Map - Combined 2.8:1 Single-Stage Supersonic Axial Compressor With USAAVLABS Centrifugal - No Inlet Guide Vanes.

Figure 58 shows a compressor map similar to that described in Figure 57. However, a variable axial inlet guide vane schedule has been added. As the inlet guide vanes are closed down, the axial surge line shifts to lower speeds and flows, and the combined surge line is likewise improved. The guide vanes were closed to 30°, which was selected as a practical limit. Also shown is the variable inlet guide vanes schedule.

Figure 59 shows a compressor map which consists of two axial transonic stages with a pressure ratio of 2.8:1 matched to the USAAVLABS high pressure ratio centrifugal. No inlet guide vanes were used.

Figure 60 shows the compressor map for the 3.1:1 pressure ratio, two transonic stage, axial compressor matched to the USAAVLABS high pressure ratio centrifugal. No inlet guide vanes were used.

Figure 61 shows the compressor map with scheduled variable inlet guide vanes and engine operating lines.

Figure 62 shows the compressor map for the same axial stages, but with scheduled variable inlet guide vanes. Engine operating lines are also shown for these two compressor configurations in a single-spool free turbine engine.

The thermodynamic effort in evaluating each compressor in single-spool engine configurations consisted of examining:

1. Free Power Turbine Configurations

    a. Design Point Analysis
    b. Off-Design Analysis
    c. Effects of Variable Geometry

2. Fixed (Connected) Power Turbine Configurations

    a. Structural and Aerodynamic Analysis
    b. Design Point Analysis

Each item is discussed in detail below.

Single-Spool Free Power Turbine

Design Point Analysis. A summary of the design point data is tabulated in Table XIII. The design point was established for each of the single-spool free power turbine cycles. The compressor match points were selected to make the single-spool engine directly comparable to the

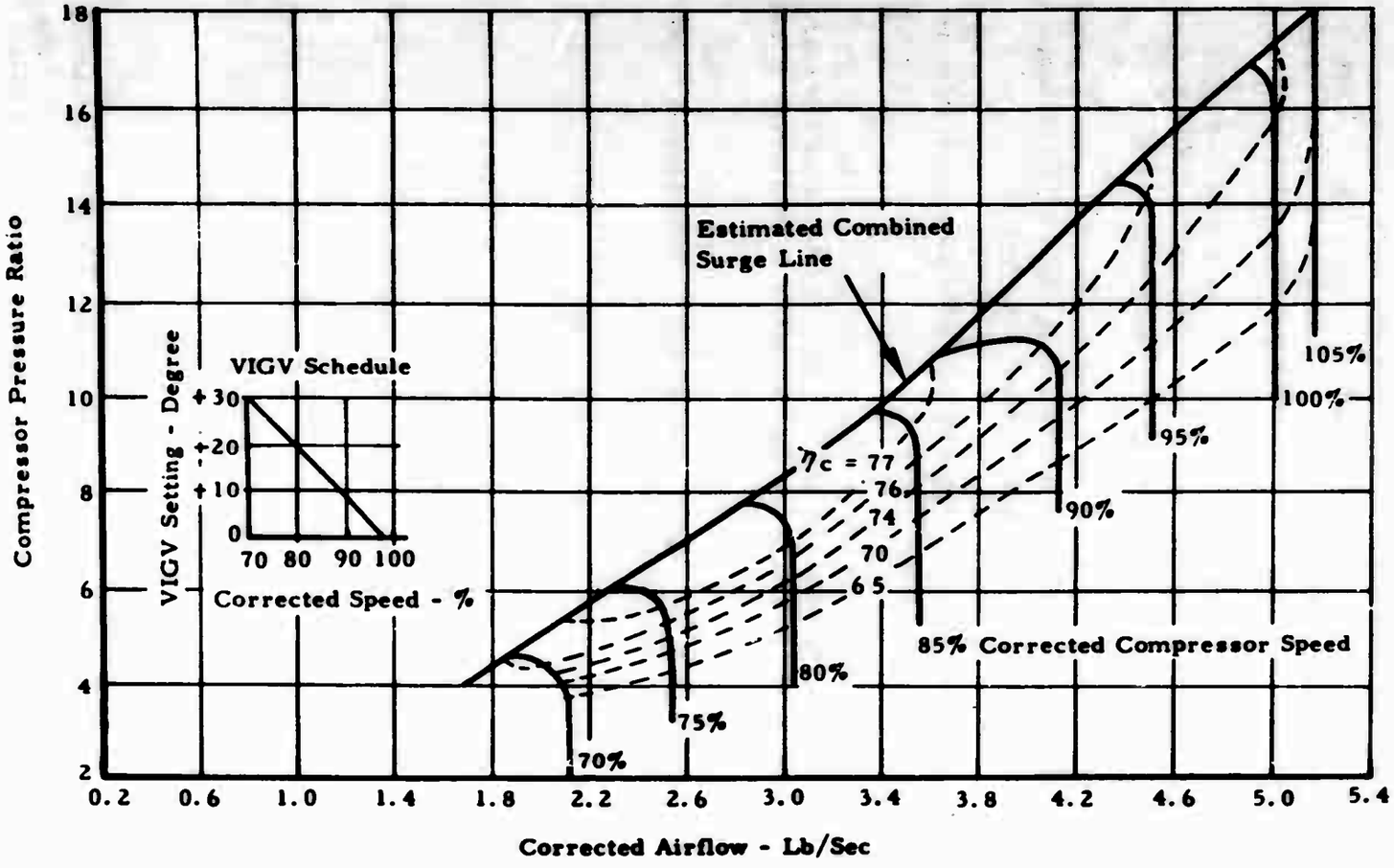

Figure 58. Estimated Performance Map - Combined 2.8:1 Single-Stage Supersonic Axial Compressor With USAAVLABS Centrifugal - Variable Inlet Guide Vanes.

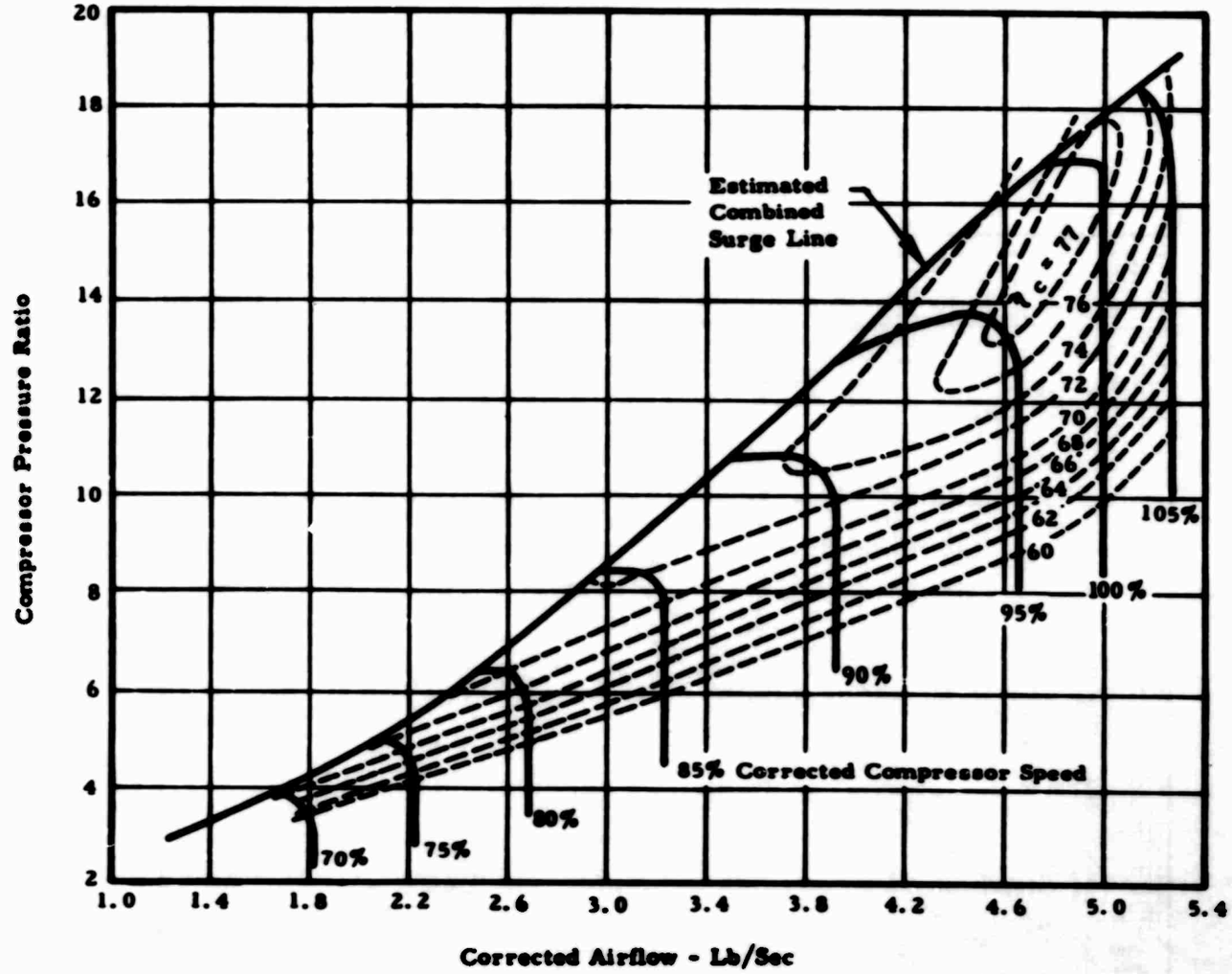

Figure 59. Estimated Performance Map - Combined Two-Stage 2.8:1 Transonic Axial Compressor With USAAVLABS Centrifugal - No Inlet Guide Vanes.

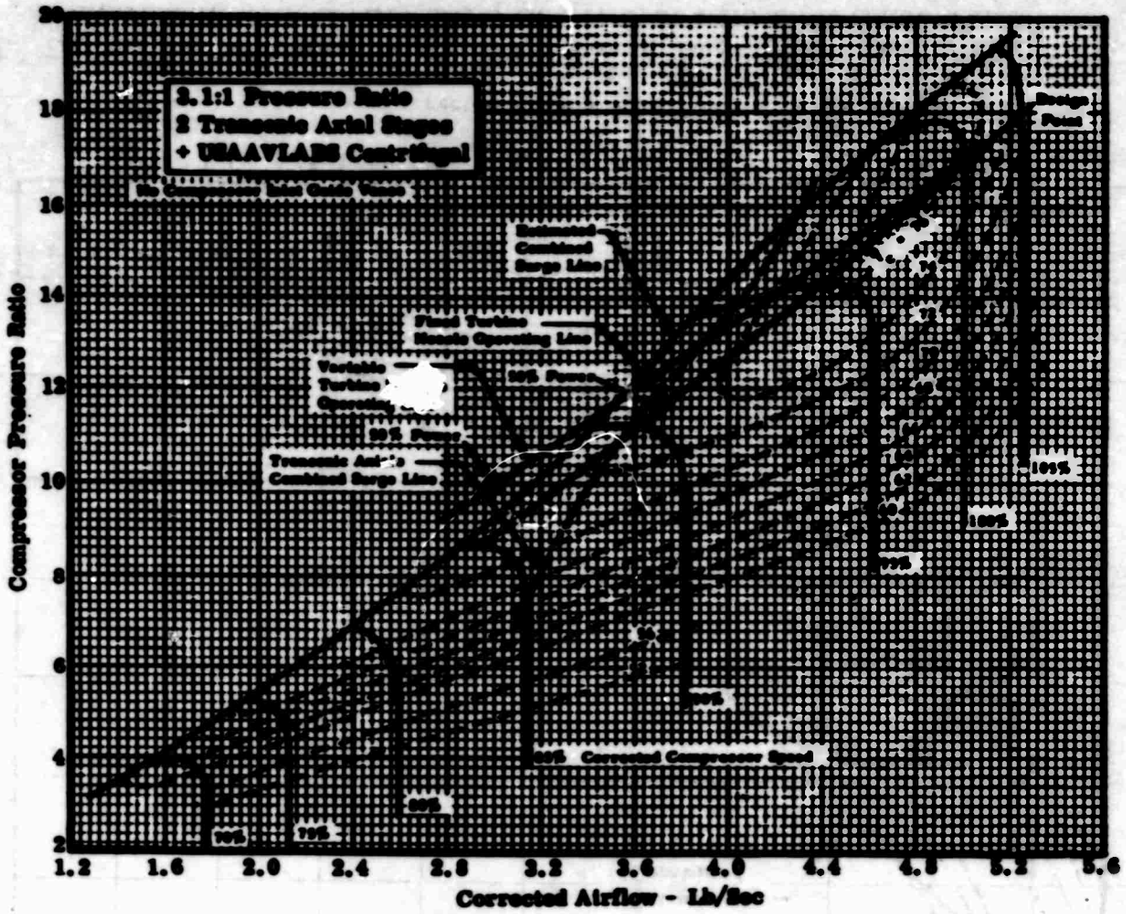

Figure 60. Estimated Combined Compressor Performance Map With Single-Spool Free Shaft Operating Lines.

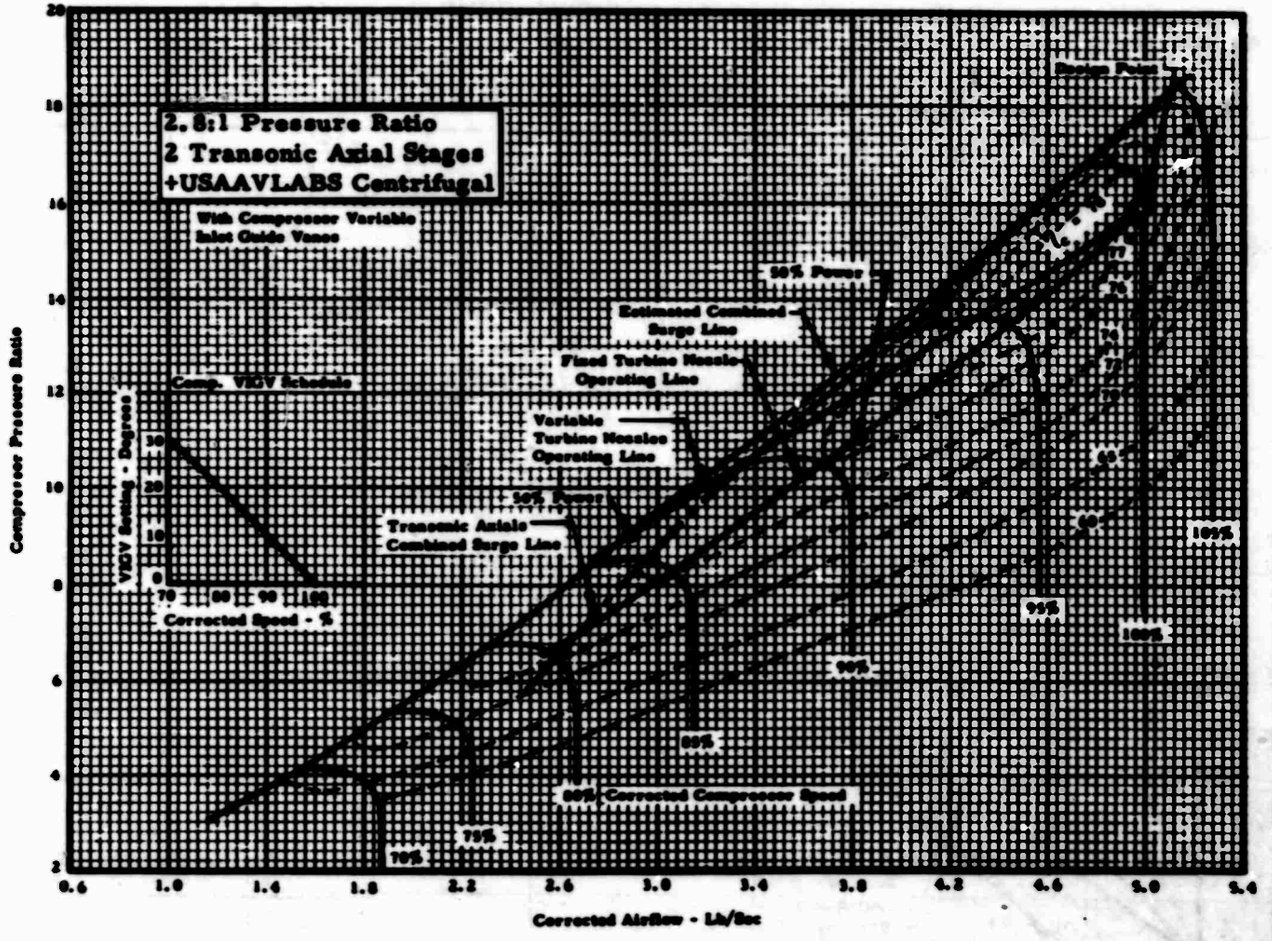

Figure 61. Estimated Combined Compressor Performance Map With Single-Spool Free Shaft Operating Lines.

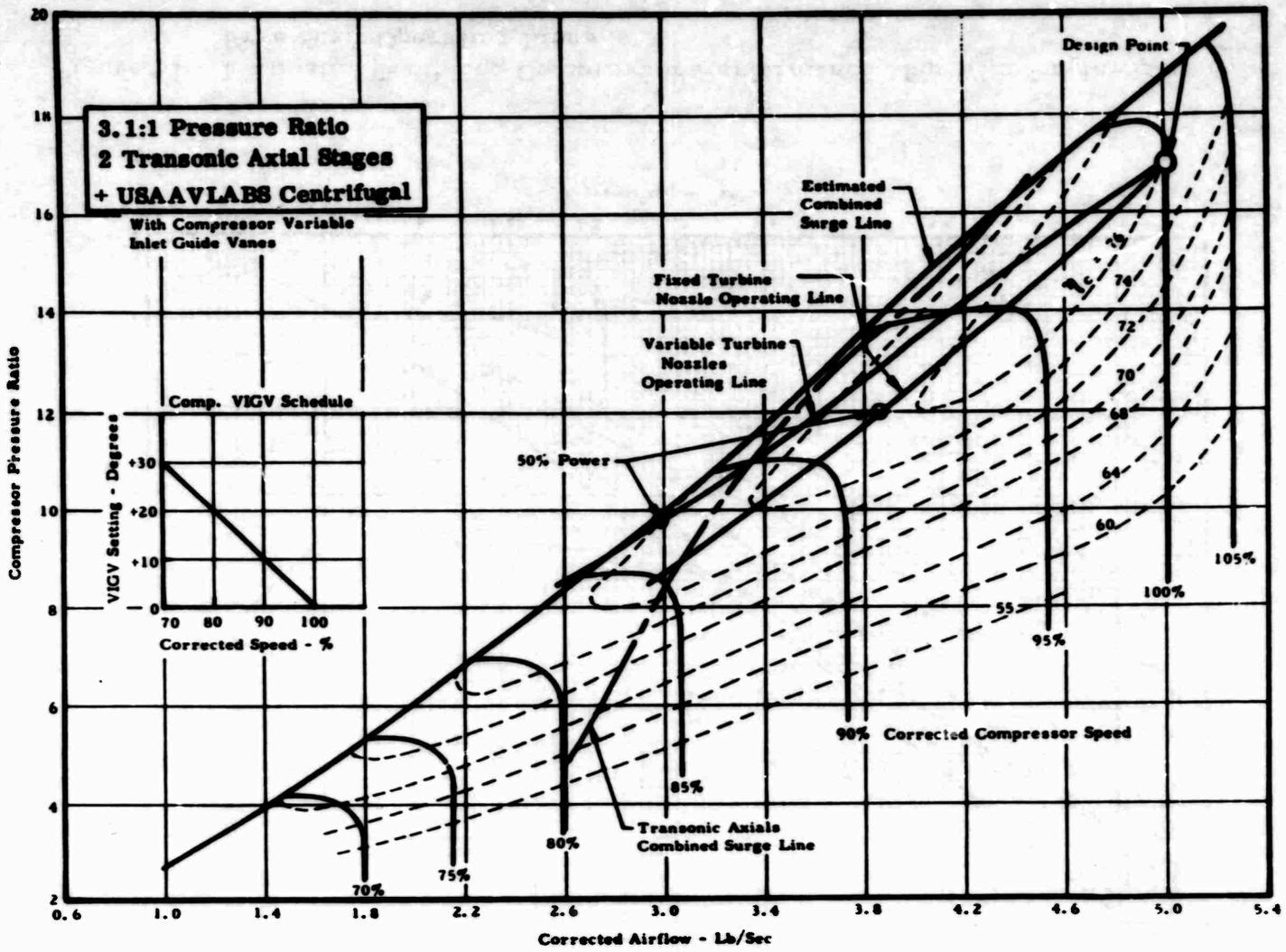

Figure 62. Estimated Combined Compressor Performance Map With Single-Spool Free Shaft Operating Lines.

two-spool engine. The complete design point output computation for these points is included in Tables XIV through XVII. The engine station designation is presented in Figure 63. The symbols used in the computer output are given on pages 104 and 105.

TABLE XIII
DESIGN POINT DATA

	One Supersonic Stage		Two Transonic Stages	
Axial Pressure Ratio	2.8:1	3.1:1	2.8:1	3.1:1
SHP	1054	1032	1100	1080
BSFC - Lb/HP-Hr	0.467	0.468	0.454	0.454
T_5-TIT - ^oR	2960	2960	2960	2960
P_3/P_2	16.0	17.0	16.0	17.0
Eff. Compressor - %	74.5	73.5	77.0	76.0
Eff. Gas Gen. Turb. - %	86.0	86.0	86.0	86.0
Eff. Power Turb. - %	88.1	88.1	88.1	88.1

The off-design analysis carried on for single-spool free-power turbine engines is discussed below.

Axial Stage = One Supersonic (With Variable Inlet Guide Vanes)

Axial Pressure Ratio = 2.8:1. As discussed previously, this configuration is not operable without compressor variable inlet guide vanes. Figure 64 shows the compressor map with scheduled variable inlet guide vanes. The schedule was optimized for maximum surge margin and efficiency. Also shown are the engine operating lines for both fixed and variable power turbine nozzles. The variable nozzle line is scheduled for constant turbine inlet temperature. It is evident that inadequate surge margin exists for operating at design temperature with variable power turbine nozzles throughout the full part-power range.

Figure 65 shows selected performance parameters for this engine. Figure 66 shows the relationship between power turbine area ratio, turbine efficiency, and flow reduction when using variable power turbine nozzles. For this particular configuration, variable power turbine nozzles result in a part-power surge problem with little improvement in BSFC.

TABLE XIV

DESIGN POINT PERFORMANCE, SINGLE-SPOOL FREE POWER TURBINE, SUPERSONIC AXIAL COMPRESSOR, 2.8:1 PRESSURE RATIO

OUTPUT 30.038

TA	5.1868E+02	PA	1.4695E+01	N/RTH2	1.0000E+02	N/RTH5C	4.2576E+01
T2	5.1868E+02	P2	1.4622E+01	WRT/D2	5.0251E+00	WN/D605	5.5230E-01
T3	1.3184E+03	P3	2.3395E+02	NPT/T7C	4.8287E+01	DHT/T5C	3.6845E+01
T4	1.3184E+03	P4	2.3395E+02	WN/D607	2.1326E+00	DHT/N2	2.0325E-02
T5	2.9600E+03	P5	2.2343E+02	DHPT/T7	3.6214E+01	DH/N2PT	1.5531E-02
T6	2.2887E+03	P6	5.7863E+01	P3/P2	1.6000E+01	ETA C	7.4500E-01
T7	2.2887E+03	P7	5.7863E+01	P5/P6	3.8613E+00	ETA T	8.6000E-01
T8	1.7540E+03	P8	1.5701E+01	P7/P8	3.6852E+00	ETA PT	8.8100E-01
		P9	1.4916E+01	P10/PA	1.0150E+00	ETA N	1.0000E+00
T10	1.7455E+03	P10	1.4916E+01	DP/PHC	0.0000E-99	ETA COM	9.8500E-01
WA	5.0000E+00	P11	1.4916E+01	DP/PC	4.5000E-02		
W3	4.9000E+00	TAU	5.5408E+04	DP/PIT	0.0000E-99		
W5	5.0368E+00			DP/PD	5.0000E-02		
W7	5.0368E+00			DP/PHH	0.0000E-99		
W10	5.1368E+00			DP/PN	0.0000E-99		
WRT/P8	1.3434E+01	BO	0.0000E-99	EHE	0.0000E-99	F/A	2.7924E-02
FN	4.7653E+01	FG	4.7653E+01	AJ	1.0866E+02	WF	4.9258E+02
SHP	1.0549E+03	BSFC	4.6691E-01	ESHP	1.0740E+03	EBSFC	4.5862E-01
ETA-CP	8.1987E-01	ETA-TP	8.4018E-01	ETA-PTP	8.6353E-01		

TABLE XV

DESIGN POINT PERFORMANCE, SINGLE-SPOOL FREE POWER TURBINE, SUPERSONIC AXIAL COMPRESSOR, 3.1:1 PRESSURE RATIO

OUTPUT 30.038

TA	5.1868E+02	PA	1.4695E+01	N/RTH2	1.0000E+02	N/RTH5C	4.2571E+01
T2	5.1868E+02	P2	1.4622E+01	WRT/D2	5.0251E+00	WN/D605	5.1954E-01
T3	1.3523E+03	P3	2.4858E+02	NPT/T7C	4.8613E+01	DHT/T5C	3.8488E+01
T4	1.3523E+03	P4	2.4858E+02	WN/D607	2.1558E+00	DHT/N2	2.1237E-02
T5	2.9600E+03	P5	2.3739E+02	DHPT/T7	3.5913E+01	DH/N2PT	1.5196E-02
T6	2.2572E+03	P6	5.7210E+01	P3/P2	1.7000E+01	ETA C	7.3500E-01
T7	2.2572E+03	P7	5.7210E+01	P5/P6	4.1495E+00	ETA T	8.6000E-01
T8	1.7323E+03	P8	1.5701E+01	P7/P8	3.6436E+00	ETA PT	8.8100E-01
		P9	1.4916E+01	P10/PA	1.0150E+00	ETA N	1.0000E+00
T10	1.7249E+03	P10	1.4916E+01	DP/PHC	0.0000E-99	ETA COM	9.8500E-01
WA	5.0000E+00	P11	1.4916E+01	DP/PC	4.5000E-02		
W3	4.9000E+00	TAU	5.4213E+04	DP/PIT	0.0000E-99		
W5	5.0342E+00			DP/PD	5.0000E-02		
W7	5.0342E+00			DP/PHH	0.0000E-99		
W10	5.1342E+00			DP/PN	0.0000E-99		
WRT/P8	1.3344E+01	BO	0.0000E-99	EHE	0.0000E-99	F/A	2.7388E-02
FN	4.7346E+01	FG	4.7346E+01	AJ	1.0796E+02	WF	4.8312E+02
SHP	1.0322E+03	BSFC	4.6804E-01	ESHP	1.0511E+03	EBSFC	4.5961E-01
ETA-CP	8.1387E-01	ETA-TP	8.3899E-01	ETA-PTP	8.6364E-01		

TABLE XVI
DESIGN POINT PERFORMANCE, SINGLE-SPOOL FREE POWER TURBINE, TWO-STAGE TRANSONIC AXIAL COMPRESSOR, 2.8:1 PRESSURE RATIO

OUTPUT 30.038

TA	5.1868E+02	PA	1.4695E+01	N/RTH2	1.0000E+02	N/RTH5C	4.2581E+01
T2	5.1868E+02	P2	1.4622E+01	WRT/D2	5.0251E+00	WN/D605	5.5251E-01
T3	1.2940E+03	P3	2.3395E+02	NPT/T7C	4.8056E+01	DHT/T5C	3.5672E+01
T4	1.2940E+03	P4	2.3395E+02	WN/D607	2.0282E+00	DHT/N2	1.9674E-02
T5	2.9600E+03	P5	2.2343E+02	DHPT/T7	3.7422E+01	DH/N2PT	1.6204E-02
T6	2.3112E+03	P6	6.0864E+01	P3/P2	1.6000E+01	ETA C	7.7000E-01
T7	2.3112E+03	P7	6.0864E+01	P5/P6	3.6709E+00	ETA T	8.6000E-01
T8	1.7541E+03	P8	1.5701E+01	P7/P8	3.8763E+00	ETA PT	8.8100E-01
		P9	1.4916E+01	P10/PA	1.0150E+00	ETA N	1.0000E+00
T10	1.7451E+03	P10	1.4916E+01	DP/PHC	0.0000E-99	ETA COM	9.8500E-01
WA	5.0000E+00	P11	1.4916E+01	DP/PC	4.5000E-02		
W3	4.9000E+00	TAU	5.7808E+04	DP/PIT	0.0000E-99		
W5	5.0387E+00			DP/PD	5.0000E-02		
W7	5.0387E+00			DP/PHH	0.0000E-99		
W10	5.1387E+00			DP/PN	0.0000E-99		
WRT/P8	1.3440E+01	BO	0.00[illegible]-99	EHE	0.0000E-99	F/A	2.8307E-02
FN	4.7665E+01	FG	4.7665E+01	AJ	1.0869E+02	WF	4.9934E+02
SHP	1.1006E+03	BSFC	4.5367E-01	ESHP	1.1197E+03	EBSFC	4.4595E-01
ETA-CP	8.3780E-01	ETA-TP	8.4100E-01	ETA-PTP	8.6283E-01		

TABLE XVII

DESIGN POINT PERFORMANCE, SINGLE-SPOOL FREE POWER TURBINE, TWO-STAGE TRANSONIC AXIAL COMPRESSOR, 3.1:1 PRESSURE RATIO

OUTPUT 30.038

TA	5.1868E+02	PA	1.4695E+01	N/RTH2	1.0000E+02	N/RTH5C	4.2575E+01
T2	5.1868E+02	P2	1.4622E+01	WRT/D2	5.0251E+00	WN/D605	5.1974E-01
T3	1.3269E+03	P3	2.4858E+02	NPT/T7C	4.8365E+01	DHT/T5C	3.7258E+01
T4	1.3269E+03	P4	2.4858E+02	WN/D607	2.0433E+00	DHT/N2	2.0554E-02
T5	2.9600E+03	P5	2.3739E+02	DHPT/T7	3.7204E+01	DH/N2PT	1.5904E-02
T6	2.2808E+03	P6	6.0384E+01	P3/P2	1.7000E+01	ETA C	7.5980E-01
T7	2.2808E+03	P7	6.0384E+01	P5/P6	3.9313E+00	ETA T	8.6000E-01
T8	1.7323E+03	P8	1.5701E+01	P7/P8	3.8458E+00	ETA PT	8.8100E-01
		P9	1.4916E+01	P10/PA	1.0150E+00	ETA N	1.0000E+00
T10	1.7244E+03	P10	1.4916E+01	DP/PHC	0.0000E-99	ETA COM	9.8500E-01
WA	5.0000E+00	P11	1.4916E+01	DP/PC	4.5000E-02		
W3	4.9000E+00	TAU	5.6739E+04	DP/PIT	0.0000E-99		
W5	5.0361E+00			DP/PD	5.0000E-02		
W7	5.0361E+00			DP/PHH	0.0000E-99		
W10	5.1361E+00			DP/PN	0.0000E-99		
WRT/P8	1.3350E+01	BO	0.0000E-99	EHE	0.0000E-99	F/A	2.7789E-02
FN	4.7359E+01	FG	4.7359E+01	AJ	1.0799E+02	WF	4.9021E+02
SHP	1.0803E+03	BSFC	4.5376E-01	ESHP	1.0992E+03	EBSFC	4.4594E-01
ETA-CP	8.3159E-01	ETA-TP	8.3988E-01	ETA-PTP	8.6288E-01		

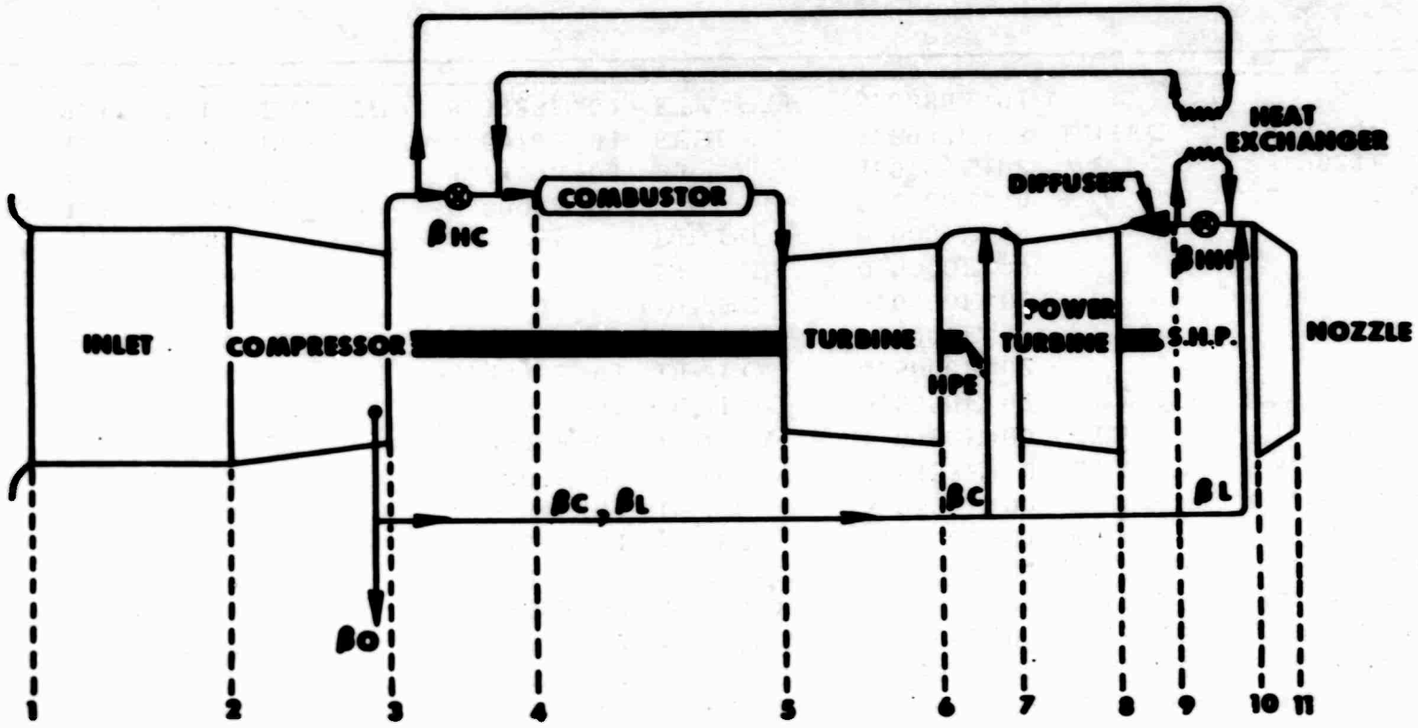

Figure 63. Station Designation, Single-Spool Free Power Turbine Turboshaft Engine.

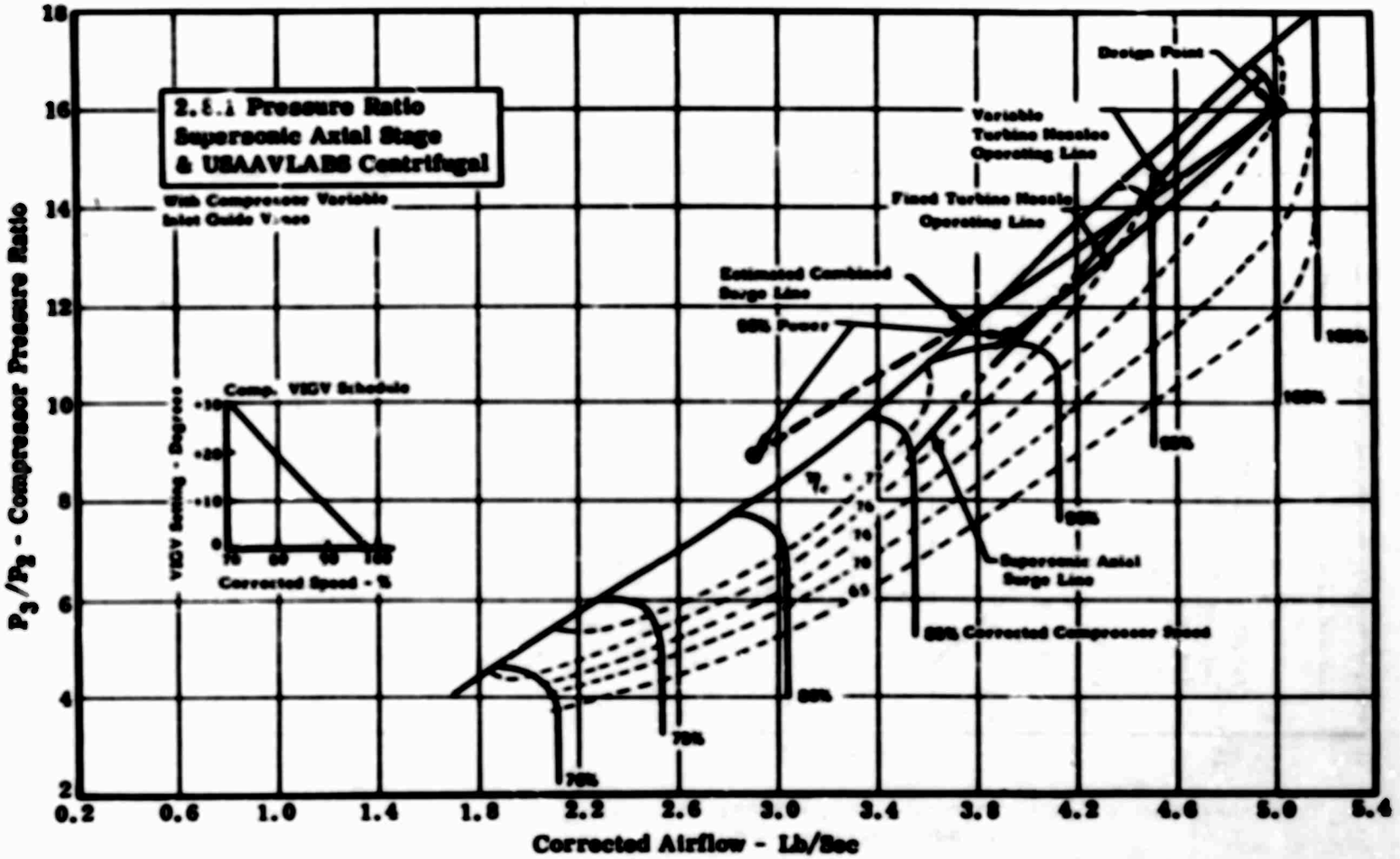

Figure 64. Estimated Combined Compressor Performance Map With Single-Spool Free Shaft Operating Lines.

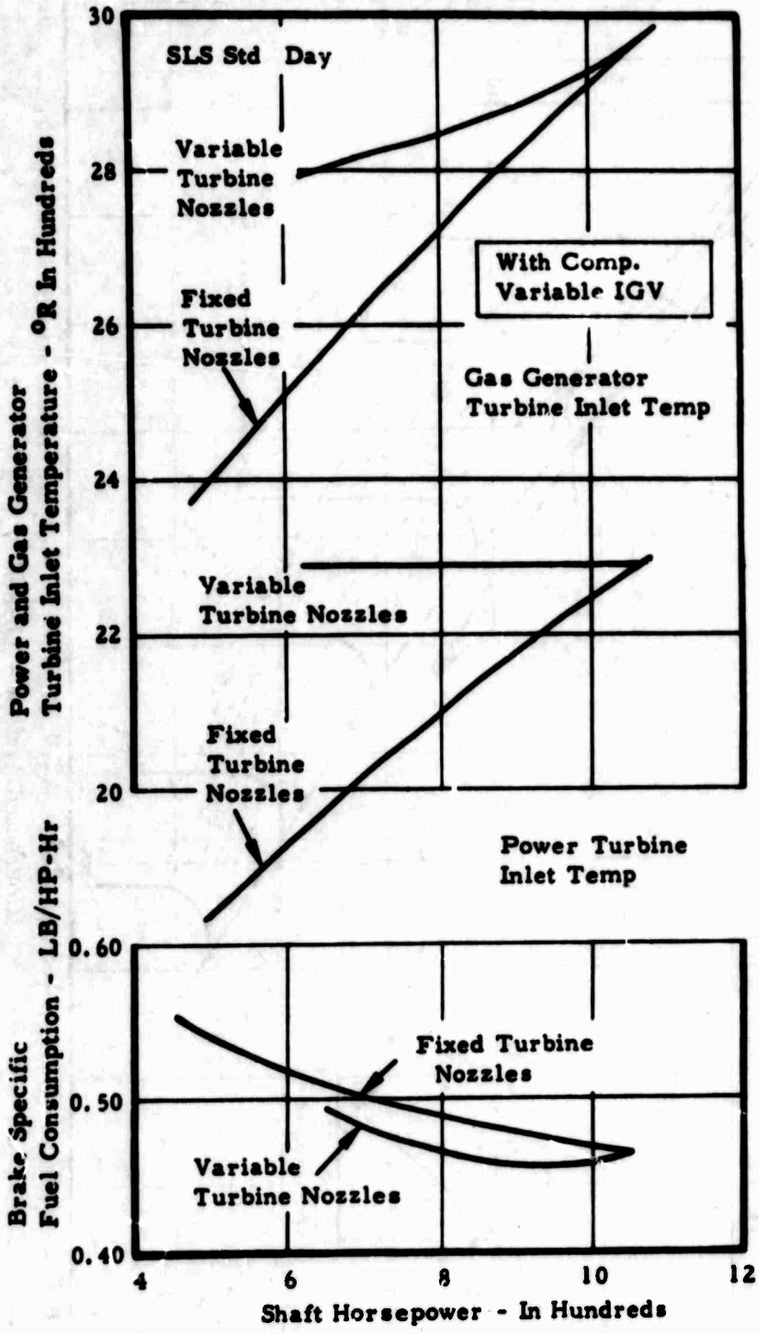

Figure 65. Selected Performance Parameters, Single-Spool Free Shaft Engine, 2.8:1 Supersonic Axial Compressor.

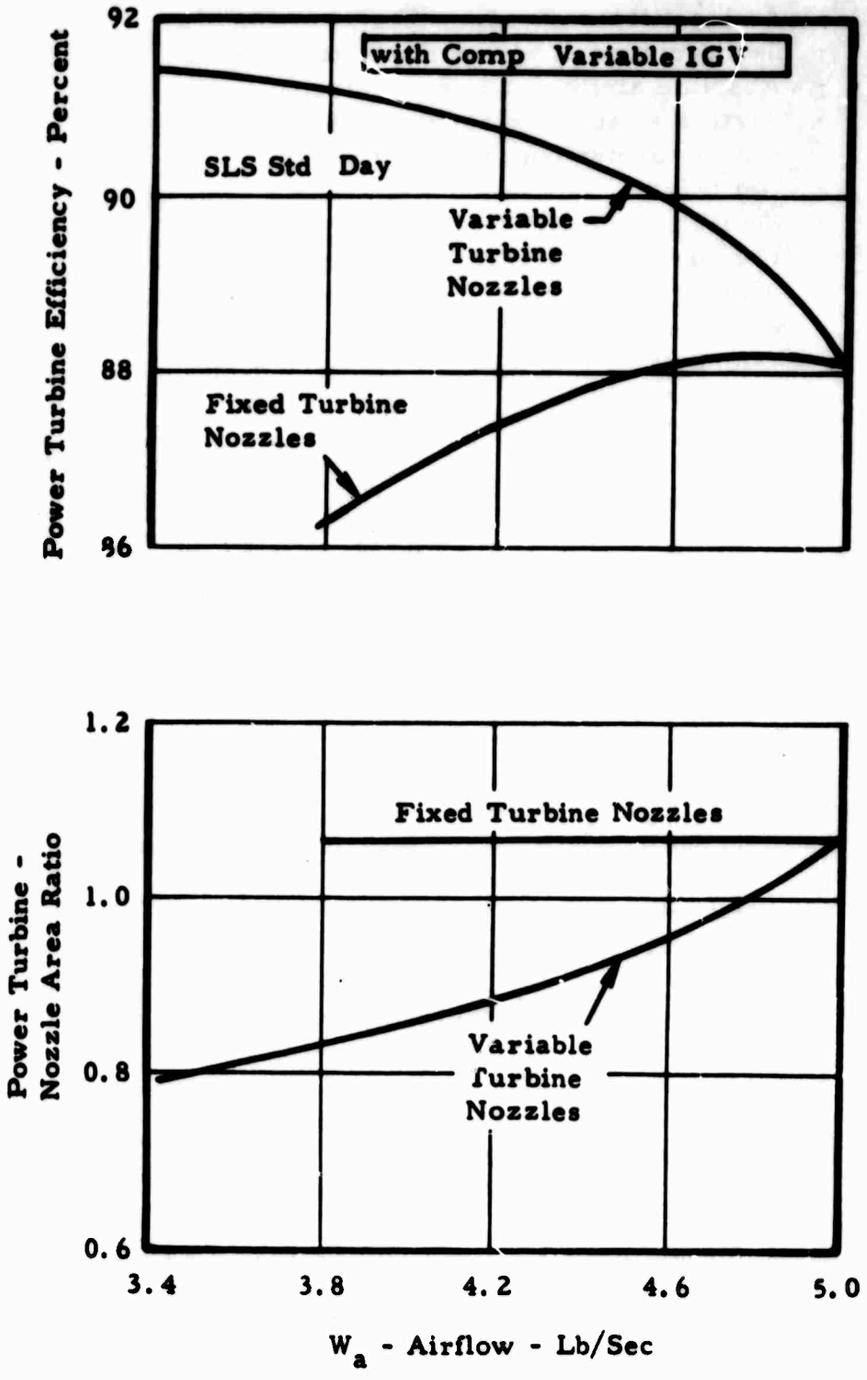

Figure 66. Estimated Power Turbine Area Ratio and Efficiency Variation, Single-Spool Free Shaft Engine, 2.8:1 Supersonic Axial Compressor.

SYMBOLS

TA	-	Ambient temperature - ^{o}R
T	-	Temperature at appropriate station - ^{o}R
WA	-	Absolute airflow at inlet - lb/sec
W	-	Airflow at appropriate stations - lb/sec
WRT/P8	-	Power turbine output flow function
FN	-	Net thrust
SHP	-	Shaft horsepower
ETA-CP	-	Compressor polytropic efficiency
PA	-	Ambient pressure - PSIA
P	-	Pressure at appropriate station - PSIA
TAU	-	Output shaft torque
BO	-	Overboard bleed
FG	-	Gross thrust
BSFC	-	Brake specific fuel consumption - lb/SHP/hr
ETA-TP	-	Turbine polytropic efficiency
N/RTH2	-	Referred compressor speed - $N/\sqrt{\theta_2}$ - rpm
WRT/D2	-	Referred airflow - $(W\sqrt{\theta}/\delta)_2$ - lb/sec
NPT/T7C	-	Referred power turbine speed - $NPT/\sqrt{\theta_{7C}}$ - rpm
WN/D607	-	Referred turbine speed flow parameter - $(WN/\delta 60)_7$ - lb-rev/sec^2
DHPT/T7	-	Referred power turbine work - $(\Delta h_{PT}/\theta)_7$ - Btu/lb
P_3/P_2	-	Compressor pressure ratio
P_5/P_6	-	Turbine pressure ratio
P_7/P_8	-	Power turbine pressure ratio
P_{10}/PA	-	Exhaust nozzle total to static pressure ratio
DP/PHC	-	Heat exchanger pressure loss - cold
DP/PC	-	Combustor pressure loss
DP/PIT	-	Inter turbine pressure loss
DP/PD	-	Exhaust diffuser pressure loss
DP/PHH	-	Heat exchanger pressure loss - hot
DP/PN	-	Exhaust nozzle pressure loss
EHE	-	Heat exchanger effectiveness
AJ	-	Exhaust nozzle area - in.^{2}
ESHP	-	Equivalent shaft horsepower
ETA-PTP	-	Power turbine polytropic efficiency
N/RTH5C	-	Referred turbine speed - $N/\sqrt{\theta_5 C}$ - rpm
WN/D605	-	Referred turbine speed flow parameter - $(WN/\delta 60)$ - lb-rev/sec^2
DHT/T5C	-	Referred turbine work - $(\Delta h_t/\theta_5 C)$
DHT/N2	-	Referred turbine work - speed parameter - $\Delta h_t/N^2$
DH/N2PT	-	Power turbine work - speed parameter - $(\Delta h/N_{PT}{}^2)$
ETAC	-	Compressor adiabatic efficiency
ETAT	-	Turbine adiabatic efficiency

ETA PT	-	Power turbine adiabatic efficiency
ETA N	-	Exhaust nozzle adiabatic efficiency
ETA COM	-	Combustor adiabatic efficiency
F/A	-	Fuel to air ratio
WF	-	Fuel flow - lb/hr
EBSFC	-	Equivalent brake specific fuel consumption - lb/SHP/hr

Axial Pressure Ratio = 3.1:1. The axial surge line crossover on the combined overall map produced a narrower operating range than that of the 2.8:1 (see Figure 57). Therefore, since the 2.8:1, with variable inlet guide vanes, results in a marginal engine, the 3.1:1 supersonic axial in a single-spool configuration was not considered further.

Axial Stages = Two Transonics (No Inlet Guide Vanes)

Axial Pressure Ratio = 2.8:1. Figure 67 shows the operating lines for both fixed and variable turbine nozzles. It is evident that inadequate surge margin exists in the part-power region with variable turbine nozzles.

Figure 68 shows selected performance parameters for this engine. Also indicated for comparison are the 3.1:1 pressure ratio data.

Figure 69 shows the turbine again moving to higher turbine efficiencies with variable nozzles resulting in slightly better part-power BSFC with variable geometry.

Axial Pressure Ratio = 3.1:1. Shown in Figure 60 is the operating line for both fixed and variable turbine nozzles. Again, it is evident that inadequate surge margin exists in the part-power region with variable turbine nozzles.

Axial Stages = Two Transonics (With Variable Inlet Guide Vanes)

Axial Pressure Ratio = 2.8:1. Figures 61, 70 and 71 present data similar to the above with the addition of variable inlet guide vanes. It is evident that the surge margin has improved considerably over the previous compressor configurations.

Axial Pressure Ratio = 3.1:1. Figure 62 shows the operating lines for both fixed and variable power turbine nozzles. The results are the same as those for the 2.8:1 pressure ratio two transonic axial stages.

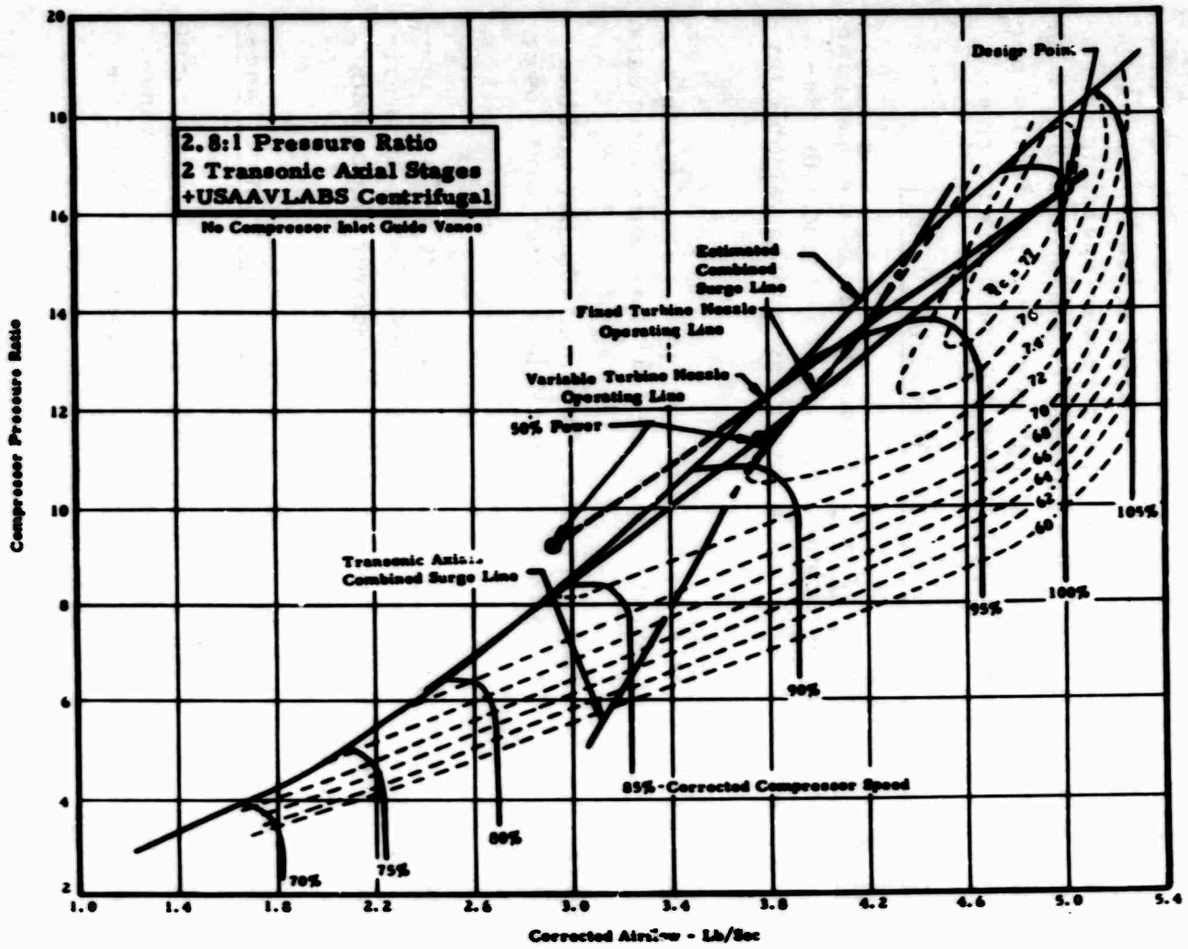

Figure 67. Estimated Combined Compressor Performance Map With Single-Spool Free Shaft Operating Lines.

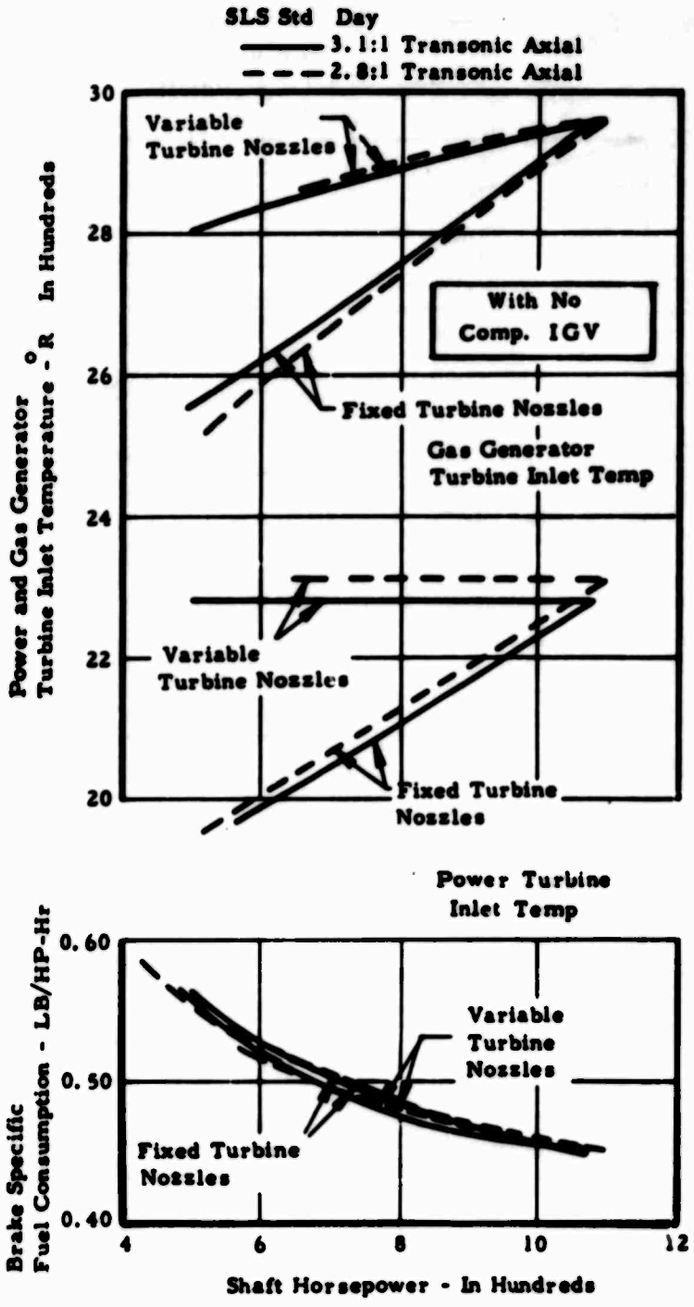

Figure 68. Selected Performance Parameters, Single-Spool Free Shaft Engine.

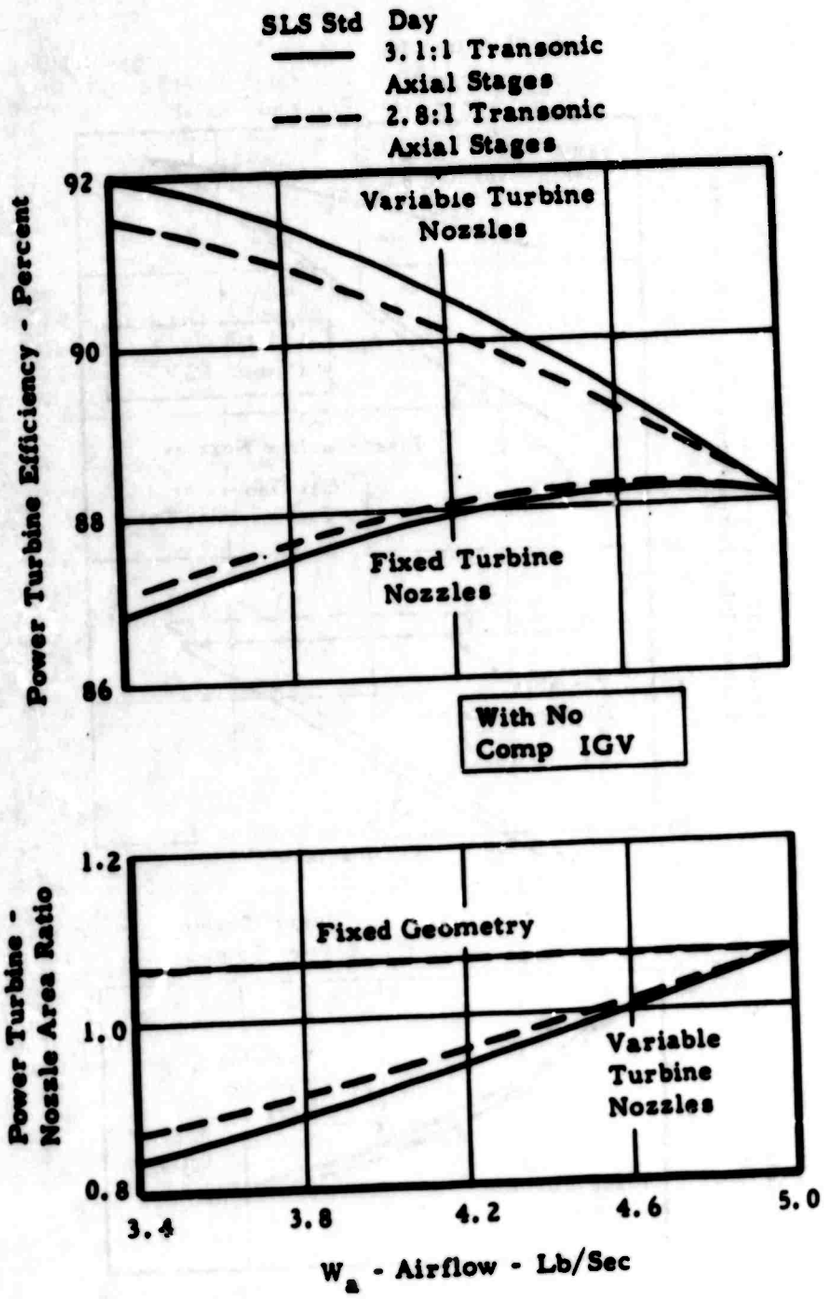

Figure 69. Estimated Power Turbine Area Ratio and Efficiency Variation, Single-Spool Free Shaft Engine.

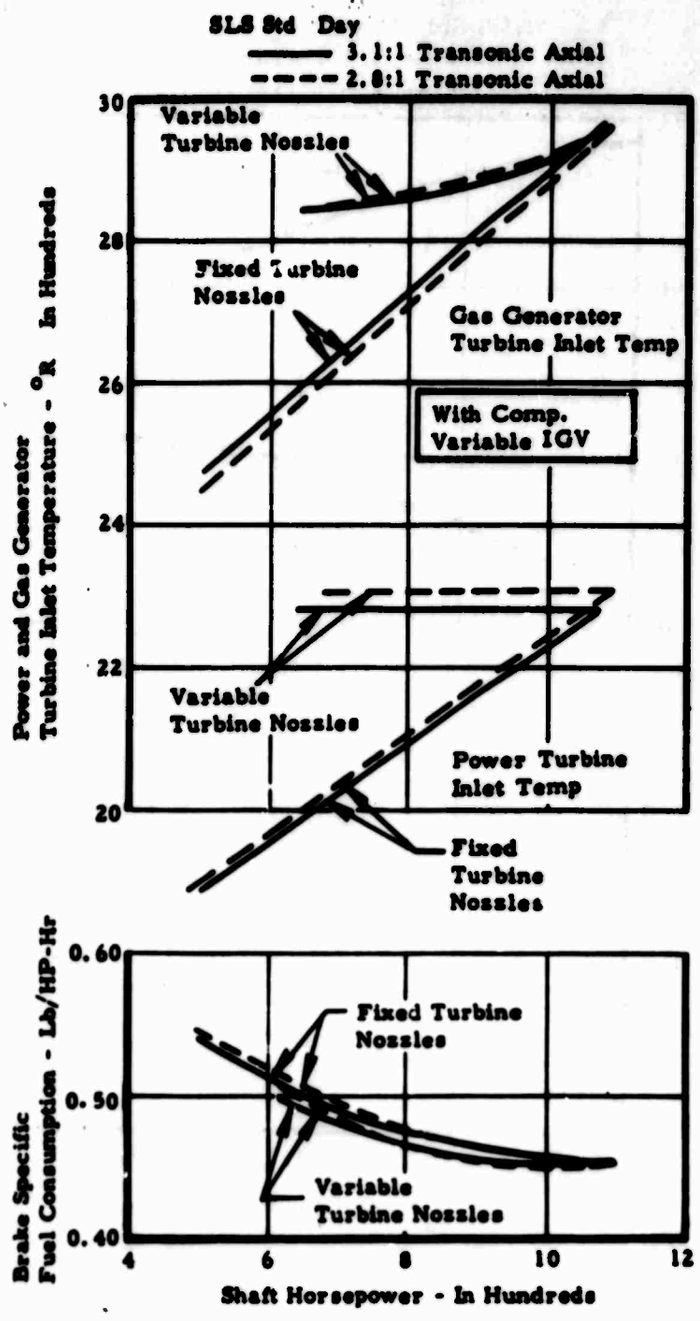

Figure 70. Selected Performance Parameters, Single-Spool Free Shaft Engine.

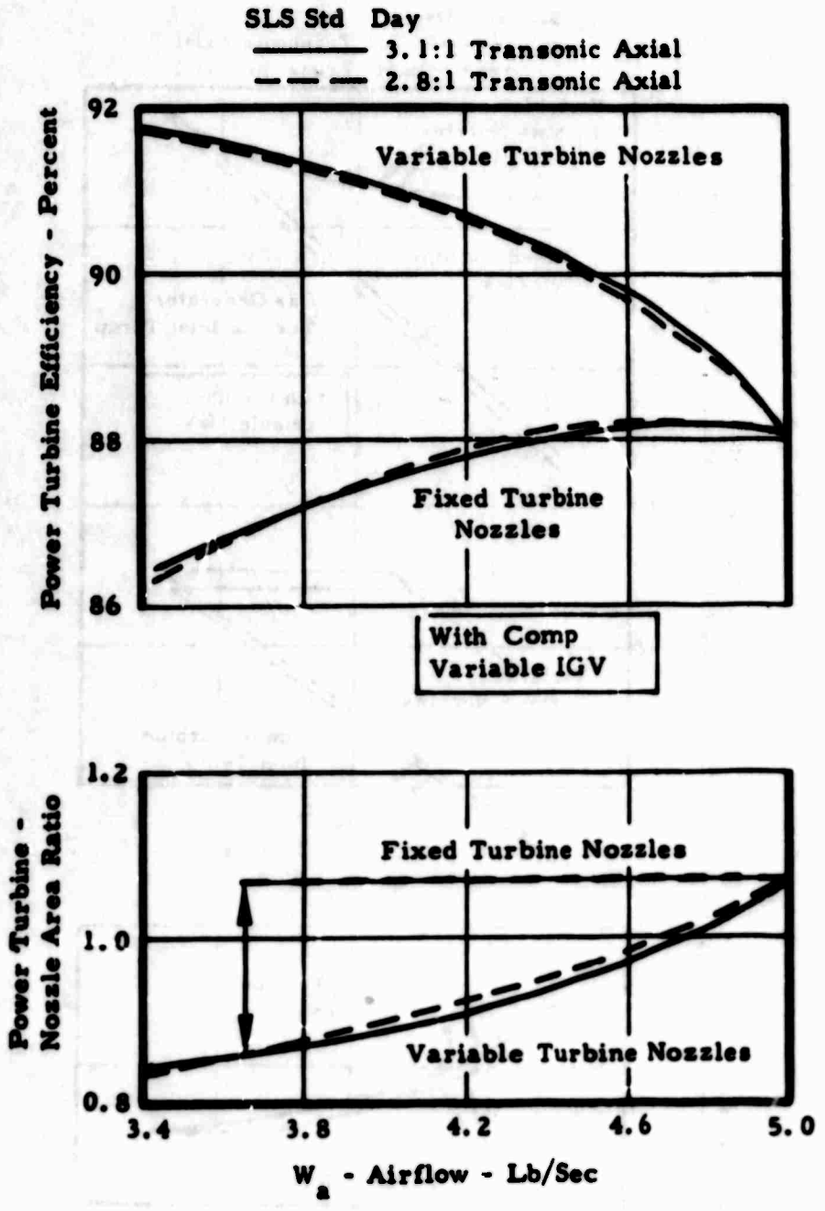

Figure 71. Estimated Power Turbine and Efficiency Variation, Single-Spool Free Shaft Engine.

Variable Geometry Analysis

Variable Inlet Guide Vanes on a Single-Spool Engine. It was noted that surge margin improvement (i.e., surge line shifts to the left on a compressor map) occurred with variable inlet guide vanes on the single-spool engine, while no improvement was realized when using variable inlet guide vanes on the low pressure compressor of the two-spool engine. The reason for this effect lies in the rematching of the spool speeds in the case of the two-spool engine. The effect is shown schematically in Figure 72 (a, b, c, d, e). Assuming a condition where the inlet guide vanes are closed while holding the high pressure spool speed constant, the engine responds in the following manner:

The compressor speed lines on the low pressure compressor shift to lower flows and pressures as indicated by the movement of line A to position B on Figure 72(a).

The low pressure and flow (point A) required to match with the high pressure compressor (point C, Figure 72(b)) remain the same. Therefore, point A is reestablished at a higher low pressure compressor speed.

The change in low pressure turbine speed does not provide any significant change in the low pressure turbine inlet flow function ($W\sqrt{T}/AP$) or in turbine efficiency. Therefore:

a. The work available from the low pressure turbine remains the same; thus the low pressure compressor pressure ratio remains unchanged.

b. The high pressure turbine discharge flow function remains the same; thus the high pressure spool remains at the same operating condition as previously experienced before the inlet guide vane change.

The net result is that a change in inlet guide vane angle on the low pressure compressor affects only the low pressure spool speed. All other parameters remain essentially unchanged. Since the surge line is not shifted, no change in surge margin is effected; therefore, no advantages are gained by the compressor variable geometry.

In the case of the single-spool engine, the rotor speeds are not self-compensating. The operating point A' is forced to move to a new point B' on the shifted speed characteristics B, Figure 72(c). In order

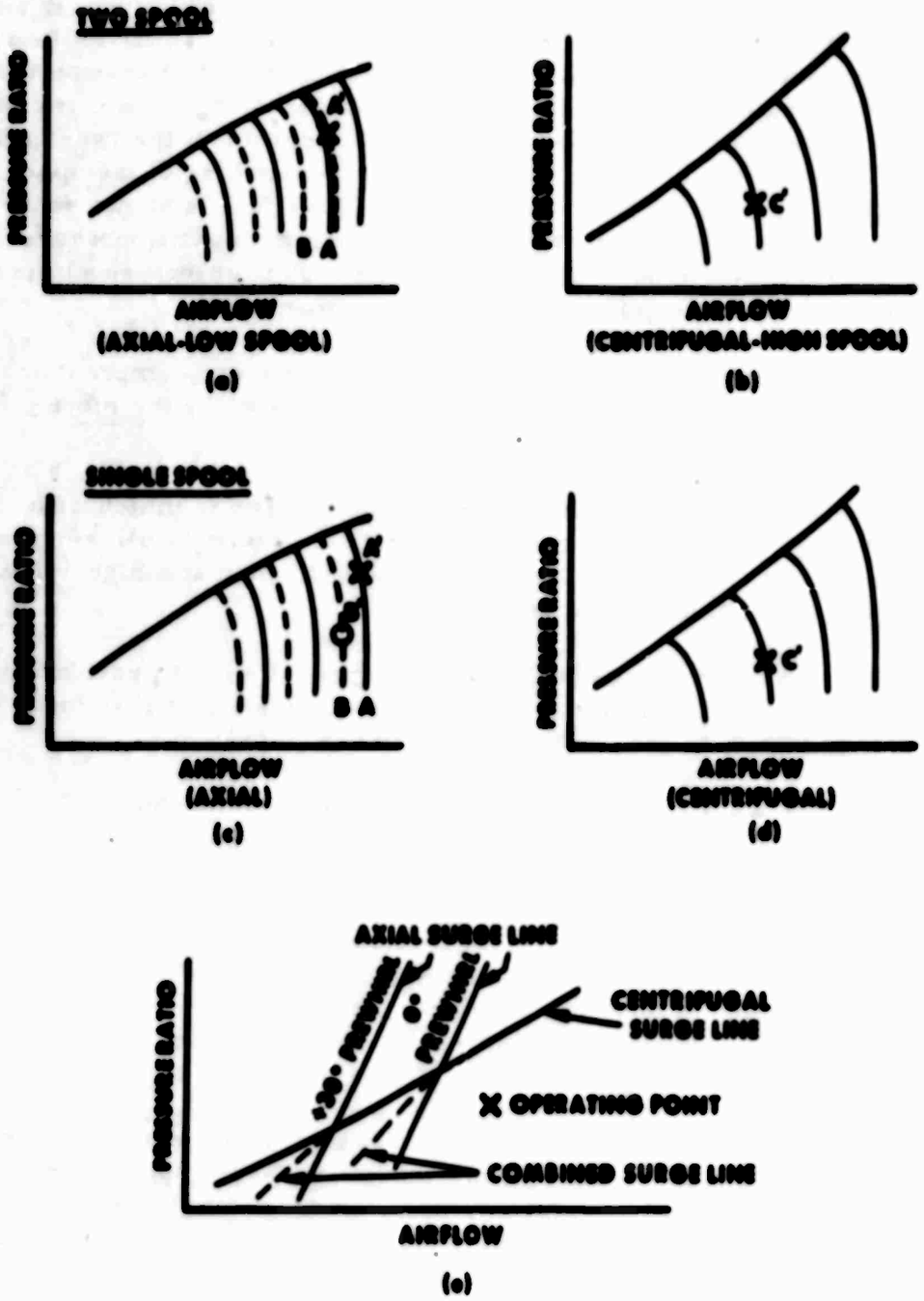

Figure 72. Effect of Variable Inlet Guide Vanes.

to maintain the match of axial exit corrected flow ($W\sqrt{T}/AP$) with the centrifugal inlet corrected flow at point C', Figure 72(d), B' must move toward a higher flow and lower pressure ratio on line B', moving away from surge and providing higher axial surge margin. This appears on the combined stage map as a shift in the match of the axial surge line to lower flows relative to the centrifugal surge line. The combined surge line is therefore moved to lower flows as described on the schematic, Figure 72(e).

Variable Power Turbine Nozzles on a Single-Spool Engine. It has been shown in this report that using variable turbine nozzles to increase part-power turbine inlet temperature causes:

- A reduction in part-power surge margin.
- Little or no improvement in part-power BSFC.

This result is consistent with past Continental studies which have shown that regeneration is required with variable turbine geometry in order to improve part-power BSFC (see Figure 73).

The above results from the following occurrences at part-power:

- With no regeneration and variable turbine geometry, the effect of the increase in turbine temperature is generally off-set (almost exactly) by the decrease in cycle pressure ratio and component efficiencies.
- The increase in cycle thermal efficiency with temperature is significantly greater with regenerator than without at the temperature levels being considered.

Single-Spool Engine - Fixed (Connected) Power Turbine. In view of the results of the fixed-shaft, two-spool engine configurations, the single-spool engine components were evaluated aerodynamically and structurally prior to overall engine performance analysis. It was found that combining the power turbine to the gas generator turbine on a single-spool engine was less severe structurally than on a two-spool engine because of the lower gas generator speed on a single-spool engine. However, the stress problems are still very severe. Using a very advanced material (forecasted for 1972-74), the turbine still suffered an efficiency penalty resulting in an overall turbine efficiency of only 84 percent.

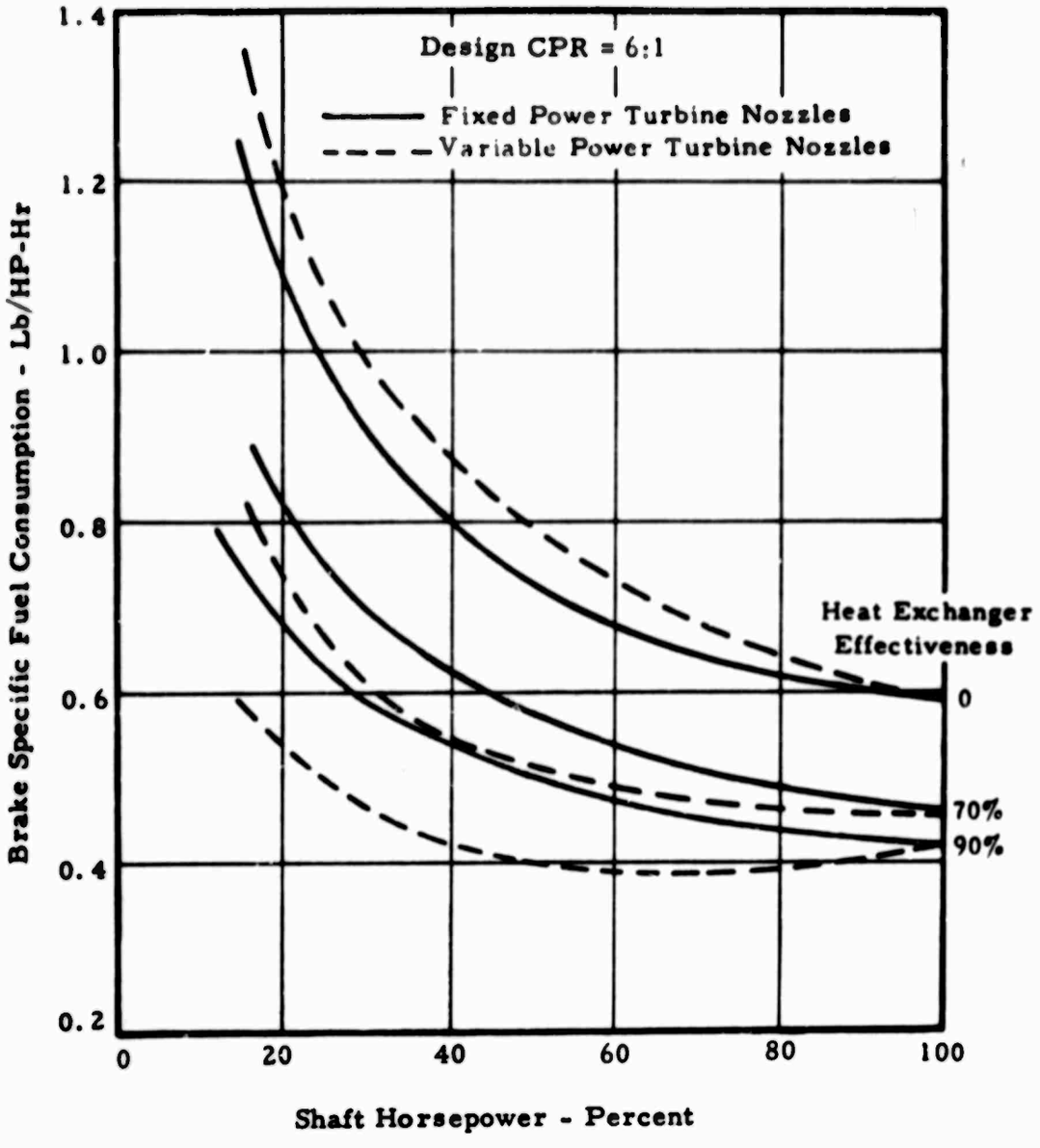

Figure 73. Past Continental Study, Effect of Regeneration and Variable Turbine Geometry on Fuel Consumption.

Design Point Analysis

A summary of the design point data is shown in Table XVIII. Using this turbine efficiency, the design point was established for each single-spool fixed-shaft turbine cycle. All of the points were selected to make the single-spool engines directly comparable to the two-spool engines. The complete input and output computations for these points are included in Tables XIX through XXII. The engine station designation is presented in Figure 74. The symbols used on the computer input and output are given below and on page 121.

TABLE XVIII
DESIGN POINT DATA

	One Supersonic Stage		Two Transonic Stages	
Axial Pressure Ratio	2.8:1	3.1:1	2.8:1	2.8:1
SHP	947	920	993	969
BSFC - Lb/HP-Hr	0.520	0.525	0.503	0.506
T5-TIT - ^{o}R	2960	2960	2960	2960
P_3/P_2	16.0	17.0	16.0	17.0
Eff. Turb - %	84.0	84.0	84.0	84.0
Eff. Comb - %	74.5	73.5	77.0	76.0

It is evident that for all engines the BSFC is above the target value. These engine configurations were therefore discarded as potential candidates, and no off-design performance was calculated.

SYMBOLS

Input	Alt	-	Altitude - feet
	N Comb	-	Combustor adiabatic efficiency
	BO	-	Overboard bleed
	DP/PHC	-	Heat exhcanger pressure loss - cold
	P_3/P_2	-	Compressor pressure ratio
	M	-	Flight Mach number
	LHV	-	Lower heating value - Btu/lb
	BC	-	Cooling bleed
	DP/PC	-	Combustor pressure loss
	NC	-	Compressor adiabatic efficiency
	TA	-	Ambient temperature - ^{o}R
	EM	-	Mechanical efficiency
	BHC	-	Heat exchanger bypass - cold side

TABLE XIX
DESIGN POINT PERFORMANCE, SINGLE-SPOOL FIXED POWER TURBINE, SUPERSONIC AXIAL COMPRESSOR, 2.8:1 PRESSURE RATIO

INPUT

ID	ALT	M	TA	PA	P2/P1	
101	0.0000E-99	0.0000E-99	0.0000E-99	0.0000E-99	9.9500E-01	
	N Comb	LHV	EM	N N	HPE	N
201	9.8500E-01	1.8400E+04	9.8000E-01	1.0000E+00	0.0000E-99	1.0000E+02
	BO	BC	BHC	BHH	BL	
301	0.0000E-99	0.0000E-99	0.0000E-99	0.0000E-99	2.0000E-02	
	DP/PHC	DP/PC	DP/PD	DP/PHH		WA
401	0.0000E-99	4.5000E-02	5.0000E-02	0.0000E-99	0.0000E-99	5.0000E+00
	P3/P2	N C	N T	TIT	P8/PA	EFFECT
501	1.6000E+01	7.4500E-01	8.4000E-01	2.9600E+03	1.0150E+00	0.0000E-99

OUTPUT 30.036

TA	5.1868E+02	PA	1.4695E+01	WA	5.0000E+00	P2/P1	9.9500E-01
T2	5.1868E+02	P2	1.4622E+01	W3	4.9000E+00	N/RTH2	1.0000E+02
T3	1.3184E+03	P3	2.3395E+02	W5	5.0368E+00	WRTH/D2	5.0251E+00
T4	1.3184E+03	P4	2.3395E+02	W7	5.0368E+00	P3/P2	1.6000E+01
T5	2.9600E+03	P5	2.2343E+02	WRT/P6	1.3681E+01	N C	7.4500E-01
T6	1.8189E+03	P6	1.5701E+01	F/A	2.7924E-02	N/RTH5C	4.2520E+01
T7	1.8189E+03	P7	1.4916E+01	DP/PN	0.0000E-99	DHT/TH5	6.1278E+01
T8	1.8091E+03	P8	1.4916E+01	DP/P6-9	5.0000E-02	N T	8.4000E-01
EFFECT	0.0000E-99	P9	1.4916E+01	P8/PA	1.0150E+00	WN/D605	5.5230E-01
N	1.0000E+02	TAU	4.9758E+04	AJ	1.1063E+02	P5/P6	1.4229E+01
FN	4.8514E+01	FG	4.8514E+01	WF	4.9258E+02	DHT/NS	3.3894E-02
SHP	9.4739E+02	BSFC	5.1993E-01	ESHP	9.6680E+02	EBSFC	5.0950E-01

TABLE XX

DESIGN POINT PERFORMANCE, SINGLE-SPOOL FIXED POWER TURBINE, SUPERSONIC AXIAL COMPRESSOR, 3.1:1 PRESSURE RATIO

INPUT

ID	ALT	M	TA	PA	P2/P1	
104	0.0000E-99	0.0000E-99	5.1868E+02	1.4695E+01	9.9500E-01	
	N COMB	LHV	EM	N N	HPE	N
204	9.8500E-01	1.8400E+04	9.8000E-01	1.0000E+00	0.0000E-99	1.0000E+02
	BO	BC	BHC	BHH	BL	
304	0.0000E-99	0.0000E-99	0.0000E-99	0.0000E-99	2.0000E-02	
	DP/PHC	DP/PC	DP/PD	DP/PHH		WA
404	0.0000E-99	4.5000E-02	5.0000E-02	0.0000E-99	0.0000E-99	5.0000E+00
	P3/P2	N C	N T	TIT	P8/PA	EFFECT
504	1.7000E+01	7.3500E-01	8.4000E-01	2.9600E+03	1.0150E+00	0.0000E-99

OUTPUT 30.036

TA	5.1868E+02	PA	1.4695E+01	WA	5.0000E+00	P2/P1	9.9500E-01
T2	5.1868E+02	P2	1.4622E+01	W3	4.9000E+00	N/RTH2	1.0000E+02
T3	1.3523E+03	P3	2.4858E+02	W5	5.0342E+00	WRTH/D2	5.0251E+00
T4	1.3523E+03	P4	2.4858E+02	W7	5.0342E+00	P3/P2	1.7000E+01
T5	2.9600E+03	P5	2.3739E+02	WRT/P6	1.3597E+01	N C	7.3500E-01
T6	1.7985E+03	P6	1.5701E+01	F/A	2.7388E-02	N/RTH5C	4.2514E+01
T7	1.7985E+03	P7	1.4916E+01	DP/PN	0.0000E-99	DHT/TH5	6.2239E+01
T8	1.7898E+03	P8	1.4916E+01	DP/P6-9	5.0000E-02	N T	8.4000E-01
EFFECT	0.0000E-99	P9	1.4916E+01	P8/PA	1.0150E+00	WN/D605	5.1954E-01
N	1.0000E+02	TAU	4.8369E+04	AJ	1.0998E+02	P5/P6	1.5119E+01
FN	4.8229E+01	FG	4.8229E+01	WF	4.8312E+02	DHT/NS	3.4434E-02
SHP	9.2094E+02	BSFC	5.2459E-01	ESHP	9.4024E+02	EBSFC	5.1383E-01

TABLE XXI
DESIGN POINT PERFORMANCE, SINGLE-SPOOL FIXED POWER TURBINE, TWO-STAGE TRANSONIC AXIAL COMPRESSOR, 2.8:1 PRESSURE RATIO

INPUT

ID	ALT	M	TA	PA	P2/P1	
101	0.0000E-99	0.0000E-99	0.0000E-99	0.0000E-99	9.9500E-01	
	N COMB	LHV	EM	N N	HPE	N
201	9.8500E-01	1.8400E+04	9.8000E-01	1.0000E+00	0.0000E-99	1.0000E+02
	BO	BC	BHC	BHH	BL	
301	0.0000E-99	0.0000E-99	0.0000E-99	0.0000E-99	2.0000E-02	
	DP/PHC	DP/PC	DP/PD	DP/PHH		WA
401	0.0000E-99	4.5000E-02	5.0000E-02	0.0000E-99	0.0000E-99	5.0000E+00
	P3/P2	N C	N T	TIT	P8/PA	EFFECT
501	1.6000E+01	7.7000E-01	8.4000E-01	2.9600E+03	1.0150E+00	0.0000E-99

OUTPUT 30.036

TA	5.1868E+02	PA	1.4695E+01	WA	5.0000E+00	P2/P1	9.9500E-01
T2	5.1868E+02	P2	1.4622E+01	W3	4.9000E+00	N/RTH2	1.0000E+02
T3	1.2940E+03	P3	2.3395E+02	W5	5.0387E+00	WRTH/D2	5.0251E+00
T4	1.2940E+03	P4	2.3395E+02	W7	5.0387E+00	P3/P2	1.6000E+01
T5	2.9600E+03	P5	2.2343E+02	WRT/P6	1.3688E+01	N C	7.7000E-01
T6	1.8194E+03	P6	1.5701E+01	F/A	2.8307E-02	N/RTH5C	4.2521E+01
T7	1.8194E+03	P7	1.4916E+01	DP/PN	0.0000E-99	DHT/TH5	6.1296E+01
T8	1.8092E+03	P8	1.4916E+01	DP/P6-9	5.0000E-02	N T	8.4000E-01
EFFECT	0.0000E-99	P9	1.4916E+01	P8/PA	1.0150E+00	WN/D605	5.5251E-01
N	1.0000E+02	TAU	5.2187E+04	AJ	1.1067E+02	P5/P6	1.4229E+01
FN	4.8532E+01	FG	4.8532E+01	WF	4.9934E+02	DHT/NS	3.3900E-02
SHP	9.9364E+02	BSFC	5.0253E-01	ESHP	1.0130E+03	EBSFC	4.9290E-01

TABLE XXII

DESIGN POINT PERFORMANCE, SINGLE-SPOOL FIXED-POWER TURBINE, TWO-STAGE TRANSONIC AXIAL COMPRESSOR, 3.1:1 PRESSURE RATIO

INPUT

ID	ALT	M	TA	PA	P2/P1	
104	0.0000E-99	0.0000E-99	5.1868E+02	1.4695E+01	9.9500E-01	
	N COMB	LHV	EM	N N	HPE	N
204	9.8500E-01	1.8400E+04	9.8000E-01	1.0000E+00	0.0000E-99	1.0000E+02
	BO	BC	BHC	BHH	BL	
304	0.0000E-99	0.0000E-99	0.0000E-99	0.0000E-99	2.0000E-02	
	DP/PHC	DP/PC	DP/PD	DP/PHH		WA
404	0.0000E-99	4.5000E-02	5.0000E-02	0.0000E-99	0.0000E-99	5.0000E+00
	P3/P2	N C	N T	TIT	P8/PA	EFFECT
504	1.7000E+01	7.5980E-01	8.4000E-01	2.9600E+03	1.0150E+00	0.0000E-99

OUTPUT 30.036

TA	5.1868E+02	PA	1.4695E+01	WA	5.0000E+00	P2/P1	9.9500E-01
T2	5.1868E+02	P2	1.4622E+01	W3	4.9000E+00	N/RTH2	1.0000E+02
T3	1.3269E+03	P3	2.4858E+02	W5	5.0361E+00	WRTH/D2	5.0251E+00
T4	1.3269E+03	P4	2.4858E+02	W7	5.0361E+00	P3/P2	1.7000E+01
T5	2.9600E+03	P5	2.3739E+02	WRT/P6	1.3604E+01	N C	7.5980E-01
T6	1.7991E+03	P6	1.5701E+01	F/A	2.7789E-02	N/RTH5C	4.2516E+01
T7	1.7991E+03	P7	1.4916E+01	DP/PN	0.0000E-99	DHT/TH5	6.2258E+01
T8	1.7899E+03	P8	1.4916E+01	DP/P6-9	5.0000E-02	N T	8.4000E-01
EFFECT	0.0000E-99	P9	1.4916E+01	P8/PA	1.0150E+00	WN/D605	5.1974E-01
N	1.0000E+02	TAU	5.0918E+04	AJ	1.1002E+02	P5/P6	1.5119E+01
FN	4.8248E+01	FG	4.8248E+01	WF	4.9021E+02	DHT/NS	3.4441E-02
SHP	9.6948E+02	BSFC	5.0564E-01	ESHP	9.8878E+02	EBSFC	4.9577E-01

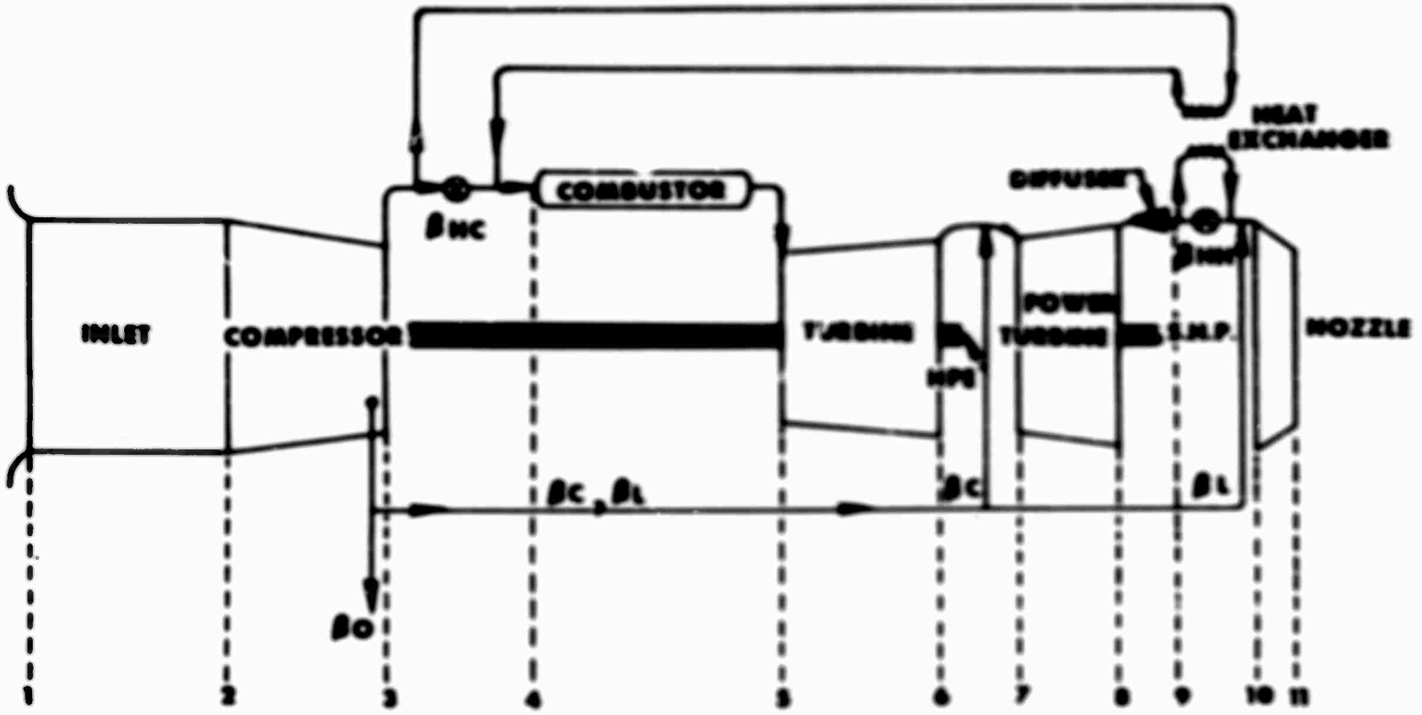

Figure 74. Station Designation, Single-Spool Fixed-Power Turbine, Turboshaft Engine.

	DP/PJ	-	Exhaust diffuser pressure loss
	NT	-	Turbine adiabatic efficiency
	PA	-	Ambient pressure - PSIA
	NN	-	Exhaust nozzle efficiency
	BHH	-	Heat exchanger bypass - hot side
	DP/PHH	-	Heat exchanger pressure loss - hot side
	TIT	-	Turbine inlet temperature - $^{\circ}R$
	P_2/P_1	-	Inlet diffuser pressure ratio
	HPE	-	Horsepower extracted
	BL	-	Heat exchanger leakage
	P_8/PA	-	Exhaust nozzle total to static pressure ratio
	N	-	Engine speed - rpm
	WA	-	Abeolute airflow at inlet - lb/sec
	Effect	-	Heat exchanger effectiveness
Output	TA	-	Ambient temperature - $^{\circ}R$
	T	-	Temperature at appropriate stations - $^{\circ}R$
	Effect	-	Heat exchanger effectiveness
	N	-	Engine speed - rpm
	FN	-	Net thrust
	SHP	-	Shaft horsepower
	PA	-	Ambient pressure - PSIA
	P	-	Pressure at appropriate stations - PSIA
	TAU	-	Output shaft torque
	FG	-	Gross thrust
	ΔSFC	-	Brake specific fuel consumption - lb/SHP/hr
	WA	-	Abeolute airflow at inlet - lb/sec
	W	-	Airflow at appropriate stations - lb/sec
	WRT/P_6	-	Turbine output flow function
	F/A	-	Fuel to air ratio
	DP/PN	-	Exhaust nozzle pressure loss
	DP/P_{6-9}	-	Exhaust diffuser pressure loss
	P_8/PA	-	Exhaust nozzle total to static pressure ratio
	AJ	-	Exhaust nozzle area - $in.^2$
	WF	-	Fuel flow - lb/hr
	ESHP	-	Equivalent shaft horsepower
	P_2/P_1	-	Inlet diffuser pressure ratio
	N/RTH2	-	Referred compressor speed - $(N/\sqrt{\theta})_2$ - rpm
	WRTH/D2	-	Referred airflow - $(W\sqrt{\theta}/\delta)_2$ - lb/sec
	P_3/P_2	-	Compressor pressure ratio
	NC	-	Compressor adiabatic efficiency
	N/RTH5C	-	Referred turbine speed - $N/\sqrt{\theta_{5C}}$ - rpm
	DHT/TH5	-	Referred turbine work - $\Delta h_t/\theta_5$ - Btu/lb
	NT	-	Turbine adiabatic efficiency
	WN/D605	-	Turbine speed flow parameters - $(WN/\delta 60)_5$ - lb-rev/sec^2

P_5/P_6	-	Turbine pressure ratio
DHT/NS	-	Turbine work - speed parameter - $\Delta h_t/N^2$
EBSFC	-	Equivalent brake specific fuel consumption lb/SHP/hr

CONCLUSIONS

Some of the conclusions which can be drawn from the engine performance evaluation are listed below:

1. Two transonic axial compressor stages incorporated in the engine produce a lower specific fuel consumption and a higher surge margin than a single-stage supersonic compressor.

2. There is no basic performance advantage of a two-spool engine configuration over a single-spool configuration. Therefore, the single-spool configurations are more desirable for their relative structural simplicity.

3. Fixed (connected) power turbine engines have significant structural and/or turbine efficiency problems, and produce inferior overall performance.

4. Free power turbines in either single- or twin-spool configurations are desirable for the broader ranges of power and fuel consumption characteristics with output speed.

5. Variable compressor inlet guide vanes improve surge margin on single-spool engines but not on two-spool engines.

6. Variable turbine geometry is not desirable for simple cycle engines.

7. Comparison of single- and twin-spool engine performance, using similar basic components, shows approximately the same change in variable power turbine geometry versus power for constant power turbine inlet temperature, as shown in Figure 75.

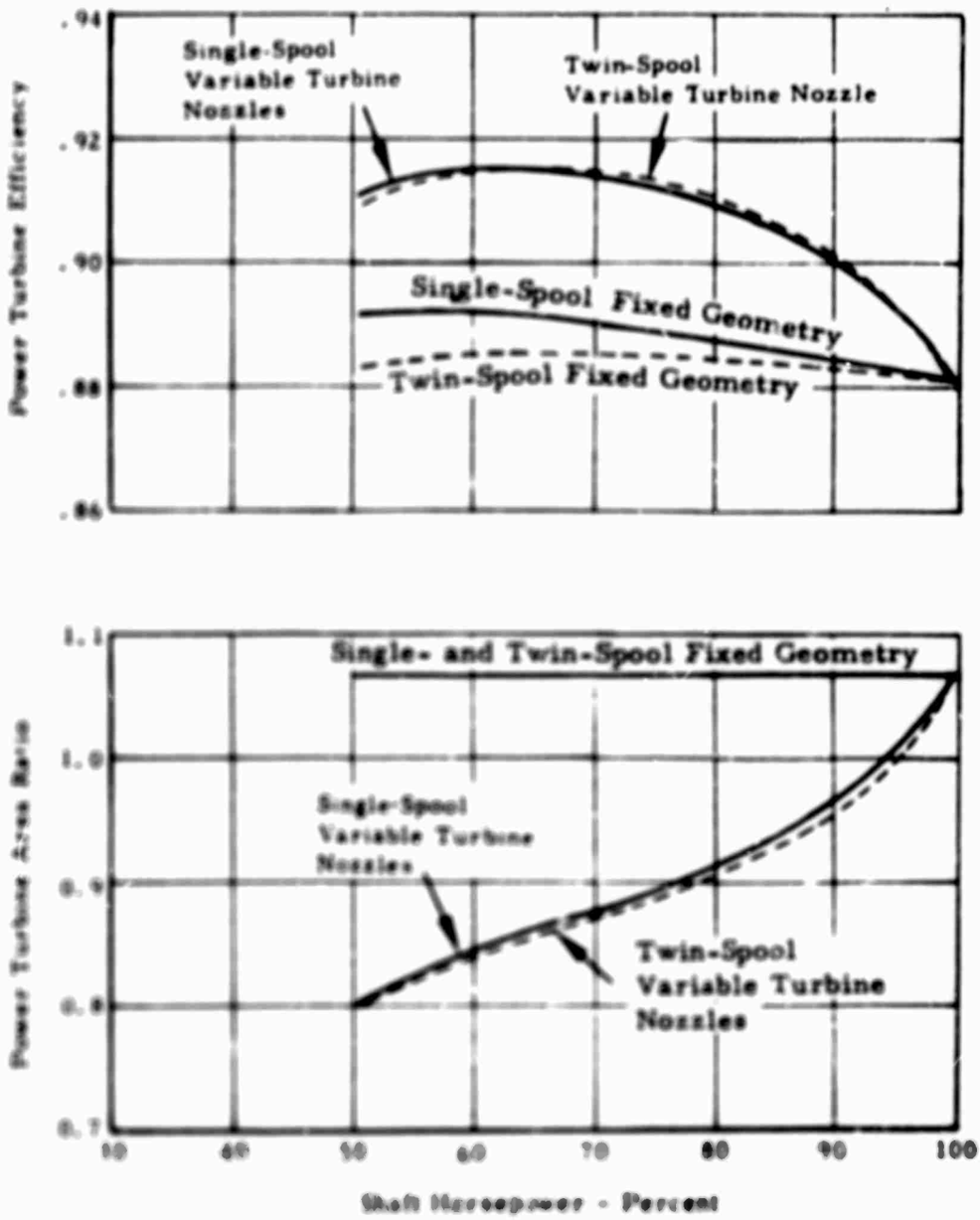

Figure 71. Comparison of Single- and Twin-Spool Variable Power Turbine Geometry Characteristics Using the 2.8:1 Two-Stage Transonic Axial Compressor.

OPTIMUM GAS GENERATOR CONFIGURATIONS

From the work performed on the gas generator cursory design, the optimum gas generator configuration shown in Figure 76 was selected.

A single-spool free-shaft power turbine configuration is preferred because of:

- Simplicity of design, i.e., single gas generator shaft, less bearings, and so forth.
- Gas generator performance essentially equivalent to that of the two-spool configurations.

Since each of the four candidate gas generators has two-stage transonic axial compressors, a comprehensive axial pressure ratio - efficiency prediction study was conducted to determine the optimum pressure ratio for maximum engine performance.

Figure 77 shows the results of this study: a prediction of the effect of axial pressure ratio on efficiency for various two-stage transonic axial compressor designs. The decrease in efficiency with increasing pressure ratio is due to the increased rotor shock losses which are associated with high relative rotor inlet Mach numbers. As the design pressure ratio of the transonic compressors is increased, higher tip speeds are needed to maintain reasonable rotor blade aerodynamic loadings. The increased tip speeds in turn necessitate the higher relative rotor inlet Mach numbers.

The pressure ratio, efficiency curve on Figure 77 becomes most significant when overlaid on Figure 78, which defines the objectives of this contract. Notice that the predicted BSFC for the axial-centrifugal compressor combination is nearly constant from an axial pressure of 2.6:1 to 3.0:1 and that the predicted BSFC rises rapidly at axial pressure ratios greater than 3.0:1. From this analysis, it is concluded that the optimum two-stage transonic axial pressure ratio for the given cycle is near 3.0:1 because:

- Minimum design point BSFC is achieved from pressure ratios from 2.6:1 to 3.0:1.
- Sufficient 50 percent power overall axial-centrifugal surge margin is obtained with the 3.0:1 pressure ratio transonic compressor design.

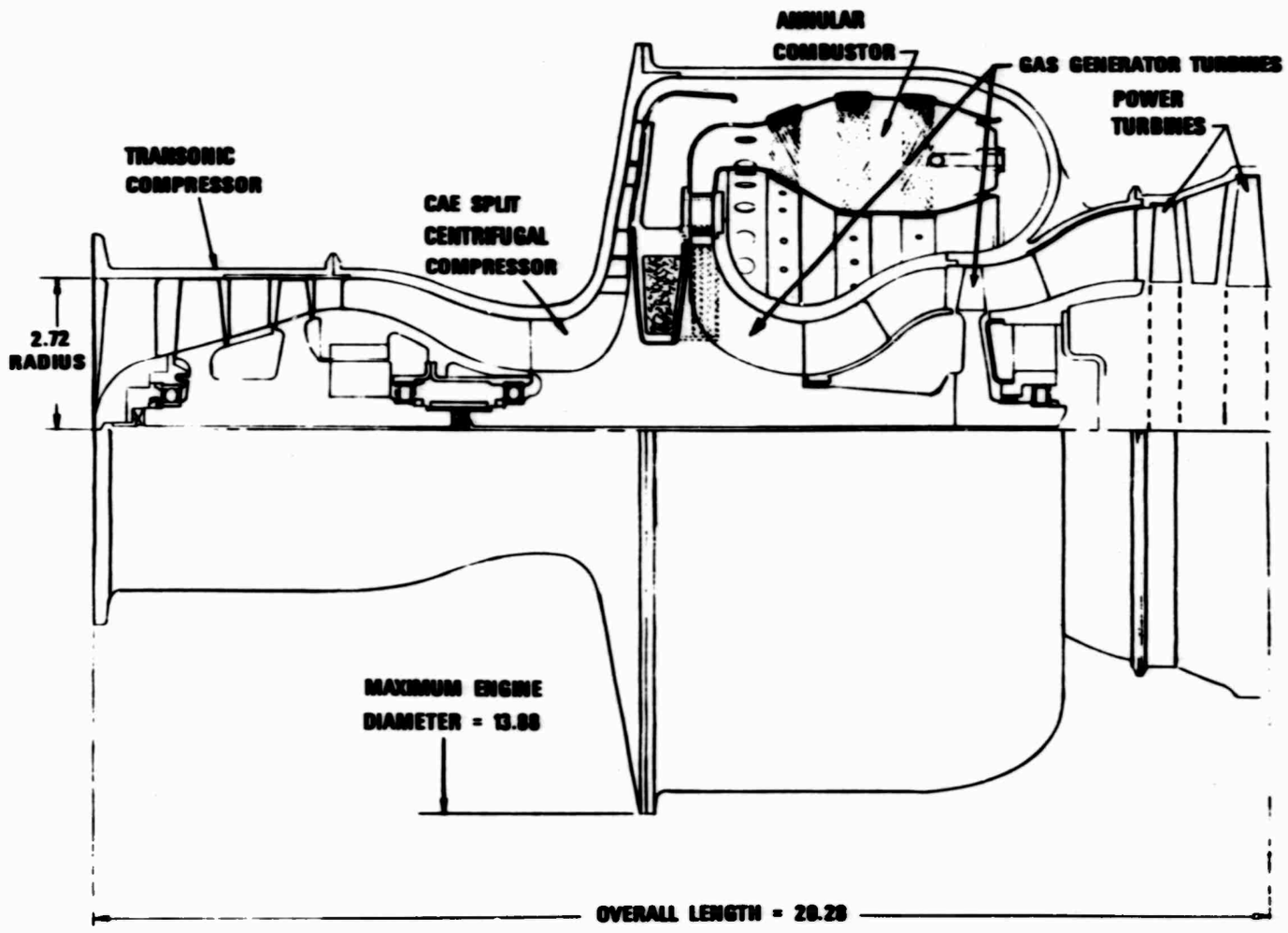

Figure 76. Single-Spool Free Shaft Power Turbine Gas Generator Flow Path, 3.0:1 Pressure Ratio, Optimum Advanced Small Axial Compressor.

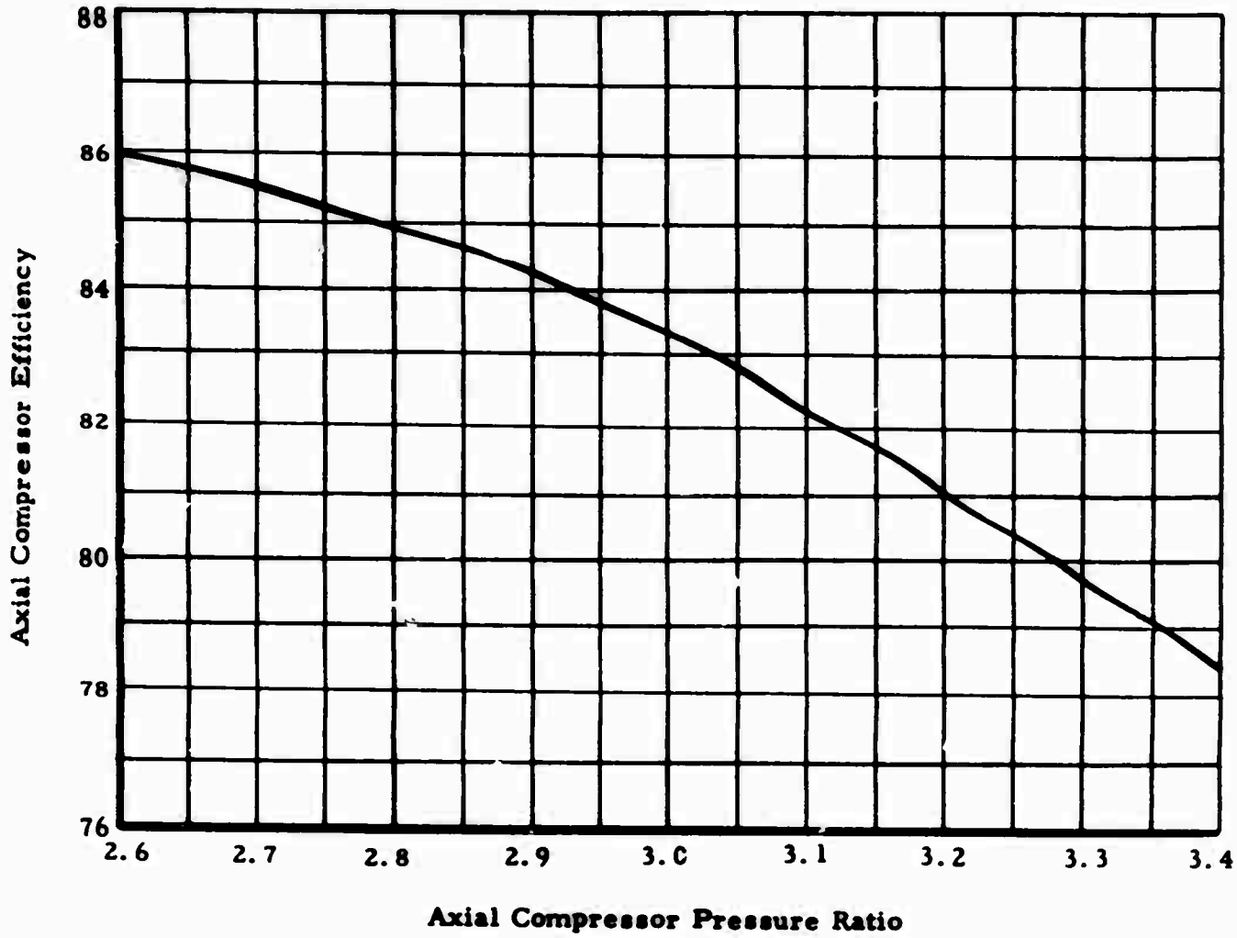

Figure 77. The Effect of Pressure Ratio on Efficiency for a Two-Stage Transonic Compressor.

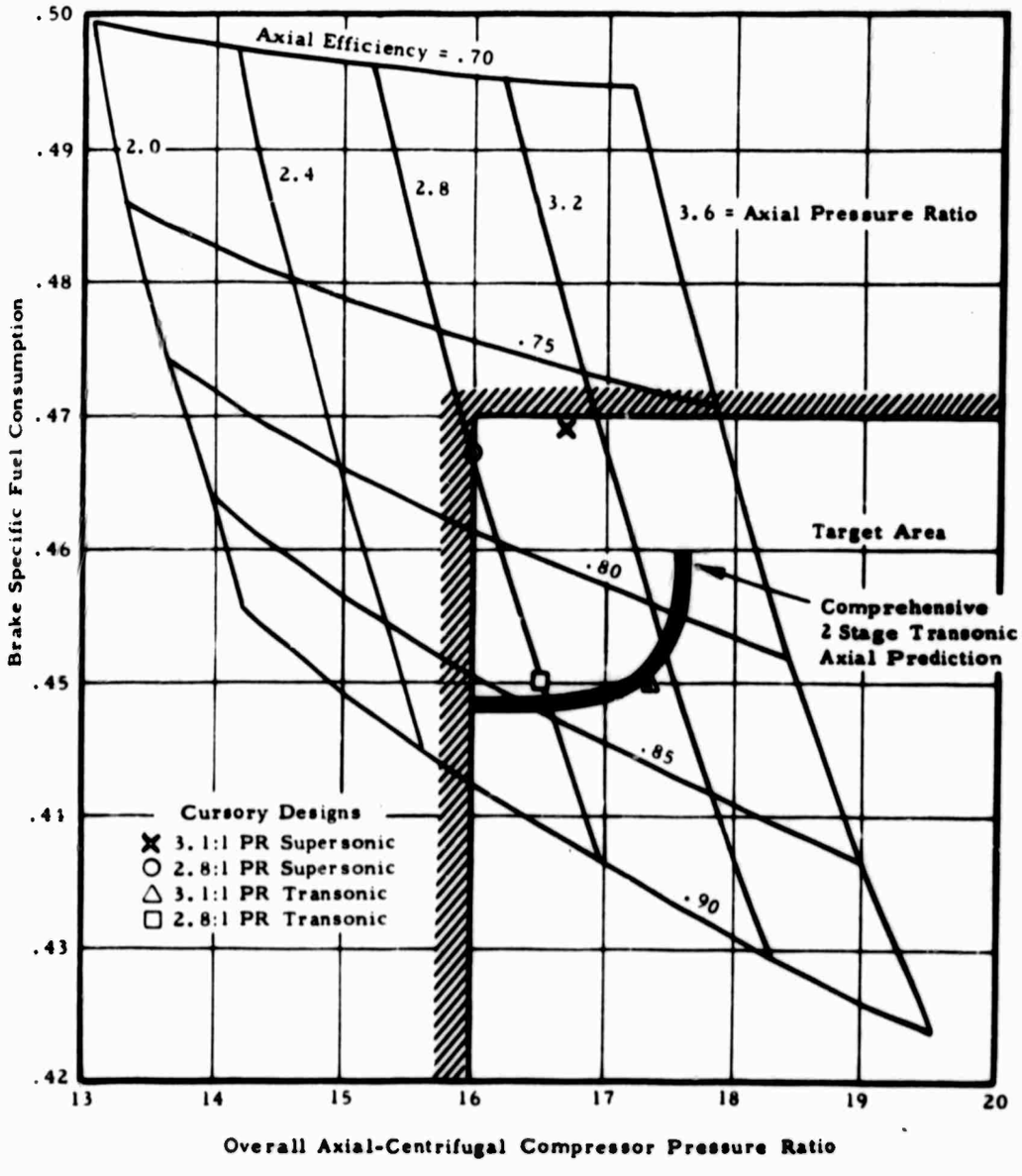

Figure 78. The Effect of Overall Axial-Centrifugal Compressor Pressure Ratio and Axial Compressor Performance on Brake Specific Fuel Consumption.

- The target BSFC is achieved with adequate margin and overall axial-centrifugal compressor pressure ratio is exceeded.

The axial compressor shown for the optimum gas generator is very close, in performance and configuration, to the two-spool, 3.1:1 pressure ratio axial compressor. It has the following approximate design parameters:

Axial Pressure Ratio	3.0:1
Axial Efficiency	83 percent
Axial Inlet Hub Tip Ratio	0.5
Axial Tip Speed	1400 feet per second

The axial compressor can be used in either a single-spool or a two-spool gas generator. This gives a design flexibility in incorporating the axial compressor into an actual engine.

The centrifugal compressor presented in Figure 76 is a Continenal "split" radial compressor configuration embodying a conventional centrifugal impeller followed, in order, by a stationary and moving row of blades. This type of compressor is ideal for high pressure ratio, low flow applications. High efficiency levels are obtained by staging the centrifugal flow path. The split compressor has higher efficiencies, lower Mach numbers, and lower tip speeds for the same pressure ratio level than the conventional centrifugal compressors.

Use of the split centrifugal compressor rather than the compressors supplied by USAAVLABS allows the rpm of the single-spool gas generator to be increased by about 25 percent. The increase in rpm is beneficial to the single-spool gas generator configurations because:

- The axial compressor is more compact.
- The centrifugal compressor runs at a higher specific speed, and thus, should be more efficient.
- The overall gas generator volume is reduced by about 41 percent.
- Greater flexibility in burner design is provided because of the lower centrifugal compressor and radial turbine profiles.

Because of these benefits, Continental believes that the compressors supplied by USAAVLABS can, and should, be designed for higher rotational speeds if eventual match with an axial compressor is intended.

The overall axial-centrifugal design performance for the optimum gas generator configuration is:

Overall Total Pressure Ratio	17.4:1
Overall Total Efficiency	0.78
Centrifugal Compressor Mechanical Tip Speed	1850 feet per second

MECHANICAL DESIGN OF ADVANCED COMPRESSOR

MECHANICAL DESCRIPTION

The Advanced Small Axial Compressor Rig (Figure 79) is designed as a compact entity which can be bench assembled into a single unit. The unit is then aligned with, coupled to, and suspended by its rear flange from the driving gearbox.

The compressor rig unit consists of three major subsections:

1. Inlet Section
2. Compressor Section
3. Exit and Exhaust Section

Inlet Section

This section includes the air inlet housing, the front bearing compartment, and the inlet guide vane housing, vanes, and linkage.

Air Inlet Housing. The air inlet housing consists of an inner bullet nose connected through three radial struts to an outer, concentric cylindrical wall. These three struts, which are streamlined and of constant radial section, are equally spaced circumferentially with one located at bottom dead center. Oil scavenge routing is through drilled passages in this bottom or 6 o'clock strut. When observing the air inlet housing from the front, the 10 o'clock strut serves to route oil into the bearing, and the 2 o'clock strut houses the bearing compartment breather or vent porting. Aside from the bearing compartment supply function, the three inlet housing struts serve as a front bearing support, transferring the residual shaft dynamic loadings from the inner bullet nose to the outer casing shell.

The front bearing compartment is contained within the limited confines of the inner bullet nose. This crowded situation was necessitated by aerodynamic requirements for the inner wall inlet flow-path boundary. The tight spacing forced severe complications in the type of oil seal used, and as a result, two systems were designed: a primary carbon face seal system and a secondary or back-up vented labyrinth seal system.

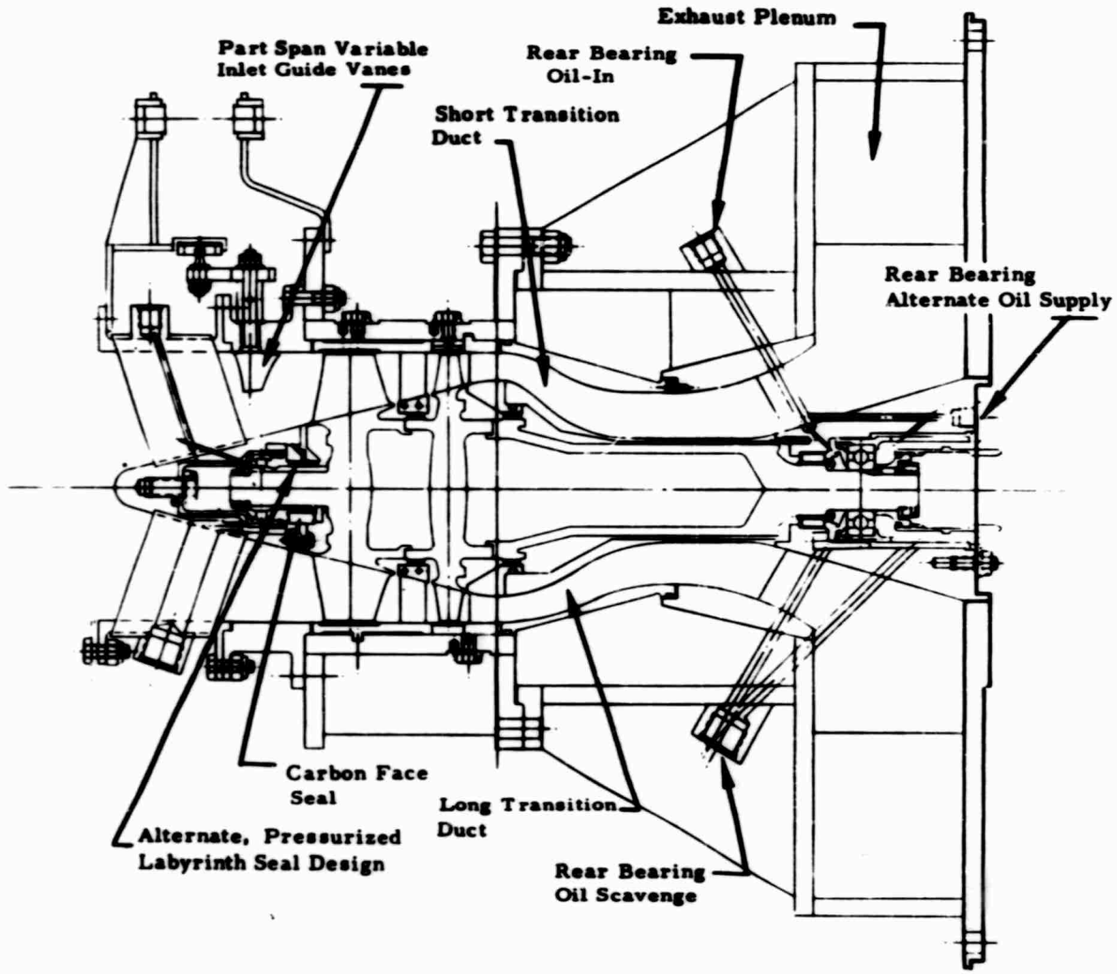

Figure 79. Advanced Axial Compressor Test Rig Design Layout.

The carbon face seal, because of sequential assembly restrictions, was designed to operate in reverse; that is, with the loaded carbon sealing face pointing away from the bearing. This puts the seal face considerably farther away from the bearing oil supply than it would be in the normal installation, possibly preventing adequate lubricating oil mist coverage of the carbon sealing face and wiper. The condition could result in local temperature rise due to friction, severe wear problems, and ineffective sealing.

If the front bearing compartment were vented to atmosphere, as is usually done, there would be a tendency for oil to be forced by the higher internal pressure through the seal into the inlet air stream, which is at subambient pressure. To prevent this, the suction or scavenge pump which drains air and oil out through the bottom housing strut must be capable of reducing the bearing compartment pressure to the same as the inlet air pressure, or below. To complement this arrangement, the vent orifice on the 2 o'clock strut terminates in a threaded boss which can accommodate a calibrated metering orifce to permit monitoring and/or controlling of the bearing compartment static pressure. With a careful balance of oil flow and breather airflow plus seal leakage flows, all adjusted to prevent exceeding of scavenge port capacity, the compartment static pressure can be regulated to an acceptable subambient level by controlling oil flow and gradually restricting breather airflow.

Again, because of size and space restrictions, a short travel carbon seal carrier had to be selected. The entire rig dimensional stackup from bearing to bearing has to be taken into account and measurements taken to afford selection of the proper carbon seal wiper shim for final running assembly.

In order to provide additional assurance of an effective seal in the front bearing compartment, a "back-up" or secondary labyrinth seal system has been designed. The labyrinth seal replaces the carbon seal and carrier component with a stationary set of radially oriented knife edges or labyrinths. The knife edges point inward toward a cylindrical shaft sleeve inner seal boundary which replaces the wiper of the carbon seal system. In the labyrinth seal system, no shimming is necessary for assembly.

In the normal operation of the labyrinth seal system, it is expected that no significant depressurization of the bearing compartment will be required. The bearing compartment should be vented to ambient through its 2 o'clock breather port. By controlling oil flow to prevent overloading the scavenge pump, a slightly subambient compartment pressurization can be achieved. If the breather airflow in through the vent is too great, a

metering restriction can be easily set up on the 2 o'clock external boss to reduce compartment pressure to the subambient condition.

It must be emphasized that the labyrinth seal design depends upon a slightly below ambient compartment pressurization for successful sealing capability. The axially centered annulus of the labyrinth seal is separately vented to ambient to produce airflow into the bearing compartment. Also, ambient vented air flows from the center labyrinth annulus to the external subambient pressurized region at the front of the stage one rotor hub.

In all cases, regardless of pressurization and vent controls utilized, the labyrinth seal depends for its successful operation upon adequate control of oil flow in and scavenge flow out. In short, the scavenge pump system must handle all oil and airflow which enters the bearing compartment with sufficient continuous suction to prevent labyrinth seal oil flooding.

Again, because of space limitations, the front bearing is lubricated through a single oil jet. This orifice is drilled through the inlet casing inner diameter at the 10 o'clock strut position. The oil jet is aimed through a hole in the bearing spring cage rear shoulder to deliver an oil flow which impinges on the bearing inner race just forward of the rollers.

The bearing spring cage is indexed to prevent blockage of this oil flow. This is accommodated on the inlet housing subassembly when the front bearing spring cage (shaft vibration damper) is bolted in by means of the center stud and locknut to the inner housing bullet nose. A pin which provides indexing for the spring cage ensures proper angular orientation for the oil jet.

The inlet housing material is type 347 stainless steel, which was chosen because its properties are satisfactory for structural loading requirements of the three struts, for weldability, and for corrosion resistance. The latter criterion is important to ensure cleanliness of the air inlet aerodynamic boundaries.

The confined space in the front bearing compartment seriously restricted the bearing spring cage geometry. The attendant requirements for reduced stiffness and optimum fatigue service life necessitated the use of 6-6-2 forged annealed titanium for bearing cage construction.

IGV Housing. The IGV housing consists of a single outer flow-path boundary with externally flanged ends. Material is SAE 1010-1020 steel cadmium plated for corrosion protection. Construction is welded.

The front flange of the IGV housing bolts to and is held concentric with the air inlet housing by doweling, thus forming a single doweled and bolted subassembly. The rear flange of the IGV housing is finish machined in this assembly in order to maintain close alignment concentricities and perpendicularities to the bearing bore.

IGV'S. The IGV housing contains 17 equally spaced radial holes near its forward end. These 17 holes accept and house the IGV stems and sleeve bearings with minimal clearances. When the rig is run without IGV's, plugs are employed to fill and seal off these 17 holes.

The IGV airfoils themselves have zero camber and extend only about halfway into the airstream from the outer flow-path boundary. Also, they are tapered from a chord of about 0.9 inch at the outer or root end to about 0.4 inch at the inner or tip end. The IGV stems protrude radially through the outer housing wall and are inserted into bronze sleeves or bushings at the housing exterior. These bushings, pinned to the IGV stems and riding in the housing holes, form journal bearings which provide for stem rotation to obtain the variations in IGV setting angle.

The actuator ring is slotted axially at 17 locations around its circumference to receive the guide pins, which transfer movement from the actuator ring through the positioning arms to the vane stems and bushings.

The inlet guide vanes are each adjusted, initially, to the same angle by means of a positioning gage; thereafter, the actuating ring causes all vanes to move by the same order of magnitude. A calibrated positioning plate with appropriate stops is used to set and monitor vane angle during testing.

The front bearing spring cage, containing the front bearing outer race, rollers, and retainer, is bolted into the inside of the bullet nose and indexed by means of a pin to provide proper alignment of the bearing oil hole. The final component of the inlet section subassembly is the carbon or labyrinth seal unit, which is bolted into the air inlet housing center section behind the bearing.

Compressor Section

The rig compressor section consists of a two-stage rotating compressor wheel and shaft assembly, two stationary vane assemblies, the rotor blade shrouds, and the mid-section external housing.

Rotor Assembly. The rotor assembly consists of integrally bladed first- and second-stage wheels and an extended rear shaft. These three components are electron beam welded together at two points on either side of the second-stage rotor. Both shaft connector stubs on the stage-two wheel are located at a diameter close to the wheel rim, thus forming a continuous axial cylindrical load path from the rear shaft, through the stage-two wheel, to the first-stage wheel. The first- and second-stage wheels have 15 and 41 blades, respectively.

The rear shaft diameter is as large as practicable throughout its length in the interests of rigidity and high third (*Free-Free*) critical speed. The confines of the inner aerodynamic exit transition ducts, coupled with thrust balance pressurization space requirement and the thrust bearing size limitations, dictated the maximum shaft size.

The rotor assembly, consisting of the stage-one and -two wheels and shaft mentioned above, is entirely of AMS 5616 (Greek Ascoloy) material. This material was chosen because of its high tensile strength, fatigue properties, availability, and weldability. This assembly is electron beam welded at two joints - one on each side of the stage-two wheel - into a unitized construction. Ample balance accommodations are provided with four planes for stock removal at:

1. Front face of stage-one wheel.
2. Rear face of stage-two wheel.
3. Rear face of shaft front end.
4. Rear OD of rear shaft cone.

The rotor weld joint diameters and face squarenesses are closely held in detail, and after welding, both front and rear bearing journal diameters and faces are turned to ensure tight control over assembled component squarenesses and center of gravity variations. The rotating knife-edge labyrinth seals located fore and aft of the stage-two rotor are also machined after welding.

Stator Assemblies. The stage-one stator assembly, located between the first- and second-stage rotors, is a split assembly. Each stator half consists of an inner and an outer 180° arc segment, forming the inner and outer shroud, joined by the stator vanes, which are brazed into the shrouds. The stator halves are doweled together at both the inner and outer shrouds for rig assembly purposes. The material selected for this component is type 347 stainless steel, which represents the optimum combination of brazeability, low cost, availability, and structural integrity.

The inner diameter of the stage-two stator assembly is silver-plated for labyrinth seal rubbing capability. The split outer shroud ring is extended axially forward to provide a stage-one rotor blade tip shrouding. To obtain tight rotor tip clearances without the risk of detrimental rubbing, a felt-metal composition strip is bonded to the outer shroud ring at its inner diameter over the stage-one blades.

The stage-two stator assembly contains 53 vanes. This assembly is a one-piece brazed entity with a single undivided inner ring shroud and a single outer shroud. The inner ring is grooved at its rear OD to house the inner exit duct "O" ring seal, and this inner ring is also silver-plated at its rear ID to provide labyrinth seal rub capability. The material is type 347 stainless steel, selected for the same reasons as the first-stage stator.

The stage-two rotor shroud is a separate piece, sandwiched axially between outer shroud rings of stage-one and stage-two stator assemblies. The stage-two rotor shroud is also coated with felt metal on the ID for abradability and close tip clearance control.

Midsection Split Housing. The compressor midsection housing encases the stage-one and -two rotors and stators. This housing is cylindrical and flanged externally at both ends. Gusseting is provided externally for flange stiffness. This housing is split longitudinally in the rig horizontal plane with doweling to ensure proper alignment of casing halves.

Inspection of compressor rotor blades and vanes is feasible by first removing the top midsection split housing half. Next, half of the stage-one stator assembly can be removed, exposing the stage-one blades. By sliding the stage-two rotor shroud ring forward, stage-two blades are also exposed and half of the stage-two stator inlet can be observed.

The mid-split housing also incorporates antitorque bolts which locally insert into slots in stage-one and -two stators and the stage-two rotor shroud. Both stator assemblies and the stage-two rotor shroud are supported at this split casing ID with closely controlled radial positioning tolerances.

SAE 1010-1020, cadmium plated steel was chosen for use in the compressor split housings because of its low cost and ready availability as well as the low strength requirements of the application and the lack of aerodynamic exposure.

Exit and Exhaust Section

The exit and exhaust section consists of the rear main frame, air exit ducts and rear bearing compartment.

Rear Main Frame. The rear main frame provides for rig mounting at its rear face; it contains a rear exit and exhaust plenum, houses the air exit ducts and rear bearing compartment, and provides the main structural static support for the entire compressor rig.

The exit plenum of the rear frame is bounded, fore and aft, by two large radial plates - the rear mount face plate and the center plate. These parallel plates are joined at their rims by a cylindrical wall spacer which encloses the exhaust plenum inside. The two plates are gusseted together through four struts located at 12, 3, 6, and 9 o'clock positions (looking from front). The four struts extend forward into the rig discharge annulus, and are streamlined at the leading edge to prevent abrupt aerodynamic blockage. The rear bearing compartment outer wall bounds the four struts at their ID, the forward part of the struts terminating at the flow-path outer wall and the rear part bridging the exhaust plenum front and rear walls out to about 1/3 the radial distance from exhaust duct exit to plenum OD. A cylindrical casing support extends forward of the front plate boundary of the exhaust plenum to join the forward external mount flange. This front flange is gusseted at four circumferential locations to the front exhaust plenum plate, and these gussets also attach to the cylindrical casing extension OD. Four internal gussets are also located radially between the outer flow-path annulus exit duct and the cylindrical casing extension. The inner gussets are angularly aligned with the inner struts at the 12, 3, 6, and 9 o'clock positions, and the external gussets are 45° offset, at the 1:30, 4:30, 7:30, and 10:30 o'clock positions.

The inner gussets and struts provide for transfer of air and oil to and from the rear bearing compartment. Scavenging is done at bottom dead center through the 6 o'clock strut and gusset which contain two axially slanted radial holes which scavenge both front and rear sides of the bearing from a common external boss located at the rear cylindrical outer casing support OD.

The 12 o'clock position strut and gusset combination houses the twin ambient vents. The forward vent provides for ambient static pressure on the back face of the second-stage compressor disc; this reduces rotor thrust and is essential to maintaining adequate thrust bearing life. The rear vent operates as a conventional breather for the rear bearing compartment.

The 9 o'clock strut and gusset house the inlet oil line which terminates in the supply oil jets. These jets are so arranged that oil is sprayed on both front and rear sides of the rear (thrust) bearing. Again, positioning of the spring cage is critical to ensure that the rear jet fires through the spring cage slot onto the bearing innner race.

The rear main housing material is 1010-1020 steel, cadmium plated except in the bearing compartment. Construction is all welded - predominately with fillet welds.

Exit Ducts. The two exit ducts, long and short, come in matched sets for aerodynamic compressor discharge variation studies. The inner duct of either set is supported at its front ID over the stage-two stator assembly inner shroud ring "O" ring groove and at its rear ID by the main frame bearing compartment outer wall. The outer duct carries its own external "O" rings at front and rear and is supported at the rear split housing flange ID and the outer discharge annulus wall front ID lip, respectively. The material of both sets of ducts is type 347 stainless steel.

Rear Bearing Compartment. The rear bearing compartment utilizes several components successfully demonstrated on the Continental TS120 gas turbine engine program at Continental. The forward carbon face seal and wiper, ball thrust bearing, and torque transfer splined adapter are all TS120 proven parts. Since there is adequate space in the rig rear section to allow flexibility in the spring cage design, SAE 4140 was used as the cage material.

Since the rig is designed for power utilization from, primarily, the TS120 gearbox, the rear bearing compartment was left unsealed and the coupling splines unlubricated. The Toledo Component Laboratory has provided necessary adaptation for mounting and aligning with the gearbox, for which a closely held diameter and squareness control is provided at the rig rear face plate ID. Oil can be supplied to the rear bearing from the gearbox, if required, by plugging the external 9 o'clock boss, removing the rear plug, and connecting the gearbox oil supply lines to the appropriate port at the rear face of the compartment.

LUBRICATION

Front Bearing

The rig front bearing is lubricated by a single 0.040-inch-diameter jet which impinges upon the bearing inner race slightly ahead of the rollers. The oil flow is designed for approximately 0.22 gallon per minute (GPM) at 50 psi pressure drop (also, assuming an orifice coefficient of 0.6) at the 100 percent speed (60,000 rpm) condition. The scavenge system is sized to handle about seven times the combined weight flow of breather and seal leakage air and oil when operating under an effective suction of 5 psi differential. This system incorporates considerable flexibility in the depressurization of the front bearing compartment by reduction of breather flow.

As stated previously, the front bearing compartment must operate at below ambient static pressure to prevent reverse flow through the carbon face seal. The external static pressure at design point (or 60,000 rpm) is about 11 psi at the front of the stage-one rotor hub. At no time will this external pressure fall below 10 psi since the rig normally will not be required to run under reduced inlet conditions. As a result, the front bearing compartment static pressure is maintained at 10 psia or slightly lower, resulting in a positive pressure drop into the compartment at all times. The same applies to the labyrinth seal back-up design configuration; direction of airflow in this case, from the external supply, should be into the bearing compartment to prevent oil and air from leaking out into the airstream.

The 0.040-inch-diameter jet provides enough oil flow to prevent skidding damage to the roller bearing. However, in the event that more oil flow is found to be necessary during rig running, the jet size will be reworked to 0.060 inch diameter, still well within the scavenge capacity.

It is emphasized that initial operation with the 0.040-inch jet orifice must be conducted with a thermocouple attached to the bearing outer race OD and that temperature must be monitored to prevent exceeding 350°F.

Rear Bearing

The rig rear (thrust) bearing is lubricated from both sides by means of two 0.040-inch-diameter jets aimed at the inner bearing race. Unlike the front bearing compartment, the rear compartment can be vented by breather directly to atmosphere since there is adequate space to permit utilization of an optimum seal without undue concern over pressure balance.

The rear compartment is designed to accommodate flexibility of oil-in, scavenge, and venting systems, depending on the gearbox adaptation. Using the TS120 gearbox, the rig rear bearing compartment can be vented to ambient through the gearbox system, through its own 12 o'clock vent orifice, or both. Also, the oil-in boss on the 9 o'clock strut can be blocked and a plug removed to connect a bearing oil inlet line from the gearbox side, if desired. Similarly, the rig rear bearing scavenge can be plugged at the 6 o'clock boss position and scavenging can be accommodated through the gearbox. However, to assure safe operation, it is strongly recommended that the rig scavenge system be used also.

The splined coupling from rig to gearbox is lubricated at its rear end by a Toledo facility-designed adapter oil jet. The front end of this coupling is lubricated from the rig side by oil mist from the aft rear bearing oil jet.

The oil flow to the rear bearing, which has two jets, is approximately twice that for the front bearing or approximately 0.44 gallon per minute. This is calculated to be sufficient for operation at the 100 percent speed and fully loaded condition. However, as in the case of the front bearing, the outer race temperature should be monitored (350°F maximum) with a thermocouple, and the two jet sizes should be increased to 0.070 inch diameter if required. The rear scavenge porting is more than adequate to handle the oil and airflows under either of the two oil jet orifice sizes.

ANALYSIS

Analytical work performed in connection with compressor test rig design included stress analyses of the discs, rotor blades, and stator vane; shaft dynamic studies; an investigation of the rig main bearings; and analysis of the gearbox speed increaser.

Stress

Discs. Analyses of both the first- and the second-stage rotor discs indicated that all stresses are within the allowable limits. Figures 80 and 81 show the variation of the biaxial stresses with radius in each disc. Discontinuity loads at the shaft junctures are included in the analysis. The electron beam welds are located in a low stress region and should present no structural problem.

Rotor Blades. A preliminary stress analysis of the first-stage rotor blades, as initially defined aerodynamically, showed a blade root tensile stress at 110 percent design speed of 114,000 psi due to centrifugal forces (direct and untwist stresses). The blade was redesigned by increasing the thickness to chord ratio from 6 to 8 percent at the blade mean hub radius, thereby reducing the blade stresses to the acceptable level of 95,000 psi. A higher thickness to chord ratio is desirable but cannot be tolerated aerodynamically.

Both the direct centrifugal and the untwist stresses are high for the first-stage blade for the following reasons:

- Low blade hub-tip ratio (0.56, mean).
- High rpm (60,000 at design).
- Large blade setting angle variation per unit height (50 degrees per inch at blade hub).

Although the vibratory stress, taken as the full gas bending stress, is low, the high steady stresses make sustained operation at 110 percent speed undesirable. Therefore, the 110 percent speed compressor characteristic will be obtained by refrigerating the inlet and running at a lower mechanical speed.

The stress levels in the second-stage rotor blade are acceptable. A summary of stresses in both rotor blades is given in Table XXIII.

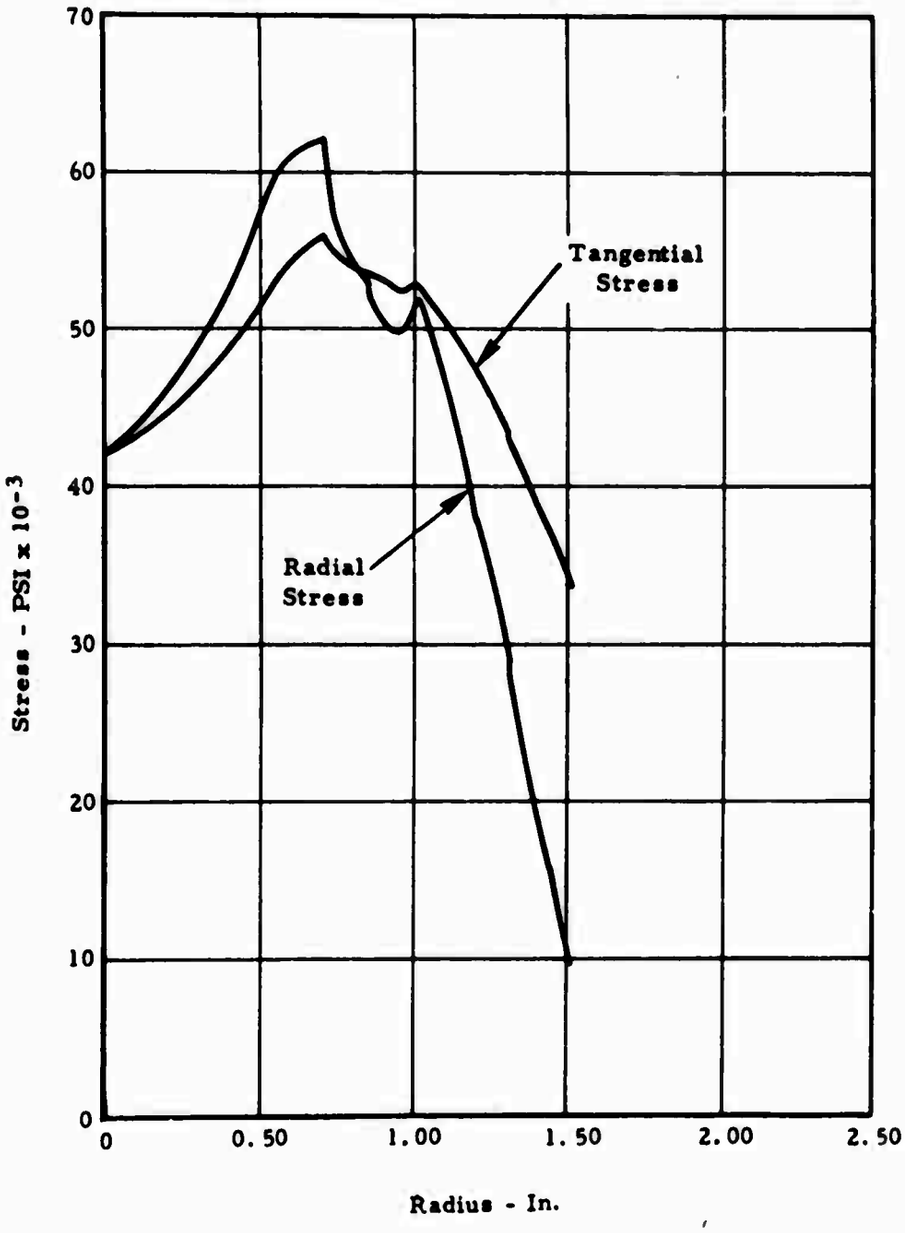

Figure 80. Advanced Axial Compressor Test Rig - First-Stage Compressor Disc - Biaxial Stress Distribution.

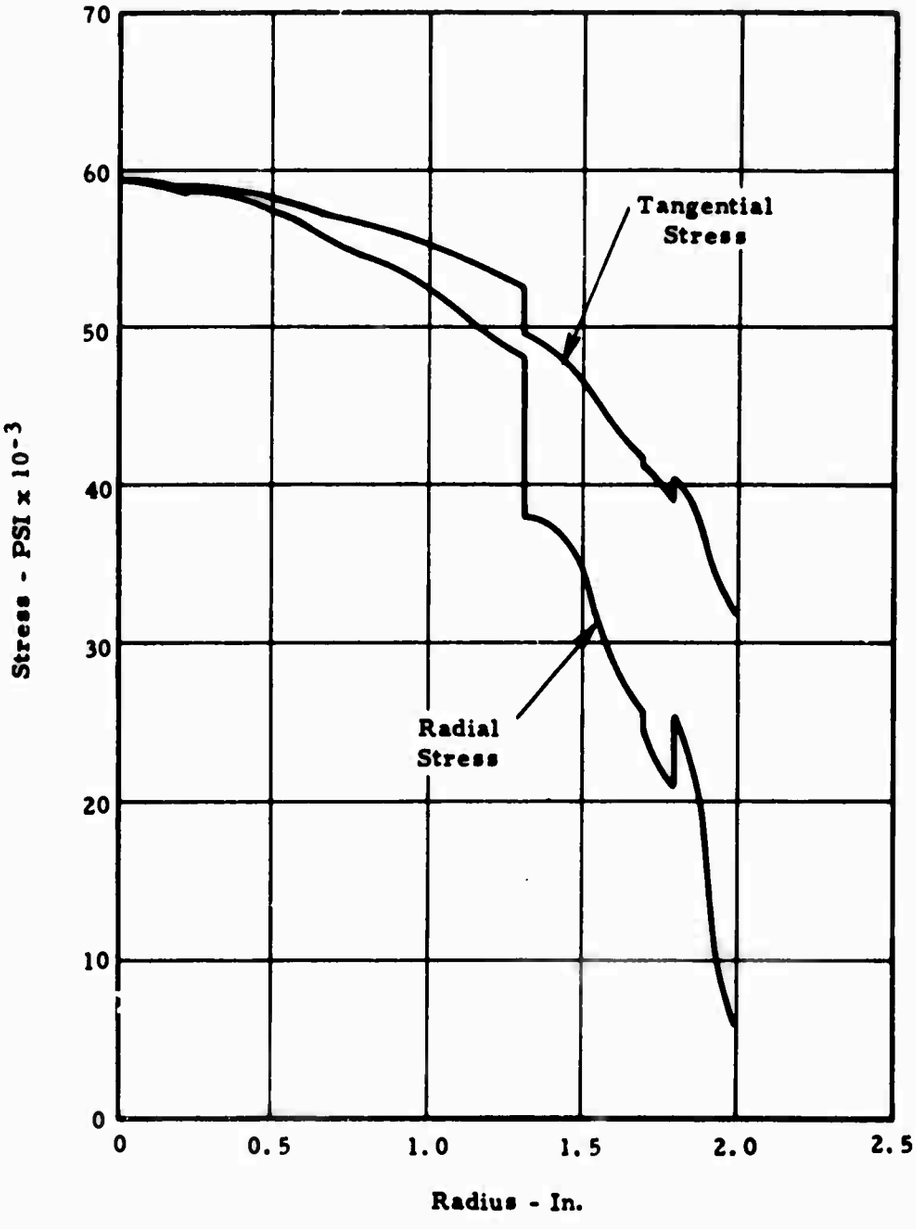

Figure 81. Advanced Axial Compressor Test Rig - Second-Stage Compressor Disc - Biaxial Stress Distribution.

TABLE XXIII
TWO-STAGE AXIAL COMPRESSOR
ROTOR BLADE STRESSES*

Stress	Leading Edge**	Midchord	Trailing Edge
		Stage-One Rotor Blade	
Centrifugal	50,300	50,300	50,300
Untwist	-102,800	+31,800	-102,800
Vibratory	1,300	- 1,100	1,500
Total	- 51,200	+81,000	- 51,000
		Stage-Two Rotor Blade	
Centrifugal	37,500	37,500	37,500
Untwist	-48,200	+15,300	-48,200
Vibratory	5,900	-5,100	6,200
Total	-4,800	+47,700	-4,500

MATERIAL PROPERTIES

Blade/Disc Material	AMS 5616 Greek Ascoloy
Ultimate Tensile Strength - psi	152,000
Yield Strength (0.2 percent offset) - psi	131,000
Fatigue Strength (10^7 cycles) - psi	78,000

* Stresses calculated at blade root at design speed (60,000 rpm). Stress values given in psi.

** Positive stresses are tensile; negative stresses are compressive.

The natural frequencies of the first- and second-stage rotor blades were calculated by treating the blades as pretwisted rotating cantilever beams. The fundamental frequencies for both blades were then adjusted for the low blade aspect ratio effect (plate analysis, as opposed to beam analysis).

Interference diagrams for both rotor blades show that the four inlet struts in the original rig design resulted in fundamental bending resonance at design speed. For this reason, three inlet struts were selected for the inlet duct. Although this number of struts creates the possibility of a fundamental bending resonance condition at 55 to 60 percent of design speed, using a number of struts less than three was impractical from the bearing support standpoint, and more than four was impractical from the aerodynamics standpoint. Further information on energy input values for the test rig will be developed by experimental confirmation of blade natural frequencies and by actual operating experience.

The stage-one rotor blade also shows the possibility of a coupling between the first torsional and second bending frequencies, which may result in a resonance condition due to the 17 inlet guide vanes. Because of this, a complete compressor performance map will be obtained first by running without the inlet guide vanes.

Stator Vanes. Both the first- and the second-stage vanes are brazed to the outer and inner shroud rings, with the inner ring free to rotate and move in the axial direction. The vanes were thus analyzed as guided cantilever beams (one end built-in, other end slope-fixed but free to translate). Under these conditions, a high transverse load would create a tensile force along the axis of each vane, but the low gas loading, combined with the short vane length, resulted in a very low deflection and a negligible tensile stress in the vanes. Sound braze joints are essential to the maintenance of low stator vane stresses, particularly along the hub profile of the necked-down first-stage stator vane. The stator vane stresses are reported in Table XXIV.

Shaft Dynamics

The principal source of mechanical vibration in high speed rotating systems is unbalance in the rotor. This unbalance may excite critical speeds of the rotor itself and/or induce resonance in any combination of structural elements that may be tuned to the running frequency of the rotor. The two-stage axial compressor test rig has been designed to minimize the effects of rotor unbalance and critical speeds through the proper combination of rotor and supporting structure compliance.

TABLE XXIV
TWO-STAGE AXIAL COMPRESSOR
STATOR VANE STRESSES

	Stage One		Stage Two	
Gas Bending Stress at:	Hub	Tip	Hub	Tip
Leading Edge	-5830	+7200	-1840	+3300
Trailing Edge	-6280	+9100	-2140	+3690
Midchord	+3400	-5230	+1370	-2160

All stresses in psi and measured at design speed (60,000 rpm)
Positive stresses are tensile; negative stresses are compressive.

The rotor suspension system of the compressor rig is based on the concept of a relatively rigid shaft assembly mounted on flexible, hydrodynamically damped bearing supports. Critical speeds are controlled by regulating the spring rates and damping constants of the bearing retainers. The flexible mounting also serves to isolate rotor unbalance from the bearings and outer structure.

Design values of bearing support flexibility are determined from a series of curves covering the complete spectrum of possible critical speeds over the compressor operating range (Figure 82). The curves are developed by a digital computer programmed to determine the flexural resonant frequencies of a variable cross section shaft rotating on elastic supports. Gyroscopic stiffening effects of large disc inertias, as well as shear deflections and the local flexure of conical shaft sections, are included in the calculations.

Spring rates are selected to place the first two critical speeds below the normal compressor operating range. The first and second modes will occur at 6,700 rpm (11 percent of design speed) and 12,200 rpm (20 percent of design speed) for front and rear bearing spring rates of 7,900 pounds per inch and 4,000 pounds per inch, respectively. Shaft deflection in these two modes is almost completely described by the bearing displacements (Figure 83). The third mode, which involves considerable shaft flexure as well as bearing displacement, occurs at 130,000 rpm, over twice the maximum rated compressor speed.

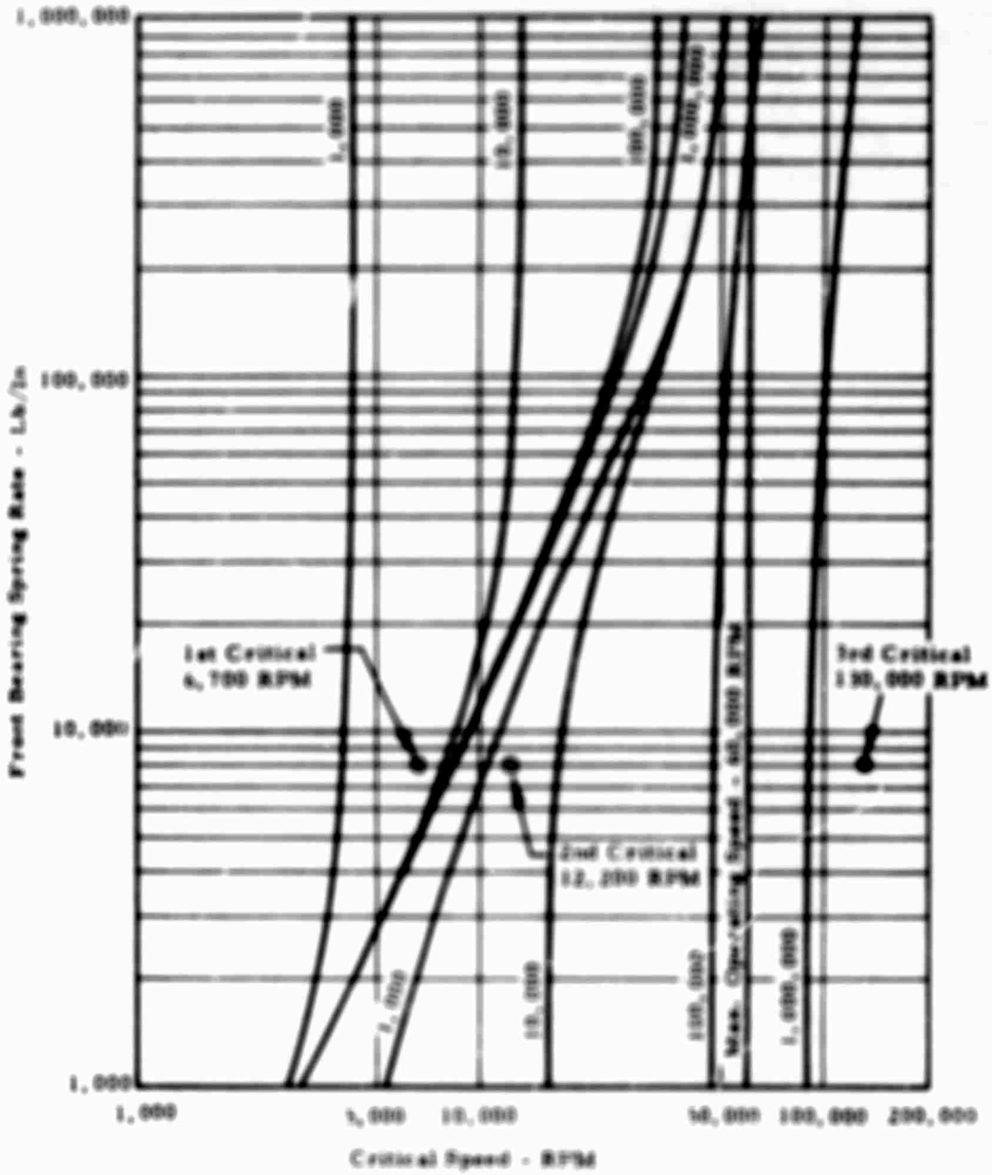

Figure 82. 3:1 Compressor Test Rig (Final Design) Critical Speed Versus Spring Rate of Front Bearing Support for Various Values of Rear Bearing Support Spring Rate.

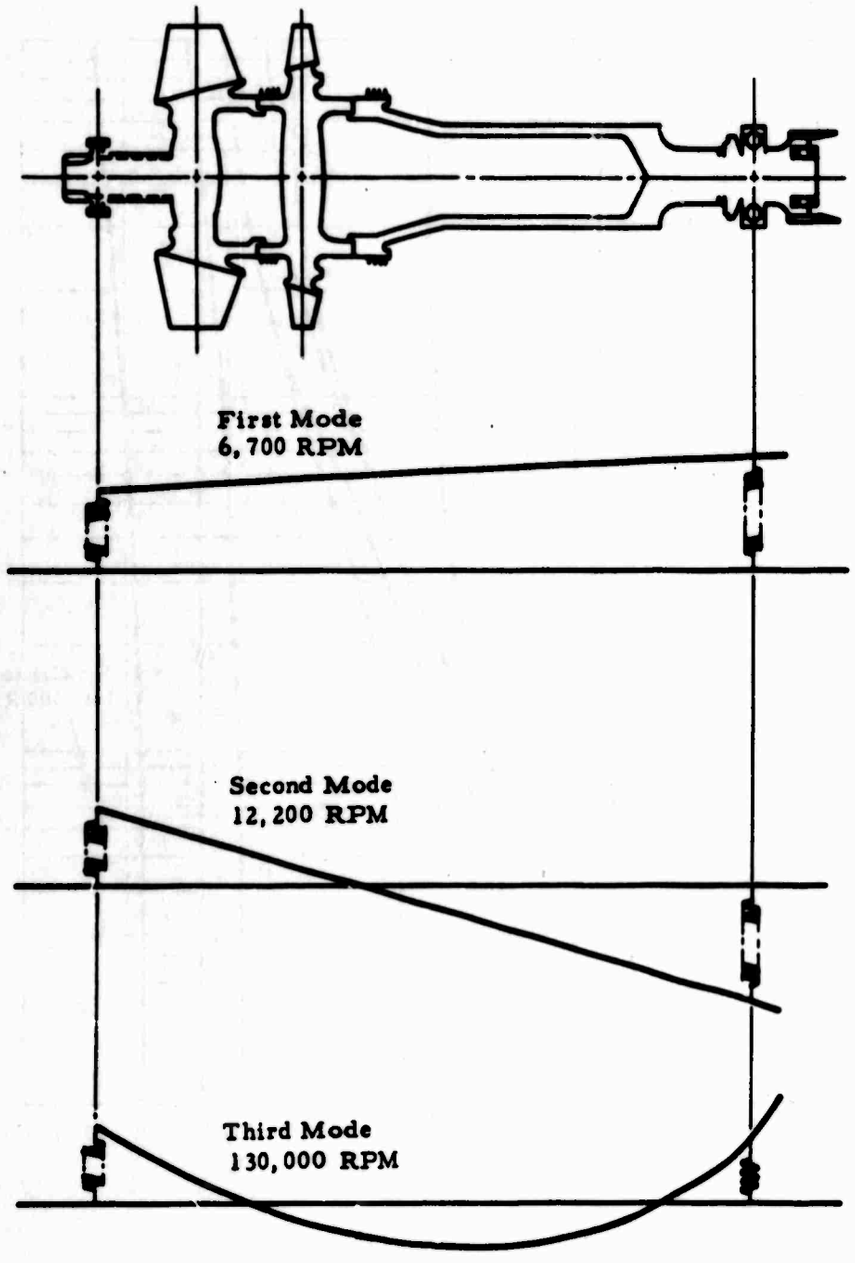

Figure 83. USAAVLABS 3:1 Compressor Test Rig - Deflection Modes for First Three Critical Speeds.

Required bearing support is provided by a cylindrical member containing a number of longitudinal slots. The slot dimensions and material modulus determine the radial spring rate of the bearing suspension, and maximum deflection is controlled by an oil-fed snubbing surface. The deflection snubber limits the maximum stringer bending stresses at resonance to 41,000 psi on the rear cage and 34,000 psi on the front cage. Although the rear bearing support is machined from steel (AMS 6382), it was necessary to specify titanium (Ti-6Al-6V-2Sn) for the front support to obtain the proper spring rate within the space limitations imposed by the flow path of the first-stage compressor.

The effect of structural compliance on the overall system is negligible compared to the relatively low spring rates of the bearing supports, and critical speeds can be accurately established. Figure 84 illustrates the application of this design feature in a typical Continental gas turbine engine main bearing support.

Operation in the region above resonance causes the shaft to seek a rotational centerline about its mass center of gravity (CG). The effect of unbalance is to displace this CG slightly from the geometric centerlines. The only force experienced by the bearings and structural support system is then equal to the product of the displacement and the spring rate of the bearing cage. For an eccentricity of 0.001 inch and a spring rate of 8,000 pounds per inch, this rotating force would be equal to 8 pounds.

Loss of a complete first-stage blade (the heaviest) would cause an unbalance load of only 62 pounds, although the centrifugal weight of this blade at full compressor speed (60,000 rpm) would be over 7,000 pounds. The capability of this system to accommodate large unbalances has been experimentally verified on similarly suspended gas turbine engines by deliberately introducing massive unbalance into the rotors and running at full speed with very little increase in external vibration levels.

The stiff construction of the electron beam welded rotor shaft minimizes any tendency to go out of balance at high speeds. If sufficient flexibility exists in a rotor system, locked in bending moments caused by the uneven distribution of unbalance along the length of the rotor will cause the shaft to deflect at high speeds, destroying the balance that was obtained at the much lower balancing speed. In some cases it is necessary to balance such flexible rotors at high speeds and in three or more planes to attain satisfactory running balance. This will not be necessary with the two-stage axial compressor test rig.

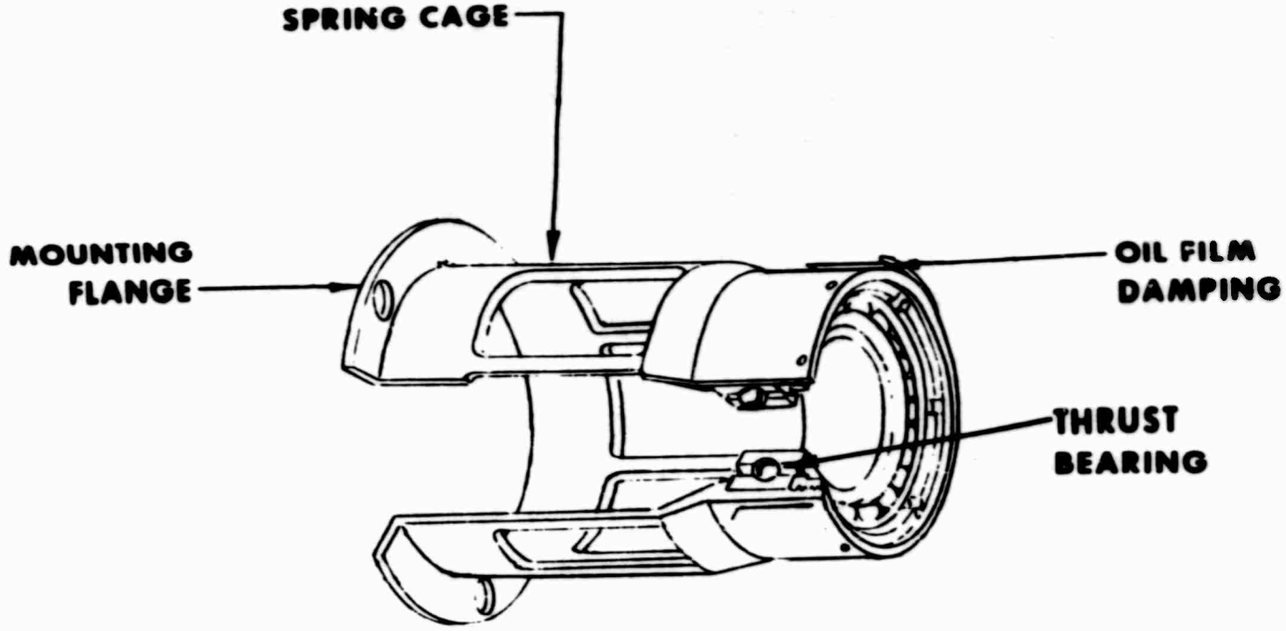

Figure 84. Typical Continental Gas Turbine Engine Flexible Main Bearing Support.

Bearing support deflection is limited at resonance by two concentric, oil-fed snubbing surfaces that also prevent excessive pounding due to the gyroscopically induced moment of the rotor under possible foundation movements. The clearance, width, and diameter of these surfaces are parameters of a viscous damping system in which the hydrodynamic force-vector generated by the rotating oil film squeeze action varies in both magnitude and direction with speed and unbalance. There is a certain optimum combination of values for which the damper is adequate to provide low frequency vibration absorption without increasing transmissibility at high speeds to such an extent that the bearing support spring no longer functions as an effective mass isolator. The design parameters used in this system have been derived through analytical methods, verified by full-scale laboratory tests, and proven by service in thousands of Continental gas turbine engines.

Compressor Main Bearings

The compressor shaft assembly is supported by a roller bearing at the front end and a ball bearing at the rear end. This seemingly unorthodox arrangement is dictated by the extremely small compartment available at the front end for a thrust bearing with a cross section capable of absorbing the rotor thrust. Since no combustion takes place in this rig, there is no extreme differential thermal expansion between the shaft and stationary structure; therefore, a rear-mounted thrust bearing can adequately maintain the required axial clearance at the compressor section. Absence of hot exhaust gases also means the rear-mounted thrust bearing will not be subjected to capacity decreasing temperature conditions.

The rear bearing, which absorbs the rotor thrust, is an angular contact split inner race type, with ball complement, contact angle, race curvatures, and retainer construction designed to accommodate high speeds and load. The bearing is currently used in the Continental Model TS120 gas turbine engine, where it has successfully accumulated many hours of development testing.

The calculated life of the thrust bearing is approximately 40 hours at maximum speed and thrust. These conditions are 60,000 rpm and 425 pounds, respectively. It is expected that the true bearing life under these conditions would be close to ten times the life calculated according to Anti-Friction Bearing Manufacturers Association (AFBMA) standards due to the combination of materials and processing specified.

The races and balls are manufactured from consumable electrode vacuum melt (CEVM) M-50 tool steel heat treated to Rockwell C-61 minimum hardness. It has been Continental's practice to assign a life factor of five to one for CEVM 52100 steel and ten to one for CEVM M-50 steel even previous to the announcements by certain bearing companies that a life factor of three to one could be applied to the catalog ratings of their bearings manufactured from vacuum degassed 52100 steel. The consumable electrode vacuum remelting process results in a cleaner grade of steel than that obtainable through vacuum degassing, and it is felt that this superior degree of cleanliness is responsible for the higher reliability of CEVM bearings. The further two-to-one improvement of M-50 over 52100 is attributable to its higher stabilized hardness of Rc 61 and its ability to retain this hardness in the ball raceways where instantaneous load-induced hot spots would reduce the local hardness of standard bearing materials and cause a resultant reduction in overall life.

The cage is machined from hardened steel, silver plated to increase corrosion resistance and improve frictional properties. Balls and cage are retained in the outer race to facilitate assembly and disassembly. The cage is outer ring guided to enhance lubrication of the guide surfaces at the high speed involved.

The DN value (an arbitrary rating parameter equal to the product of the bearing bore diameter in millimeters and the shaft speed in rpm) of the bearing is 1.2×10^6 at maximum compressor speed, and this parameter is well within the range of successful Continental experience. The internal geometry of the bearing is based on configurations which have allowed bearing companies to successfully test this size bearing at a speed of 120,000 rpm, about 100 percent higher than the maximum rated speed of this rig.

The outer race of the bearing is positively retained by a nut and lock ring in its flexible housing. The inner race is pressed on the shaft with an interference fit and held through a spline coupling member by a nut and lockwasher.

The front bearing is a double lipped outer race roller bearing with a wider than standard inner race to accommodate expansion between the housings and the rotor shaft. The roller complement and retainer construction are set up primarily to favor high speed capability rather than radial load capacity since most of the unbalance will be absorbed in the flexible bearing mount. By allowing the shaft to rotate about its mass center of gravity rather than its geometric center, the maximum radial force seen by the bearing will be less than 50 pounds and the resulting bearing life is calculated to be in excess of 20,000 hours.

Rollers and races on this bearing are manufactured from CEVM M-50 tool steel. The material is stabilized to retain hardness and dimensional stability at 600°F although it is not expected that operating temperature will exceed 300°F with the scheduled oil supply. The cage for this bearing is a one-piece, outer land riding, high strength, hardened steel machining, silver-plated to improve frictional characteristics. The bearing is press fitted on the shaft and held by a nut and lock washer. The outer race is retained by a nut and lock ring against a solid shoulder in the flexible support.

MECHANICAL DESIGN OF TEST RIG INSTRUMENTATION AND ASSOCIATED HARDWARE

TEST RIG AND ASSOCIATED HARDWARE

The adaptation design work for mounting of the USAAVLABS compressor in the 1400 horsepower test rig area at Continental's Toledo Component Testing Laboratory included the design of the compressor inlet duct, the discharge collector, the throttle valve adapters, and the inlet plenum cover plate. An existing inlet bellmouth will be utilized, and inlet airflow will be determined by an American Society of Mechanical Engineers nozzle in the test cell supply line. Inlet pressure depression and refrigeration capabilities, as required, are provided by means of the sealed inlet configurations.

Gearbox

An existing high speed gearbox utilizing the same internal rotating components as the gear reduction unit used on the Continental TS120 gas turbine engine, but with housing and basic static structure fabricated from steel rather than cast from magnesium as in the engine gearbox, was selected as the speed increasing unit to drive the 3:1 compressor test rig. It must be pointed out that the gearbox represents a conservative long-life approach to its original design objectives; namely, 120 horsepower at 66,800 rpm input speed with output at 6061 rpm. Under its proposed usage, the unit is highly stressed and has a limited life expectancy.

An analysis of the gear and bearing loads, stresses, and life was conducted for a compressor input of 410 horsepower at 60,000 rpm. This would correspond to 5444 rpm input to the gearbox. The results of this analysis indicate that a gearbox life of 100 hours at full rated power and speed should be attained. The most critical component in the drive train is the high speed pinion thrust bearing which has a calculated B10 life of 250 hours.

The gear train is shown in Figure 85 with the bearings identified numerically. A summary of bearing loads, speeds, and lives is presented in Table XXV. The reduction gear data are summarized in Table XXVI.

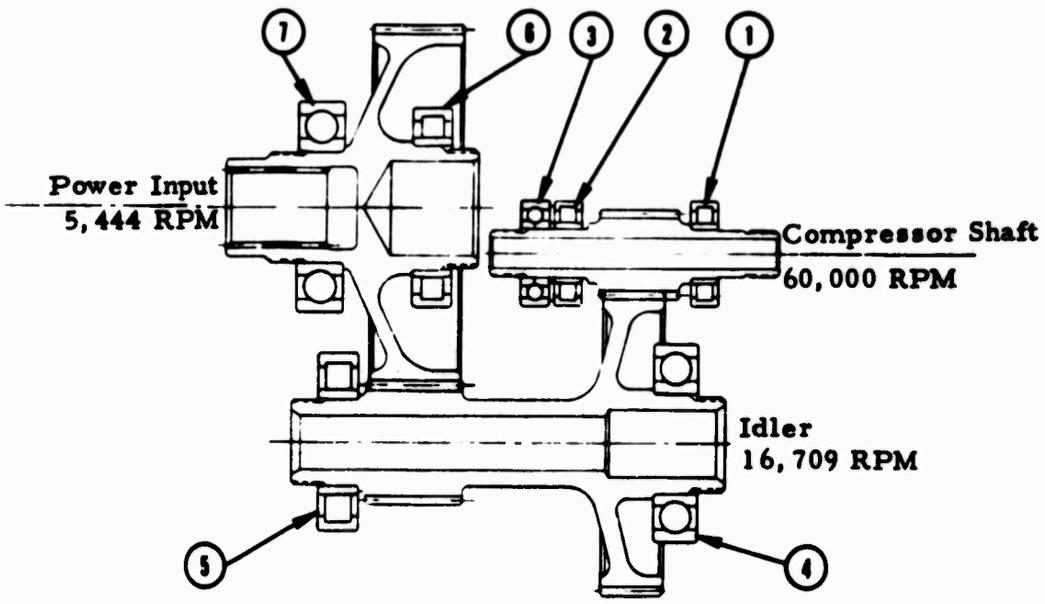

Figure 85. USAAVLABS 3:1 Compressor Gearbox Schematic.

TABLE XXV
USAAVLABS 3:1 COMPRESSOR SPEED INCREASER GEARBOX BEARINGS

SUMMARY

Brg. No.	CAE P/N	Manufacturer's Cat. No.	Function or Drive	Speed, RPM	Radial Ld., Lb	Thrust Ld., Lb	Equivalent Loads Lb	Life, Hours
1	306669	MR-104-KE	High Speed Pinion, Rear	60,000	359	-	359	924
2	306669	MR-104-KE	High Speed Pinion, Front	60,000	341	-	341	1,096
3	307023	9104-UK-204	High Speed Pinion, Thrust	60,000	-	183	183	254
4	306681	208-S	Compound Idler, Rear	16,709	381	171	411	2,460
5	306682	MR-207-E	Compound Idler, Front	16,709	1,339	-	1,339	1,085
6	306680	MR-110-KG	Power Input, Rear	5,444	1,289	-	1,289	2,896
7	306679	209-S	Power Input, Front	5,444	745	355	797	1,280

TABLE XXVI
SUMMARY OF 3:1 COMPRESSOR SPEED INCREASER GEAR DATA

	High Speed Mesh		Low Speed Mesh	
	Pinion 711148	Gear 711074	Pinion 711074	Gear 711011
No. of Teeth	22	79	29	89
Pitch Diameter (In)	1.3463	4.8343	1.853	5.6868
Normal Diametral Pitch	17	17	16	16
Normal Pressure Angle	20°	20°	20°	20°
Helix Angle	16°RH	16°LH	18°LH	18°RH
Effective Face Width (In)	1.05	1.05	1.45	1.45
Horsepower	410	410	410	410
Speed (RPM)	60,000	16,709	16,709	5,444
Pitch Line Velocity FPM	21,147	21,147	8,106	8,106
Wear Stress (PSI)	234,000	- -	232,700	- -
Static Hertz Stress (PSI)	132,100	- -	165,400	- -
Dynamic Beam Stress (PSI)	83,000	- -	106,300	- -
PVT Factor	1,326,000	1,488,000	485,000	892,000
Contact Ratio	3.2	3.2	3.2	3.2
Life (Hrs)	670		500	

It is anticipated that the original TS120 oil supply, particularly to the high speed pinion bearings, will be inadequate. Therefore, changes in the lubricating system to supply oil to both sides of all pinion bearings were incorporated. Gear jet sizes were increased by 50 percent to allow over twice the cooling capacity that the present oil flow provides. Also, the high speed pinion roller bearing clearance was increased from the present 0.0001 to 0.0003 inch (which was specified to prevent roller skidding under zero or light load) to approximately 0.0004 to 0.0008 inch to prevent excessive heat generation which might cause the bearings to seize up from loss of internal clearance due to differential thermal expansion.

INSTRUMENTATION

The fixed rake and survey instrumentation required for one test is defined in Table XXVII. Instrumentation plane locations are shown on Figure 86. The number and type of traverse probes and actuators, including spares, needed for one test are listed below.

	No. Probes	Spares	Total
Static Pressure Angle	3	1	4
Total Pressure and Temperature, Angle	3	1	4
Total Pressure, Angle	1	1	2
Total Pressure, Static Pressure Angle	3	1	4
Total No. Traverse Probes	10	4	14
Total No. Actuators	9	1	10

A standard American Society of Mechanical Engineers 5 inch diameter nozzle is used to measure airflow. Rotation speed is measured by a magnetic speed pick-up indicator.

TABLE XXVII

USAAVLABS SMALL AXIAL COMPRESSOR INSTRUMENTATION REQUIREMENTS

[illegible]	[illegible]	[illegible]	[illegible]
1	[illegible]	a. [illegible] b. [illegible]	[illegible]
2	[illegible]	a. [illegible] b. [illegible]	[illegible]
3	[illegible]	a. [illegible] b. [illegible] c. [illegible]	[illegible]
4	[illegible]	a. [illegible] b. [illegible]	[illegible]
5	[illegible]	[illegible]	[illegible]
6	[illegible]	[illegible]	[illegible]
7 8 9	[illegible]	a. [illegible] b. [illegible] c. [illegible]	[illegible]
	[illegible]	a. [illegible] b. [illegible] c. [illegible] d. [illegible] e. [illegible]	[illegible]
		[illegible]	

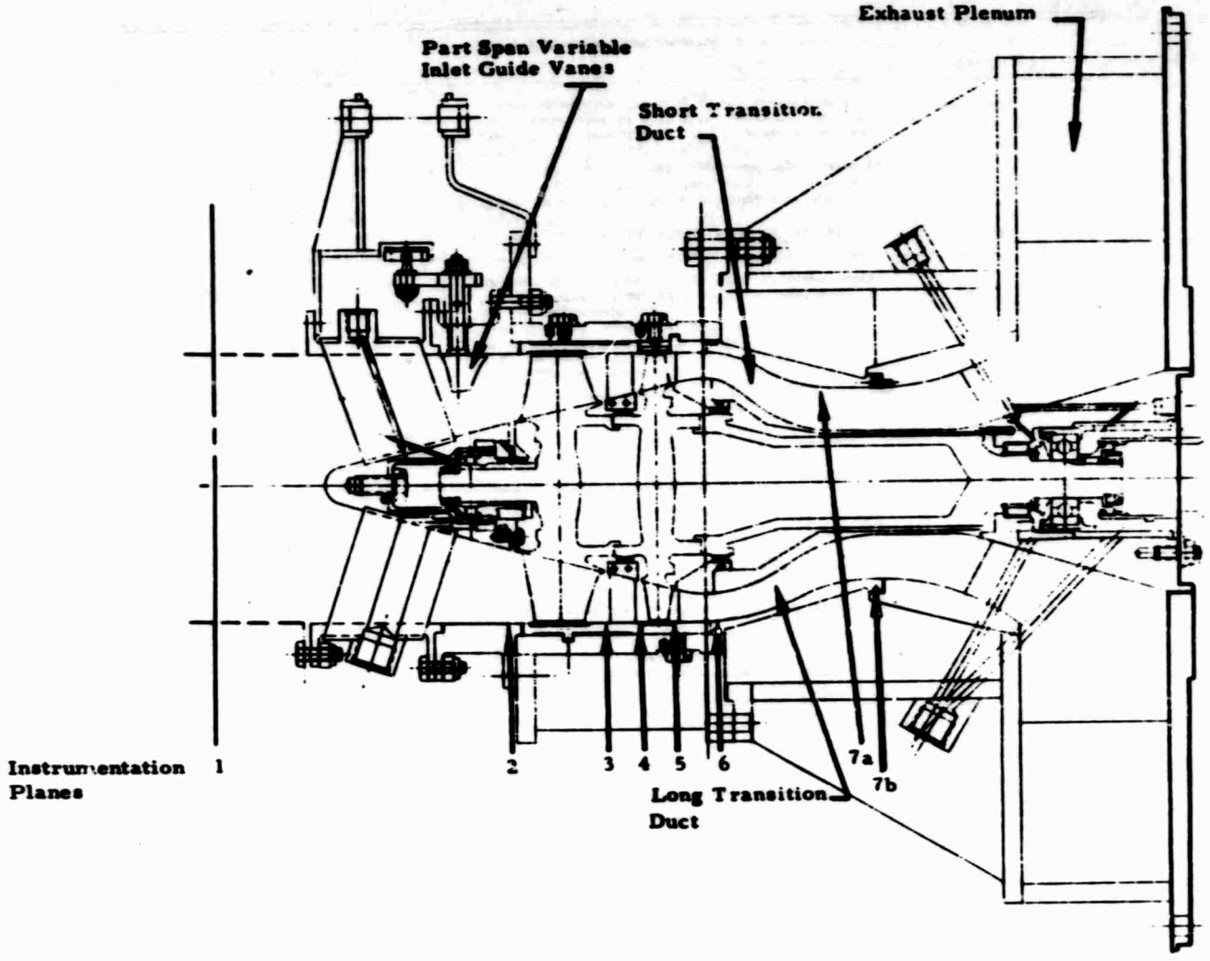

Figure 86. Advanced Axial Compressor Test Rig Design Layout - Instrumentation Planes.

UNCLASSIFIED

Security Classification

DOCUMENT CONTROL DATA - R & D

(Security classification of title, body of abstract and indexing annotation must be entered when the overall report is classified)

1. ORIGINATING ACTIVITY (Corporate author) Continental Aviation and Engineering Corporation 12700 Kercheval Avenue Detroit, Michigan 48215	2a. REPORT SECURITY CLASSIFICATION Unclassified 2b. GROUP

3. REPORT TITLE

ADVANCEMENT OF SMALL GAS TURBINE, COMPONENT TECHNOLOGY
ADVANCED SMALL AXIAL COMPRESSOR VOLUME I - ANALYSIS AND DESIGN

4. DESCRIPTIVE NOTES (Type of report and inclusive dates)

5. AUTHOR(S) (First name, middle initial, last name)

James V. Davis

6. REPORT DATE	7a. TOTAL NO. OF PAGES	7b. NO. OF REFS
December 1969	175	

8a. CONTRACT OR GRANT NO.	9a. ORIGINATOR'S REPORT NUMBER(S)
DA 44-177-AMC-296(T) b. PROJECT NO. 1G162203 D14413 c. d.	USAAVLABS Technical Report 69-10A 9b. OTHER REPORT NO(S) (Any other numbers that may be assigned this report) Continental Report No. 1033

10. DISTRIBUTION STATEMENT

This document is subject to special export controls, and each transmittal to foreign governments or foreign nationals may be made only with prior approval of US Army Aviation Materiel Laboratories, Fort Eustis, Virginia 23604.

11. SUPPLEMENTARY NOTES	12. SPONSORING MILITARY ACTIVITY
Advanced Axial Compressor Family Study - Volume I	U.S. Army Aviation Materiel Laboratories, Fort Eustis, Virginia

13. ABSTRACT

A cursory design study of the gas generator involving the preliminary design and analysis of a family of axial compressors was conducted. Each axial compressor was designed to be capable of match with the USAAVLABS advanced centrifugal technology. The minimum overall axial-centrifugal design pressure ratio for each compressor configuration was 16:1. The engine performance using the characteristics of the compressor designs was evaluated and an optimum gas generator configuration was selected.

The axial compressor for the optimum gas generator configuration was detail designed for test rig evaluation. This axial compressor has two stages and a 3.0:1 design pressure ratio. The design flow rate is 5.0 pound-per-second and the inlet tip radius is 2.72 inches.

DD FORM 1 NOV 68 1473 REPLACES DD FORM 1473, 1 JAN 64, WHICH IS OBSOLETE FOR ARMY USE.

UNCLASSIFIED

Security Classification

UNCLASSIFIED

Security Classification

14. KEY WORDS	LINK A		LINK B		LINK C	
	ROLE	WT	ROLE	WT	ROLE	WT
Axial Compressor Design Component Technology Small Gas Turbine						

UNCLASSIFIED

Security Classification